



Cape Peninsula
University of Technology

**DESIGN AND IMPLEMENTATION OF A NONLINEAR CONTROLLER IN PLC AS
A PART OF AN ADROIT SCADA SYSTEM FOR OPTIMAL ADAPTIVE CONTROL
OF THE ACTIVATED SLUDGE PROCESS**

by

PASEKA AUGUSTINUS NKETOANE

Thesis submitted in fulfilment of the requirements for the degree

Master of Technology: Electrical Engineering

in the Faculty of Engineering

at the Cape Peninsula University of Technology

Supervisor: Prof R. Tzoneva

Bellville Campus
December 2009

DECLARATION

I, Paseka Augustinus Nketoane, declare that the contents of this dissertation/thesis represent my own unaided work, and that the thesis has not previously been submitted for academic examination towards any qualification. Furthermore, it represents my own opinions and not necessarily those of the Cape Peninsula University of Technology.

Signed

Date

ABSTRACT

More than 70% of the earth's surface is covered by water, only a small part of which is suitable for either human consumption or agricultural use. Due to pollution from agriculture, households and industry reaching rivers, lakes and seas it is important for wastewater to be properly treated in order to remove harmful substances before it reaches the environment.

Strict environmental and health regulations together with a demand for cost effective ways of wastewater treatment have made control technology in Wastewater Treatment Plants an important priority. Dissolved oxygen (DO) is the amount of oxygen in the effluent and it plays a vital role of controlling WWTP. Oxygen dissolves in water through mixing water surface with the atmosphere. The dissolved oxygen concentration in the aerobic part of an activated sludge process should be sufficiently high to supply enough oxygen to the microorganisms in the sludge. But, an excessive high DO leads to high energy consumption and may also deteriorate the sludge quality. A high DO concentration in the internally recirculated water also makes the denitrification less efficient. Hence, both for economical and process reasons, it is of interest to control the DO. The used controllers are normally linear controllers, proportional integral (PI) or proportional integral derivative (PID) ones. The work of these controllers leads to bad system performance, because, the process of dissolving oxygen into the wastewater is a nonlinear process and requires nonlinear control.

The aim of the research project is to develop methods for design of linear and nonlinear controllers of the concentration of the DO in the aeration tank of the WWTP and to implement the designed controllers in the frameworks of PLC. The nonlinear linearizing controller based on a reference model and Lyapunov second method is designed. Additionally, a linear controller is developed in a form of PI controller based on pole placement method to improve the performance of the closed loop system. The resultant controller is to be implemented on a PLC as a part of Adroit SCADA system. The developed programmes are used to control the wastewater treatment process in laboratory scale plant and can be applied as a part of SCADA software for control of the wastewater treatment plants.

ACKNOWLEDGEMENTS

I wish to thank:

- My creator for giving courage, wisdom and strength for guiding me through out my studies
- My family for their everlasting support and encouragement, especially 'Makhautla Makhetha, 'Malisema Ramashamole and Nthabiseng Taole
- My supervisor Prof Raynitchka Tzoneva for her supervision, guidance, dedication, assistance, patience, and understanding and let me say Prof without your support this work would have been possible.
- Mr Carl Kriger for his assistance with Adroit SCADA and Modicon PLCs
- Mr Nthuthuko Dube insightful words, comments and support
- Ms Koketso Kujane comments and her support
- Mr Christopher Quigley of Oxleyinc for his assistance with Adroit SCADA and Modicon M340 PLCs

If you have received funding from the NRF, include the following:

The financial assistance of the National Research Foundation towards this research is acknowledged. Opinions expressed in this thesis and the conclusions arrived at, are those of the author, and are not necessarily to be attributed to the National Research Foundation.

DEDICATION

This thesis is dedicated to the late 'MANTSEBO EXINIA SEKOTA

TABLE OF CONTENTS

Declaration	ii
Abstract	iii
Acknowledgements	iv
Dedication	v
Glossary	xvii

CHAPTER ONE: STATEMENT OF THE PROBLEM: PROJECT OBJECTIVES HYPOTHESIS AND ASSUMPTIONS

1.1	Awareness of the problem	1
1.1.1	The process variables	3
1.1.2	Main operation problems	3
1.1.2.1	Operator's application of concepts and testing to process control	3
1.1.2.2	Infiltration Inflow	3
1.1.2.3	Process control testing	3
1.1.2.4	Operational and management manual adequacy	3
1.1.2.5	The industrial loading	3
1.1.2.6	Process controllability	4
1.1.3	Sludge wasting and return	4
1.2	Statement of the problem	5
1.3	Design based problems	6
1.3.1	Sub-problem1: Activated Sludge Process study	6
1.3.2	Sub-problem2: Mathematical Modelling	6
1.3.3	Sub-problem3: Control design and Implementation	6
1.3.4	Sub-problem4	7
1.4	Real time implementation sub-problems	7
1.4.1	Sub-problem5	7
1.4.2	Sub-problem6	7
1.4.3	Sub-problem7	8
1.4.4	Sub-problem8	8
1.5	Research Aim and Objectives	8
1.5.1	Aim	8
1.5.2	Objectives	8
1.6	Hypothesis	9
1.7	Delimitations of the research	9
1.8	Motivation for the project development	9
1.9	Assumptions	10
1.10	Research methods	10
1.10.1	Literature review method	10
1.10.2	Design method	10
1.10.3	Experimental method	10
1.10.4	Description method	10
1.11	Outline of the thesis	10

CHAPTER TWO: OVERVIEW OF THE METHODS FOR MODELLING AND CONTROL OF WASTEWATER TREATMENT PROCESS

2.1	Introduction	13
2.2	Wastewater treatment process description	13
2.2.1	Mechanical (Primary) treatment	13
2.2.2	Biological treatment	14
2.2.3	Chemical treatment	14

2.2.4	Sludge treatment	14
2.2.5	The Activated Sludge Process	15
2.2.6	Biological nitrogen removal	17
2.3	A process of dissolving oxygen in wastewater	18
2.3.1	The role of dissolved oxygen (DO) concentration in nature	18
2.3.2	The role of dissolved oxygen in the activated sludge process	19
2.4	Mass balance model of dissolved oxygen	21
2.4.1	Mass balances	21
2.4.1.1	The definition of the oxygen transfer function	22
2.4.1.2	The dissolved oxygen dynamics	22
2.5	Methods for measurement of dissolved oxygen concentration based on respirometry	23
2.5.1	Respirometry	23
2.5.2	Significance of respirometry	25
2.5.3	Measuring principles	27
2.5.4	Principles based on measuring DO concentration in liquid phase	27
2.5.5	Respirometric principles based measuring dissolved oxygen in the gas phase	29
2.5.6	Static gas-static liquid	31
2.5.7	Flowing gas-static liquid	31
2.5.8	Static gas-flowing liquid	33
2.5.9	Hybrid respirometer	34
2.6	Methods for estimation of the oxygen transfer function and oxygen uptake rate	34
2.7	Methods for control of the dissolved concentration	40
2.7.1	First dissolved oxygen control systems	40
2.7.2	Diffused aeration control	41
2.7.3	Mechanical aerator control	42
2.7.4	Elementary control concepts of the aerated sludge process	42
2.7.4.1	Objectives of control	42
2.7.4.2	Dissolved oxygen levels	44
2.7.4.3	Standard control schemes for DO concentration and respiration rate control	44
2.7.5	Respirometry in control	46
2.8	Analysis of the existing situation	47
2.9	Conclusion	50

CHAPTER THREE: DEVELOPMENT OF A MATHEMATICAL MODEL OF THE DISSOLVED OXYGEN CONCENTRATION PROCESS

3.1	Introduction	51
3.2	Structure of the Activated Sludge Process (ASP) mass balance model	51
3.3	Description of the COST Benchmark process based on ASM1 biological	52
3.3.1	Process flows and oxygen transfer functions	53
3.3.2	Values of the ASM1 model parameters	54
3.3.3	Process variables	54
3.4	Mass-balance model of the dissolved oxygen concentration for the Benchmark plant	55
3.5	Mathematical model of the oxygen transfer function	56
3.6	An exponential model of oxygen transfer function	58
3.7	Dissolved oxygen model equation representation in standard affine form	59
3.8	Simulation of the DO model in Simulink	61

3.8.1	Importance of simulation	61
3.8.2	Objectives of DO concentration model simulation	62
3.8.3	Input data fro simulation	63
3.8.4	Results from the simulation	63
3.8.5	Discussion of the results	74
3.9	Conclusion	77

CHAPTER FOUR: ESTIMATION OF THE OXYGEN TRANSFER FUNCTION AND OXYGEN UPTAKE RATE

4.1	Introduction	78
4.2	The method of least squares for parameter estimation	79
4.3	Data used for parameter estimation	78
4.4	Application of the least squares method to different models of the oxygen transfer function	80
4.4.1	Oxygen transfer function represented by a time varying parameter	80
4.4.2	Oxygen transfer function represented by a linear function	83
4.4.3	Oxygen transfer function represented by a power function	83
4.4.4	Oxygen transfer function represented by an exponential function	84
4.4.5	Oxygen transfer function represented by a square root function	85
4.4.6	Oxygen transfer function represented by a second order polynomial	86
4.4.7	Oxygen transfer function represented by a Monod type model	87
4.5	Calculation of the parameters in the software environment of Matlab	87
4.6	Conclusion	88

CHAPTER FIVE: OVERVIEW OF THE METHODS FOR ANALYSIS AND CONTROL DESIGN OF NONLINEAR SYSTEMS

5.1	Introduction	89
5.2	Nonlinear system determination	89
5.2.1	Improvement of the existing control systems	91
5.2.2	Analysis of hard nonlinearities	92
5.2.3	Dealing with model uncertainties	92
5.3	Mathematical models of the nonlinear systems	92
5.4	Nonlinear control design	93
5.4.1	Feedback linearization	94
5.4.2	Input/Output linearization	94
5.4.3	Sliding mode control	95
5.4.4	Lyapunov stability theory	95
5.4.5	Adaptive control	96
5.5	Methods for analysis of the nonlinear systems	97
5.5.1	Phase plane analysis	97
5.5.2	Describing functions	98
5.5.3	Lyapunov method	99
5.6	Conclusion	99

CHAPTER SIX: DESIGN OF A NONLINEAR LINEARIZING CONTROL OF DISSOLVED OXYGEN CONCENTRATION

6.1	Introduction	100
6.2	Feedback linearization	100
6.3	Linearization approaches	103
6.3.1	Input-State linearization	103

6.3.2	Input/Output linearization	105
6.3.3	Comparison between the two approaches	106
6.4	Importance of the dissolved oxygen concentration control	107
6.5	Nonlinear linearizing controller design on the basis of the geometrical approach	109
6.5.1	PI controller design	112
6.5.2	Transfer function of the linearized process	112
6.5.3	Transfer function of the PI controller	112
6.5.4	Transfer function of the closed loop system	113
6.5.5	Characteristics equation of the closed loop system	113
6.5.6	Desired characteristic equation	114
6.5.7	Comparison of the equations	114
6.6	Design of the final nonlinear linearizing controller	115
6.7	Simulink block diagram of the nonlinear linearizing controller	116
6.8	Matlab program for the nonlinear linearizing controller	117
6.9	Simulation results of the nonlinear linearizing controller	118
6.10	Discussion of the results	127
6.11	Conclusion	128

CHAPTER SEVEN: DESIGN OF NONLINEAR LINEARIZING CONTROL OF THE DISSOLVED OXYGEN PROCESS ON THE BASIS OF LYAPUNOV THEORY

7.1	Introduction	129
7.2	Nonlinear systems and Equilibrium points	129
7.2.1	Autonomous and Non-autonomous systems	129
7.2.2	Equilibrium points	130
7.2.3	Concepts of stability	130
7.2.4	Stability and Instability	131
7.2.5	Asymptotic stability and Exponential stability	131
7.2.6	Local and Global stability	132
7.2.7	Linearization and Local stability	133
7.3	Lyapunov's direct method	133
7.3.1	Positive definite functions and Lyapunov functions	134
7.3.2	Barbalat's lemma	135
7.4	Controller design	136
7.4.1	Nonlinear continuous control of dissolved oxygen concentration	136
7.4.2	Model reference control systems, design of a nonlinear controller in common case	137
7.4.3	The plant is described by a nonlinear state equation	137
7.4.4	Determination for the behaviour of the closed loop system	137
7.4.5	Determination of the error between the reference model and plant state	138
7.4.6	Design of a controller	138
7.4.6.1	Construction of a Lyapunov functions for the system	138
7.4.6.2	Calculation of the derivative of the function of Lyapunov according to the trajectory of the error equation	139
7.4.6.3	Calculation of the control vector u	139
7.5	Design of the nonlinear Lyapunov controller for the model of the dissolved oxygen concentration	140
7.5.1	Dissolved oxygen model	140
7.5.2	The model of the desired system (reference model)	140
7.5.3	Determination of the error between reference model and plant states	141
7.6	Design of the control	142
7.6.1	Construction of a Lyapunov function of the error differential equation	142

7.6.2	Calculation of the first derivative of the function of Lyapunov	142
7.6.3	Calculation of the control u	142
7.7	Design of a controller for the reference model	143
7.7.1	Design of the PI controller	144
7.7.2	Final expression of the control u	144
7.8	Simulation study of the behaviour of the designed closed loop system	145
7.8.1	Simulink block diagrams	146
7.8.2	Matlab program for the Lyapunov based nonlinear controller with reference model	148
7.8.3	Simulation results	149
7.9	Discussion of the results	157
7.10	Conclusion	158

CHAPTER EIGHT: IMPLEMENTATION OF THE NONLINEAR CONTROLLER IN PLC AS A PART OF THE THREE LAYER STRATEGY

8.1	Introduction	159
8.2	Programmable Logic Controller (PLC)	159
8.3	PLC Hardware	161
8.3.1	Programming Device	161
8.3.2	Central Processing Unit (CPU)	161
8.3.3	Power Supply	161
8.3.4	Input/Output Modules	162
8.3.4.1	Discrete Input Modules	162
8.3.4.2	Discrete Output Modules	163
8.3.4.3	Analog Input Modules	163
8.3.4.4	Analog Output Modules	163
8.4	Program Scan	163
8.5	Programming of PLCs	164
8.5.1	Ladder logic diagram	164
8.5.2	Symbols used in Ladder Logic diagrams	164
8.5.3	Input Devices (Contacts)	165
8.5.4	Normally open contact	165
8.5.5	Normally closed contact	165
8.5.6	Output Devices (Coils)	165
8.5.7	Rung	166
8.6	Modicon M340 PLC using Unity Pro S V4.0 Software	166
8.7	The closed loop system of Waste Water Treatment plant.	169
8.8	Process Variables to be measured	171
8.8.1	pH	171
8.8.2	Turbidity	172
8.8.3	Conductivity	172
8.8.4	DO	172
8.8.5	Communication	173
8.9	Implementation of the designed controllers in PLC	173
8.9.1	PLC program for input and output data	173
8.9.1.1	PLC program for implementation of PI controller	174
8.9.1.2	PLC program implementation of the linearizing controller	175

8.9.2	PLC program for implementation of the nonlinear Lyapunov reference based model controller	177
8.9.3	Definition of variables in the PLC programs	179
8.10	Conclusion	180

CHAPTER NINE: CONCLUSION AND FUTURE DIRECTION OF RESEARCH

9.1	Introduction	182
9.1.1	Aims and objectives	182
9.2	Deliverables	183
9.2.1	Literature review, analysis and comparison of the models and approaches for control of DO concentration	183
9.2.2	Review of the theory for design of the nonlinear controller	183
9.2.3	Development of a method for parameter estimation of the nonlinear model of DO with different representations of the oxygen transfer function	184
9.2.4	Development of a method for nonlinear linearizing reference model control of the dissolved oxygen process on the basis of Lyapunov theory	184
9.2.5	Development of a method for design of a nonlinear linearizing control of dissolved oxygen concentration	185
9.2.6	Software development	185
9.3	Application of the results	186
9.4	Future research	186
9.5	Publications	187

REFERENCES

LIST OF FIGURES

Figure 1.1:	Three layers of adaptive control structure.	7
Figure 2.1:	Layout of a wastewater treatment plant	14
Figure 2.2:	Basic ASP structure consisting of an aeration tank and a settler.	16
Figure 2.3:	The biological renewal process (Henze <i>et al</i> , 1995)	18
Figure 2.4:	A schematic diagram of the aeration tank.	23
Figure 2.5:	Schematic representation of substrate consumption process (H. Spanjers <i>et al</i> , 1996).	26
Figure 2.6:	Closed loop control of dissolved oxygen control	37
Figure 2.7:	Estimator of $K_{La}(u(t))$ and $r_{SO}(t)$	38
Figure 2.8:	(a) Standard feedback control, (b) Feedforward control and (c) Feedforward-feedback control	46
Figure 2.9:	Hierarchy of control tasks	49
Figure 3.1:	Common model of the DO process for design of control using the airflow rate as a manipulated variable	52
Figure 3.2:	The benchmark structure	53
Figure 3.3:	Exponential model curve of K_{La}	59
Figure 3.4:	Block diagram of the dissolved oxygen concentration.	59
Figure 3.5:	Representation of dissolved oxygen model in Simulink	63

Figure 3.6: Open loop response of the dissolved oxygen model using $S_{oin}=0.2$ and r_{so} calculated for XBA of 149.797 and XBH of 2559.444	63
Figure 3.7: Open loop response of the dissolved oxygen model using $S_{oin}=0.6$ and r_{so} calculated for XBA of 149.797 and XBH of 2559.444	64
Figure 3.8: Open loop response of the dissolved oxygen model using $S_{oin}=1$ and r_{so} calculated for XBA of 149.797 and XBH of 2559.444	64
Figure 3.9: Open loop response of the dissolved oxygen concentration using $S_{oin}=0.2$ and r_{so} calculated for XBA of 134.8173 and XBH of 2815.3884	64
Figure 3.10: Open loop response of the dissolved oxygen concentration using $S_{oin}=0.6$ and r_{so} calculated for XBA of 134.8173 and XBH of 2815.3884	65
Figure 3.11: Open loop response of the dissolved oxygen concentration using $S_{oin}=1$ and r_{so} calculated for XBA of 134.8173 and XBH of 2815.3884	65
Figure 3.12: Open loop response of the dissolved oxygen concentration using $S_{oin}=0.2$ and r_{so} calculated for XBA of 164.7767 and XBH of 2303.4996	65
Figure 3.13: Open loop response of the dissolved oxygen concentration using $S_{oin}=0.6$ and r_{so} calculated for XBA of 164.7767 and XBH of 2303.4996	66
Figure 3.14: Open loop response of the dissolved oxygen concentration using $S_{oin}=1$ and r_{so} calculated for XBA of 164.7767 and XBH of 2303.4996	66
Figure 3.15: Open loop response of the dissolved oxygen concentration using $S_{oin}=0.4$ and r_{so} calculated for XBA of 119.8376 and XBH of 3071.3328	66
Figure 3.16: Open loop response of the dissolved oxygen concentration using $S_{oin}=0.2$ and r_{so} calculated for XBA of 119.8376 and XBH of 3071.3328	67
Figure 3.17: Open loop response of the dissolved oxygen concentration using $S_{oin}=1$ and r_{so} calculated for XBA 119.8376 of and $+20\%XBH$ of 3071.3328	67
Figure 3.18: Open loop response of the dissolved oxygen concentration using $S_{oin}=1$ and r_{so} calculated for XBA 179.7564 of and XBH of 2047.5552	67
Figure 3.19: Open loop response of the dissolved oxygen concentration using $S_{oin}=0.2$ and r_{so} calculated for XBA of 179.7564 and XBH of 2047.5552	68
Figure 3.20: Open loop response of the dissolved oxygen concentration using $S_{oin}=1$ and r_{so} calculated for XBA of 179.7564 and XBH of 2047.5552	68
Figure 3.21: Open loop response of the dissolved oxygen concentration using $S_{oin}=0.6$ and r_{so} calculated for XBA of 104.8579 and XBH of 3327.2772	68
Figure 3.22: Open loop response of the dissolved oxygen concentration using $S_{oin}=0.2$ and r_{so} calculated for XBA of 104.8579 and XBH of 3327.2772	69
Figure 3.23: Open loop response of the dissolved oxygen concentration using $S_{oin}=1$ and r_{so} calculated for XBA of 104.8579 and XBH of 3327.2772	69
Figure 3.24: Open loop response of the dissolved oxygen concentration using $S_{oin}=0.6$ and r_{so} calculated for XBA of 194.7361 and XBH of 1791.6108	69
Figure 3.25: Open loop response of the dissolved oxygen concentration using $S_{oin}=0.2$ and r_{so} calculated for XBA of 194.7361 and XBH of 1791.6108	70
Figure 3.26: Open loop response of the dissolved oxygen concentration using $S_{oin}=1$ and r_{so} calculated for XBA of 194.7361 and XBH of 1791.6108	70
Figure 3.27: Open loop response of the dissolved oxygen concentration using $S_{oin}=0.8$ and r_{so} calculated for XBA of 89.8782 and XBH of 3583.2216	70
Figure 3.28: Open loop response of the dissolved oxygen concentration using $S_{oin}=0.2$ and r_{so} calculated for XBA of 89.8782 and XBH of 3583.2216	71
Figure 3.29: Open loop response of the dissolved oxygen concentration using $S_{oin}=1$ and r_{so} calculated for XBA of 89.8782 and XBH of 3583.2216	71
Figure 3.30: Open loop response of the dissolved oxygen concentration using $S_{oin}=0.8$ and r_{so} calculated for XBA of 209.7158 and XBH of 1535.6664	71
Figure 3.31: Open loop response of the dissolved oxygen concentration using $S_{oin}=0.2$ and r_{so} calculated for XBA of 209.7158 and XBH of 1535.6664	72
Figure 3.32: Open loop response of the dissolved oxygen concentration using $S_{oin}=1$ and r_{so} calculated for XBA of 209.7158 and XBH of 1535.6664	72
Figure 3.34: Open loop response of the dissolved oxygen concentration using $S_{oin}=1$ and r_{so} calculated for XBA of 74.8985 and XBH of 3839.166	72

Figure 3.35: Open loop response of the dissolved oxygen concentration using $S_{oin}=0.2$ and r_{so} calculated for XBA of 74.8985 and XBH of 3839.166	73
Figure 3.36: Open loop response of the dissolved oxygen concentration using $S_{oin}=0.6$ and r_{so} calculated for XBA of 74.8985 and XBH of 3839.166	73
Figure 3.37: Open loop response of the dissolved oxygen concentration using $S_{oin}=1$ and r_{so} calculated for XBA of 224.6955 and XBH of 1279.722	73
Figure 3.38: Open loop response of the dissolved oxygen concentration using $S_{oin}=0.2$ and r_{so} calculated for XBA of 224.6955 and XBH of 1279.722	74
Figure 3.39: Open loop response of the dissolved oxygen concentration using $S_{oin}=0.6$ and r_{so} calculated for XBA of 224.6955 and XBH of 1279.722.	74
Figure 4.1: Input/output model of DO concentration	80
Figure 5.1: General nonlinear system model.	91
Figure 6.1: Control strategy for the DO concentration process.	109
Figure 6.2: Block diagram of the closed loop system with PI controller	113
Figure 6.3: Structure of the nonlinear linearizing controller.	116
Figure 6.4: Closed loop of the nonlinear linearizing controller Simulink diagram	116
Figure 6.5: The nonlinear linearizing controller Simulink diagram	117
Figure 6.6: Output response of PI controller.	119
Figure 6.7: Output response of the nonlinear linearizing controller	119
Figure 6.8: Closed loop response for the nonlinear controller when $S_{oin}=0.2$, $a=-0.8$, $r_{so}=-764.6982$, and set point of 1.8	120
Figure 6.9: Closed loop response for the nonlinear controller when $S_{oin}=0.2$, $a=-0.8$, $r_{so}=-746.7435$ and set point of 1.8	120
Figure 6.10: Closed loop response for the nonlinear controller when $S_{oin}=0.2$, $a=-0.8$, $r_{so}=-782.6757$, and set point of 1.8	120
Figure 6.11: Closed loop response for the nonlinear controller when $S_{oin}=0.2$, $a=-0.8$, $r_{so}=-719.7945$, and set point of 1.8	121
Figure 6.12: Closed loop response for the nonlinear controller when $S_{oin}=0.2$, $a=-0.8$, $r_{so}=-809.6251$, and set point of 1.8	121
Figure 6.13: Closed loop response for the nonlinear controller when $S_{oin}=0.2$, $a=-0.8$, $r_{so}=-692.8452$, and set point of 1.8	121
Figure 6.14: Closed loop response for the nonlinear controller when $S_{oin}=0.2$, $a=-0.8$, $r_{so}=-836.5741$, and set point of 1.8	122
Figure 6.15: Closed loop response for the nonlinear controller when $S_{oin}=0.2$, $a=-0.8$, $r_{so}=-764.6982$, and set point of 2	122
Figure 6.16: Closed loop response for the nonlinear controller when $S_{oin}=0.2$, $a=-0.8$, $r_{so}=-746.7435$ and set point of 2	122
Figure 6.17: Closed loop response for the nonlinear controller when $S_{oin}=0.2$, $a=-0.8$, $r_{so}=-782.6757$, and set point of 2	123
Figure 6.18: Closed loop response for the nonlinear controller when $S_{oin}=0.2$, $a=-0.8$, $r_{so}=-719.7945$, and set point of 2	123
Figure 6.19: Closed loop response for the nonlinear controller when $S_{oin}=0.2$, $a=-0.8$, $r_{so}=-809.6251$, and set point of 2	123
Figure 6.20: Closed loop response for the nonlinear controller when $S_{oin}=0.2$, $a=-0.8$, $r_{so}=-692.8452$, and set point of 2	124
Figure 6.21: Closed loop response for the nonlinear controller when $S_{oin}=0.2$, $a=-0.8$, $r_{so}=-836.5741$, and set point of 2	124
Figure 6.22: Closed loop response for the nonlinear controller when $S_{oin}=0.2$, $a=-0.8$, $r_{so}=-764.6982$, and set point of 3	124
Figure 6.23: Closed loop response for the nonlinear controller when $S_{oin}=0.2$, $a=-0.8$, $r_{so}=-746.7435$ and set point of 3	125
Figure 6.24: Closed loop response for the nonlinear controller when $S_{oin}=0.2$, $a=-0.8$, $r_{so}=-782.6757$, and set point of 3	125
Figure 6.25: Closed loop response for the nonlinear controller when $S_{oin}=0.2$, $a=-0.8$, $r_{so}=-719.7945$, and set point of 3	125
Figure 6.26: Closed loop response for the nonlinear controller when	126

Soin=0.2, a=-0.8 rso=-809.6251, and set point of 3	
Figure 6.27: Closed loop response for the nonlinear controller when Soin=0.2, a=-0.8, rso=-692.8452, and set point of 3	126
Figure 6.28: Closed loop response for the nonlinear controller when Soin=0.2, a=-0.8, rso=-836.5741, and set point of 3	126
Figure 7.1: The closed loop system configuration diagram	137
Figure 7.2: Closed loop system of the nonlinear controller.	144
Figure 7.3: Closed loop Lyapunov direct based model Simulink block diagram	146
Figure 7.4: Reference model Simulink block diagram	147
Figure 7.5: Nonlinear Linearizing controller Simulink block diagram	147
Figure 7.6: Respiration Simulink block diagram	147
Figure 7.7: PI controller signal	149
Figure 7.8: Nonlinear controller output	149
Figure 7.9: Closed loop response for the nonlinear controller when Soin=0.2, a=-0.8, rso=-764.6982, and set point of 1.8	150
Figure 7.10: Closed loop response for the nonlinear controller when Soin=0.2, a=-0.8, rso=-746.7435 and set point of 1.8	150
Figure 7.11: Closed loop response for the nonlinear controller when Soin=0.2, a=-0.8, rso=-782.6757, and set point of 1.8	150
Figure 7.12: Closed loop response for the nonlinear controller when Soin=0.2, a=-0.8, rso= -719.7945, and set point of 1.8	151
Figure 7.13: Closed loop response for the nonlinear controller when Soin=0.4, a=-0.8 rso=-809.6251, and set point of 1.8	151
Figure 7.14: Closed loop response for the nonlinear controller when Soin=0.2, a=-0.8, rso=-692.8452, and set point of 1.8	151
Figure 7.15: Closed loop response for the nonlinear controller when Soin=0.2, a=-0.8, rso=-836.5741, and set point of 1.8	152
Figure 7.16: Closed loop response for the nonlinear controller when Soin=0.2, a=-0.8, rso=-764.6982, and set point of 2	152
Figure 7.17: Closed loop response for the nonlinear controller when Soin=0.2, a=-0.8, rso=-746.7435 and set point of 2	152
Figure 7.18: Closed loop response for the nonlinear controller when Soin=0.2, a=-0.8, rso=-782.6757, and set point of 2	153
Figure 7.19: Closed loop response for the nonlinear controller when Soin=0.2, a=-0.8, rso=-719.7945, and set point of 2	153
Figure 7.20: Closed loop response for the nonlinear controller when Soin=0.4, a=-0.8 rso=-809.6251, and set point of 2	153
Figure 7.21: Closed loop response for the nonlinear controller when Soin=0.2, a=-0.8, rso=-692.8452, and set point of 2	154
Figure 7.22: Closed loop response for the nonlinear controller when Soin=0.2, a=-0.8, rso=-836.5741, and set point of 2	154
Figure 7.23: Closed loop response for the nonlinear controller when Soin=0.2, a=-0.8, rso=-764.6982, and set point of 3	154
Figure 7.24: Closed loop response for the nonlinear controller when Soin=0.2, a=-0.8, rso=-746.7435 and set point of 3	155
Figure 7.25: Closed loop response for the nonlinear controller when Soin=0.2, a=-0.8, rso=-782.6757, and set point of 3	155
Figure 7.26: Closed loop response for the nonlinear controller when Soin=0.2, a=-0.8, rso= -719.7945, and set point of 3	155
Figure 7.27: Closed loop response for the nonlinear controller when Soin=0.4, a=-0.8 rso=-809.6251, and set point of 3	156
Figure 7.28: Closed loop response for the nonlinear controller when Soin=0.2, a=-0.8, rso=-692.8452, and set point of 3	156
Figure 7.29: Closed loop response for the nonlinear controller when Soin=0.2, a=-0.8, rso=-836.5741, and set point of 3	156
Figure 8.1: Block diagram of the standard components of PLC (NIIT,2005)	162

Figure 8.2: Program's scan process Diagram.	163
Figure 8.3: Normally Open Contact.	165
Figure 8.4: Normally Closed Contact.	165
Figure 8.5: Structure of a coil.	166
Figure 8.6: Simple ladder logic diagram	166
Figure 8.7: A diagram for a configuration example for the Modicon M340 PLC with one rack	167
Figure 8.8: The closed loop system of wastewater treatment plant.	169
Figure 8.9: The PLC has to communicate with database and Adroit.	170
Figure 8.10: The interfacing structure of the controller and plant.	171
Figure 8.11: PLC bus	173
Figure 8.12: I/O Mapping diagram for the input sensors and output actuators	174
Figure 8.13: PI Controller diagram	174
Figure 8.14: Linearizing controller structure for PLC implementation	175
Figure 8.15A: Linearizing controller diagram	176
Figure 8.15B: Linearizing controller diagram-continuation	176
Figure 8.16: Error calculation structure	177
Figure 8.17: Nonlinear Lyapunov reference based controller structure for PLC implementation	177
Figure 8.18: Reference model diagram	178
Figure 8.19A: Nonlinear controller	178
Figure 8.19B: Nonlinear controller-continuation	178
Figure 8.20: Calculations of errors in the nonlinear controller structure	179
Figure E1.1: BMX XPB 0600 rack diagram	212
Figure E1.2: The BMX CPS 2000 power supply module and components numbers	213
Figure E1.3: BMX P34 2020 diagram showing an RJ45 Ethernet port.	214
Figure E1.5: MAC diagram for selection an IP address	215
Figure E1.6: Ethernet port on a BMX P34 2020 processor	215
Figure E1.7: Ethernet network diagram	216
Figure E1.8: The components of a BMX P34 2020 processor diagram	216
Figure E1.9: The diagnostic diagram of LEDs on the BMX P34 2020 processor	218
Figure E1.10: A discrete input/output module with 40-pin connectors:	220
Figure E1.11: 24 VDC discrete module connected via a 20-pin terminal block	220
Figure E1.12: Wiring diagram for a 20 pin out for a digital output module	221
Figure E1.13: 20 pin out digital module diagram	222
Figure E1.14: Wiring diagram for a 20 pin out for a digital output module	223
Figure E1.15: 40 pin Analog module diagram	225
Figure E1.16: 20 pin Analog module diagram	226
Figure E1.17: wiring diagram of the Analog module for a 20 pin out connection	227
Figure E2.1: M-File for Export of data	228
Figure E2.2: M-File for Import of data	228
Figure E2.3: MySQL DB Manager	229
Figure E2.4: MySQL DB Manager Import data from Matlab and Adroit.	229
Figure E2.5: MySQL DB Manager import DO Value from PLC and Adroit.	230
Figure E2.6: Dialog box diagram	230
Figure E2.7: DbAcces dialog box	231
Figure E2.8: DbAcces agent diagram	231
Figure E3.1: Adroit Program	232
Figure E4.1: DO Transmitter	234
Figure E4.2: Solenoid Valve.	235

Figure E4.3: Proportional Pressure Regulators	235
Figure E5.1: DO Sensor Wiring	236
Figure E5.2: DO Transmitter inside view	236
Figure E5.3: Conductivity Sensor Wiring	237
Figure E5.4: Conductivity Transmitter Inside view	237
Figure E5.5: pH Sensor Wiring	238
Figure E5.6: pH Transmitter Inside view	238

LIST OF TABLES

Table 2.1: Summary of the measuring principles for respiration rate	32
Table 3.1: Process flows and oxygen transfer functions	53
Table 3.2: Kinetic parameter values for ASM1	54
Table 3.3: State Variables for the IAWQ Activated Sludge Model #1 (ASM1)	54
Table 3.4: Different models for oxygen transfer function	58
Table 3.5: Values of the model parameters	62
Table 3.6: Parameters table for open loop control	62
Table 3.7: Simulation results comparison table	76
Table 6.1: Values of the model parameters	118
Table 6.2: Values of the model parameter for controller calculation	118
Table 6.3: Parameters table for nonlinear control design	118
Table 6.4 Simulation results comparison	127
Table 7.1: Parameters table for nonlinear control design	145
Table 7.2: Values of the model parameters	149
Table 7.3: Values of the model parameter for controller calculation	149
Table 7.4: Simulation results comparison	157
Table 8.1: Number Table	167
Table 8.2: Elementary variables for the design of both Nonlinear Linearizing and Nonlinear reference model, Lyapunov based controllers	179
Table 9.1: Programs used for parameter estimation of different models of the oxygen transfer function	185
Table 9.2: Programs used for nonlinear linearizing controllers design and nonlinear controller design and simulation of the closed loop system	185
Table 9.3: Programs for nonlinear controller implementation in the embedded environment of PLC	186
Table E1.1: The following table describes the components of a power supply module.	213
Table E1.2: The following illustration shows the pin assignment of the Ethernet port for the BMX P34 2020/2030 processor:	215
Table E1.3: The following table shows the components of a BMX P34 2020 processor	216
Table E1.4: The characteristics of the BMX P34 2020 processor	218
Table E1.5: Different characteristics of discrete input/output module	219
Table E1.6: General Characteristics for the BMX DDI 1602 module	221
Table E1.7: General characteristics of the BMX DDO 1602 module	223
Table E1.8: The general input characteristics of BMX AMM 0600 module	224
Table E1.9: Different characteristics of analog input/output module	225
Table E1.10: Connection points for Analog module	226
Table E4.1: MPPE valve data	235

APPENDICES

Appendix A:

Appendix B:

Appendix C:

Appendix D:

GLOSSARY

Terms/Acronyms/Abbreviations	Definition/Explanation
A.C	Alternating Current
AE	Aerobic
AN	Anoxic
ASM1	Activated Sludge Model 1
ASP	Activated Sludge Process
ATP	Adenosine triphosphate
BNR	Biological Nutrient Removal
BOD	Biochemical Oxygen Demand
CPU	Central Processing Unit
D/A	Digital to Analog Converter
FB	Feedback
FF	Feedforward
D	Disturbance
DC	Direct Current
DO	Dissolved Oxygen
IAWQ	International Association on Water Quality
IEC	International Electrotechnical Commission
I/O	Input/Output
LS	Least Squares
MATLAB	Matrix Laboratory
MV	Manipulated Variable
O	Output
OUR	Oxygen Uptake Rate
PC	Personal Computer
PI	Proportional Integral
PID	Proportional Integral Derivative
PLC	Programmable Logic Controller
RBOS	Readily Biodegradable Organic Substrate
RISC	Reduced Instruction Set Computer
SCADA	Supervisory Control and Data Acquisition
SIMULINK	Simulation and Link
SISO	Single-input Single-output
SQL	Structured Query Language
STR	Scientific and Technical Report
UCT	University of Cape Town
WWT	Wastewater Treatment
WWTP	Wastewater Treatment Plants

MATHEMATICAL NOTATION

Symbols/Letters	Definition/Explanation
Q_r	Return flow rate of aerobic tank
Q_w	Wastage flow rate of aerobic tank
Q_{air}	Airflow rate of aerobic tank
N	Nitrogen
H_2O	Water
NH_3	Ammonia
NH_4^+	Ammonium
NO_3^-	Nitrate
NO_2^-	Nitrite
s_O	DO concentration in the aeration tank
O_2	Gaseous Oxygen
K_{La}	Oxygen transfer function
$s_{O,sat}$	Saturated value of the DO concentration in wastewater
$u(t)$	Control input
r_{SO}	Respiration rate or Oxygen Uptake Rate
$s_{O,in}$	DO concentration of the input flow
V	Volume of the wastewater
Q	Influent wastewater flow rate
s_{OL}	DO concentration in the liquid phase
s_{OL}^*	Saturation concentration of DO
$s_{OL,in}$	DO concentration in the liquid phase entering the system
K_{LaL}	Oxygen transfer coefficient based on liquid volume
Q_{in}	Flow rate of the liquid entering the system
Q_{out}	Flow rate of the liquid leaving the system
V_L	Volume of the liquid phase
s_{OG}	Dissolved oxygen in the gas phase
V_G	Volume of the gas phase
$s_{OG,in}$	DO concentration in the gas phase entering the system
K_{LaG}	Oxygen transfer coefficient based on gas volume
F_{in}	Flow rate of gas entering the system
F_{out}	Flow rate of gas leaving the system
Q_{in}	Input flow rate for the aeration tank
$r_{SO,end}$	Endogenous Oxygen uptake rate
$r_{SO,ex}$	Exogenous Oxygen uptake rate
s_O^{sp}	DO concentration set-point in the aeration tank
$e_r(t)$	Zero mean white noise
f	Filter pole

q	Backward shift operator
$\varepsilon(t)$	Predictor error
K_S	Half-saturation (hetero.growth)
μ_{mH}	Maximum heterotrophic growth rate
K_{OH}	Half-saturation (hetero.oxygen)
K_{NO}	Half-saturation (nitrate)
b_H	Heterotrophic decay
η_g	Anoxic growth rate correction factor
η_h	Anoxic hydrolysis rate correction factor
K_h	Maximum specific hydrolysis rate
K_x	Half-saturation (hydrolysis)
μ_{mA}	Maximum autotrophic growth rate
K_{NH}	Half-saturation (auto. growth)
b_A	Autotrophic decay
K_{OA}	Half-saturation (auto.oxygen)
k_a	Ammonification rate
x	Soluble inert organic matter
s_S	Readily biodegradable substrate
x_I	Particulate inert organic matter
x_S	Slowly biodegradable substrate
$x_{B,H}$	Active heterotrophic biomass
$x_{B,A}$	Active autotrophic biomass
x_P	Particulate product arising from biomass decay
s_{NO}	Nitrate and nitrite nitrogen
s_{NH}	$\text{NH}_4^+ + \text{NH}_3$ nitrogen
s_{ND}	Soluble biodegradable organic nitrogen
x_{ND}	Particulate biodegradable organic nitrogen
s_{ALK}	Alkalinity
Y_H	Heterotrophic yield
Y_A	Autotrophic yield
$x(t)$	State vector
u	Control vector
$f(x)$	Nonlinear function
$g(x)$	Nonlinear function
w	Disturbance vector
$u(k)$	Airflow rate
$x \in R^n$	State vector
$u \in R^m$	Control vector
$y \in R^l$	Output vector
$A \in R^{n \times n}$	Input state matrix
$B \in R^{n \times m}$	Control output state matrix
$C \in R^{l \times n}$	Output control matrix
$D \in R^{l \times m}$	Output control matrix

x_0

$f \in R^n$

$h \in R^l$

Initial state space vector

Vector of the nonlinear function of the state

Vector of the nonlinear output function of the state

CHAPTER ONE

STATEMENT OF THE PROBLEM: PROJECT OBJECTIVES HYPOTHESIS AND ASSUMPTIONS

1.1 Awareness of the problem

Water is said to be tasteless, odourless and colourless. It can be described as a giver of life as the early stages of human development is spent in water and 60% of human body consists of water. Clean water is a valuable resource lacking in many parts of the world, especially in Africa where people have died from diseases related to water contamination (e.g. cholera). Every living thing on earth (micro-organisms, plants, animals, humans and even our brain) consists mostly of water. More than 70% of the earth's surface is covered by water, only a small part of which is suitable for either human consumption or agricultural use (approximately 0.5% of all water in the world), (Lindberg, 1997) Due to pollution from agriculture, households and industry reaching rivers, lakes and seas it is important for wastewater (Sewage) to be properly treated in order to remove harmful substances before it reaches the environment. More material regarding wastewater treatment in general can be found in (Ingildsen and Olson, 2001).

Strict environmental and health regulations together with a demand for cost effective ways of wastewater treatment have made control technology in Wastewater Treatment Plants an important priority. The control system is used to supervise the inherently dynamic WWT processes from the input wastewater through biological process (Activated Sludge Process) to effluent dispersal. This is expected to reduce the need for larger volumes, improve the effluent water quality, decrease the use of chemicals, and save energy and operational costs. Sensors for dissolved oxygen and nutrients such as ammonium, nitrate and phosphorus have been developed and improved in recent years, thus increasing the potential for effective monitoring, automation and control of wastewater treatment plants. This assists in reaching the objective of the wastewater treatment process operation, which is to provide reliable and stable process control with highly efficient results at minimum cost.

Wastewater can be attributed to as both liquid and solid wastes. It may be defined as a combination of domestic wastewater, industrial wastewater, together with groundwater, surface water and storm water. The accurate composition of wastewater differs from region to region, from season to season, from day to day, from hour to hour and from minute to minute. It depends on a number of different reasons such as time of the day, weather etc (Metcalf and Eddy, 1979). The main aim of wastewater treatment is to

reduce as much as possible the undesired ingredients such as organic matter, nitrogen and phosphorus, although phosphorus is not considered in this thesis. Wastewater treatment process is a process based on biological process of activated sludge. The function of wastewater treatment plant is mainly to speed up the natural process whereby water purifies itself. The main objective regarding WWTP is to produce an effluent that meets the required standards at the least possible cost. The historical development of the wastewater treatment logically leads to the necessity of proper control of this complex, nonlinear process. Wastewater treatment plant is becoming more and more pivotal in the community of today because of urbanisation. In the past waste disposal was not too much of a problem as the number of people was small. The expansion of rural populations and immigration of people to urban areas with disposal and accumulation of human waste products rapidly became a hygienic problem. The connection between hygiene problems, health issues and wastewater led to new way of dealing with human waste products. Water closet and the development of sewer systems transporting the water from households into nearby rivers and lakes were introduced. In 1930, sedimentation tanks were introduced to solve visual problems related to waste disposal.

With time, new negative impacts were discovered. Problems concerning oxygen depletion in the water pumped to rivers and lakes emerged. The oxygen depletion occurred since pollutants (mainly organic matter) were oxidized in the rivers and lakes. To improve the situation, biological treatment evolved. This treatment consisted of adding oxygen to the wastewater in reactors, thus allowing organic matter to oxidize before the water was pumped to the rivers and lakes. The process is working in two directions meaning:

1. Reduction of organic bound energy to such a level that, the heterotrophic growth and their associated deoxygenating effects in the receiving body of water are acceptably low.
2. Reducing autotrophic substances, phosphates, ammonia and nitrates, to levels such that photosynthetic autotrophic growth and capacity to fix solar energy as organic energy in the receiving body of water are acceptably low.

Wastewater treatment process monitoring, optimization and control are very important these days, especially in South Africa when considering the number of contributing factors in the form of:

1.1.1 The process variations

There is a great need for consideration of the dynamic behaviour and operational characteristics of wastewater treatment process as they prove to be frequently larger than that of industrial process given their large temporal variations which occur in wastewater composition, concentration and flow rate. But, in reality most wastewater treatment plants are in a primitive state with respect to process operation as opposed to industrial process. The reason being gross failures due to bulking of activated sludge and "sour" anaerobic digesters are all too frequent. Additionally, there are significant variations in treatment plant efficiency, not only from plant to plant, but also from day to day and hour to hour in the same plant.

1.1.2 Main operational problems

The main problems that influence the process performance have been identified as follows:

1.1.2.1 Operator's application of concepts and testing to process control

The necessary knowledge pertaining to the process is not applied accordingly for control purposes.

1.1.2.2 Infiltration inflow

The most notable process caused by it "washout" of the suspended growth system during the high flow periods. The second problem is the dilution of raw wastewater, with the results that, the biological process loadings were less than that of design intent and healthy biomass could be sustained as result.

1.1.2.3 Process control testing

Some of the basic test for proper operation of the plant pertaining to the mixed liquor suspended solids, dissolved oxygen, sludge settleability, return sludge solids concentration are not performed or used for process control.

1.1.2.4 Operational and management manual adequacy

There is a shortage of operating procedures for key process variable in the operational manuals.

1.1.2.5 The industrial loading

Characteristics of wastewater and micro-organisms poisoning can be changed through it.

1.1.2.6 Process controllability

Included is the inability to vary return sludge rate and air input given how the device is constructed. This means that an adequate attention had not been paid during the design phase of the process control.

1.1.3 Sludge wasting and return

Proper process control requires the control of sludge age and substrate removal rate. These parameters are controlled through the regulation of the inventory of active solids under aeration via the mechanism of sludge wasting. The plant should have design capabilities for sludge wasting and return, particularly from the aeration basin.

Conclusion can be drawn from the above that difficulties mentioned are due to a number of factors, ranging from lack of proper application process control techniques to plant understanding; hence the improved performance of wastewater can be attributable to many different ways. Included amongst others can be the increasing of quality and quantity of operational personal, paying more attention to the dynamic behaviour and operational characteristics of the plant during design phase and the improved control strategies for plant operation. Presently, there are many well-designed wastewater treatment plants capable of high degree of pollutants removal. However, it is of great importance to note that, well-constructed facilities are not only important, but also form one part of the solution to the problem that is at hand. Good operation, routine maintenance and good administrative programs are needed too. However, there are some drawbacks in terms of control as most wastewater treatment processes are in primitive state with respect to process operation when compared to industrial processes. In addition, there are significant variations in treatment plant efficiency, not only from one plant to another, but also from day to day and hour to hour monitoring and control in the same plant.

Drawbacks such as

- Lack of suitable engineering understanding of many of the control process characteristics
- Lack of fully reliable on-line sensors and other equipment for process monitoring and control.
- Lack of understanding of how to use and maintain the equipment properly.
- Use of daily average type data not on-line data to control the process.

The above drawbacks lead to poor monitoring and control of the wastewater treatment process

Controls strategies exist in today's plants but are primarily involved with the handling and use of information. The control process can either be done manually or automatically. Automatic control systems are of different forms and they can range from on/off control to on-line optimal computer control of the plant as a whole. Not considering which type of control, some of the fundamental questions need to be answered. These questions are as follows:

1. What type of information should be collected for the process monitoring and control?
2. How should this information be transmitted in a real system?
3. How should the information be processed?
4. What control actions should be taken?

The theses answer the above questions through application of the new modern control approaches and methods in the process of development of a control system. The main research problem of the project is to investigate application of the nonlinear control theory for design of real time control for dissolved oxygen concentration in the aeration tank of the activated sludge process as a part of an adaptive optimal control strategy of the activated sludge process in the wastewater treatment.

The control strategy, used sensors, developed models and control algorithms will be based on the complex dependencies between the process variables and on the complex self-regulatory mechanisms within the cell. Activated sludge process is a dynamic process, which involves both rapidly and slowly changing parameters. In order to control product quantity and quality, or the dynamic state of the process, the control strategy has to be capable to control both types of variables in real time, with real on-line data.

1.2 Statement of the Problem

Dissolved oxygen (DO) is the concentration of oxygen in the water of the rivers, lakes, dams etc. If there is no oxygen or it is insufficient then aquatic animals will die or their growth or production will be affected. The dissolved oxygen should be as high as possible.

Problem: To investigate application of the nonlinear control theory for design of real time control of dissolved oxygen concentration in the aeration tank of the activated sludge

process using the on-line measurement of DO concentration in the process aeration tank.

The problem is solved as a part of 3 layers structure for adaptive optimal control of the activated sludge process based on the real plant dynamics, their structural and biological models, and control theory, pilot plant in the lab with different possibilities for using various plant structures, and SCADA and computational software environment, as follows:

1. Benchmark and Athlone plant structures.
2. UCT and ASM1 biological models.
3. Optimal control theory.
4. Nonlinear control theory.
5. Pilot plant of the wastewater treatment.
6. Adroit, MATLAB, MySQL, and concepts software.

The three layers adaptive control structure, Figure 1.1 has layers of adaptation, optimization, and direct control. The structure is implemented using a personal computer (PC) with Adroit SCADA, MATLAB, and MySQL database software and PLC with Unity software. The top two layers are implemented in PC and the third layer is implemented in PLC. The model estimation is done on the level of optimization. The problem for design of dissolved oxygen control is solved on the layer of optimization. The controller implementation is done on the layer for direct control as a part of PLC software.

1.3 Design based problems

1.3.1 Sub-problem1: Activated Sludge Process study

To investigate and understand every concept about the activated sludge process biological reactions as described by UCT and ASM1 biological models.

1.3.2 Sub-problem2: Mathematical Modelling

To develop mathematical models of the dissolved oxygen concentration with different models of the oxygen transfer function and different representations of the oxygen uptake rate.

1.3.3 Sub-problem3: Control design and Implementation

To design and implement nonlinear controllers based on the nonlinear control theory and applying the method of reference model control using Lyapunov second method and nonlinear linearizing controllers.

1.3.4 Sub-problem4

Development of MATLAB/SIMULINK programmes for simulation of the developed models, and of the closed loop systems.

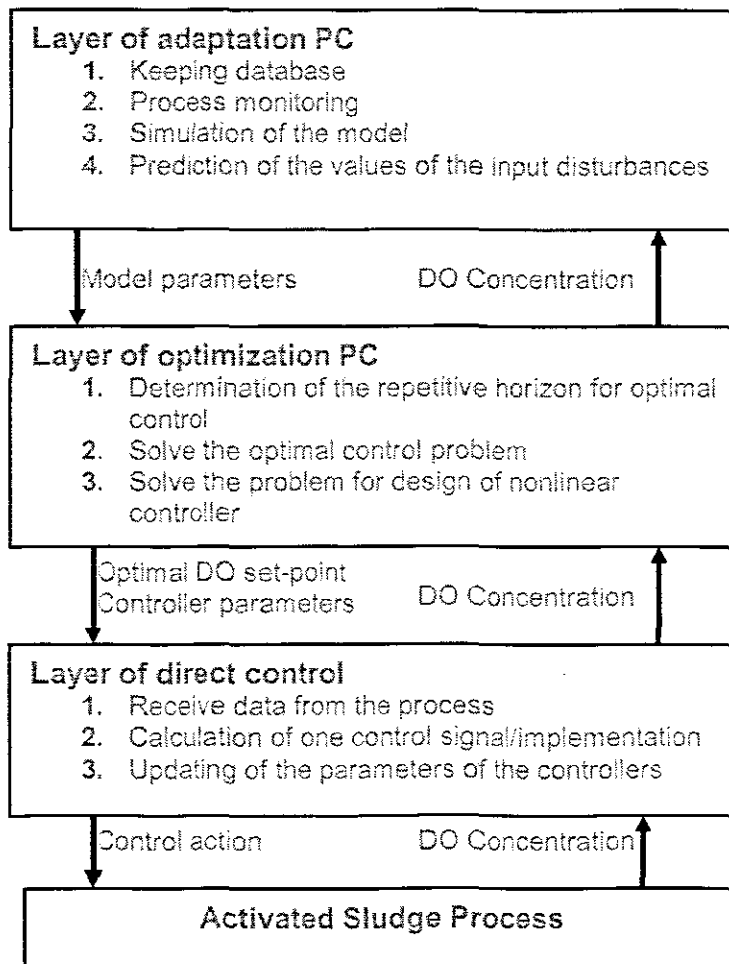


Figure1.1: Three layers of adaptive control structure.

1.4 Real time implementation sub-problems

1.4.1 Sub-problem5

Developing a communication link between PLC (Programmable Logic Controller) and DO (Dissolved Oxygen) sensor and between PLC and the supervising computer.

1.4.2 Sub-problem6

Developing a PLC programme for uploading of the nonlinear controller in PLC for real-time control.

1.4.3 Sub-problem7

Developing programs for communication between MySQL database and MATLAB/SIMULINK software for control design purposes.

1.4.4 Sub-problem8

Interfacing PLC with SCADA software

1.5 Research Aim and Objectives

1.5.1 Aim

The aim of the research project is to develop models of DO concentration process and methods for design of linear and nonlinear controllers of the concentration of the DO in the aeration tank of the ASP and to implement the designed controllers in the frameworks of Modicon PLC. Adroit SCADA, MySQL database and MATLAB/SIMULINK software as a part of Optimal Adaptive strategy for control of the activated sludge process are used as an environment for the research investigations.

1.5.2 Objectives

The objectives are:

1. To develop models of the DO concentration with different representations of the oxygen transfer function.
2. To develop method for design of parameter estimation of the DO model coefficients and oxygen uptake rate for different mathematical representations of the oxygen transfer function
3. To develop method for design of a linear controller of the DO concentration based on pole placement theory.
4. To develop method for design of a nonlinear controller of the DO concentration based on Lyapunov stability theory and reference model control theory.
5. To develop method for design of a nonlinear linearizing controller of the DO concentration based on the nonlinear geometrical control theory.
6. To implement the controllers in the frameworks of the PLC as a part of the Adroit SCADA system.
7. To develop software for communication between SCADA, MySQL, Matlab and PLC in real time

1.6 Hypothesis

The thesis proves that the nonlinear controller of DO concentration gives better performance of the closed loop system than that of the linear controller. The hypothesis is connected with the possibilities of developing software for programming PLC in order to implement the nonlinear controller. The parameters of the nonlinear controller could be changed in real time from the SCADA system and the set point of the nonlinear controller could also be changed in real time from the SCADA system.

1.7 Delimitation of the research

The research is mainly based on designing and implementing nonlinear controller because the linear controller will not give good performance of the nonlinear activated sludge process. The monitoring of the process is realised by acquiring real-time data by sensors for dissolved oxygen concentration. The real data is collected by using data acquisition system built for the pilot plant in the research laboratory on the basis of PC and Modicon M340 PLC with help of Adroit software. The problem for design of nonlinear control is solved using the Benchmark and Athlone wastewater treatment plant models data. Linear and nonlinear control theories are used for design of the controllers in state space domain. The classic control theory based on Laplace domain is used for design of linear controller.

1.8 Motivation for the project development

The control and monitoring of the wastewater treatment process dynamic behaviour and operational characteristics are frequently more important than that of industrial processes because of the large temporal variations which occur in wastewater composition, concentration and flow. The project development is in accordance with the mention at the beginning of the chapter important characteristics and drawbacks of the process and its control and aims to develop a hardware and software system, implementing a strategy of real time optimization and control, based on: the characteristics of the process as an object of control, the existing at the moment instrumentation and control devices and structures in the considered processes, the possibilities to apply new instrumentation techniques for measurement, monitoring, modelling and control.

1.9 Assumptions

The assumptions in this research project are based on different parts of the research work that have to be done and are classified as follows:

- The process conforms to the current control technology.

- The mass balance equations describe the real time process at Athlone plant and the benchmark process with accuracy good enough for the control design.
- The oxygen uptake rate in the aeration tank can be estimated on line on the basis of measurements of the DO concentration.
- The structure of the nonlinear model of DO allows application of the nonlinear geometric control theory for design of a nonlinear linearizing controller.
- Optimal control implementation done with the help of nonlinear controller parameters calculation, Adroit software, PC and PLC programming environment will allow quick problem solving according to the dynamics of the process in real time

1.10 Research Methods

1.10.1 Literature review method

Literature review study of different models of nonlinear control systems.

1.10.2 Design method

- Method of Lyapunov theory for stability is used for design of a nonlinear controller on the basis of linear reference model.
- Method of geometrical control theory is used for design of a nonlinear linearizing controller on the basis of the linear reference model.

1.10.3 Experimental method

- Development of strategies for using PLC and Adroit software environment.
- PLC and PC will be used for controlling of the pilot plant.

1.10.4 Description method

- The system is described with all its specifications, characteristics and functions and also the obtained results are described in the thesis.

1.11 Outline of the thesis

This thesis is made up of nine chapters:

Chapter 2 gives an overview of the methods for modelling, estimation and control of the process for dissolving of oxygen in wastewater. Discussion of the use of automatic control and state estimation of dissolved oxygen concentration in wastewater treatment plants is done. In particular, the activated sludge process modelling and control is

considered. A design method, which gives a high performance controller for all operating conditions, is discussed on the basis of different papers. The design method consists of two parts: estimation part where the oxygen transfer function and oxygen uptake rate (respiration) are determined and a controller design part.

Chapter 3 introduces the structure of the activated sludge process (ASP) and the description of the COST Benchmark process based on the ASM1 biological model. The mass-balance model of the dissolved oxygen concentration for the Benchmark layout is also given together with development of the mathematical model of the oxygen transfer function as an exponential model. Development of dissolved oxygen model equation in standard affine form is introduced and is applied to the controller design.

Chapter 4 Discusses least-squares method for parameter estimation for different models of oxygen transfer function. The equations for calculations of the transfer function coefficients and oxygen uptake rate are derived. Matlab software for estimation of the parameters of different representations of oxygen transfer function is developed. The results from the calculations are given.

Chapter 5 provides nonlinear control theory used for the analysis and designing of nonlinear control systems. The nonlinear methods for analysis and control design of nonlinear systems are given. Different types of nonlinear controller design methods for analysis of the nonlinear systems for the purpose developing controllers are analysed.

Chapter 6 presents nonlinear controller design which is based on the feedback linearization method. The nonlinear controller is designed in such way that the closed loop system consisting of the nonlinear controller and the nonlinear process is equivalent to a desired linear system. Then linear PI controller is designed for the linearized closed system. Results from the simulation for the different values of the inflow DO concentration and oxygen uptake rate are presented.

Chapter 7 gives the common nonlinear controller design based on the Lyapunov's direct method and reference control method applied to the model of dissolved oxygen concentration. Simulink block diagrams are provided for the sole purpose of simulations and their simulation results given for different cases of the inflow DO concentration and oxygen uptake rate.

Chapter 8 describes the real-time implementations platform structure of the nonlinear controllers based on PLC software. The connections between different parts of control strategy are described and programmed on the basis of DO control problem.

Chapter 9 gives a detailed conclusions and future research in the field of wastewater treatment processes.

CHAPTER TWO

OVERVIEW OF THE METHODS FOR MODELLING AND CONTROL OF WASTEWATER TREATMENT PROCESS

2.1 Introduction

The aim of this chapter is to give an overview of the methods for modelling, estimation and control of the process for dissolving of oxygen in wastewater. Discussion of the use of automatic control and state estimation of dissolved oxygen concentration in wastewater treatment plants is done. In particular, the activated sludge process modelling and control is considered. A design method, which gives a high performance controller for all operating conditions, is discussed on the basis of different papers. The design method consists of two parts: estimation part where the oxygen transfer function and oxygen uptake rate (respiration) are determined and a controller design part.

2.2 Wastewater treatment process description

In modern societies proper management of wastewater is a necessity not an option. Wastewater often is classified as industrial wastewater or municipal wastewater, with industrial wastewater deemed compatible with municipal wastewater, usually discharged to municipal sewers. Basically, wastewater treatment processes consists of mechanical treatment, biological treatment, chemical treatment and sludge treatment. The wastewater commonly for it to be released to the recipient, t steps are taken into consideration, hence shown is the typical schematic diagram of the wastewater treatment plant process in Figure 2.1. The Activated Sludge Process (ASP) is one of the most used types of the biological treatment processes.

2.2.1 Mechanical (primary) treatment

The mechanical treatment is used for removal of large objects and heavy materials from the incoming wastewater. To a considerable degree this process is supposed to safe guard the subsequent processes against various types of grits and larger particles. The process actually consists of networks that get rid of large substances in the wastewater: an aerated sand filter which is responsible for the removal of sand and a primary sedimentation unit accountable for reducing the content of suspended solids in the wastewater through sedimentation. By using primary treatment large amount of organic matters in particulate form may be removed and by doing so, reducing the need for aeration later in the process.

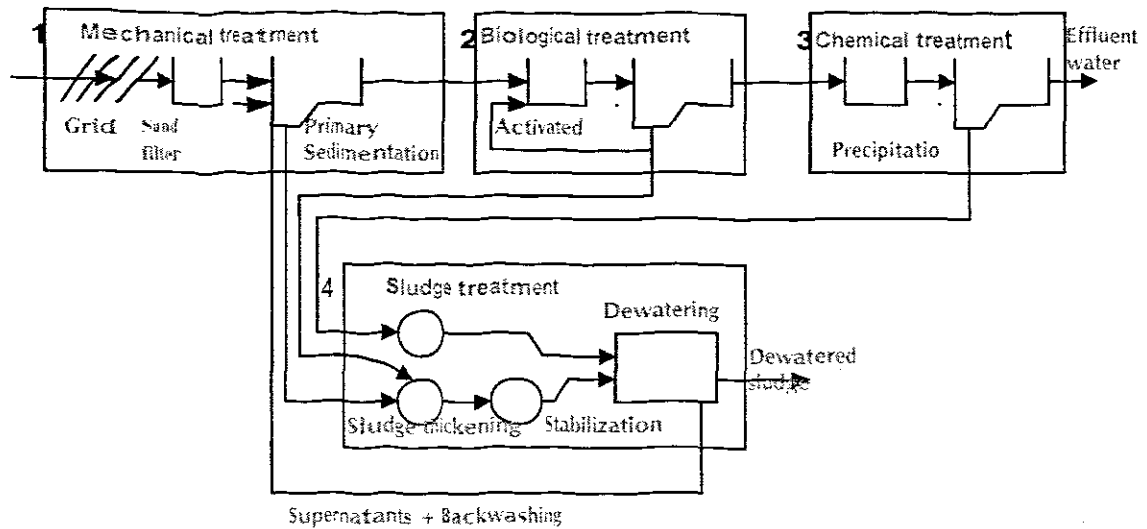


Figure 2.1: Layout of a wastewater treatment plant

2.2.2 Biological treatment

In this part of the wastewater treatment plant, micro-organisms degrade organic matter and in some configurations nutrients are also removed. Different types of WWT processes exist but larger wastewater treatment plants make use of the activated sludge process. In its basic configuration the activated sludge process consists of an aerated tank and a settler. Microorganisms grow slowly in the aerated tank and in order to maintain their population sizes, sludge from the settler is re-circulated back to the aerated tank. Excess sludge is removed for both to avoid sludge in effluent water and to maintain a reasonable suspended solids concentration.

2.2.3 Chemical treatment

In chemical treatment process, phosphorus removal is the priority hence it is common for precipitation to take place. Precipitation chemical is added which turns phosphate into insoluble fractions. Precipitation chemicals also stimulate creation of flocks. The insoluble phosphates together with organically bounded phosphate then absorb or adhere to flocks. The flocks are separated by either sedimentation or floatation. Instead of chemicals enhanced phosphorus removal can be applied by the activated sludge process.

2.2.4 Sludge treatment

The sludge consists of organic material which has to be stabilised to avoid odour and reduce the pathogenic content. Aerobic stabilisation can be performed simultaneously in

an activated sludge plant whereby primary and secondary sludges are continuously aerated for long periods of time. In aerobic digestion the microorganisms extend into a respiration phase where materials previously stored by the cell are oxidized, resulting in a reduction of the biologically degradable organic matter. Bio-gas, methane and carbon dioxide are produced during digestion. Before sludge is transported away, it is dewatered by means of mechanical, centrifuging or filtering, the reason being to reduce the transportation cost due to the fact that sludge contains 95% water. After treatment sludge may be dumped or used as fertilizer and soil conditioning.

2.2.5 The Activated Sludge Process

The activated sludge process is an aerobic, biological treatment method that uses the metabolic reactions of microorganisms to produce an acceptable effluent quality by removing substances that have an oxygen demand. This treatment method, considered to be a secondary treatment process, generally follows a primary clarifier. However, depending on wastewater characteristics and plant design, the clarifier may be eliminated (Activated sludge, manual of practice OM-9). Bacteria constantly need energy in order to grow and support essential life activities. Growing cells make use of substrate and nutrients situated outside their membrane for growth and for energy development.

Traditionally the ASP mainly served to remove organics and ammonium from the wastewater (Metcalf and Eddy, 1979), (Arceivala and Asolekar, 2007), (Richard, 1989), (Jeppson, 1996). In its basic design, ASP plant takes the organics in the influent flow which are transformed into settleable biomass (activated sludge flocs) by biomass growth. In the next step the sludge settles at the bottom of the secondary settler. Figure 2.2 shows that the treated effluent of the plant flows over weirs at the top of the settler, while the settled sludge is withdrawn from the bottom. The major part of it is recycled back to the reactor, and a small part is wasted. Sludge recycling prevents the washout of biomass by decoupling the sludge residence time from the hydraulic residence time in the plant. The main control hurdles are the rates (1/h) of return flow Q_r , wastage flow Q_w , and airflow Q_{air} . During the last decade the interest in total-Nitrogen N removal from wastewater has risen due to increasing attention for the problem of eutrophication in the aquatic environment. Total-N removal requires two biological processes, namely nitrification and de-nitrification. Nitrification is a two step process, based on the nitrifiers *Nitrosomonas* and *Nitrobacter* of which both are autotrophic organisms. Autotrophic organisms are able to build up their biomass from inorganic carbon and water H_2O by

reduction process. Nitrification takes place when the autotrophs meet NH_4 under aerobic conditions. De-nitrification is fulfilled by heterotrophic organisms. De-nitrifiers or "heterotrophic organisms which are able to de-nitrify" preferably use dissolved oxygen (DO) as electron acceptor, but switch to NO_x in case no DO is available. The de-nitrification process only takes place when de-nitrifiers meet Readily Biodegradable Organic Substrate (RBOS) in an anoxic environment (presence of NO_x , absence of DO). Under those conditions de-nitrifiers consume organics, using nitrate and nitrite as oxidiser.

Activated sludge process keeps microorganisms suspended either by blowing air in the aeration tank or by the use of agitators. Oxygen is being utilized by the micro-organisms to oxidize the organic matters.

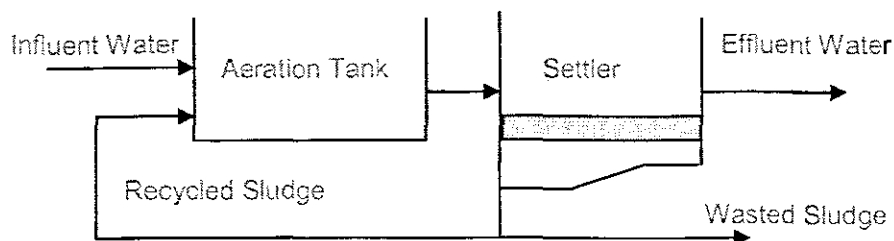


Figure 2.2: Basic ASP structure consisting of an aeration tank and a settler.

Figure 2.3 illustrates the basic biological renewal process in wastewater plant (Henze *et al.*, 1995). The reactions happening in the process have different time scales. The organic matter enters the process in several forms. It is converted to other forms by the biological process. The hydrolysis process converts larger molecules of slowly biodegradable matter into smaller, more easily accessible molecules, meaning, into readily biodegradable matter. The speed of hydrolysis may be of great concern in the activated sludge process as the influent wastewater mainly consists of slowly biodegradable matter. The fact of the matter pertaining to the hydrolysis process is that it is relatively slower than the growth rate of the micro-organisms. The growth rate of the micro-organisms (biomass) depends on many different things, including the amount of biomass (number of micro-organisms), substrate (food, readily-biodegradable matter), temperature, pH, toxins, etc.

2.2.6 Biological Nitrogen Removal (BNR)

Nitrogen can be presented in different forms, for instance, as ammonia NH_3 , ammonium NH_4^+ , nitrate NO_3^- , nitrite NO_2^- and as organic compounds. In the raw wastewater, nitrogen is mostly represented by NH_4^+ and organic nitrogen (Lindberg, 1997).

Nitrogen forms an integral nutrient for biological growth. It is one of the main components in living organisms. Nevertheless, when nitrogen is present in effluent wastewater, problems may take place (Lindberg, 1997):

- Ammonia is toxic to aquatic organisms, especially those of higher life forms such as Fish, invertebrates, plants, and aerobic bacteria which all require oxygen for respiration.
- When ammonium is oxidized to nitrate, a significant oxygen demand in the receiving body may give rise to a severe depletion of the dissolved oxygen concentration.
- In drinking water nitrate is toxic, especially for infants.
- Nitrogen is an essential plant nutrient. Overloading can stimulate undesirable growth of aquatic plants and algae. When the plants die, oxygen is consumed by organisms degrading the litter.
- The presence of ammonia in drinking water supplies requires an increased chlorine dosage.

The ammonium can be removed in two-steps like it has been stated earlier (nitrification and de-nitrification)

The formulae describing the chemical reaction in the nitrification process are as follows;



The two equations show how ammonia is oxidized to nitrate and then to nitrite. Nitrate can be converted to nitrogen gas by de-nitrification and the process takes place in anoxic environment. Hence the formula describing the chemical reaction is



For Nitrogen removal, Nitrification process (conversion of ammonium into nitrate) requires the presence of oxygen. De-nitrification process (conversion of nitrate to gaseous nitrogen) does not require the presence of oxygen (Lindberg, 1997).

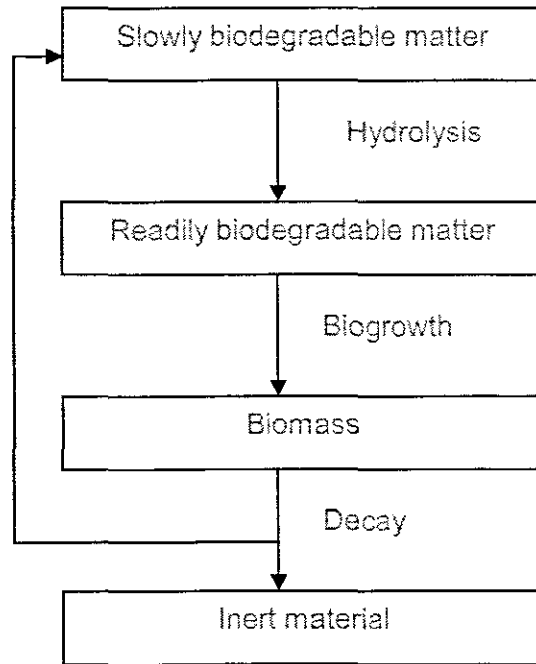


Figure 2.3: The biological renewal process (Henze et al, 1995).

2.3 A process of dissolving oxygen in wastewater

2.3.1 The role of the dissolved oxygen concentration in nature

Dissolved oxygen (DO) is the concentration of oxygen in the surface water and it plays a vital role as a measure of the health of the stream. Oxygen gets into water by diffusion from the surrounding air, by aeration (rapid movement), and as a waste product of photosynthesis. If there is no oxygen or it is insufficient then aquatic animals will die or their growth or production will be affected. The dissolved oxygen should be as high as possible. The following are the few examples of the role of DO as an important factor in nature (Lindberg and Carlsson, 1996), (Application Data Sheet, 2006).

- Much of the dissolved oxygen in water comes from the atmosphere. After dissolving at the surface, oxygen is distributed by current and turbulence. Algae and rooted aquatic plants also deliver oxygen to water through photosynthesis.
- The main factor contributing to changes in dissolved oxygen levels is the build-up of organic wastes. Decay of organic wastes consumes oxygen; this consumption is higher in summer, when aquatic animals require more oxygen to support higher metabolisms.
- Depletions in dissolved oxygen can cause major shifts in the kinds of aquatic organisms found in water bodies.
- Temperature, pressure, and salinity affect the dissolved oxygen capacity of water. The ratio of the dissolved oxygen content to the potential capacity gives the percent saturation, which is an indicator of water quality.
- Oxygen depletion is referred to as low levels of DO which may result in fish mortality. It is recommended that 5mg/L of DO concentration be available for optimum fish health. Most species of fish turn to distress when DO levels fall to 2-4mg/L, as they are sensitive to low levels of dissolved oxygen, more specifically larger fish as they react quickly to oxygen depletion than their smaller counterparts.

Oxygen depletion takes place when oxygen consumption exceeds oxygen production. Increase in oxygen consumption is due to an over-abundance of aquatic plants or algae in the ecosystem, increased organic waste in water, demise and decomposition of organic matters, or certain chemicals that are being directly used.

2.3.2 The role of dissolved oxygen in the activated sludge process.

Dissolved oxygen concentration is one of the principal control parameters in the activated sludge systems (Lindberg and Carlsson, 1996). (Vanrolleghem and Lee, 2003) stated that, Oxygen plays an integral part in activated sludge process. If the associated aeration is done in an optimal way it will lead to substantial reduction in the process energy consumption. This gives operators in control and management of wastewater treatment plants a more manageable task to do. The proper control of dissolved oxygen probes which are probably the most widely applied sensors in biological wastewater treatment plants is very important. Numerous efforts have been devoted to maximize the information extracted from the raw data. Control of the dissolved oxygen concentration (DO) in an activated sludge process is of considerable importance because of economy

and process efficiency. Dissolved oxygen analysis measures the amount of gaseous oxygen O_2 dissolved in an aqueous solution.

An oxygen depletion event can be envisaged and therefore, be averted by continuous monitoring of dissolved oxygen levels in the aeration tank of the activated sludge process. The most efficient way or tool to carry out the task is by measuring DO with an electrode and electronic meter or with field test kits. The electronic meter does not measure oxygen directly; rather, it uses electrodes to measure the partial pressure of oxygen in the water, which is converted to oxygen mass weight concentration. The amount of solution required to change the colour of the sample reflects the concentration of DO in the sample. The amount of oxygen dissolved in water is expressed as a concentration, in milligrams per litre (mg/l) of water. The primary objective of the activated sludge process is to maintain low concentration of biodegradable matter and nutrients in the effluent together with low sludge production. But since it is a known fact that activated sludge process is a very complex and very nonlinear in nature it presents a challenge to control. Controlling dissolved oxygen concentration plays an important part in operating the facility.

Dissolved oxygen concentration control is deemed one of the most important parameters in wastewater treatment plants (WWTP). (Reiger et al, 2006), stated that owing to the extreme nonlinearity and time variation of the activated sludge process maintenance a reliable performance of aeration control might prove to be a very difficult task. However, a number of control candidate schemes for improving DO have been tested.

Aeration takes place in the aerobic reactors, but practically, DO concentration s_o in the activated sludge process is maintained by manoeuvring aeration airflow Q_{air} (Lindberg, 1997). The aeration input can be represented by the oxygen transfer rate function K_{La} . Two factors that affect the dynamics of the DO are oxygen uptake rate (respiration) and nonlinear oxygen transfer function. Determination of their values is a challenging topic for the application of recursive identification due to nonlinear characteristics of the oxygen transfer function (Ljung and Söderström, 1983). On-line estimation of respiration rate of the microorganisms is based on current values of dissolved oxygen concentration and airflow signals. Control efficiency improvement for dissolved oxygen concentration can be achieved through fast estimation of respiration taking into account that respiration is the most important disturbance signal in controlling dissolved oxygen concentration.

Respiration rate is directly linked to substrate removal and biomass growth of which is evident that respirometry is an effective tool in the activated sludge process control. However, neither respiration rate nor other process variables are generally deployed directly in conjunction with control strategies in order to secure the primary objectives (Lira *et al*, 2004).

Respiration rate can be used as a controlled variable and this is achievable through the actual rate or endogenous rate being kept at the certain value by influencing some process handle, measurement being used to designate disturbances or by triggering the alarm. In most instances though, respirometry can be used to extract information with a particular biological significance from measurements (Lira *et al*, 2004).

When the oxygen uptake rate is used as controlled variable, respirometry strategy is manipulated to maintain the endogenous respiration rate in the aeration tank at a set-point value. The underlying idea is that endogenous respiration rate is a measure of active biomass concentrations.

2.4 Mass balance model of dissolved concentration

2.4.1 Mass balances

The dissolved oxygen concentration (DO) in the aerobic part of an activated sludge process should be sufficiently high to supply enough oxygen to the microorganisms in the sludge. An excessively high DO (which requires a high air flow rate) leads to a high-energy consumption and may also deteriorate the sludge quality. A high DO concentration in the internally recirculated water also makes the denitrification less efficient. Hence, both for economical and process reasons, it is of interest to control the DO.

The difficulty in controlling the DO is that, the process dynamics is nonlinear. This means that high control performance for all operating conditions may be hard to achieve with a linear controller. The key idea is to explicitly take the nonlinear characteristics of the oxygen transfer function K_{La} into account in the control design. The design method consists of two separate parts: an estimation part where K_{La} is determined and a controller design part (Carlsson, 1997).

2.4.1.1 The definition of the oxygen transfer function

In the dissolved oxygen concentration dynamics, the oxygen transfer function K_{La} is included. It describes the rate at which oxygen is transferred to the wastewater by the aeration system as a function of the airflow rate (u). The most common way to describe the oxygen transfer is by the following equation (Carlsson, 1997):

$$K_{La}(u(t))(s_{O_{sat}} - s_O(t), s_{O_{sat}})s_O(t) \quad (2.4)$$

In (2.4), the oxygen transfer function K_{La} only depends on the air flow rate $u(t)$. However, K_{La} depends also on several other factors, for example type of diffusers, wastewater composition, temperature, design of aeration tank, tank depth, placement of diffusers etc. The main time-varying dependence is on the air flow rate $u(t)$.

2.4.1.2 The dissolved oxygen dynamics

In an activated sludge process, biodegradable matter is degraded by micro organisms which consume oxygen. Figure 2.4 below shows the aerating basin with its inflows and outflows. This diagram is used for development of the mass balance model of the process. Dynamic behaviour of the DO concentration is described by the following mass balance equation:

$$\dot{s}_O(t) = \frac{Q(t)}{V}(s_{O_{in}} - s_O(t)) + K_{La}(u(t))(s_{O_{sat}}(t) - s_O(t)) + r_{SO}(t) \quad (2.5)$$

where $s_O(t)$ is the DO concentration in the aeration tank

$s_{O_{in}}(t)$ is the DO concentration of the input flow

$s_{O_{sat}}$ is the saturated value of the DO concentration in wastewater

$Q(t)$ is the influent wastewater flow rate

V is the volume of the wastewater tank

$K_{La}(u)$ is the oxygen transfer function depending on the control input

$u(t)$ is the airflow rate into the zone from the air production system

$r_{SO}(t)$ is the respiration rate (oxygen utilisation rate or oxygen uptake rate)

When the mass balance equation of the DO concentration is used for control design, the oxygen transfer coefficient K_{La} is considered as a linear or nonlinear function of the airflow rate. This is based on the strong dependence of the value of K_{La} and the value of

the airflow rate. The variables that are assumed to be measured are $s_o(t)$, $s_{o,in}(t)$, $u(t)$ and $Q(t)$; $s_{o,sat}$ and V are known constants.

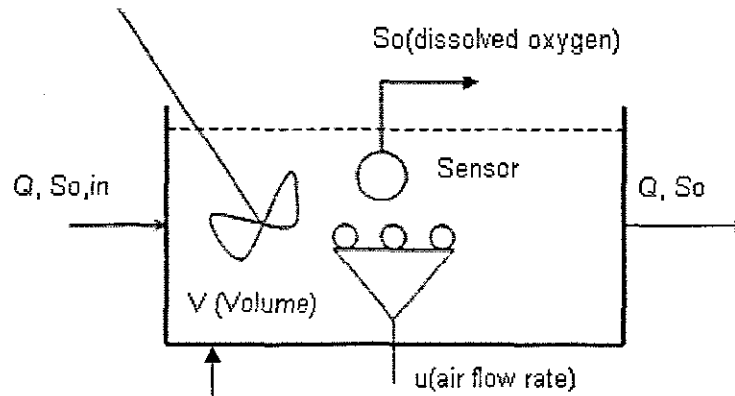


Figure 2.4: A schematic diagram of the aeration tank.

2.5 Methods for measurement of dissolved oxygen concentration based on the respirometry

2.5.1 Respirometry

Respirometry techniques measure the respiration rate which is used to determine:

1. The rate of biodegradation by sludge bacteria.
2. Toxic wastes which inhibit both respiration and biodegradation.
3. The process optimization and control.

In the aerobic tanks of a biological treatment plant, the complex molecules of the wastewater are broken down by the combined activities of heterotrophic bacteria, nitrifying bacteria and other microorganisms. In terms of process control, there are three major processes (Spanjers *et al.* 1996):

- Biodegradation
- Growth
- Respiration

The above three processes are interdependent, resulting in changing of rate of respiration, which is a measure of the rate of biodegradation attained. It is for the above reason that the oxygen uptake rate may be used as a control variable in process optimization. If toxicity in the influent wastewater inhibits the respiration rate of the

activated sludge, it follows that there will be an associated reduction in the rate of biodegradation. A scientific and technical report on respirometry control of activated sludge process has been compiled by IAWQ Task Group (Spanjers *et al*, 1996). It explained the significance of respirometric analysis in activated sludge systems from the environmental view of the biochemical engineering. The reason being that respiration rate is directly related with two important biochemical processes i.e. biomass growth and substrate consumption which must be controlled in wastewater treatment plant. Included in the report are respirometry-based control strategies and all measuring techniques for respiration rate are classified accordingly (Spanjers, Vanrolleghem, Olsson and Dold, 1996). Measurement and interpretation of the respiration rate of the activated sludge is done by respirometry. The respiration rate is the amount of oxygen per unit of volume and time that is consumed by microorganisms. For a long time respirometry has been known as an important source for controlling the activated sludge process. The explanation given for this is that respiration rate is directly linked to two important biochemical processes that must be controlled in wastewater treatment plant namely biomass growth and substrate consumption (Lukasse *et al*, 2000).

Respiration rate and dissolved oxygen concentration in activated sludge form a strong attachment amongst them. These results in that the dissolved oxygen measurement can be easily and reliably done and it has been used recurrently in the control of the activated sludge process. Nevertheless, the fixed value of dissolved oxygen concentration does not give adequate information on the growth and substrate utilization as such. But it must be noted that there is a difference between dissolved oxygen concentration-based control and respiration rate-based control (Spanjers *et al*, 1996).

Measurement of respiration rate has been the research topic for many investigators and a number of measuring procedures have been developed. Regrettably, in the narrative of respirometers there is more disorientation about the working principles than with any other instrument, it is being portrayed with terms like: continuous, semi-continuous, batch, in-line, on-line, in-situ, etc. The explanation for this confusion is that the description can be relevant to the operation of the respirometer, which over and over again is a small activated sludge reactor by itself, or to the way it relates with the treatment plant.

A number of respirometry-based control schemes have been proposed in the literature but very few real implementations are reported. Owing to inadequate measurement

techniques and lack of understanding of the information content of respirometric data, there have been a small number of successful practical applications (Marsili-Libelli, Vaggi, 1997), (Marsili-Libelli, Tabani, 2002), (Checchi, Marsili-libelli, 2005). Additionally, confusion cropping up from inconsistency in implementation methods and employment of terminology has held back the introduction of respirometry-based control.

In 1993 the International Association on Water Quality (IAWQ) established a task group with the mission to write a Scientific and Technical Report (STR) on respirometry-based control after realising the need for an extensive evaluation of respirometry in control of the activated sludge process. The aim of the STR was to generate new insights by evaluating existing knowledge present in literature and practice and identify further needs (H. Spanjers *et al.* 1996).

2.5.2 Significance of respirometry

The main purpose in wastewater treatment systems more often than not is the removal of carbonaceous material from the waste stream through growth of heterotrophic bacteria. The bacteria convert the energy of intramolecular bonds in the organic substrate to the high-energy phosphate bonds of adenosine triphosphate (ATP). This energy is then used to produce the various molecular components required for cell growth and reproduction. Alteration of energy from substrate to ATP occurs by means of a series of oxidation-reduction reactions. The most important ATP generation process within the cell is expressed as an oxidative phosphorylation. ATP is generated as electrons removed from the substrate by oxidation are transferred along the electron transport chain to the terminal electron acceptor-oxygen in the aerobic activated sludge process. Generally the process of the aerobic respiration is represented schematically in Fig.2.5. A portion $(1-Y)$ – of the used up substrate is oxidized to supply the energy to reorganise the remainder (Y) of the substrate molecules into new bacterial cell mass, where Y is substrates remnants and $1-Y$ is substrates consumed.

The removal of carbonaceous material and related processes are not essentially the only sinks for oxygen in activated sludge systems. Nitrification, which entails oxidation of ammonia nitrogen to nitrate nitrogen by autotrophic organisms, often will account for approximately 40 percent of the total oxygen demand.

The rate, upon which the oxygen is utilized as an electron acceptor (i.e. the respiration rate) can be tracked with relative ease as the measurement involves simply monitored

variables like, dissolved oxygen concentration or partial pressure of oxygen. The above is not applicable for certain important state variables such as active biomass concentration which cannot be measured directly, that's why respirometry is a powerful alternative tool for assessing the condition of a system. Respiration has been identified as the most sensitive parameter in research and model development, against which activated sludge theory can be tested. Several experimental protocols based on respiration rate have developed to isolate and study different aspects of process behaviour such as biomass growth rate and decay rate, nitrification rate, and hydrolysis. Respiration rate can also be regarded as the basis for a number of wastewater characterization protocols.

Oxygen demand and respiration rate are interrelated to all the aerobic organism activities in an activated sludge system, and differ in space and time. Many factors have an impact. These include:

- The time-varying influent loading rate and the composition of the influent
- The flow regime in the system e.g. plug flow versus completely mixed one
- The inclusion of unaerated zones for nutrient removal
- Heterotrophic and autotrophic organism growth rates
- Return activated sludge and mixed liquor recycle rates
- Operating sludge age (or solids retention time)
- The spatial distribution and efficiency of devices

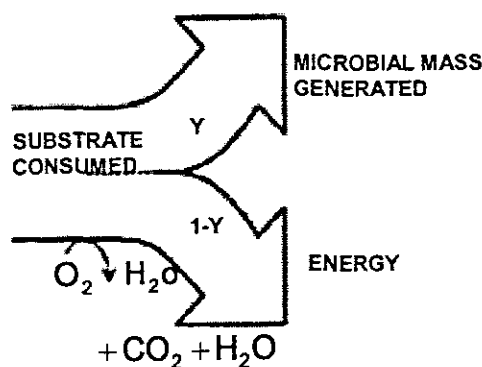


Figure 2.5: Schematic representation of substrate consumption process (H. Spanjers et al, 1996).

Since oxygen consumption is directly linked to process behaviour it is to be expected that respiration rate can be used as an important tool in the system control and for recognizing disturbances which have an impact on process performance (Spanjers *et al*, 1996).

2.5.3 Measuring principles

Respirometers are usually used to measure respiration rate. They are normally ranging from a simple, manually operated bottle equipped with dissolved oxygen sensor to complicated instruments that are operated fully automatically. In several cases, the aeration tank of the treatment plant itself can serve as respirometer. With the exception of the latter case, a characteristic known to all respirometers is a reactor, separated from the activated sludge tank, where different components (biomass, substrate, etc.) are brought together.

The operation of all respirometers engages some technique for calculating the rate at which the biomass takes up oxygen dissolved in the liquid. Various techniques have been developed in the past. But, it was found by the task group that all measuring techniques for the respiration rate can be classified into only eight basic principles according to two criteria (H. Spanjers *et al*, 1996):

- The phase where oxygen concentration is measured (gas or liquid)
- Whether or not there is input and output of liquid and gas (flowing or static).

The operation of all existing respirometers can be described in terms of the above principle. At the moment, the principles are being discussed according to the phase where oxygen is measured.

2.5.4 Principles based on measuring DO concentration in the liquid phase.

Respirometers that are based on measuring DO concentration in the liquid phase make use of a DO mass balance over the liquid phase. Consider a system consisting of a liquid phase, having biomass and substrate, and a gas phase both being ideally mixed and having an input and output. It is believed that the DO concentration in the liquid phase can be measured. The DO mass balance over the liquid phase is:

$$\frac{d}{dt}(V_L s_{OL}) = Q_{in} s_{OL,in} - Q_{out} s_{OL} + V_L K_{LaL} (s_{OL}^* - s_{OL}) - V_L r_{SO} \quad (2.6)$$

where: s_{OL} = DO concentration in the liquid phase

s_{OL}^* = saturation concentration of the DO

$s_{OL,in}$ = DO concentration in the liquid phase entering the system

K_{LaL} = oxygen mass transfer coefficient (based on liquid volume)

Q_{in} = flow rate of the liquid entering the system

Q_{out} = flow rate of the liquid leaving the system

r_{SO} = respiration rate of the biomass in the liquid

V_L = volume of the liquid phase

Mass balance over the liquid phase, Equation (2.6) does not contain gas flow terms. The first and second term on the right side represent advective flow of DO in the input and output liquid streams. In most systems Q_{in} and Q_{out} will be equal so that the liquid volume is constant. The mass transfer balance is described in the third term. The respiration rate is included in the last term which is to be derived. Therefore, s_{OL} must be measured and all other coefficients be known or neglected. Practically, determination of r_{SO} can be simplified in several ways. One approach is to make use of a method exclusive of liquid flow and oxygen input. Followed by, the first three terms on the right hand side of Equation. (2.6) fall away and the mass balance reduces to:

$$\dot{s}_{OL} = -r_{SO} \quad (2.7)$$

Therefore, the differential term has to be determined in order to obtain the respiration rate only. This can be done by measuring the decrease in DO as a function of time due to respiration, in correspondence with the approximation of the differential term with a finite difference term.

The significance of this approach is that the DO becomes exhausted after some time to give each new measurement of r_{SO} a reaeration needed to bring the DO concentration a higher level. DO and substrate are limited when their concentrations turn out to be too low, causing a nonlinear DO to decrease. The procedure for the determination of r_{SO} according to "standard methods" is based on this principle. The principle is often used for manually measuring of r_{SO} but it is also implemented in automatic respirometers which sample activated sludge from an aeration basin and do one or more measurements of

the DO decrease. In general, it is highly impractical for the principle to be implemented directly in an aeration tank.

The negative aspect required for reaerations can be eliminated by continuously aerating the sludge. Then, the oxygen mass transfer term $K_{LaL}(s_{OL}^* - s_{OL})$ must be included in the mass balance Equation (2.7). To obtain r_{SO} both the differential term and the mass transfer term must be determined. For the latter to be calculated, the mass transfer coefficient K_{LaL} and DO saturation concentration s_{OL}^* must be known. These coefficients have to be determined on a regular basis because they depend on environmental conditions such as temperature, barometric pressure and properties of the liquid. The simplest approach is to determine these coefficients by using separate reaeration tests and look-up tables. Another move towards coefficients estimation from the dynamics of the DO concentration response is through application of parameter estimation techniques as developed in chapter 4. The advantage of the latter is that the values of the response can be updated relatively easily. This respirometric principle allows the measurement of r_{SO} at a constant DO concentration, thereby eliminating the dependency of r_{SO} on the DO concentration (provided $DO \gg 0 \text{ mg/l}$). This principle can be implemented in a separate respirometer or directly in the aeration tank (H. Spanjers et al, 1996).

Repetitive aeration or estimation of oxygen transfer coefficients can be avoided when liquid with a high enough input DO concentration is pumped continuously through a closed completely mixed or plug flow cell without gas phase. The liquid flow terms now have to be included in the mass balance Equation (2.7). Both DO concentrations $s_{OL,in}$ and s_{OL} must be measured continuously to allow the calculation of r_{SO} . In a respirometer Q_{in} and V_L are instrument constants and therefore assumed known or calibrated. This principle is in fact the continuous counterpart of the one described in Equation (2.6). It is also sensitive to the effect of substrate and dissolved oxygen concentration limitation. However, the effect of the limiting substrate can be reduced by the continual addition of substrate (wastewater) to the respiration cell (H. Spanjers *et al*, 1996).

2.5.5 Respirometric principles based on measuring oxygen in the gas phase

Respirometric principles based on the measurement of gaseous oxygen might as well use of oxygen mass balances to receive the respiration rate. However, in addition to the

mass balance on liquid phase Equation (2.6), a balance on the gas phase must be considered (H. Spanjers *et al*, 1996):

$$\frac{d}{dt}(V_G s_{OG}) = F_{in} s_{OG,in} - F_{out} s_{OG} - V_G K_{LaG} (s_{OG}^* - s_{OG}) \quad (2.8)$$

where: s_{OG} = DO concentration in the gas phase

$s_{OG,in}$ = DO concentration in the gas entering the system

F_{in} = flow rate of the gas entering the system

F_{out} = flow rate of the gas leaving the system

V_G = volume of the gas phase

The term $K_{LaG} (s_{OG}^* - s_{OG})$ represents the mass transfer rate from the gas phase to the liquid phase and it consists of the connection between the two phases. As opposed to measuring s_{OG} directly, it can be related to volume or pressure changes by using the gas law. Additional assumptions to be made are that the gas behaviour be ideal and that measured changes are only caused by changes in oxygen concentration. Since carbon dioxide is produced in the activated sludge process this gas must be absorbed chemically to avoid interference with the oxygen measurement.

Following mass balances Equations (2.6) and (2.8), in order to allow calculation of r_{SO} , s_{OG} must be measured and also the information about s_{OL} is required. If mass transfer is sufficiently fast it can be alleged that the oxygen concentrations are in balance so that the gas phase measurement is a true representation of the condition in the liquid phase. In particular for full scale situations where the aeration tank is used as a respirometer (off-gas or exhaust gas measurement), the legality of this statement should be seriously confirmed. The measuring of r_{SO} in respirometers is usually simplified under static liquid phase operation. In the simplest case, when both liquid and gas phase are static, the same restriction as with the simplest DO based principle exists: in case the oxygen turns out to be worn out it must be refilled by, for example, venting the gas phase. Another option is to supply oxygen from an external tank and measure the amount of oxygen supplied, or generate the oxygen by electrolysis. The latter technique enables deduction of r_{SO} from the electrolysis current. Constant pressure and temperature must be kept in both instances.

Table 2.1 sums up the measuring principles; the first column encloses the names of the mass balance terms and the second column contains the mathematical equivalents. The succeeding columns list the respirometric principles, the first four being liquid phase principles and the others being gas phase principles. The mass balances for each principle are formed by multiplying the terms with the coefficients in the column of the appropriate principle. The totting up of all terms must be equivalent to zero (H. Spanjers *et al*, 1996).

2.5.6 Static gas-static liquid

A static gas-static liquid respirometer is normally controlled by monitoring the decline in dissolved oxygen concentration s_o with time in a closed vessel after a short aerated phase. By omitting transport and aeration terms the calculated mass balance equation of respirometer becomes

$$\dot{s}_o = -r_{s_o} \quad (2.9)$$

An entirely closed respiration chamber with no headspace is required as no aeration of the activated sludge sample may take place during experiment. If an open respiration chamber is used surface aeration may influence the measured data given by Equation (2.9). This type of respirometer is limited, because of the absence of aeration and thereby the danger of oxygen limitation, particularly for the determination of the sludge kinetics and wastewater characteristics.

2.5.7 Flowing gas-static liquid

Since they are continuously aerated, flowing gas-static liquid respirometers have the advantage that higher sludge concentrations can be used, mainly because there is a continuous input of oxygen to avoid oxygen limitation. It is recommended that higher sludge concentration will typically allow a shortening of the experiment.

The transport term of equation (2.6) is not needed giving the following mass balance equation.

$$\dot{s}_o = K_{La}(s_o^0 - s_o) - r_{s_o} \quad (2.10)$$

The figures at the top schematically illustrate the different principles. Signified are: the two segments gas and liquid, the flow system of both segment and the position where oxygen is measured in either form (gas or liquid)

Table 2.1: Summary of the measuring principles for respiration rate

Respirometric principle process		Measurement in liquid phase				Measurement in gas phase			
Liquid phase balance	respiration	$V_L r_{SO}$	-1	-1	-1	-1	-1	-1	-1
	dissolved oxygen accumulation	$\frac{d}{dt}(V_L s_{OL})$	-1	-1	-1	-1	-1	-1	-1
	liquid flow	$Q_{in} s_{OL,in} - Q_{out} s_{OL}$		1		1	1		1
	gas exchange	$V_L K_{L,aL} (s_{OL}^* - s_{OL})$			1	1	1	1	1
Gas phase balance	Gaseous oxygen accumulation	$\frac{d}{dt}(V_G s_{OG})$				-1	-1	-1	-1
	gas flow	$F_{in} s_{OG,in} - F_{out} s_{OG}$						1	1
	gas exchange	$V_L K_{L,aL} (s_{OL}^* - s_{OL})$				-1	-1	-1	-1

In case the oxygen transfer coefficient (function) K_{La} is too high, then it be noted that oxygen dynamics might not be visible. Furthermore, too high aeration intensity may perhaps increase the risk of measurement noise. It is therefore significant to optimise the aeration in the respirometer in such a way that a consistent r_{sO} value can be obtained. In most cases, the oxygen uptake rate r_{sO} may be considered to consist of two components namely the exogenous oxygen uptake rate $r_{sO,ex}$, meaning the immediate oxygen uptake needed to degrade the substrate, and the endogenous uptake rate $r_{sO,end}$. In the absence of substrate, $r_{sO,ex}$ is zero and this results in oxygen concentration in the flowing gas-static liquid respirometer to reach a steady-state concentration $s_{O,eq}$ which represents the equilibrium between oxygen transfer and endogenous respiration. Under the statement that $r_{O,end}$ is constant for which a reasonable assumption for short-term experiments were performed, out of which Equation (2.10) is being formulated.

$$\dot{s}_O = K_{La}(s_{O,eq} - s_O) - r_{sO,ex} \quad (2.11)$$

In applying the above equation attention can be focused on the substrate degradation-induced respiration $r_{sO,ex}$ only. A flowing gas-static liquid respirometer makes it easy to record r_{sO} data with a higher frequency as compared to most static-gas respirometers. As for the above Equation (2.11), the exogenous oxygen uptake rate can be calculated from s_O data which is measured during the substrate degradation when values of ds_O/dt , $s_{O,eq}$, and K_{La} are known. The factor ds_O/dt is the slope of the s_O curve, and it is usually obtained by a moving data window regression on the s_O data.

2.5.8 Static gas-flowing liquid

In static-gas flowing liquid respirometers the s_O concentration at both the inlet and the outlet of a closed respiration chamber is measured. Aerated sludge is pumped incessantly through the respiration chamber. The r_{sO} is calculated by making an oxygen mass balance over the respiration chamber using the inlet $s_{O,in}$ and the outlet s_O dissolved oxygen concentration and the residence time V/Q_{in} in the chamber and this is illustrated by Equation (2.12) below.

$$\dot{s}_O = \frac{Q_{in}}{V}(s_{O,in} - s_O) - r_{sO} \quad (2.12)$$

It can be noted from equation (2.12) above that knowledge of K_{La} is not necessary, which gives to this type of the respirometer an advantage in the study of more complex substrates such as wastewater for which K_{La} estimation may be challenging. The residence time V/Q_{in} is believed to be known in this approach and ought to be properly chosen to avoid oxygen limitation in the respiration chamber. The drawback is that a relatively small difference $s_{O,in} - s_O$ must be calculated from the signals of two dissolved oxygen probes, indicating that a drift of the electrodes may cause incorrect r_{sO} data. To deal with this, the s_O concentrations in the inlet and outlet of the respiration chamber are measured by the same dissolved oxygen probe in the static gas-flowing liquid respirometers. The results were achieved by regular switching of the flow direction in the respiration vessel. On the other hand, the regular flow direction switch means that the response time of the electrode itself turns out to be an important data for the data interpretation.

2.5.9 Hybrid respirometer

Taking the good and leaving out the bad elements of the different existing respirometers, a compromise for the theoretical concept of a hybrid respirometric measurement principle had been proposed. The proposed respirometer is based on the principles of flowing gas-static liquid and static gas-flowing liquid respirometer combination.

The combined respirometric-titrimetric monitoring of the degradation process during batch experiment with activated sludge is presented and done by (Gerneae, Petersen, Ottøy and Vanrolleghem, 2001). They found improved confidence intervals for using the combined data set as opposed to separate respirometric or titrimetric data sets for parameter value estimation. On the other hand oxygen concentration control can be improved for the purposes of efficiency.

2.6 Methods for estimation of the oxygen transfer function and oxygen uptake rate

The availability of on-line information about the microbiological activity is of vital importance in monitoring and control of the activated sludge of the wastewater process. The lack of reliable sensors and high cost of advanced instrumentation are of major problems in the monitoring and control of wastewater treatment plants.

Many respirometric methods are described in the literature, but their implementation in the activated sludge process is difficult. Development of the methods for model based control resulted in development of the investigation of different approaches for estimation of the oxygen uptake rate and oxygen transfer function by using software sensors. Some overview of the existing methods is given below.

Model-based on-line estimation of respiration from current values of dissolved oxygen concentration and airflow signals was developed in (Gerškšič *et al*, 2006). It is based on fast estimation of respiration, because respiration is the most important disturbance signal in controlling dissolved oxygen concentration and is used as a factor improving control efficiency.

Estimation of the respiration rate and the nonlinear oxygen transfer function using software sensor (Lindberg and Carlsson, 1996) for the measurement of the dissolved oxygen concentration and airflow rate by a Kalman filter was proposed. The respiration rate is time varying. Generally it has a daily variation around a nonzero mean value; however it might change unexpectedly due to disturbances. The oxygen transfer function depends on a number of factors, for instance aeration type, wastewater composition etc, as well as the airflow rate. Discrete extended Kalman filter for estimation of oxygen uptake (respiration) and nonlinear oxygen transfer function (Sotomayor *et al*, 2001) used numerical simulations for simultaneous estimation of both respiration rate and oxygen transfer function through software sensor was developed.

Nonlinear adaptive control for improved control of dissolved oxygen concentration in the aeration tank of the wastewater treatment process based on a bilinear model of the dissolved oxygen concentration was done in (Ko, McINNIS and Goodwin, 1982). They effectively showed through simulation results that both OUR (oxygen uptake rate) and nonlinear oxygen transfer coefficient can be estimated using on-line methods.

Controlling activated sludge process on the bases of dissolved oxygen concentration measurement profile providing a distinct advantage of exploring the use of reliable sensors was done in (Olsson and Andrews, 1978). The reason for this being that it makes it possible to get information for variables that are not easily measurable.

(Lindberg and Carlsson, 1996) suggested another strategy that only involves nonlinear oxygen transfer function and in this case comparison was made on the basis of the

designed controller outperforming the normal PI controller. The challenge in controlling DO is that the process is inherently nonlinear; indicating that high control performance for all operating conditions may be a problem to attain with a linear controller. Hence, the decision taken for the development of a design method that gives a high performance controller for all operating conditions is convenient for the control of dissolved oxygen concentration. Further, in the design of the controller, the nonlinear characteristics of oxygen transfer function K_{La} had been taken into consideration. A design method which consisted of two parts in the form of: an estimation part and a controller design part is developed. The control design is based on a linearization of the DO process, obtained by using the inverse of an estimated oxygen transfer function. It should be noted though that it is of importance to choose a set-point for DO concentration controller, meaning, a suitable DO in the zone. However, in practice the set-point is often kept at a fixed level. A set-point controller which uses measurements of ammonia concentration had been suggested. The DO set-point was controlled as to obtain a prespecified ammonia concentration.

Estimation techniques issued from control and systems theory are applied in the development of software sensors for on-line estimation of bio-process variables. Software sensor can be said to be in association between an estimator and a sensor. Software gathers the on-line estimation of the variable from measurements made by the sensor.

Bio-activities in the activated sludge process are closely linked to the dissolved oxygen concentration. The heterotrophic bacteria degrade the carbonaceous organic matter making use of oxygen to oxidize and mineralize organic matter to produce carbon dioxide. The effect of dissolved oxygen concentration on the rate of nitrification using both pure and mixed cultures, and cultures found in wastewater treatment systems have been investigated by (Stenstrom and Pudaska, 1980). Nitrification is made up by a special group of autotrophic bacteria, called nitrifiers. In this process, the nitrosomonas oxidize into nitrite and the nitrobacters oxidize nitrite into nitrate. In association with heterotrophic microorganisms, nitrifiers need more oxygen for their growth, so the nitrification process is responsible for approximately 40% of the total oxygen demand.

Different automatic techniques have been applied to control dissolved concentration in wastewater treatment plants in the past and the reason is that there are benefits including the following, but not limited to:

- On-line sensors for measurement of DO concentration have been developed in recent years.
- There is a lot to be gained when controlling the DO concentration, because it is very expensive for blowing air in the deep basins.
- The quality and process efficiency of effluent water depend largely on appropriate DO concentration.

A nonlinear model-based control algorithm for dissolved oxygen control is developed in (Yoo *et al*, 2004). Dissolved oxygen (DO) concentration in mixed liquor is an important process parameter in the biological wastewater treatment process as a result of economic reasons and performance. The proper control of DO can give an improved process performance and provide an economic incentive to minimize the excess oxygen consumption by making available the needed amount of air to meet the time-varying oxygen demand of the mixed liquor. Nevertheless, the major technical hitches in the control of biological process are the variety of the kinetic parameters and limited availability of on-line information; consequently, an adaptive and nonlinear controller is the cream of the crop for the biological process control.

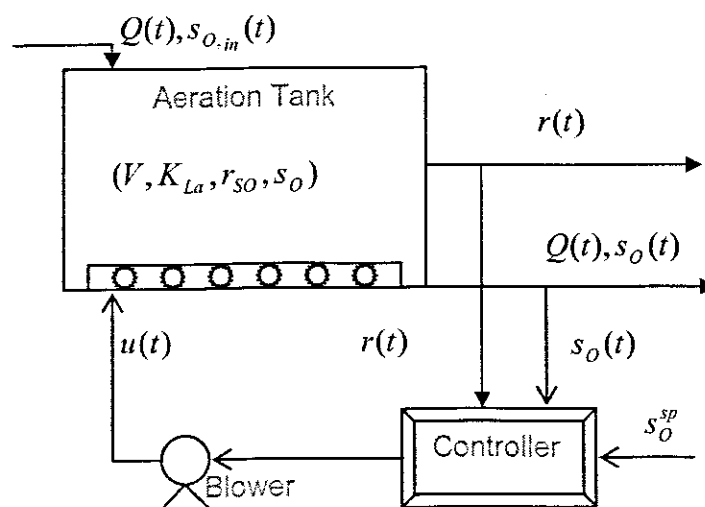


Figure 2.6: Closed loop control of dissolved oxygen control.

The estimation of the oxygen transfer rate $K_{La}u(t)$ and the respiration rate ($r_{SO}(t)$) is needed to construct a nonlinear controller for controlling the DO concentration more effectively. Several recursive approaches were proposed in order to estimate $K_{La}u(t)$ and $r_{SO}(t)$ from the measurement of DO and airflow rate (Holmberg et al., 1989), (Carlsson, 1993); (Marsili-Libelli and Voggi, 1997). Here the Lindberg's method [1997] is described. The proposed Kalman filter estimates the values of $K_{La}(t)$ and $r_{SO}(t)$ on the basis of the measurements of the DO concentrations and airflow rate. The filter equations are shown on Figure 2.7., where F and K are filter coefficients.

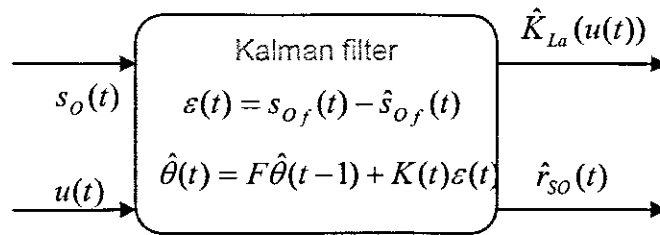


Figure 2.7: Estimator of $K_{La}(u(t))$ and $r_{SO}(t)$

Because the respiration rate is affected by microbial activity, influent characteristics, influent loads and flow rate, it is not possible to decide its mathematical formulation and specific form, that is, the $r_{SO}(t)$ is a kind of a stochastic process. The respiration rate in many biological treatment processes which treat domestic wastewater exhibits sinusoidal behaviour due to large diurnal fluctuations in the flow rate and the composition of the feed stream; and the respiration rate in industrial WWTP shows a step-like behaviour. Several models for modelling the respiration rate as a stochastic process, such as random walk model, a filtered random walk model, and an integrated random walk model, are suggested (Olsson and Newell, 1999).

In the paper considered above, the respiration rate is modelled as a filtered random walk based on a deviation variable,

$$r_{SO}(t) = \frac{1}{(1-q^{-1})(1-fq^{-1})} e_r(t) \quad (2.13)$$

where f is a filter pole between 0.9 and 1, $e_r(t)$ is zero mean white noise, and q is backward shift operator. Here, the respiration rate is considered as a filtered random

walk model among stochastic processes. The filtered random walk model can give better tracking performance of the respiration rate than a random walk model in the presence of measurement noises (Lindberg, 1997). The exponential oxygen transfer rate model K_{La} can be a good choice, because it can give a similar shape of the K_{La} function, which is natural in a physical sensor (the oxygen transfer deteriorates for high airflows). Further, only two parameters are necessary to be estimated and it is easy to invert the K_{La} function. An exponential model of the oxygen transfer rate is modelled suggested by (Lindberg, 1997),

$$K_{La}(u(t)) = k_1(1 - e^{-k_2 u(t)/a}) \quad (2.14)$$

where a is a scaling factor and k_1 and k_2 are parameters in the exponential K_{La} model. The parameters of k_1 and k_2 can be estimated during the laboratory batch experiment under an assumption of a fixed airflow rate which gives a fixed K_{La} .

The Kalman filter equations for the exponential model of the K_{La} are used as follows (Ljung, 1987).

$$\varepsilon(t) = s_{O_f}(t) - \hat{s}_{O_f}(t|t-1; \hat{\theta}(t-1)) \quad (2.15)$$

$$\hat{\theta}(t) = F\hat{\theta}(t-1) + K(t)\varepsilon(t) \quad (2.16)$$

$$K(t) = \frac{FP(t-1)\varphi(t)}{1 + \varphi^T(t)P(t-1)\varphi(t)} \quad (2.17)$$

$$P(t) = FP(t-1)F^T - \frac{FP(t-1)\varphi(t)\varphi^T(t)P(t-1)F^T}{1 + \varphi^T(t)P(t-1)\varphi(t)} + R_1 \quad (2.18)$$

$$F = \begin{bmatrix} 1 & 0 & 0 & 0 \\ 0 & 1 & 0 & 0 \\ 0 & 0 & 1+f & -f \\ 0 & 0 & 1 & 0 \end{bmatrix} \quad (2.19)$$

where $\varepsilon(t)$ is the predictor error, $s_{O_f}(t)$ is the filtered DO signal, and $\hat{s}_{O_f}(t)$ is the predicted filtered signal, f is a filter pole between 0.9 and 1. The parameter vector θ is defined as $\theta = [\hat{k}_1 \quad \hat{k}_2 \quad \hat{r}_{SO}(t) \quad \hat{r}_{SO}(t-1)]^T$, where \hat{k}_1 and \hat{k}_2 are the estimated value of exponential K_{La} model, and the respiration rate $\hat{r}_{SO}(t)$, is the estimated value of respiration rate. The covariance matrix R_1 is a 4×4 diagonal matrix,

$R_1 = \text{diag}(\gamma_1, \gamma_1, \gamma_2, 0)$ which should have appropriate values. The parameter γ_1 is a small number, which reflects the slow variation in the K_{La} parameters. The much faster variation in the respiration rate is turned into a larger value of γ_2 . A too small value of γ_2 may give (a larger) bias in the estimate, since the Kalman filter will not be able to follow the variations in the true respiration rate. On the other hand, a too large value of γ_2 results in unnecessary large variations (due to measurement noise) of the estimated respiration rate (Lindberg, 1997). The regressor $\varphi(t)$ is given by:

$$\begin{aligned} \varphi(t) &= h^* [(s_{O_{sat}} \quad s_{O_f}(t-1)) [1 \quad e^{-k_2 u(t)/a} \quad k_1 u(t) e^{-k_2 u(t)/a} \quad 1 \quad 0]^T \\ h &= \frac{1}{K_{La}(u) + Q/V} e^{-(K_{La}(u) + Q/V)h} \quad 1 \end{aligned} \quad (2.20)$$

where h^* is a sampling time.

The predictor $\hat{s}_{O_f}(t)$ is given by:

$$\begin{aligned} \hat{s}_{O_f}(t|t-1) &= s_{O_f}(t-1) + h^* \left\{ \frac{Q(t-1)}{V} [s_{O_{in}}(t-1) \quad s_{O_f}(t-1)] + \right. \\ &+ K_{La}[u(t-1)] [s_{O_{sat}} \quad s_{O_f}(t-1)] \quad \hat{r}_{SO}(t-1) \} \end{aligned} \quad (2.21)$$

The presented results showed that a nonlinear model-based control algorithm for dissolved oxygen control really outperforms PID controller when both the oxygen uptake rate and the nonlinear oxygen transfer function are considered in the design of the controller. In this simulation, the time delay that always exists in the real biological treatment process is also considered, where the time delay was ten times the sampling time. The estimated respiration rate can also be useful for the determination of a suitable DO set point. It is important that the input signal should be sufficiently exciting, both in amplitude and in frequency to obtain good estimation result, especially with the measurement noise corrupted data.

When approximating the respiration rate and oxygen transfer function from measurement of DO and airflow rates, it is essential that a high excitation in the airflow rate be used. A high excitation in airflow rate entails rapid changes in DO. If the DO sensor is not fast, the estimates will be influenced. (Carlsson and Lindberg, 1996) considered a filtering procedure, developed by (Ahlen and Sternard, 1989). It is applied to reduce the influence of the DO sensor dynamic. The filtered DO measurements can then be used for estimating respiration rate and oxygen transfer function.

2.7 Methods for control of the dissolved oxygen concentration

2.7.1 First Dissolved Oxygen Control systems

The initial use of dissolved oxygen control systems for the activated sludge started as far as 1963 when it was for the activated sludge and post-aeration process control at the 120,000m³/day capacity wastewater treatment facility at Reno-Sparks, Nevada. After the initial success, the dissolved oxygen control systems were designed for activated sludge treatment plants at Oro Loma Sanitary District in San Lorenzo, California, the University of California at Davis, Carmel, California, and the San Francisco International Airport (Ryder, 1972).

In the plant Reno-Sparks, the requirement was for dissolved oxygen post-aeration control to economically assure that the discharge standards would be achieved. Furthermore, the stringent effluent BOD and solids standards required that the activated sludge system selected for secondary wastewater treatment operates at nearly maximum efficiency all the time.

Improvement of electrochemical sensing elements for the measurements of dissolved oxygen had been introduced as early as 1970's. And it has made it possible for the automation control of this most important factor of the activated sludge by maintaining a selected concentration of dissolved oxygen readily available for the purpose of control and operation (Ryder, 1972).

2.7.2 Diffused Aeration Control

The most primitive illustrations of aeration were applied to diffused aeration plants utilizing centrifugal blowers (Ryder, 1972). In one example, a multiple system of electrodes were monitored. A different approach to control the centrifugal blowers was utilized at Reno-Sparks (Ryder, 1972). In this case there was a control to both activated sludge aeration tanks and post-aeration tank following the secondary sedimentation tanks using the same group of aeration blowers. The desired range of dissolved oxygen could vary from 0.5 to 3mg/l in the mixed liquor and above a minimum of 6mg/l in the post-aeration tanks.

Regulation of the amount of air to each of three aeration tanks and the post-aeration tank had been accomplished through modulating of butterfly valves which response to both the wastewater flow and dissolved oxygen concentration. From the aeration tanks a triple pass is provided and can be operated flexibly for a number of modifications of the

activated sludge process for which it relies on the loading conditions and operational choice.

2.7.3 Mechanical Aerator Control

Dissolved oxygen may be controlled with equal facility in the mechanical aeration systems as readily as those with diffused air. The example given was that of Oro Loma Water Pollution Control Plant where three aeration tanks, each with 18.6 kW or 25 h.p. surface aerators are installed in pairs in each of the aeration tanks (Ryder, 1972). The first quarter of the tanks were utilized for returned sludge reaeration. The remaining three-quarters of the tanks could optionally be operated as plug flow or continuous mixed aeration patterns.

The utilization of dissolved oxygen signal in cascaded control system for adjustment of the set-point of the immersed controllers is to maintain a predetermined concentration of dissolved oxygen in aeration tanks, usually at 1 or 1.5 mg/l. Only one of the surface aerators in each tank was positioned from the DO control system. Other units were just following the leader to maintain the same submergence setting. The two aerators in reaeration zone of each tank were controlled by similar but independent system.

The cost of providing dissolved oxygen control was approximated at \$5000 for the sensor, amplifier, transducer, controller, and positioner. Oro Loma Wastewater Treatment Plant had six control loops of this kind, representing a cost in the region of \$30,000. It had been concluded that since it cost around \$15,000 to operate aerators at Oro Loma by continuous dissolved oxygen control, considerable economic savings would be provided through the set control system (Ryder, 1972).

2.7.4 Elementary control concepts of the aerated sludge process

2.7.4.1 Objectives of control

A wastewater treatment plant is certainly not at steady state, but it is for ever subjected to disturbances. The influent flow rate, composition and concentrations will vary significantly. Internal streams are purposefully or unintentionally changed. In an advanced nutrient removal plant there are many biological processes happening concurrently. Each of these needs special operating conditions and reacts differently to the disturbances. An example being whereby carbonaceous removal and nitrification compete for dissolved oxygen (Spanjers *et al*, 1996).

In control it is of great importance to determine an objective, but this is not always stated clearly. Typically, the primary objective is to keep the plant running, while meeting the effluent standards. The overall challenge is often to run the plant consistently in the absence of all disturbances, with the help of measurement information and manipulated variables. Usually the coupling between the influent loading circumstances and the effluent quality is extremely tricky to measure.

Owing to that it is important to describe operational objectives. Given the necessary conditions, they will both guarantee a satisfactory final effluent. Distinctive operating objectives are (Spanjers *et al*, 1996): growing of the right biomass population, maintaining a good mixture where appropriate, and avoiding the clarifier overloading. The control problem is made more complicated by the several couplings within the plant (caused by internal recycles) as well as to the sewer system. Moreover, there are couplings that couples together water and sludge treatment. Many fundamental problems as result of lack of proper functioning of the plant are due to biochemical/microbiological reactions. Some desired operating conditions often seem to be too limited to control the plant due to the fact that the availability of the variables is being influenced.

Measurements are the foundation of the control. It is demonstrated that respirometers can add critical information for the control of a treatment plant. All the variables that influence the process are called inputs. A few of them can be manipulated, so they are manipulated variables. Typically those manipulated variables are: air flow rate, chemical dosage rate, waste flow rate and recycle flow rate. Other inputs that can affect the process are externally generated. The reason is that they cannot be manipulated for influencing the process and are thus defined as disturbances. The example being the influent flow rate which sometimes can be manipulated, if not it is considered a disturbance. Some of the disturbances can be measured.

Many of the disturbances in a treatment plant are related to the influent, like the influent flow rate and concentration changes. Others are attributed to the operation of other unit processes, like filter backwashing, or digester supernatant recycling (Spanjers *et al*, 1996). They are inputs to the aerator as long as they influence the behaviour of the aerator. The process is defined by state variables, typically the concentrations of different types of substrate and organisms. It is of firm believed that these are not directly measurable. Instead, the process is observed by measurements that are related to the

In control it is of great importance to determine an objective, but this is not always stated clearly. Typically, the primary objective is to keep the plant running, while meeting the effluent standards. The overall challenge is often to run the plant consistently in the absence of all disturbances, with the help of measurement information and manipulated variables. Usually the coupling between the influent loading circumstances and the effluent quality is extremely tricky to measure.

Owing to that it is important to describe operational objectives. Given the necessary conditions, they will both guarantee a satisfactory final effluent. Distinctive operating objectives are (Spanjers *et al*, 1996): growing of the right biomass population, maintaining a good mixture where appropriate, and avoiding the clarifier overloading. The control problem is made more complicated by the several couplings within the plant (caused by internal recycles) as well as to the sewer system. Moreover, there are couplings that couples together water and sludge treatment. Many fundamental problems as result of lack of proper functioning of the plant are due to biochemical/microbiological reactions. Some desired operating conditions often seem to be too limited to control the plant due to the fact that the availability of the variables is being influenced.

Measurements are the foundation of the control. It is demonstrated that respirometers can add critical information for the control of a treatment plant. All the variables that influence the process are called inputs. A few of them can be manipulated, so they are manipulated variables. Typically those manipulated variables are: air flow rate, chemical dosage rate, waste flow rate and recycle flow rate. Other inputs that can affect the process are externally generated. The reason is that they cannot be manipulated for influencing the process and are thus defined as disturbances. The example being the influent flow rate which sometimes can be manipulated, if not it is considered a disturbance. Some of the disturbances can be measured.

Many of the disturbances in a treatment plant are related to the influent, like the influent flow rate and concentration changes. Others are attributed to the operation of other unit processes, like filter backwashing, or digester supernatant recycling (Spanjers *et al*, 1996). They are inputs to the aerator as long as they influence the behaviour of the aerator. The process is defined by state variables, typically the concentrations of different types of substrate and organisms. It is of firm believed that these are not directly measurable. Instead, the process is observed by measurements that are related to the

state variables. Together the DO concentration and respiration rate r_{SO} are examples of measured variables.

2.7.4.2 Dissolved Oxygen Levels

The readily available methods of continuously maintaining a selected concentration of dissolved oxygen keep the plant operation at the level required by this concentration. From the economic perspective operations related to power consumption, for effective activated sludge results for oxygen concentration should be at minimum. The larger the gradient between saturation and maintained oxygen concentrations, the greater the oxygen transfer for an equivalent amount of aeration and power consumption. There are lower limits imposed by the period when the sludge is in the secondary sedimentation tank and the dissolved oxygen is depleted by the metabolic organisms.

Higher dissolved oxygen concentrations can result in excessive nitrification, proliferation of filamentous organisms, and by mechanical shear result in poorly settling activated sludge. It had been evident from the initial start-up of the Reno-Sparks, Oro Loma and Davis plants whereby those problems were clearly defined. It had been found that a dissolved oxygen concentration of mixed liquor in the aeration tanks ranges from 0.75 to 1 mg/l in the aeration tank, and it permitted zero dissolved oxygen in the final sedimentation tanks, which imposed an unfavourable environment for the filamentous organisms, and the control of the sludge bulking.

The practical implication is getting the optimum conditions for an efficient and rapidly settling of activated sludge, which could be obtained as a result of controlled dissolved oxygen within close limits in the region of 0.5 to 1.5 mg/l. This is of particular importance considering overloading or high carbohydrates fed contributing to the enhancement of the growth of filamentous organisms.

2.7.4.3 Standard control schemes for DO concentration and respiration rate control

The simple closed Feedforward and mixed loop schemes are very much used in wastewater treatment plants for DO concentration or respiration rate control. The summary of these schemes is given in Figure 2.8 where D is a disturbance input, O is the output, and MV is the manipulated variable. Standard feedback (FB) control scheme is illustrated in Figure 2.8 (a). One or more measured variables are inputs to the controller and they are weighed against the set-point (reference) values. The idea is for the

controller to hold the measured variables as closely as possible to the set-point values, regardless of the disturbances (Spanjers *et al*, 1996). To illustrate the concepts, two control loops are considered, DO control and respiration rate control. Traditionally in DO controls, DO concentration is measured and compared with the desired DO concentration. The air flow rate is influenced in such way that the DO concentration would reach the desired value. Respiration rate here is considered as a disturbance; the reason for this is that it is the one that changes the DO concentration. The control system does not recognize that r_{SO} may be influenced by air flow rate and it does not explicitly take r_{SO} into consideration. It can be alleged that a toxic substance has entered the plant as a result of the slump in r_{SO} . The DO controller will notice that less flow rate is needed to reach the DO set-point value, but it does not identify that the toxic disturbance has entered the plant. A decrease in substrate concentration would have caused the similar control action, but such a strategy would need to be implemented with caution using complicated measurements (Spanjers *et al*, 1996).

When considering a respiration control system, it is a known fact that the respiration rate is measured and the results are compared with the desired r_{SO} (the r_{SO} set-point). Like it is in DO control, the air flow rate is manipulated so that the set-point is reached. (Note that in this case the DO concentration will also be changed, but only that value that corresponds to the change of the respiration rate). Before, r_{SO} was considered to be a disturbance. But here it is the controlled variable, and the disturbances consist of, for instance, substrate concentration changes, pH or toxic changes, that will cause r_{SO} to change. Such a change is directly noticeable through the measured value. It is of great importance to notice that a further analysis needs to be undertaken to determine exactly what is causing the change in r_{SO} . It is demonstrated using the above two examples, that one has to define the boundary between the controller and the surrounding in each case, so that the inputs and disturbances are properly recognized.

Feedforward (FF) control is applicable when disturbances are measured. The manipulated variable is adjusted to compensate for the effect of the disturbance. The idea is that the effect of the disturbance and the FF control action compensate each other out, and there is no deviation from the set-point. The basic design principle is shown in Figure.2.8 (b). The FF control is such that a model is needed for it to calculate how much of the MV is required for cancelling out the disturbance. Since the result of the

disturbance on the output has not yet been seen, the controller has to be able to calculate its outcome before it actually happens. It is not possible to completely cancel out the influence of a disturbance with FF control, the reason being that the models and measurements are not always perfect. Therefore, it is always strongly advisable to merge FF controller with a FB controller together (Figure.2.8(c)). The FF controller makes a swift compensation for the disturbance, while the FB controller adjusts in slower time scale, resultant respond is combination of accuracy and speed.

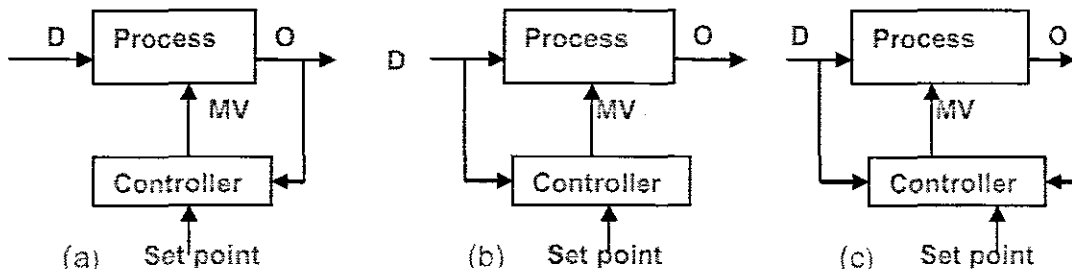


Figure 2.8: (a) Standard feedback control, (b) Feedforward control and (c) Feedforward-feedback control.

2.7.5 Respirometry in control

Through personal interactions and literature review, the overview of existing suggestions and applications of respirometry-based control strategies of the activated sludge process are provided by IAWQ Task Group (Spanjers *et al*, 1996). The authors classified the different applications to support further developments of activated sludge process control systems that include respirometry. In the review all the proposals in which respiration rate was directly implicated in the control system were considered giving sufficient explanation where necessary. Both automatic and manual controls were considered.

Classification of the strategies as based on different elements of respirometry-based control system, meaning the location of the respirometer, measured or deduced (input or output) variable, controlled variable, manipulated variable. For each of these elements, a number of possibilities were found in the literature and classifications could be based on any characteristic. IAWQ Task Group recommended a classification that is based on the manipulated variable to identify the control scheme. The decision was based on the idea that it had to be revealed as some classifications are more prone to confusion and

misunderstanding than others, and such measures were taken at Copenhagen Specialised Conference on Sensors in 1995.

The list of the manipulated variables that were proposed to act on the activated sludge process on the basis of respirometry included most control handles available in current treatment plants. The authors have found references where air flow rates, influent, return activated sludge, waste, sludge storage, internal nitrate recycle, chemical dosage, and sludge treatment return liquor are controlled using respirometry.

Most of the practical applications of oxygen measurements are performed in the liquid phase. Hence, respirometric methods described in the development of this introduction will be limited to respirometers where oxygen is measured in the liquid phase using dissolved oxygen electrode. The respiration rate is calculated by making a general mass balance for oxygen over liquid phase. The equation includes among other things, a transport term, an aeration term and a term describing the oxygen uptake rate r_{sO} by the microorganisms. Nevertheless, depending on the design of the respirometer the transport and aeration terms may not be needed.

$$\frac{ds_o}{dt} = \frac{Q_{in}}{V}(s_{o,in} - s_o) + K_{La}(s_o^0 - s_o) - r_{sO} \quad (2.22)$$

2.8 Analysis of the existing situation

The dissolved oxygen concentration (DO) in the aerobic part of an activated sludge process should be sufficiently high to supply adequate oxygen to the micro-organisms in the sludge, as it plays an integral part for control of wastewater treatment plants. On the other hand, an excessively high DO (which requires a high airflow rate) leads to high energy consumption and may also deteriorate the sludge quality. A high DO concentration in the internally re-circulated water also means the denitrification less efficient. Hence, both for economical and process reasons, it is of great importance to control the DO. (Lindberg and Carlsson, 1996) developed a strategy for DO controller based on the nonlinear DO transfer function, the reason being to illustrate that nonlinear DO controller can outperform a standard PI controller.

Dissolved oxygen is a nonlinear process which makes it difficult to be controlled. A lot of different control techniques have been tried in the past, but none came close to solving the exact problem. High control performance for all operating conditions is not easily

achievable with any type of linear controllers. In order to attain a high performance controller for all operating conditions, the main focus is to take into consideration the nonlinear characteristics of the oxygen transfer function K_{La} when designing the controller.

Dissolved oxygen concentration is characterised by two important parameters, oxygen transfer function K_{La} and oxygen uptake rate r_{SO} (Respiration). The oxygen transfer depicts that it depends on several variables in the form of oxygen transfer rate and mass transfer coefficient as the literatures describe.

Automatic control techniques were used for DO control in wastewater treatment processes for many years, the reason being:

- The sensors for measurement of DO were available.
- The DO control reduces the amount of energy for blowing of air in the aeration basin.
- The effluent characteristics and process performance depend on the proper DO.

The normally used controllers over the years are proportional integral (PI) or proportional integral differential (PID). The work performed by the said controllers above led to not very good system performance, simply because

- The set-points are selected according to some nominal system requirements and not according to the operating conditions of the process at moment of control.
- The parameters of the controllers are not determined according to the operating conditions of the process.
- The controllers are designed for linear process, whereas the process of dissolving of oxygen into the wastewater is a nonlinear process.

These drawbacks are being dealt with in by considering the problem for DO control in a scheme of 3 layer hierarchy in Figure 2.9 where;

1. Layer 3 is where the model parameters are estimated on the basis of the predicted process variables. The model parameters are estimated every two hours on the basis of predicted values of process disturbances and real values of the measured process variables.
2. Layer 2 is where the optimal set-point for the DO controller is determined through the solution of optimal control problem on the basis of measurement of the

process variables and prediction of the process disturbances. The problem for optimal control is solved in the scheme of repetitive optimization every two hours depending on the dynamics of the system disturbances. The obtained optimal DO trajectory is used to determine set points for the design of the nonlinear controller on layer 2 and for stabilizing control on layer 1. The controller is designed on the basis of the estimated model parameters and optimal set point for the DO concentration.

3. Layer 1 is where the controller parameters are programmed in PLC and the control action is produced.

The problems solved in the thesis are for estimation of the values of the parameters of the model of the dissolved oxygen concentration on layer 3, for design of the linearizing and linear controllers on the layer 2, and for the implementation of the controller in PLC for direct control.

The design of the controller parameters is done by the methods developed in the thesis and these methods are based on the consideration that DO process is a nonlinear one. The idea is still to keep the industry standard PI controller, but some additional control to be introduced in order to cope with the nonlinear character of the process.

The methods proposed consist of two steps:

- Design of a nonlinear linearizing controllers using the second method of Lyapunov or the input/output linearization theory
- Design of a linear (PI) controller

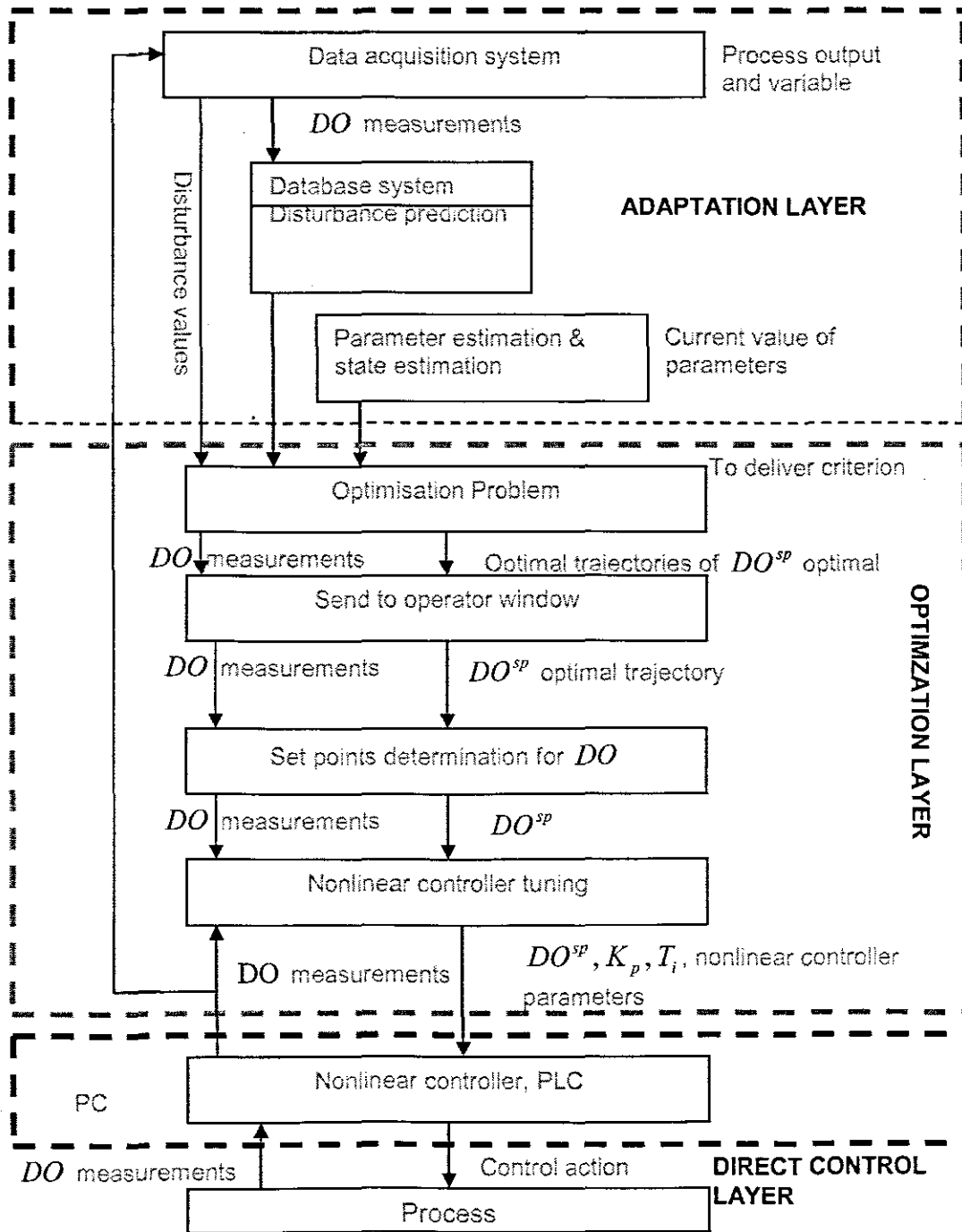


Figure 2.9: Hierarchy of control tasks

2.9 Conclusion

This chapter gives an introduction of wastewater treatment process. For the effective removal of the nutrients, the structure of WWTP together with the processes such as primary, biological, chemical, and sludge treatment are looked at. The biological treatment of wastewater, particularly, the activated sludge process is discussed.

In ensuring the effective control of the process (ASP) by controlling dissolved oxygen concentration, two factors that affect the dynamics of the DO, oxygen uptake rate (respiration) and nonlinear oxygen transfer function were taken into consideration. Review of the methods for application of respiration and of the DO model parameter estimation was performed. Since the thesis deals with designing the nonlinear controller, then an overview of the existing control methods of DO was done.

Chapter 3 provides the overview of the mathematical modelling of the dissolved oxygen concentration of the ASP based on ASM1 biological model. Also different models of oxygen transfer function are discussed and simulated.

CHAPTER THREE

DEVELOPMENT OF A MATHEMATICAL MODEL OF THE DISSOLVED OXYGEN CONCENTRATION PROCESS

3.1 Introduction

Dissolved oxygen concentration is one of the principal control parameters in the activated sludge systems (Lindberg and Carlsson, 1996). (Vanrolleghem and Lee, 2003) stated that, "Oxygen plays an integral part in activated sludge process." If the associated aeration is done in an optimal way it will lead to substantial reduction in the process energy consumption. Aeration takes place in the aerobic reactors, but practically, DO concentration s_o in the activated sludge process is maintained by manoeuvring aeration airflow Q_{air} considered as a control input u . The aeration input can be represented by the oxygen transfer function K_{La} . Different types of K_{La} are analyzed for the purpose of developing a nonlinear controller for controlling dissolved oxygen concentration in the aeration tank of the Activated sludge process (Lindberg, 1997)

This chapter introduces the structure of the activated sludge process (ASP) and the description of the COST Benchmark wastewater treatment process based on the ASM1 biological model in sections 3.2 and 3.3 respectively. Section 3.4 gives mass-balance model of the dissolved oxygen concentration for the Benchmark layout. Development of the mathematical model of the oxygen transfer function is in section 3.5. An exponential model of oxygen transfer function is given in section 3.6 and this model is used in section 3.7 to develop dissolved oxygen model equation in standard affine form which is applied to the controller design for the model of dissolved oxygen concentration. Simulink block diagrams are provided for the sole purpose of simulations and their simulation results are shown in section 3.8

3.2 Structure of the Activated Sludge Process (ASP) mass balance model

Dissolved oxygen concentration is one of the main control variables of the ASP when the process of carbon and nitrogen removal is considered. There is influence of the diurnal variation of the flow and concentrations of the inflow over the activities of the microorganisms and in this way over the concentrations of the DO. This requires improved control of the required concentration of the DO.

The ASP is a complex nonlinear process and proper control of the airflow rate is necessary to be implemented. This means that proper controller has to be designed and implemented in order to follow requirements of the microorganisms for dissolved oxygen. Different control design methods can be applied. These methods are based on mathematical models of the ASP incorporating both mass balances of the flows and process variables in the plant, with biochemical activities of microorganisms and mass balance of the oxygen with the processes of dissolving and uptaking of oxygen in the wastewater. These two models can be considered in a series in the following way as depicted in Figure 3.1, where s_{od} is the concentration of DO as a result of dissolving oxygen in water.

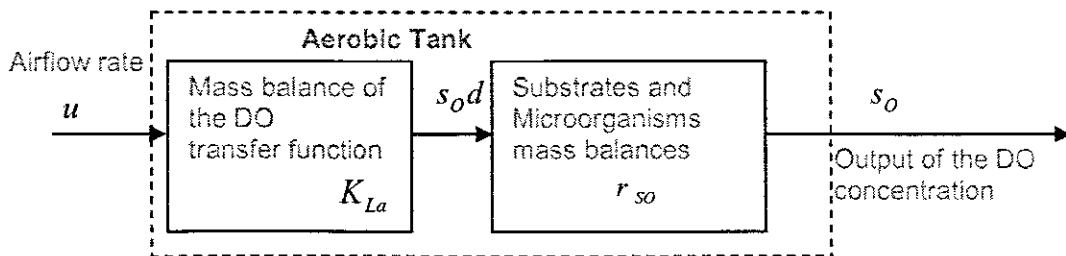


Figure 3.1: Common model of the DO process for design of control using the airflow rate as a manipulated variable

Various aeration strategies can be implemented on the basis of different models of DO concentration, different types of DO controllers and different types of design methods can be used to design the controllers. These aeration strategies can be considered as a part of the three-layer control strategy of the ASP described in Chapter 2. The research work in the thesis concentrates on the modelling and control of the DO concentration. All derivations are done for the COST Benchmark process based on the ASM1 biological model.

3.3 Description of the COST Benchmark process based on ASM1 biological model

Benchmark model Figure 3.2 is defined as a protocol to obtain a measure of performance of control strategies for activated sludge plants based on numerical, realistic simulations of the controlled plants. The benchmark consists of a description of the plant layout, a simulation of biological model (ASM1) and definitions of controller performance. The benchmark is not correlated to any particular simulation platform, meaning any

commercial WWTP simulation software packages can be used as well direct coding (C, C++ or FORTRAN), (IWA Taskgroup,2008),(Copp, 2002).

The benchmark process is composed of a five-compartment of the activated sludge reactor consisting of two anoxic tanks, which are not aerated, but fully mixed, followed by three aerobic tanks. The plant consequently merges nitrification with predenitrification in a configuration that is usually used for realizing biological nitrogen removal in full-scale plants. The activated sludge reactor is followed by a secondary settler.

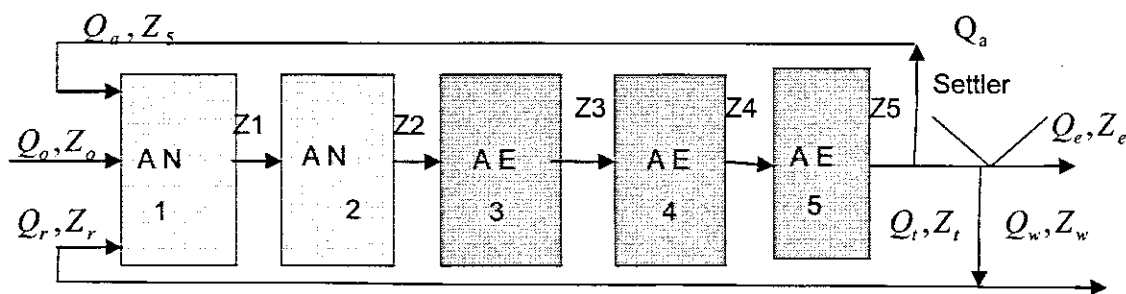


Figure 3.2: The benchmark structure

The notations on the model are:

- For the flow rates: Q_o is the input flow rate, Q_r is the return flow rate, Q_a is the internal recycle flow rate, Q_t is the input for the settler flow rate, Q_w is the wasting sludge flow rate, and Q_e is the effluent flow rate.
- For the variables concentrations, the vector Z is for all process variables concentrations, one of its components is the DO which is noted as s_o .

3.3.1 Process flows and oxygen transfer functions

The list of system parameters with their units is given in Table 3.1.

Table 3.1: Process flows and oxygen transfer functions

	Default System Values	units
Influent flow rate	18446	m ³ day ⁻¹
Recycle flow rate	12446	m ³ day ⁻¹
Internal recycle flow rate	55338	m ³ day ⁻¹
Wastage flow rate	385	m ³ day ⁻¹
K_{La} -Tank 1 and Tank 2	n/a	-

commercial WWTP simulation software packages can be used as well direct coding (C, C++ or FORTRAN), (IWA Taskgroup,2008),(Copp, 2002).

The benchmark process is composed of a five-compartment of the activated sludge reactor consisting of two anoxic tanks, which are not aerated, but fully mixed, followed by three aerobic tanks. The plant consequently merges nitrification with predenitrification in a configuration that is usually used for realizing biological nitrogen removal in full-scale plants. The activated sludge reactor is followed by a secondary settler.

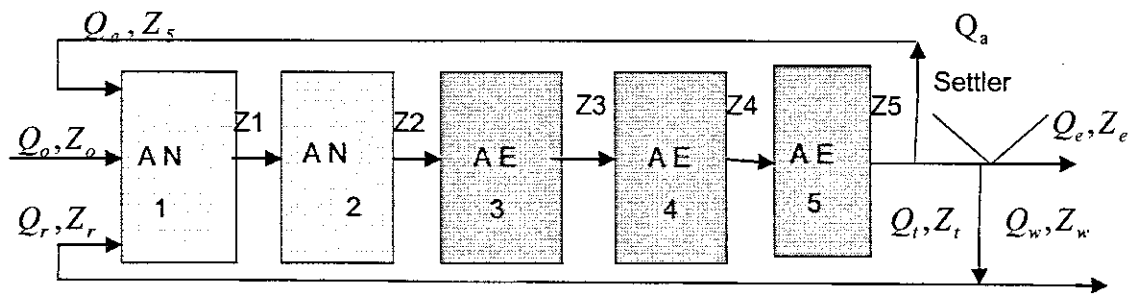


Figure 3.2: The benchmark structure

The notations on the model are:

- For the flow rates: Q_o is the input flow rate, Q_r is the return flow rate, Q_a is the internal recycle flow rate, Q_t is the input for the settler flow rate, Q_w is the wasting sludge flow rate, and Q_e is the effluent flow rate.
- For the variables concentrations, the vector Z is for all process variables concentrations, one of its components is the DO which is noted as s_o .

3.3.1 Process flows and oxygen transfer functions

The list of system parameters with their units is given in Table 3.1.

Table 3.1: Process flows and oxygen transfer functions

	Default System Values	units
Influent flow rate	18446	m ³ day ⁻¹
Recycle flow rate	18446	m ³ day ⁻¹
Internal recycle flow rate	55338	m ³ day ⁻¹
Wastage flow rate	385	m ³ day ⁻¹
K_{La} -Tank 1 and Tank 2	n/a	-

K_{La} - Tank 3	10	hr ⁻¹
K_{La} - Tank 4	10	hr ⁻¹
K_{La} - Tank 5	3.5	hr ⁻¹

3.3.2 Values of the ASM1 model parameters

The kinetic parameter values are listed below in Table 3.2. Included in the table are parameter descriptions, parameter symbols, units and their associated values

Table 3.2: Kinetic parameter values for ASM1

Parameter Description	Parameter Symbol	Value	Units
Maximum heterotrophic growth rate	μ_{mH}	4.0	day ⁻¹
Half-saturation (hetero. growth)	K_S	10.0	g COD m ⁻³
Half-saturation (hetero. oxygen)	K_{OH}	0.2	g O ₂ m ⁻³
Half-saturation (nitrate)	K_{NO}	0.5	g NO ₃ -N m ⁻³
Heterotrophic decay	b_H	0.3	day ⁻¹
Anoxic growth rate correction factor	η_g	0.8	No dimension
Anoxic hydrolysis rate correction factor	η_h	0.8	No dimension
Maximum specific hydrolysis rate	K_h	3.0	$g x_S (g x_{B,H} COD \cdot day)^{-1}$
Half-saturation (hydrolysis)	K_X	0.1	$g x_S (g x_{B,H} COD)^{-1}$
Maximum autotrophic growth rate	μ_{mA}	0.5	day ⁻¹
Half-saturation (auto. growth)	K_{NH}	1.0	g NH ₂ -N m ⁻³
Autotrophic decay rate	b_A	0.05	day ⁻¹
Half-saturation (auto. oxygen)	K_{O_d}	0.4	G O ₂ m ⁻³
Ammonification rate	k_a	0.05	$m^{-3} (g COD \cdot day)^{-1}$

3.3.3 Process variables

Table 3.3 lists the ASM1 13 state variables, their associated symbols and their units (Henze *et al*, 1987).

Table 3.3: State Variables for the IAWQ Activated Sludge Model #1 (ASM1)

State Variable description	State Symbol	Units
Soluble inert organic matter	X	g COD m ⁻³

Readily biodegradable substrate	s_S	g COD m ⁻³
Particulate inert organic matter	x_I	g COD m ⁻³
Slowly biodegradable substrate	x_S	g COD m ⁻³
Active heterotrophic biomass	$x_{B,H}$	g COD m ⁻³
Active autotrophic biomass	$x_{B,A}$	g COD m ⁻³
Particulate product arising from biomass decay	x_P	g COD m ⁻³
Oxygen	s_O	g COD m ⁻³
Nitrate and nitrite nitrogen,	s_{NO}	g N m ⁻³
NH ₄ ⁺ + NH ₃ nitrogen	s_{NH}	g N m ⁻³
Soluble biodegradable organic nitrogen	s_{ND}	g N m ⁻³
Particulate biodegradable organic nitrogen	x_{ND}	g N m ⁻³
Alkalinity	s_{ALK}	mol L ⁻¹

3.4 Mass-balance model of the dissolved oxygen concentration for the Benchmark plant (layout)

The process dynamics are obtainable through the application of the principles of mass balances to the aeration tank in the wastewater process structure. The considered structure has 3 aeration basins. The considerations will be done for one of them as the basins are similar. Dynamic of the dissolved oxygen concentration in the n^{th} aeration tank can be described by the following mass balance equation:

$$\dot{s}_O(t) = \frac{1}{V_n} [Q_{n-1}s_{O,n-1}(t) + V_n r_{SO,n}(t) + V_n K_{La,n} u(t)(s_{O,sat} - s_{O,n}(t)) - Q_n s_{O,n}(t)] \quad (3.1)$$

where $Q_n = Q_{n-1} = Q_o + Q_r + Q_a$, $s_{O,n}(0) = s_{OO,n}$. $s_{OO,n}$ is the initial state, $s_{O,n}(t)$ [mg/l] is the dissolved oxygen concentration in the n^{th} tank, K_{La} is the oxygen transfer function, $s_{O,sat}$ [mg/l] is the dissolved oxygen concentration at saturation point, $r_{SO,n}(t)$ [d⁻¹] is the oxygen uptake rate, V [m³] is the volume of the tank and u is the airflow rate, $r_{SO,n}$ is the respiration rate. The index n will be omitted further in the thesis because the structure of the DO model for every aerobic tank is the same. The oxygen utilisation rate is given by ASM1 biological model as:

$$\begin{aligned}
r_{So}(t) = & -\hat{\mu}_H \left(\frac{1-Y_H}{Y_H} \right) \left(\frac{s_{S,n}(t)}{K_S + s_{S,n}(t)} \right) \left(\frac{s_{O,n}(t)}{K_{OH} + s_{O,n}(t)} \right) x_{BH}(t) - \\
& -\hat{\mu}_A \left(\frac{4.57-Y_A}{Y_A} \right) \left(\frac{s_{NH,n}(t)}{K_{NH} + s_{NH,n}(t)} \right) \left(\frac{s_{O,n}(t)}{K_{OA} + s_{O,n}(t)} \right) x_{BA}(t)
\end{aligned} \tag{3.2}$$

where μ_H is the maximum heterotrophic growth rate, Y_H is the heterotrophic yield, μ_A is the maximum autotrophic growth rate, Y_A is the autotrophic yield, $s_{S,n}(t)$ is the readily biodegradable substrate, $s_{NH,n}(t)$ is the $NH_4^+ + NH_3$ nitrogen, $K_{NH}, K_{OA}, K_{OH}, K_S$ are the half-saturation coefficients for heterotrophic growth rate, autotrophic growth, and autotrophic decay respectively.

Here the respiration rate is determined by other process variables. This is a very complex equation to be used for real time control. That is why oxygen uptake rate will be considered as a nonlinear function which can be calculated on the basis of measurements of the dissolved oxygen concentration and the air flow rate $u(t)$ following estimation procedure. It is assumed that $s_{O,n}(t), s_{O,n-1}(t), u$ and wastewater flow rates Q are measured and $s_O, s_{O,sat}$ and V_n are constants. The equation for the DO can be rewritten in the following way:

$$\dot{s}_{O,n}(t) = \frac{1}{V_n} [Q_n(s_{O,n-1}(t) - s_{O,n}(t))] + r_{SO,n}(t) + K_{La,n}u(t)(s_{O,sat} - s_{O,n}(t)) \tag{3.3}$$

Taking into account that the tanks are identical, then for simplicity it is accepted that $s_{O,n} = s_O, Q_n = Q, V_n = V, s_{O,n-1} = s_{O,in}$. The equations (3.2) and (3.3) represent the model of the process for dissolved oxygen control.

The control action of this process is airflow rate, controlled output is the concentration of dissolved oxygen and uncontrolled disturbances are the inflow DO concentration and the oxygen utilisation rate. The disturbances depend on the input flow characteristics and will change requirements of the microorganisms for oxygen. The results of these changes are required for changing the set-point and controller parameters.

3.5 Mathematical model of the oxygen transfer function K_{La}

In the dissolved oxygen concentration dynamics, the oxygen transfer function K_{La} describes the dissolving of oxygen on the basis of the flow rate of air into the water. It

describes the rate at which oxygen is being transferred to the wastewater by the system for the aeration, as a function of airflow rate.

$$K_{La}(u(t))(s_{O_{sat}} - s_O(t)), s_{O_{sat}} > s_O(t) \quad (3.4)$$

The oxygen transfer function (coefficient) can be related to the changes in the intensity of aeration, which is considered as a control input $u(t)$. There are different models of K_{La} proposed in the existing literature as follows:

- Linear relationship with a nonzero intercept (Reinius and Hultgren, 1988), (MaKinia, 1998), (Bocken *et al*, 1989), (Holmberg *et al*, 1989) $K_{La}u(t) = k_1(t)u(t) - k_2(t)$, where k_2 and k_1 are empirical constants or time varying parameters
- Power function of the airflow rate (Cheng, Roth, Eckenfelder, 1980) $K_{La}u(t) = k_1(t)u(t)^{k_2(t)}$
- Exponential model (Lindberg, 1997) $K_{La}(u(t)) = k_1(1 - e^{-k_2u(t)^a})$, where a is a scaling factor, k_1 and k_2 are parameters
- No aeration control, meaning that, the aerators are continuously on during the whole time $K_{La}u(t) = k_1(t)$
- Linear transfer function (Haarsma, Keesman, 1995), (Holmberg, 1990), (Lukasse *et al*, 1996) $K_{La}u(t) = k_1(t)u(t)$
- Square root function (Holmberg *et al*, 1989) $K_{La}u(t) = k_1(t)\sqrt{u(t)}$
- Monod type model $K_{La}u(t) = \frac{k_1(t)u(t)}{u(t) + k_2(t)}$

The transfer function K_{La} as a function of its parameters varies slowly in a matter of hours or even days. The transfer function depends on the aerator type, water depth, basin shape and even airflow rate. Aerator clogging accounts for much of the variations of K_{La} . That is why K_{La} is time dependant and has to be determined on-line. The oxygen respiration rate is determined in both, the primary respiration, used in synthesis and in the endogenous respiration, during decay. The respiration rate changes significantly in a number of hours; while K_{La} differs slightly from day to day.

Summary of the existing literature of the oxygen transfer function models is given below in Table 3.4.

Table 3.4: Different models for oxygen transfer function

Model	Equation
Step	$K_{La} = (0, k_1)$
Linear A	$K_{La} = k_1 \cdot u$
Linear B	$K_{La} = k_1 \cdot u + k_2$
Arctan	$K_{La} = k_1 \cdot \tan^{-1}(k_2 \cdot u)$
Square root	$K_{La} = k_1 \cdot \sqrt{u}$
Power	$K_{La} = k_1 \cdot u^{k_2}$
Exponential	$K_{La} = k_1 \cdot (1 - e^{-k_2 u})$
Polynomial	$K_{La} = k_1 \cdot u + k_2 \cdot \sqrt{u + k_3}$
Piecewise linear	$K_{La} = (k_1 + k_2 \cdot t) \cdot u$
Cubic spline	$K_{La} = f(u)$
Second order model	$K_{La} = k_1 u + k_2 u^2$
Monod type	$K_{La}(u) = \frac{k_1 u}{u + k_2}$

Fast estimation of respiration (oxygen uptake rate) is important given the fact that respiration appears to be the most important disturbance signal in the control of dissolved oxygen concentration and therefore could be used in improvement of control efficiency; the whole exercise is achievable through on-line estimation of respiration from the current values of dissolved oxygen concentration and airflow signals (S.Gerkšič *et al*, 2006). Estimation of oxygen transfer function K_{La} and oxygen uptake rate r_{SO} is determined in the thesis on the basis of least square method using the measurements of the airflow rate and DO.

3.6 An exponential model of K_{La}

(Lindberg, 1997) suggested that an exponential K_{La} might be a suitable choice as it gives a curve with a shape similar to the natural one, Figure 3.3. It can be noted though that only two parameters are necessary to estimate and is also possible to invert the K_{La}

function as inverting would make it easy to design a nonlinear controller. A typical curve of the $K_{La}(u)$ functions is given on Figure 3.3.

The designs of nonlinear controllers in the thesis are based on the exponential model of the oxygen transfer rate. It can be substituted in equation (3.4) to form the process model.

$$\dot{s}_o(t) = \frac{1}{V} Q(s_{O,in}(t) - s_o(t)) + r_{SO} + k_1(1 - e^{-k_2 u(t)})(s_{O,Sat} - s_o(t)) \quad (3.5)$$

The equation (3.5) is used for the design of the controller.

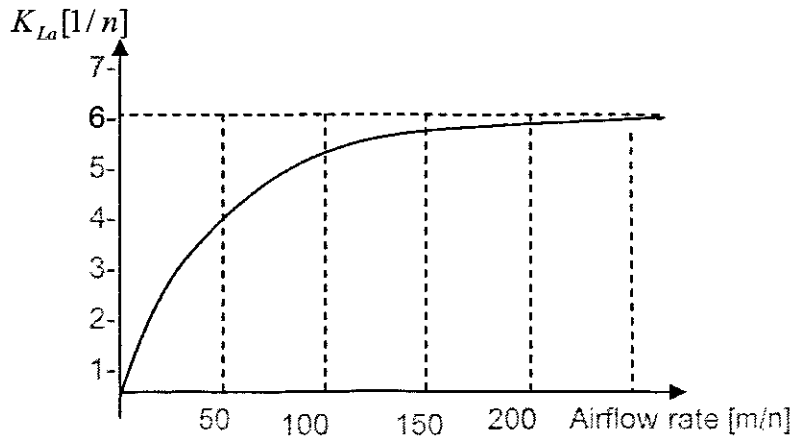


Figure 3.3: Exponential model curve of K_{La}

3.7 Dissolved Oxygen Model Equation representation in a standard affine form

The equation of the dissolved oxygen mass balance describes the model of the aerobic tank with one control input $u(t)$, two disturbance inputs $s_{O,in}$ and r_{SO} and one state/output s_o . A block diagram of this model is shown on Figure 3.4.

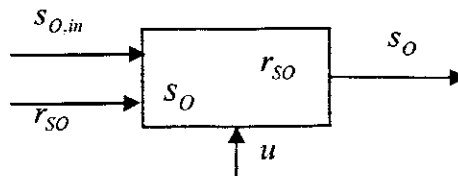


Figure 3.4: Block diagram of the dissolved oxygen concentration.

The equation (3.5) is a nonlinear one because of the nonlinear transfer function and because of the product between it and the dissolved oxygen variable. Equation (3.5) can be rewritten in a nonlinear affine standard form. This equation is used later for the design of the nonlinear controllers.

$$\dot{x}(t) = f(x) + g(x)u(t) + g_1(x)w(t) \quad (3.6)$$

where x is a state vector, u is the control vector, w is the disturbance vector and $f(x)$ and $g(x)$ are nonlinear functions. The following transformations are implemented in order to represent equation (3.5) in the form of equation (3.6). Introducing of the equivalent control $u_1(t) = -k_1 e^{-k_2 u(t)}$. Then

$$\begin{aligned} \dot{s}_o(t) &= \frac{Q}{V}(s_{o,in}(t) - s_o(t)) + K_{La}(s_{o,sat} - s_o(t)) + r_{SO}(t) = \\ &= \frac{Q}{V}s_{o,in}(t) - \frac{Q}{V}s_o(t) + r_{SO}(t) + k_1(1 - e^{-k_2 u})(s_{o,sat}(t) - s_o(t)) = \\ &= \frac{Q}{V}s_{o,in}(t) - \frac{Q}{V}s_o(t) + k_1(s_{o,sat}(t) - s_o(t)) - k_1 e^{-k_2 u(t)}(s_{o,sat}(t) - s_o(t)) + r_{SO}(t) = \\ &= \frac{Q}{V}s_{o,in}(t) - \frac{Q}{V}s_o(t) + r_{SO}(t) + k_1(s_{o,sat} - s_o(t)) + u_1(t)(s_{o,sat} - s_o(t)) \end{aligned} \quad (3.7)$$

The representation is obtained in the form

$$\dot{s}_o(t) = f(s_o(t)) + g(s_o(t))u_1(t) + g_1(s_o(t))s_{o,in}(t) + g_2(s_o(t))r_{SO}(t) \quad (3.8)$$

where $f(s_o) = -\frac{Q}{V}s_o(t) + k_1(s_{o,sat} - s_o(t))$; $g(s_o) = (s_{o,sat}(t) - s_o(t))$,

$$g_1(s_o) = \frac{Q}{V} = \text{Constant}, \text{ and } g_2(s_o) = 1 = \text{Constant}$$

The equation (3.9)

$$\dot{s}_o(t) = f(s_o(t)) + g(s_o(t))u_1(t) + g_1(s_o(t))s_{o,in}(t) + g_2(s_o(t))r_{SO}(t) \quad (3.9)$$

has 4 terms. First one describes the free dynamics of the dissolved oxygen. The second one describes the forced dynamics of the dissolved oxygen. The third and fourth terms describe the influence of the disturbances, i.e. inflow dissolved oxygen concentration and the oxygen uptake rate.

The control $u(t)$ can be calculated back from the control $u_1(t)$ using \ln function as follows;

$$\begin{aligned}
u_1(t) &= -k_1 e^{-k_2 u(t)} \\
\ln u_1(t) &= \ln(-k_1) + \ln(e^{-k_2 u(t)}) \\
\ln u_1(t) &= \ln(-k_1) - k_2 u(t) \\
\ln u_1(t) - \ln(-k_1) &= -k_2 u(t) \\
\ln \frac{u_1(t)}{-k_1} &= -k_2 u(t) \\
u(t) &= \frac{1}{-k_2} \ln \frac{u_1(t)}{-k_1}
\end{aligned} \tag{3.10}$$

The model (3.10) is used for design of the nonlinear controllers.

3.8 Simulation of the DO model in Simulink

3.8.1 Importance of simulation

Simulation is the route taken to use a numerical solution of the given model equations to approximate the behaviour of the system. In control engineering, the models are most often a collection of integro-differential equations, the solution to which represents the response of the system to specific ecological circumstances and inputs. Computer models differ in complexity from a few first-order differential equations to systems with multiple state variables such as a model of the space shuttle. More and more, control models of complicated systems are hybrids of differential equations working together with dynamic digital logic. For such systems simulation is necessary to study the potential response in different conditions.

Simulation is one of the most important resources in the field of control engineering and is the only common method of analysis able to find solutions to illogical nonlinear differential and difference equations. Evidently simulation locates only particular solutions, to be precise, solutions to the equations with specific inputs, initial conditions, and parameters. It is in support of that reason that simulation does not supplant other methods of analysis. Properties of significance such as stability or conditional stability cannot be verified with simulations.

3.8.2 Objectives of DO concentration model simulation

The objectives of the simulation of the DO concentration model are:

- To obtain solution of the model differential equation for the given step input of the airflow rate and steady state values of the process variables describing the oxygen uptake rate

- Investigating the influence of the external $s_{O,in}$ and internal r_{SO} disturbances over the dynamics of the DO concentration

Simulation and investigations are done in the software environment of Matlab/Simulink

3.8.3 Input data for simulation

Parameters for simulation of the Dissolved Oxygen Concentration are introduced in Matlab workspace by the program "DO_Open_Loop_Parameters.m". The program is given in the Appendix A. The corresponding Simulink model "DO_Mdel_2.mdl" is given in Figure 3.5. The input variables are the disturbances $s_{O,in}$, and r_{SO} the control signal u , and the parameters are $\mu_H, Y_H, \mu_A, Y_A, s_{S,n}, s_{NH,n}, K_{NH}, K_{OA}, K_{OH}, K_S$. The output variable is dissolved oxygen concentration s_O . The values of the parameters are taken from the ASM1 biological model and are given in Table 3.5. The values of k_1 and k_2 are calculated from the value $K_{La} = 240 \text{ day}^{-1}$ by a curve fitting for a given value of the airflow rate $u = 50000 \text{ m}^3/\text{day}$.

Table 3.5: Values of the model parameters

Par	μ_H	Y_H	μ_A	Y_A	$s_{S,n}$	$s_{NH,n}$	K_{NH}	K_{OA}	K_{OH}	K_S	k_1	k_2
Val	4	0.67	0.5	0.24	0.889	1.733	1.0	0.4	0.2	10.	240	$1.961e^{12}$

Table 3.5 gives the calculation of the parameters for the open loop control for internal and external disturbances variations. In order to achieve dynamic behaviour of the dissolved oxygen concentration for different cases of $s_{O,in}$ and r_{SO} , the latter is calculated for $\pm 10\% - \pm 50\%$ of both x_{BA} and x_{BH} and their calculated values are given in Table 3.6 below.

Table 3.6: Parameters table for open loop control

r_{SO}				$s_{O,in}$		
Xba	149.797	Xbh	2559.444	0.2	0.6	1
Xba-10%	134.8173	Xbh+10%	2815.3884	0.2	0.6	1
Xba+10%	164.7767	Xbh-10%	2303.4996	0.2	0.6	1
Xba-20%	119.8376	Xbh+20%	3071.3328	0.4	0.2	1
Xba+20%	179.7584	Xbh-20%	2047.5552	0.4	0.2	1
Xba-30%	104.8579	Xbh+30%	3327.2772	0.6	0.2	1
Xba+30%	194.7361	Xbh-30%	1791.6108	0.6	0.2	1
Xba-40%	89.8782	Xbh+40%	3583.2216	0.8	0.2	1

Xba+40%	209.7158	Xbh-40%	1535.6664	0.8	0.2	1
Xba-50%	74.8985	Xbh+50%	3839.166	1	0.2	0.6
Xba+50%	224.6955	Xbh-50%	1279.722	1	0.2	0.6

Simulink diagram of the dissolved oxygen concentration model is shown below on Figure 3.5. The model is used for simulation results for different behaviour of the dissolved concentration for steady state values of variables given above on Tables 3.5 and 3.6.

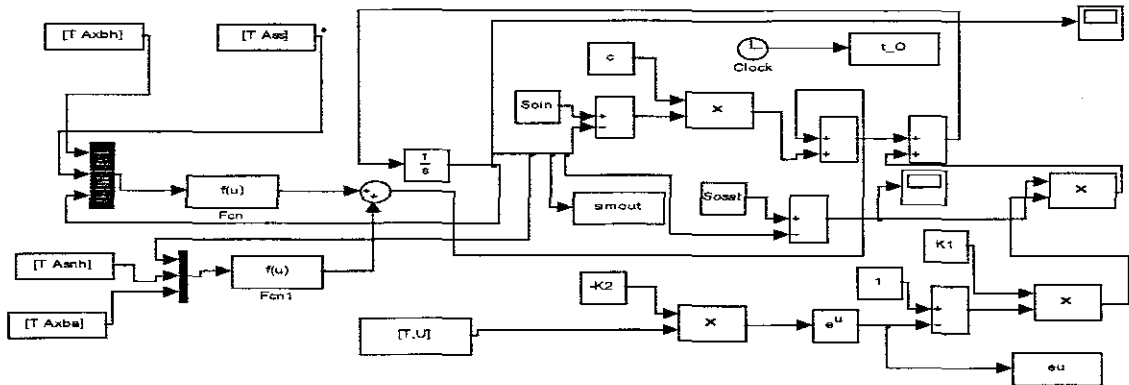


Figure 3.5: Representation of dissolved oxygen model in Simulink

3.8.4 Results from the simulation

The dynamic behaviour of the DO concentration for steady state values of the variables obtained from the Benchmark process with ASM1 biological model is shown in Figure 3.6. The dynamic behaviour of the DO concentration for different cases of disturbances $s_{O,in}$ and r_{SO} are shown in Figure 3.7 to 3.39.

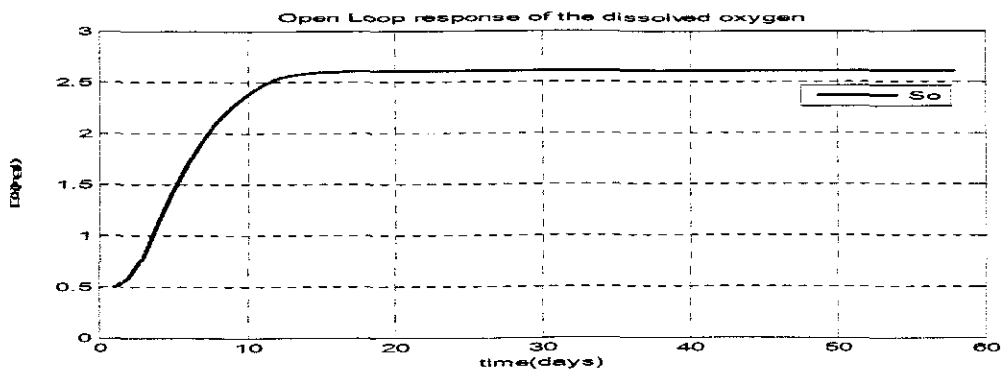


Figure 3.6: Open loop response of the dissolved oxygen model using $S_{O,in}=0.2$ and r_{SO} calculated for XBA of 149.797 and XBH of 2559.444

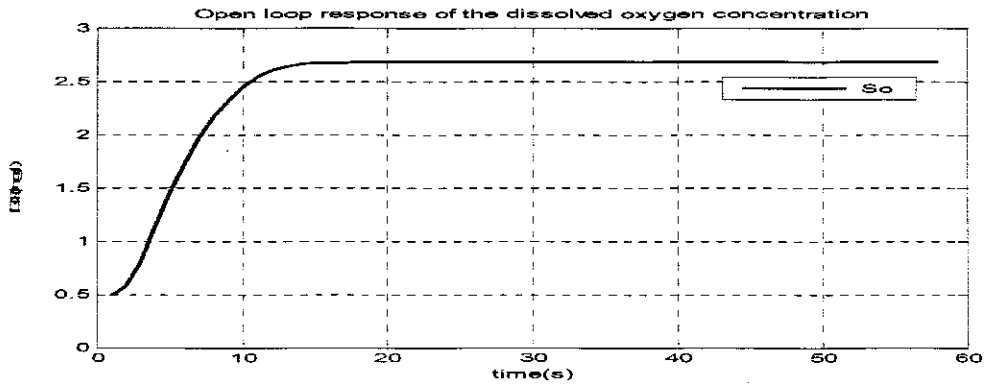


Figure 3.7: Open loop response of the dissolved oxygen model using $S_{oin}=0.6$ and r_{so} calculated for XBA of 149.797 and XBH of 2559.444

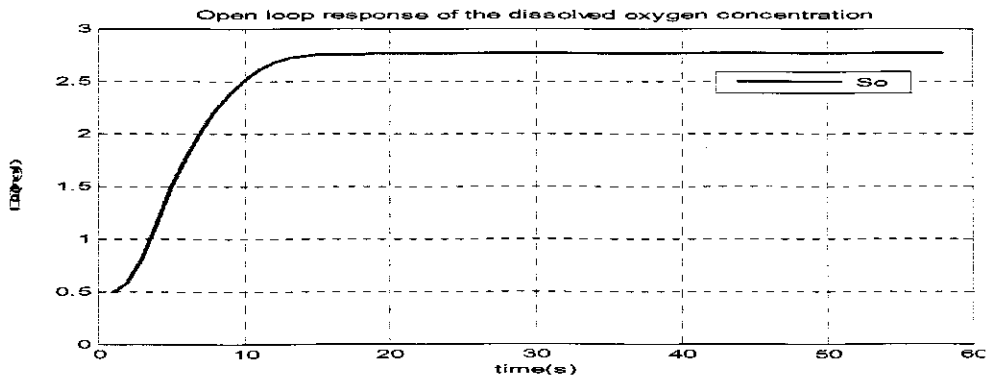


Figure 3.8: Open loop response of the dissolved oxygen model using $S_{oin}=1$ and r_{so} calculated for XBA of 149.797 and XBH of 2559.444

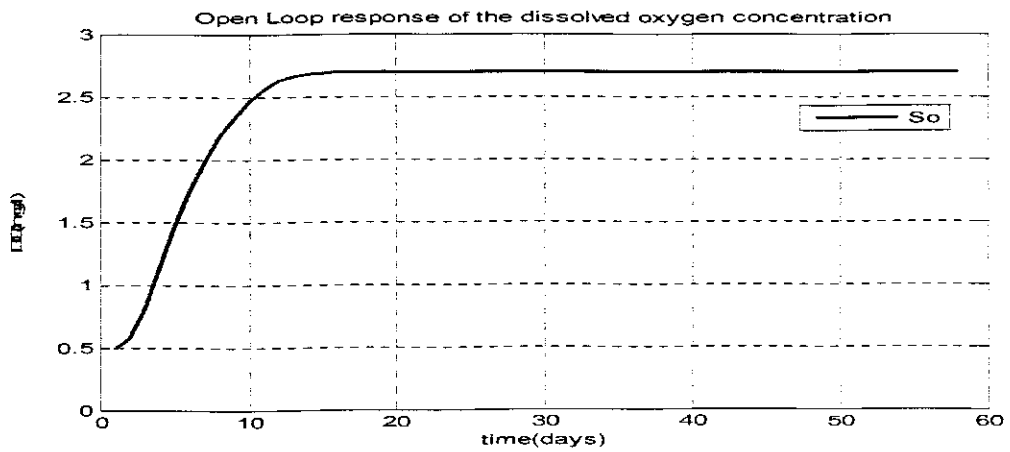


Figure 3.9: Open loop response of the dissolved oxygen concentration using $S_{oin}=0.2$ and r_{so} calculated for XBA of 134.8173 and XBH of 2815.3884

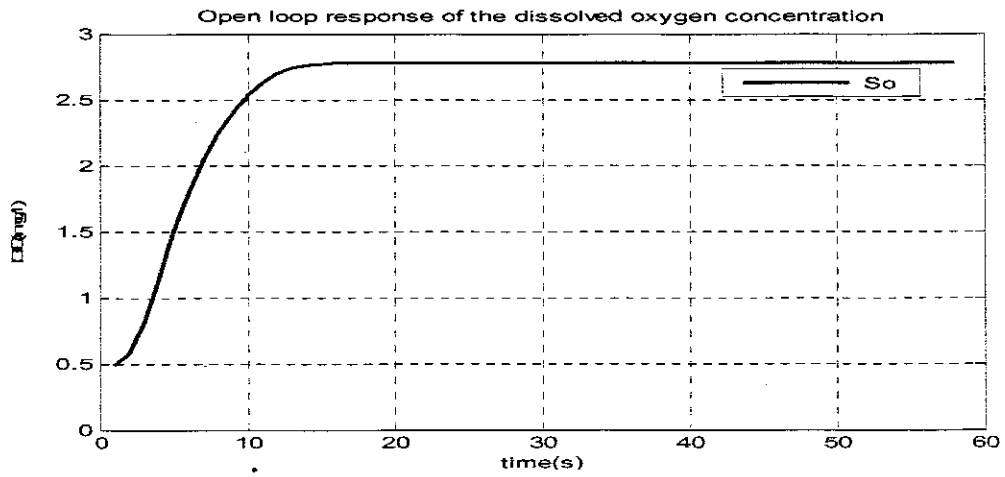


Figure 3.10: Open loop response of the dissolved oxygen concentration using $S_{oin}=0.6$ and r_{so} calculated for XBA of 134.8173 and XBH of 2815.3884

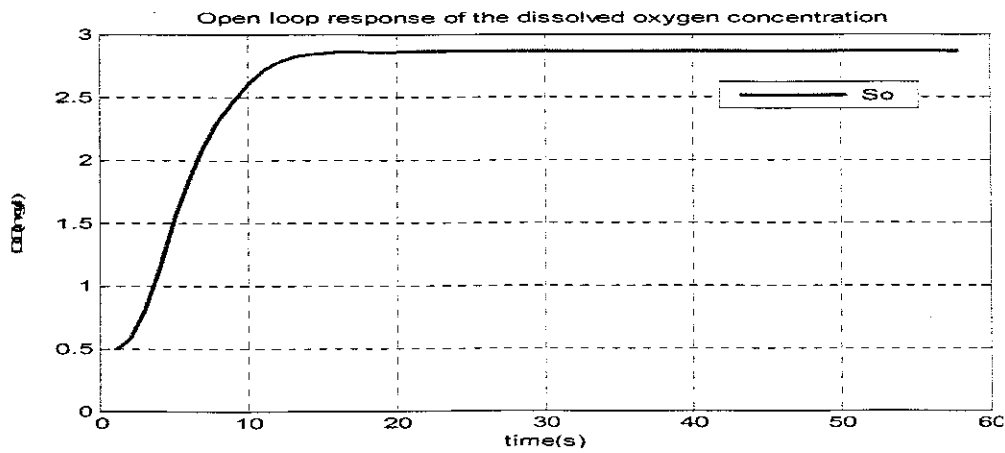


Figure 3.11: Open loop response of the dissolved oxygen concentration using $S_{oin}=1$ and r_{so} calculated for XBA of 134.8173 and XBH of 2815.3884

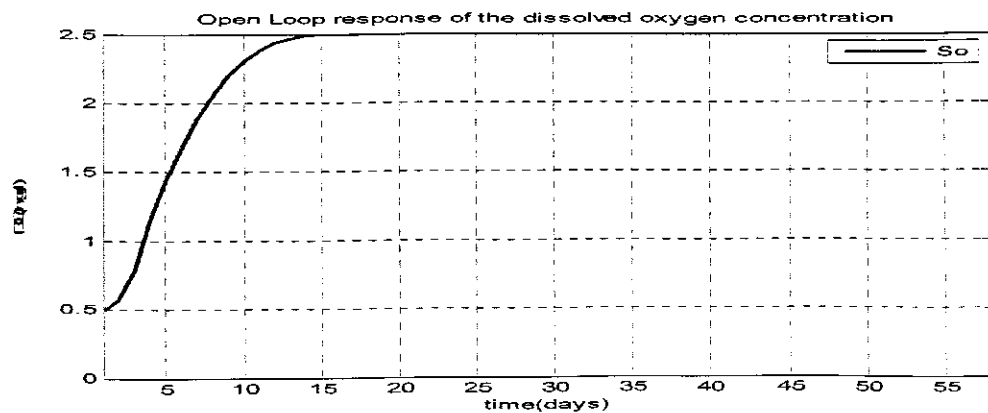


Figure 3.12: Open loop response of the dissolved oxygen concentration using $S_{oin}=0.2$ and r_{so} calculated for XBA of 164.7767 and XBH of 2303.4996

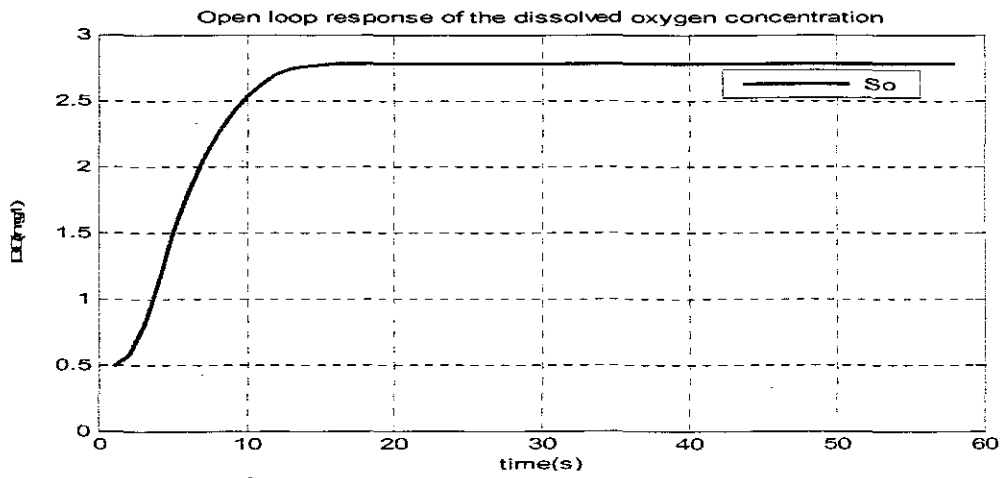


Figure 3.10: Open loop response of the dissolved oxygen concentration using $S_{oin}=0.6$ and r_{so} calculated for XBA of 134.8173 and XBH of 2815.3884

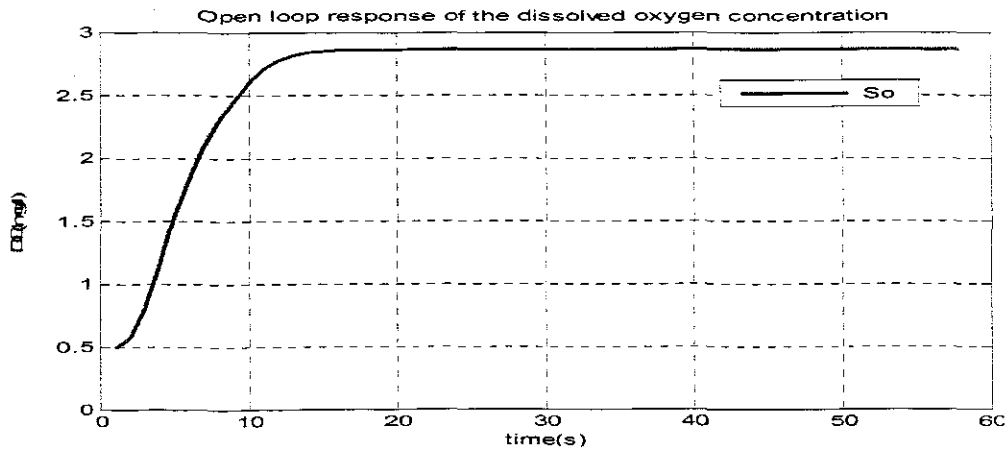


Figure 3.11: Open loop response of the dissolved oxygen concentration using $S_{oin}=1$ and r_{so} calculated for XBA of 134.8173 and XBH of 2815.3884

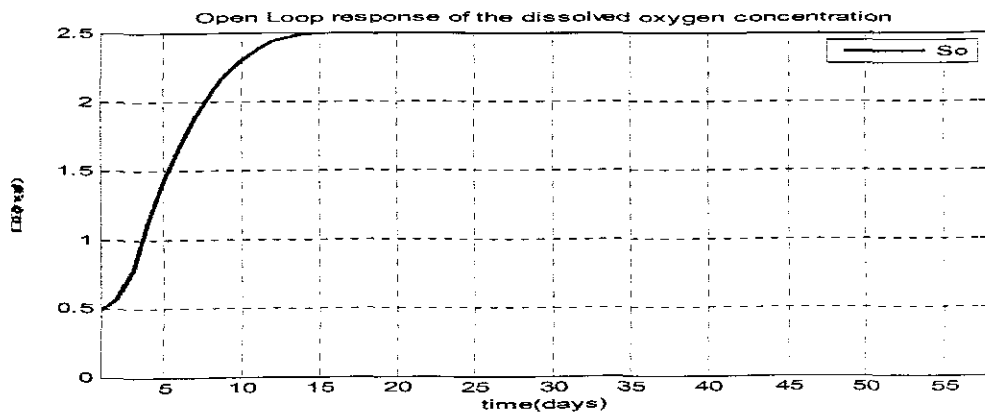


Figure 3.12: Open loop response of the dissolved oxygen concentration using $S_{oin}=0.2$ and r_{so} calculated for XBA of 164.7767 and XBH of 2303.4996

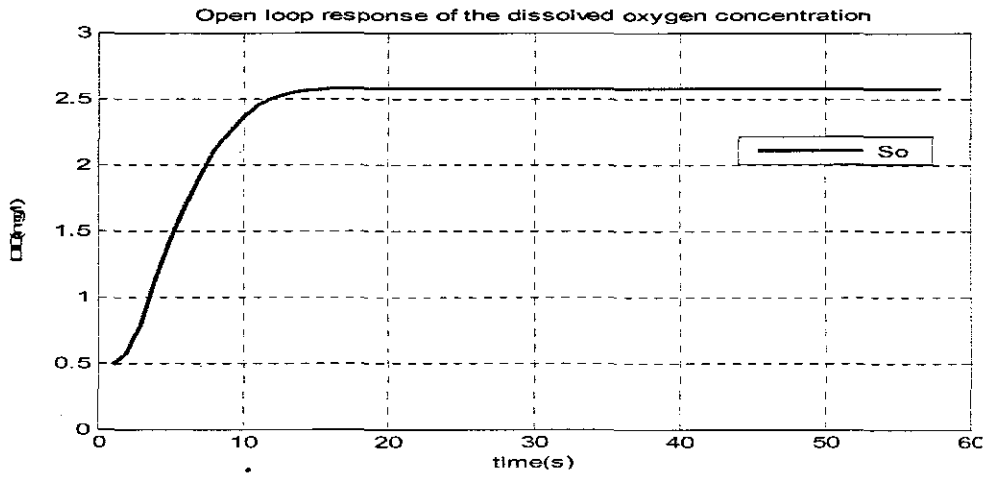


Figure 3.13: Open loop response of the dissolved oxygen concentration using $S_{oin}=0.6$ and r_{so} calculated for XBA of 164.7767 and XBH of 2303.4996

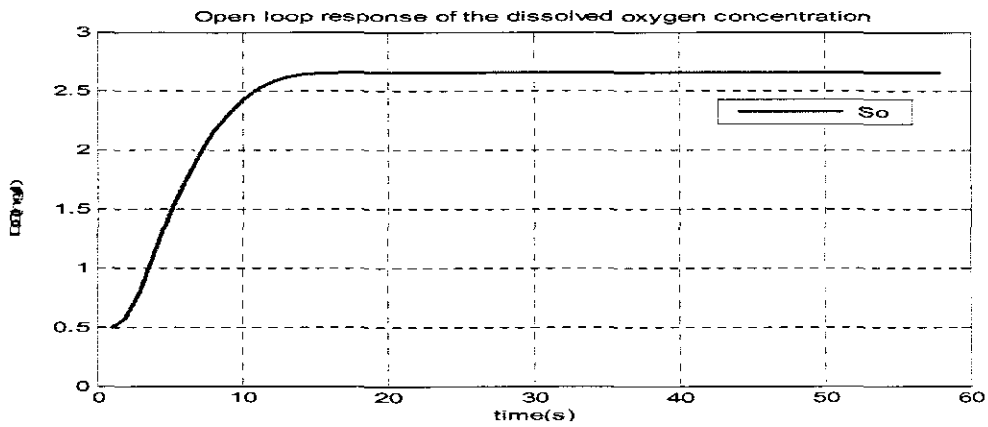


Figure 3.14: Open loop response of the dissolved oxygen concentration using $S_{oin}=1$ and r_{so} calculated for XBA of 164.7767 and XBH of 2303.4996

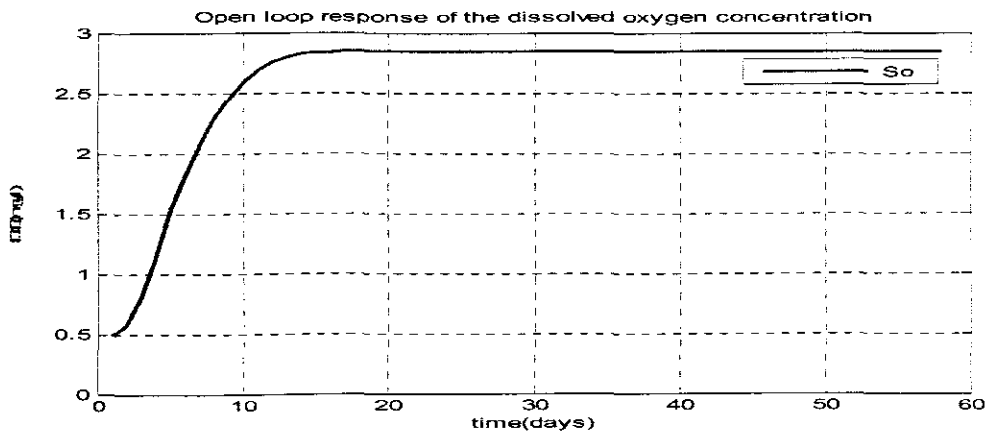


Figure 3.15: Open loop response of the dissolved oxygen concentration using $S_{oin}=0.4$ and r_{so} calculated for XBA of 119.8376 and XBH of 3071.3328

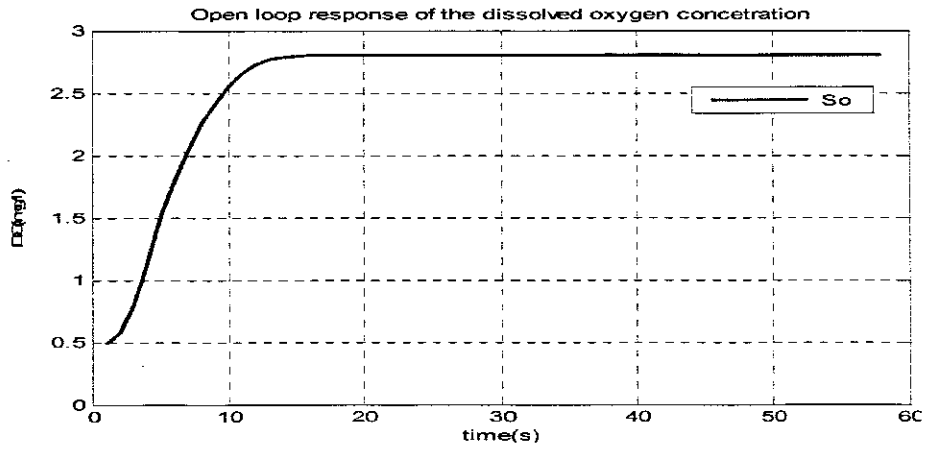


Figure 3.16: Open loop response of the dissolved oxygen concentration using $S_{oin}=0.2$ and r_{so} calculated for XBA of 119.8376 and XBH of 3071.3328

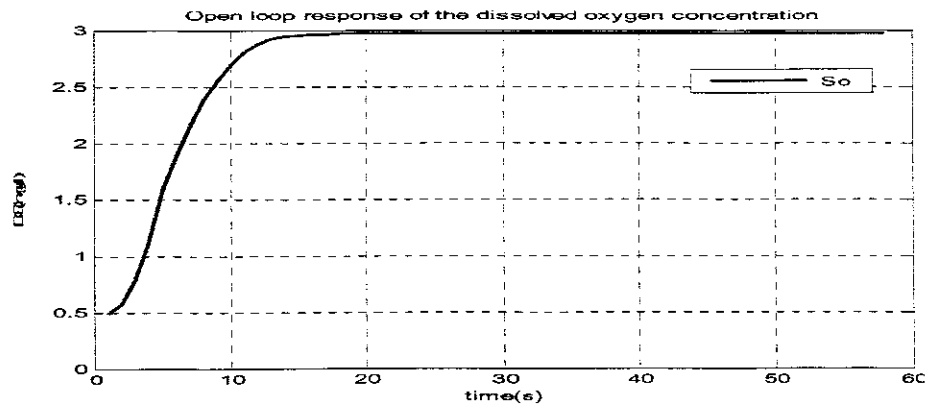


Figure 3.17: Open loop response of the dissolved oxygen concentration using $S_{oin}=1$ and r_{so} calculated for XBA 119.8376 of and +20%XBH of 3071.3328

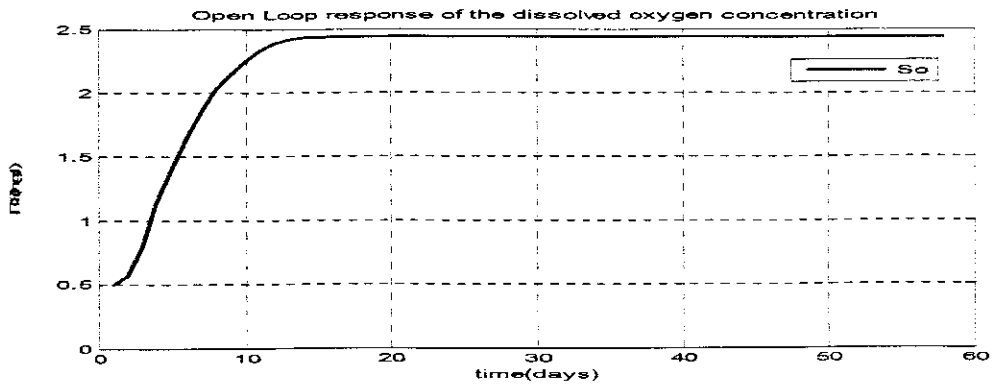


Figure 3.18: Open Loop response of the dissolved oxygen concentration using $S_{oin}=1$ and r_{so} calculated for XBA 179.7564 of and XBH of 2047.5552

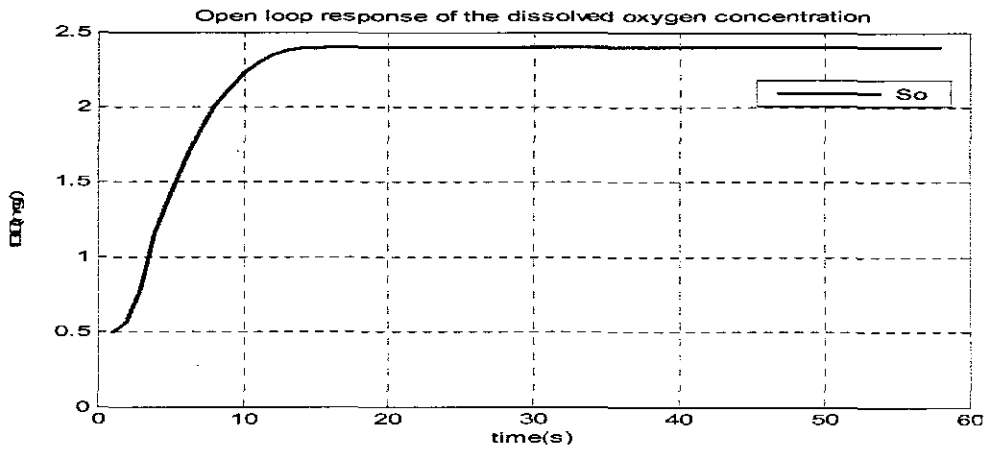


Figure 3.19: Open loop response of the dissolved oxygen concentration using $S_{oin}=0.2$ and r_{so} calculated for XBA of 179.7564 and XBH of 2047.5552

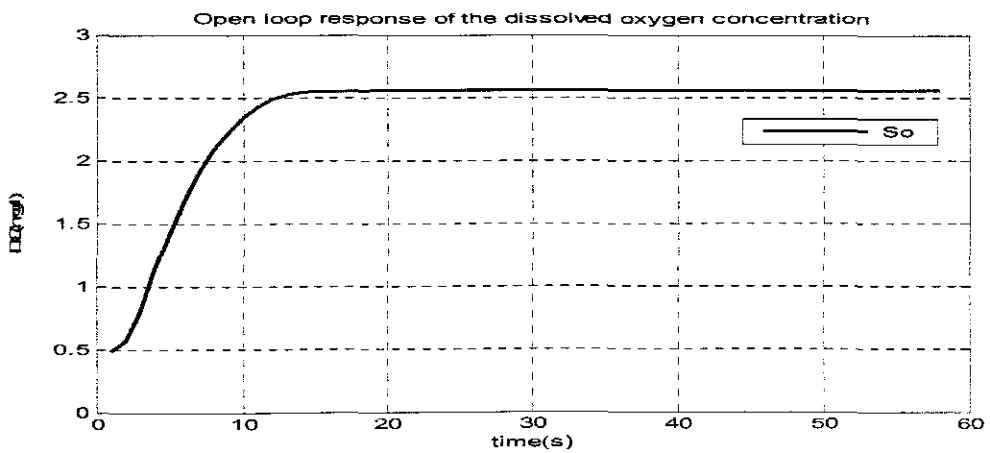


Figure 3.20: Open loop response of the dissolved oxygen concentration using $S_{oin}=1$ and r_{so} calculated for XBA of 179.7564 and XBH of 2047.5552

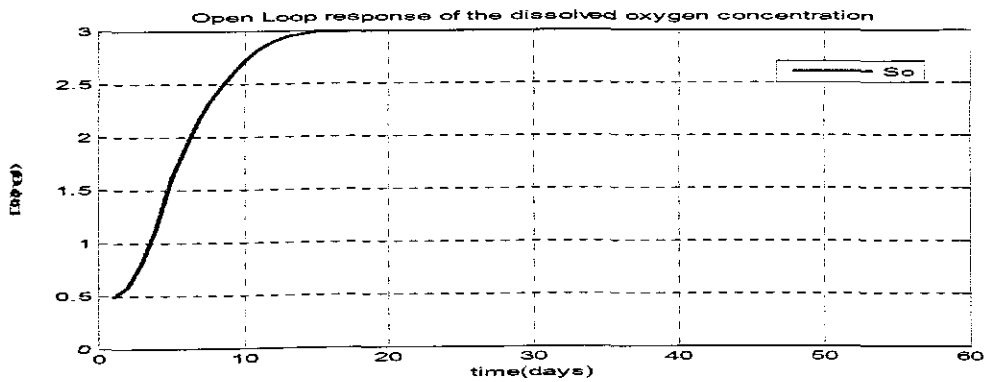


Figure 3.21: Open loop response of the dissolved oxygen concentration using $S_{oin}=0.6$ and r_{so} calculated for XBA of 104.6579 and XBH of 3327.2772

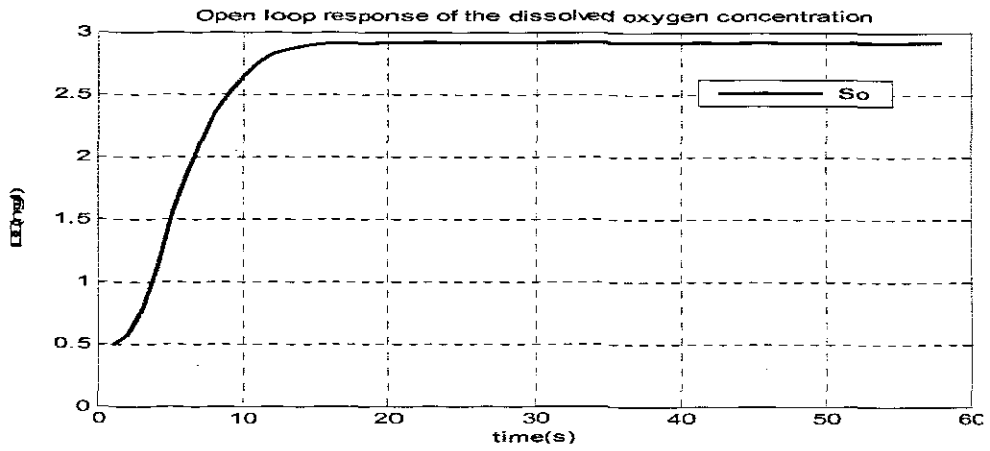


Figure 3.22: Open loop response of the dissolved oxygen concentration using $S_{oin}=0.2$ and r_{so} calculated for XBA of 104.8579 and XBH of 3327.2772

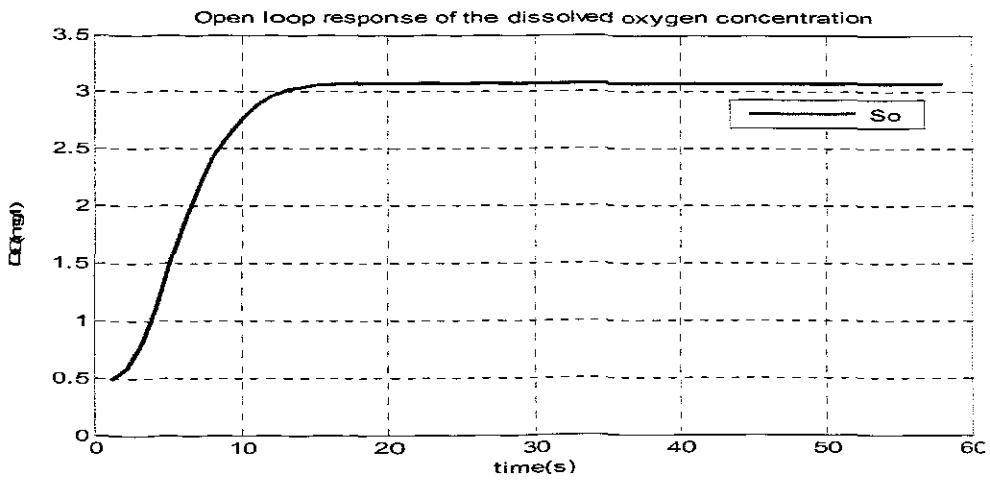


Figure 3.23: Open loop response of the dissolved oxygen concentration using $S_{oin}=1$ and r_{so} calculated for XBA of 104.8579 and XBH of 3327.2772

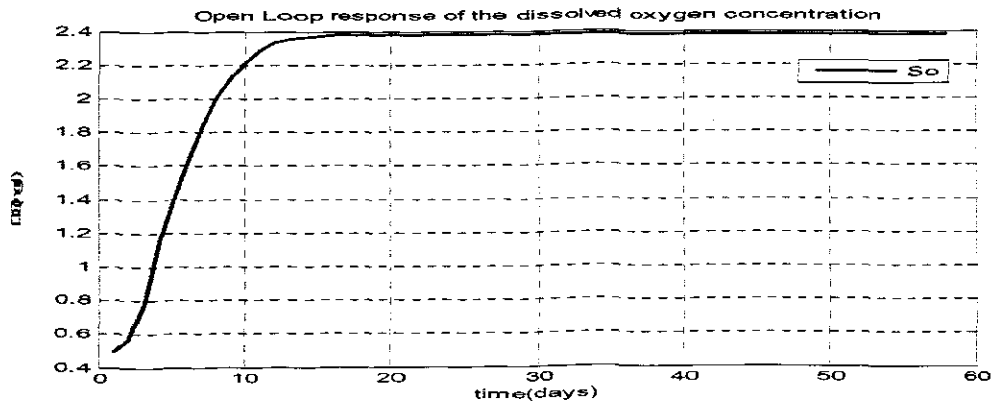


Figure 3.24: Open loop response of the dissolved oxygen concentration using $S_{oin}=0.6$ and r_{so} calculated for XBA of 194.7361 and XBH of 1791.6108

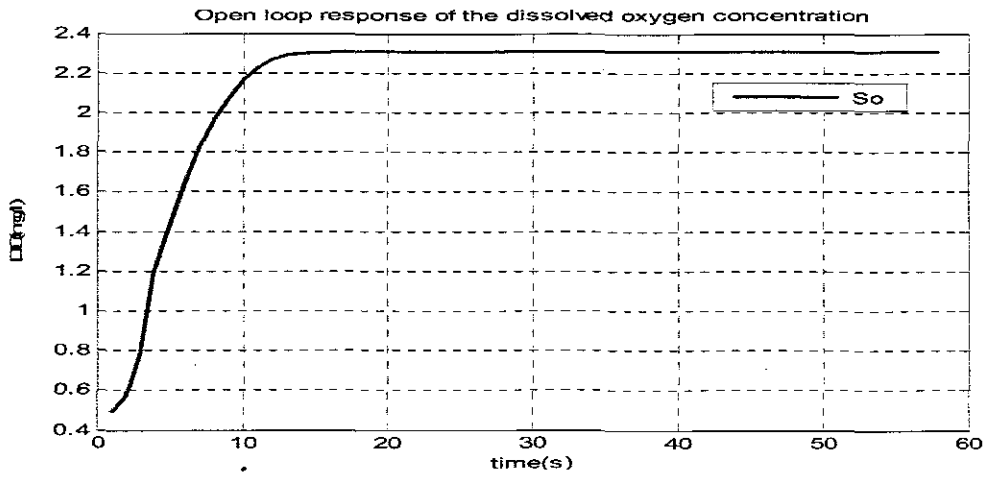


Figure 3.25: Open loop response of the dissolved oxygen concentration using $S_{oin}=0.2$ and r_{so} calculated for XBA of 194.7361 and XBH of 1791.6108

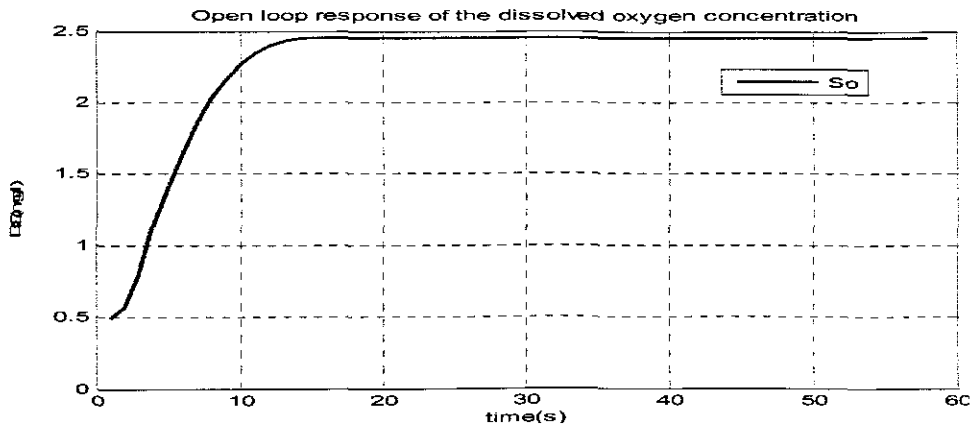


Figure 3.26: Open loop response of the dissolved oxygen concentration using $S_{oin}=1$ and r_{so} calculated for XBA of 194.7361 and XBH of 1791.6108

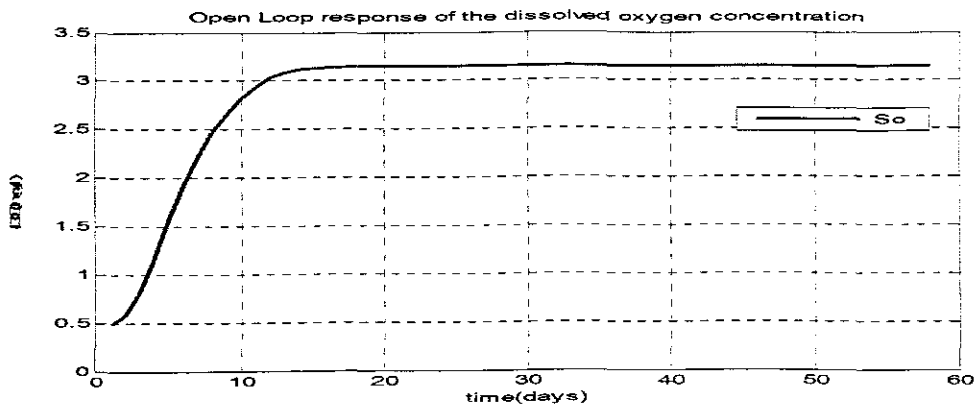


Figure 3.27: Open loop response of the dissolved oxygen concentration using $S_{oin}=0.8$ and r_{so} calculated for XBA of 89.8782 and XBH of 3583.2216

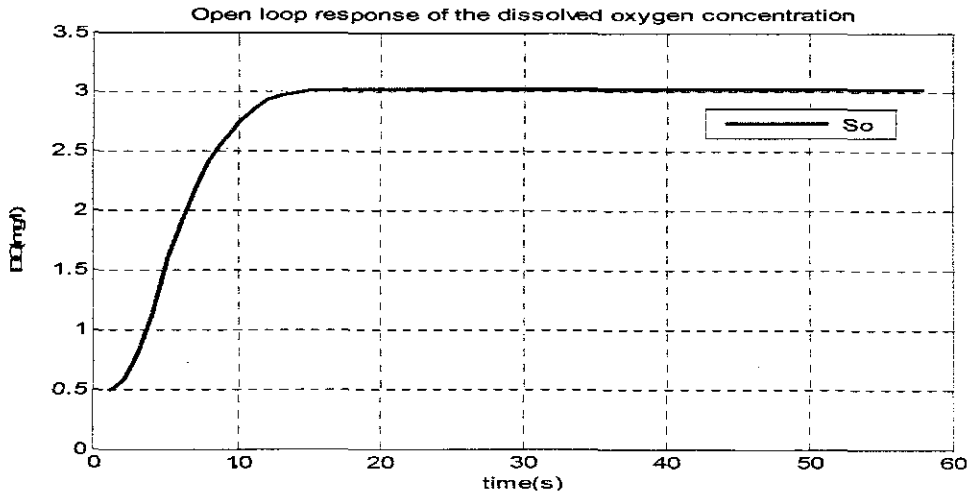


Figure 3.28: Open loop response of the dissolved oxygen concentration using $S_{oin}=0.2$ and r_{so} calculated for XBA of 89.8782 and XBH of 3583.2216

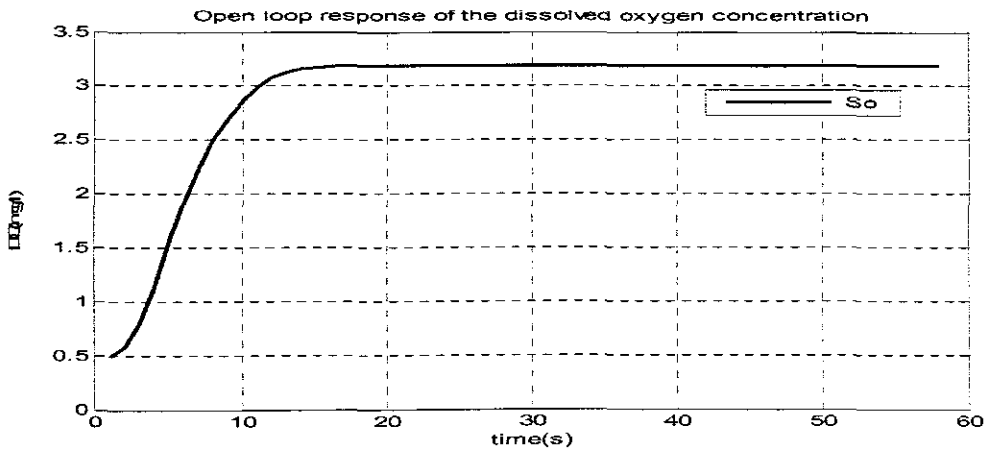


Figure 3.29: Open loop response of the dissolved oxygen concentration using $S_{oin}=1$ and r_{so} calculated for XBA of 89.8782 and XBH of 3583.2216

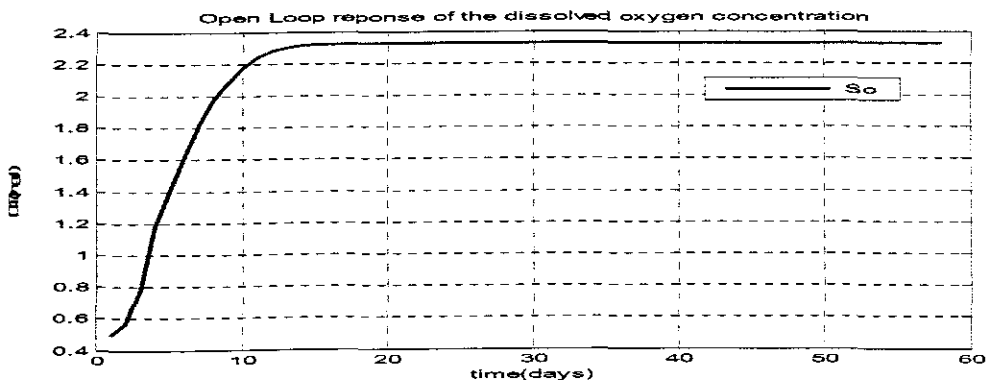


Figure 3.30: Open loop response of the dissolved oxygen concentration using $S_{oin}=0.8$ and r_{so} calculated for XBA of 209.7158 and XBH of 1535.6664

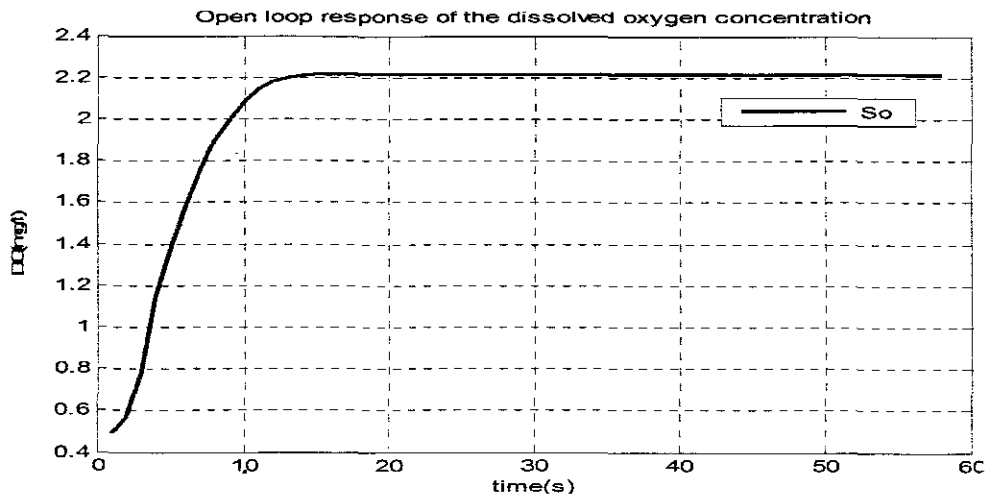


Figure 3.31: Open loop response of the dissolved oxygen concentration using $S_{oin}=0.2$ and r_{so} calculated for XBA of 209.7158 and XBH of 1535.6664

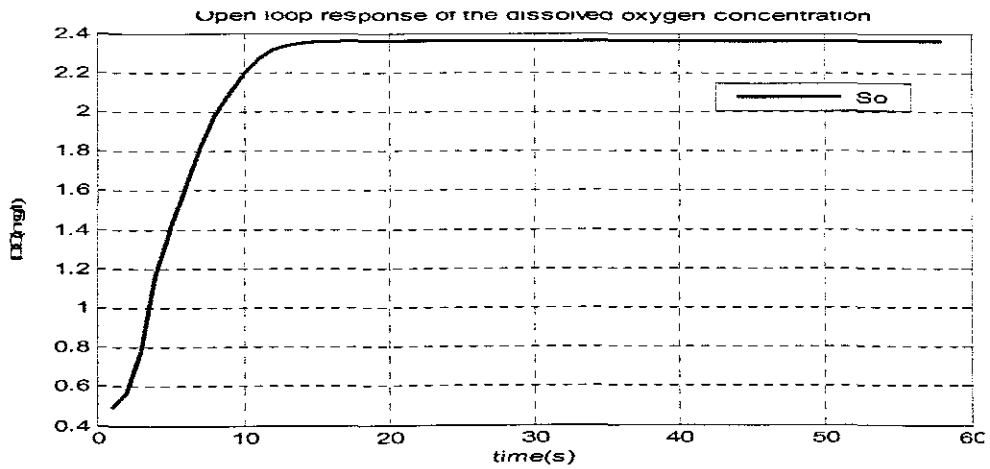


Figure 3.32: Open loop response of the dissolved oxygen concentration using $S_{oin}=1$ and r_{so} calculated for XBA of 209.7158 and XBH of 1535.6664

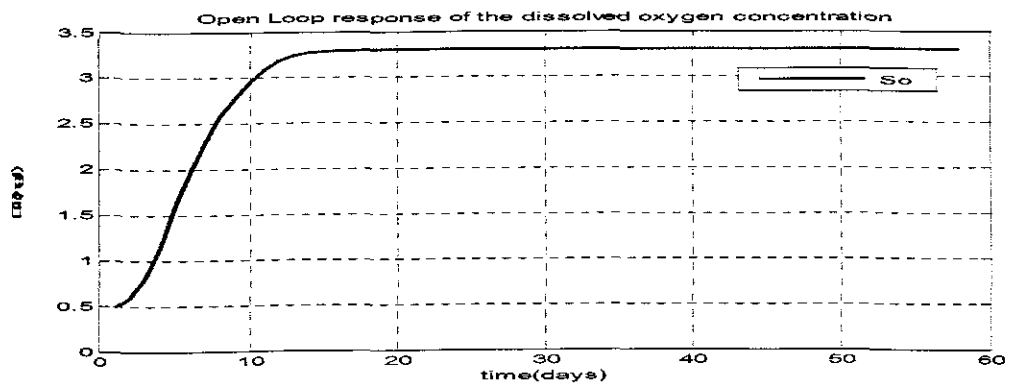


Figure 3.34: Open loop response of the dissolved oxygen concentration using $S_{oin}=1$ and r_{so} calculated for XBA of 74.8985 and XBH of 3639.166

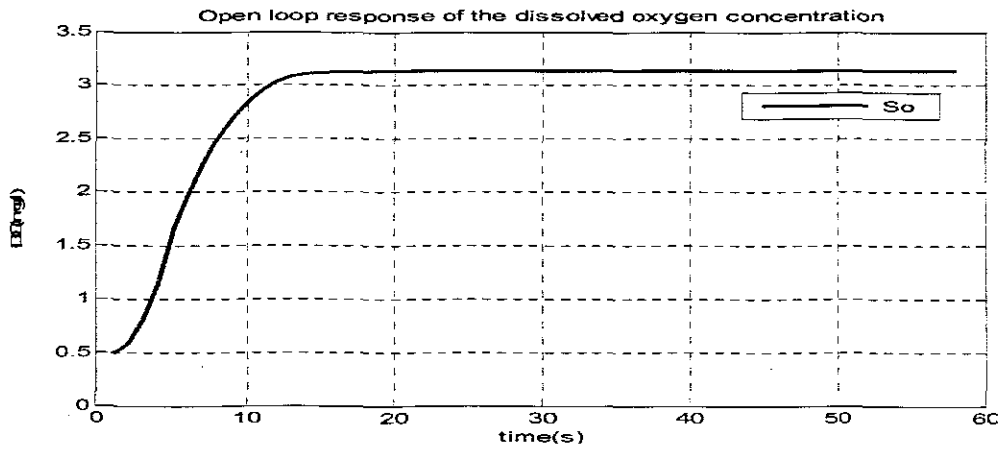


Figure 3.35: Open loop response of the dissolved oxygen concentration using $S_{oin}=0.2$ and r_{so} calculated for XBA of 74.8985 and XBH of 3839.166

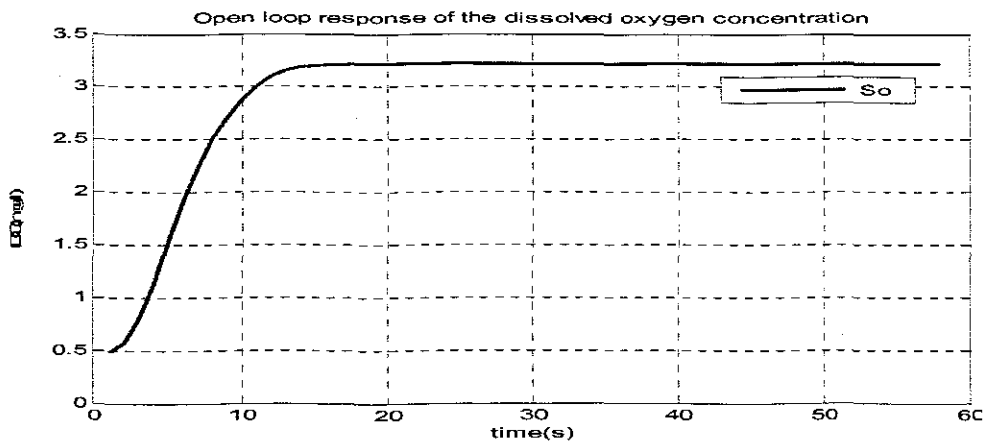


Figure 3.36: Open loop response of the dissolved oxygen concentration using $S_{oin}=0.6$ and r_{so} calculated for XBA of 74.8985 and XBH of 3839.166

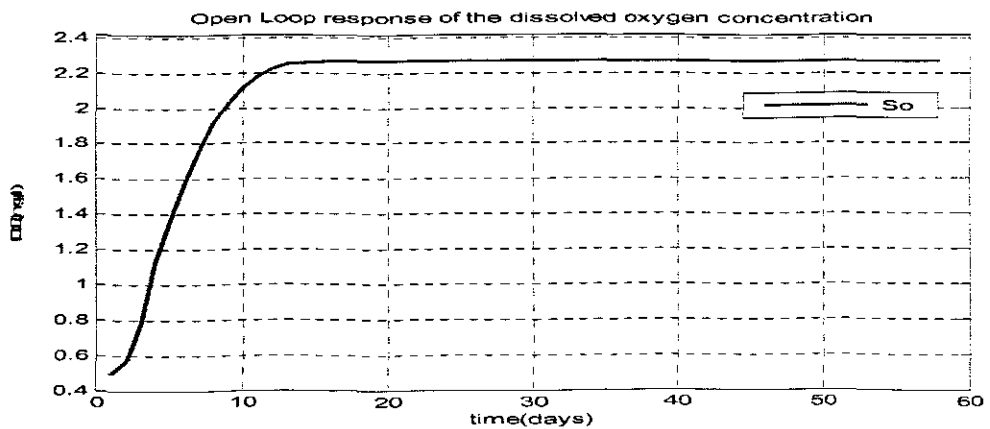


Figure 3.37: Open loop response of the dissolved oxygen concentration using $S_{oin}=1$ and r_{so} calculated for XBA of 224.6955 and XBH of 1279.722

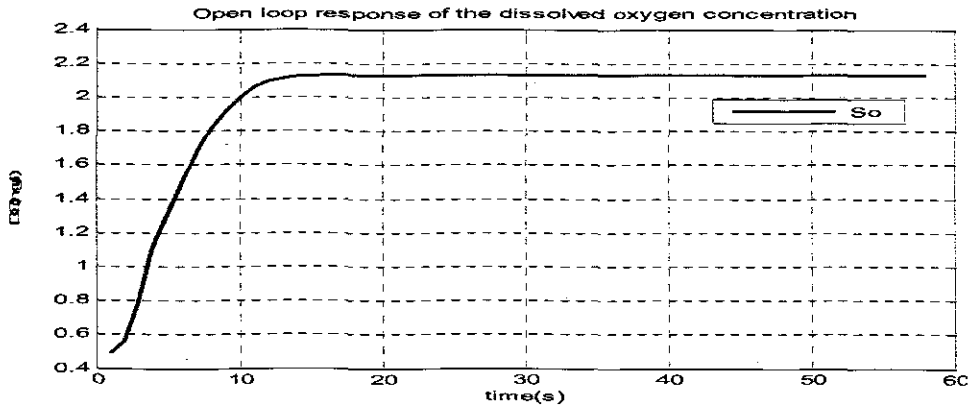


Figure 3.38: Open loop response of the dissolved oxygen concentration using $S_{o,in}=0.2$ and r_{SO} calculated for XBA of 224.6955 and XBH of 1279.722

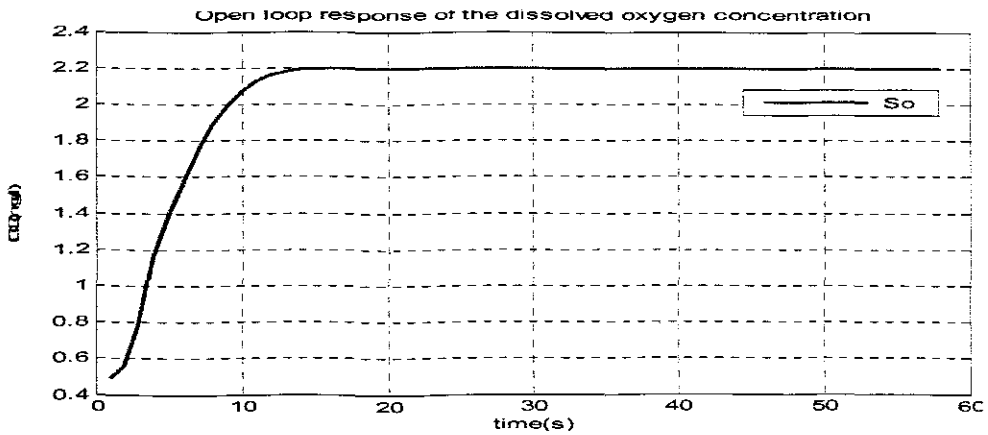


Figure 3.39: Open loop response of the dissolved oxygen concentration using $S_{o,in}=0.6$ and r_{SO} calculated for XBA of 224.6955 and XBH of 1279.722.

3.8.5 Discussion of the results

For the simulation results of open loop trajectories of the dissolved oxygen concentration the following parameters were varied: the two disturbance; external $s_{O,in}$, and internal r_{SO} and for calculation of r_{SO} the values of x_{BA} and x_{BH} were calculated from $\pm 10\%$ to $\pm 50\%$ of the original steady state value from the Benchmark plant. The following parameters of transition behaviours were observed to investigate the performance of the open loop response: time delay, steady state error, settling time, rising time. The values are provided in Table 3.7. On the basis of Table 3.7 the following observations and conclusions can be made:

- The time delay of the process is not very sensitive towards the value of disturbances. The biggest values of time delays of 0.2 seconds are for the steady state of process biomass and small values of the $s_{O,in}$
- The steady state values of the s_o is the most sensitive parameter of the transition behaviour. It is higher for higher values of the process heterotrophic bacteria x_{BA} , the bigger values of the steady state s_o are for smaller values of $s_{O,in}$.
- Reduction of x_{BA} with big percentage leads to reduction of s_o in steady state

The settling time parameter is very sensitive toward variation of $s_{O,in}$. Smaller variations of x_{BA} and x_{BH} give bigger value of the settling time than the bigger variations. The rising time is approximately the same for all variations of disturbances.

Table3.7: Simulation results comparison table

Parameters				Characteristics											
t_{SO}	$S_{O,m}$			Time delay			Steady state value			Settling time			Rising time		
				(td)			(ss)			(ts)			(tr)		
Original x_{BA} x_{BH}	0.2	0.6	1	0.2	0.2	0.15	2.49	2.3	2.2	12	12	14	0.4	0.4	0.2
-10% x_{BA} +10% x_{BH}	0.2	0.6	1	0.15	0.15	0.15	2.3	2.2	2.1	12	12	12	0.2	0.2	0.2
+10% x_{BA} -10% x_{BH}	0.2	0.6	1	0.15	0.15	0.15	2	0.49	2.4	14	14	14	0.2	0.2	0.2
-20% x_{BA} +20% x_{BH}	0.4	0.2	1	0.15	0.15	0.15	2.1	2.2	2	14	14	14	0.2	0.2	0.2
+20% x_{BA} -20% x_{BH}	0.4	0.2	1	0.15	0.15	0.15	2.01	2.1	2.49	12	12.5	12.5	0.2	0.2	0.2
-30% x_{BA} +30% x_{BH}	0.6	0.2	1	0.15	0.15	0.15	2	2.1	2.49	14	12.5	13	0.2	0.2	0.2
+30% x_{BA} -30% x_{BH}	0.6	0.2	1	0.15	0.15	0.15	2.01	2.1	2.01	12.5	13	12.5	0.2	0.2	0.2
-40% x_{BA} +40% x_{BH}	0.8	0.2	1	0.15	0.15	0.15	2.3	2.5	2.3	13	12	13	0.2	0.2	0.2
+40% x_{BA} -40% x_{BH}	0.8	0.2	1	0.15	0.15	0.15	2.1	2.2	2.01	12.5	12	12	0.2	0.2	0.2
-50% x_{BA} +50% x_{BH}	1	0.2	0.6	0.15	0.15	0.15	2.1	2.4	2.3	12	13	15	0.2	0.2	0.2
+50% x_{BA} -50% x_{BH}	1	0.2	0.6	0.15	0.15	0.15	2.18	2.15	2.2	13	12	12	0.2	0.2	0.2

Table3.7: Simulation results comparison table

Parameters				Characteristics											
I_{SD}	$S_{D.in}$			Time delay			Steady state value			Settling time			Rising time		
				(td)			(ss)			(ts)			(tr)		
Original x_{BA} x_{BH}	0.2	0.6	1	0.2	0.2	0.15	2.49	2.3	2.2	12	12	14	0.4	0.4	0.2
-10% x_{BA} +10% x_{BH}	0.2	0.6	1	0.15	0.15	0.15	2.3	2.2	2.1	12	12	12	0.2	0.2	0.2
+10% x_{BA} -10% x_{BH}	0.2	0.6	1	0.15	0.15	0.15	2	0.49	2.4	14	14	14	0.2	0.2	0.2
-20% x_{BA} +20% x_{BH}	0.4	0.2	1	0.15	0.15	0.15	2.1	2.2	2	14	14	14	0.2	0.2	0.2
+20% x_{BA} -20% x_{BH}	0.4	0.2	1	0.15	0.15	0.15	2.01	2.1	2.49	12	12.5	12.5	0.2	0.2	0.2
-30% x_{BA} +30% x_{BH}	0.6	0.2	1	0.15	0.15	0.15	2	2.1	2.49	14	12.5	13	0.2	0.2	0.2
+30% x_{BA} -30% x_{BH}	0.6	0.2	1	0.15	0.15	0.15	2.01	2.1	2.01	12.5	13	12.5	0.2	0.2	0.2
-40% x_{BA} +40% x_{BH}	0.8	0.2	1	0.15	0.15	0.15	2.3	2.5	2.3	13	12	13	0.2	0.2	0.2
+40% x_{BA} -40% x_{BH}	0.8	0.2	1	0.15	0.15	0.15	2.1	2.2	2.01	12.5	12	12	0.2	0.2	0.2
-50% x_{BA} +50% x_{BH}	1	0.2	0.6	0.15	0.15	0.15	2.1	2.4	2.3	12	13	15	0.2	0.2	0.2
+50% x_{BA} -50% x_{BH}	1	0.2	0.6	0.15	0.15	0.15	2.18	2.15	2.2	13	12	12	0.2	0.2	0.2

3.9 Conclusion

This chapter provides an overview of Benchmark structure based on Activated Sludge Model #1. System variables, state variables and parameter values from ASM1 are given. Mathematical modelling of the different types of oxygen transfer function and oxygen uptake rate is discussed.

Normal nonlinear affine form of the mass balance equation is derived. Simulation in Matlab/Simulink environment is done for the case of exponential function of the oxygen transfer function. The influence of two types of disturbances over the process dynamics is investigated and the obtained trajectories are compared. The obtained trajectory of the dissolved oxygen model is used in the chapters 6 and 7 for the design of nonlinear controllers.

Chapter 4 deals with parameter estimation of different models of oxygen transfer function K_{La} based the method of least squares.

CHAPTER FOUR

ESTIMATION OF THE OXYGEN TRANSFER FUNCTION AND OXYGEN UPTAKE RATE

4.1 Introduction

The oxygen uptake rate has a very complex nonlinear representation according to the Patterson matrix of ASM1 model. This representation includes different variables of the ASP. Their on-line measurement is not possible because of lack of respective sensors. This means that real-time use of the model of dissolved oxygen (DO) for control purposes is not possible if the oxygen uptake rate is calculated according to Patterson matrix. It is necessary to find some estimated value of the oxygen uptake rate (OUR) on the basis of the available measurements, which are the DO concentration values.

When the value of the oxygen uptake rate (OUR) is known, the specific growth rate or the variations of the substrate can be calculated. The knowledge of r_{SO} is good for the sludge inventory control. The respiration rate depends directly on the wastewater and it is not possible to control it. This means that it could be considered as a disturbance input to the process. The estimator can be part of an adaptive controller for DO concentration control.

The thesis considers different models of the oxygen transfer function. In order to develop a method and algorithm for this estimation is necessary to know the values of K_{La} . The value of K_{La} varies according to the wastewater quality and diffusers clogging. It shows the efficiency of the aerator system. K_{La} has a typically nonlinear character: as the airflow rate increases, then K_{La} tends to a saturation value characterized by different parameters, which are not known. Their estimation is also necessary to be performed. The least squares method is developed for estimation of the OUR and the oxygen transfer function parameters. The considered models are used for design and simulation of the nonlinear closed loop control.

Discussed in this chapter is least-squares method for parameter estimation in section 4.2. Section 4.3 introduces data used for parameter estimation. Section 4.4 is the application of least squares methods to different models of oxygen transfer function, the

subsequent models are given in subsections 4.41 to 4.47. Section 4.5 gives simulation results of the parameter estimation for different models of oxygen transfer function.

4.2 The Method of Least Squares for parameter estimation

The Method of Least squares for parameter estimation describes a frequently used approach to solving over determined or inaccurately specified systems of equations in a fitting sense. It is an alternative to interpolation for fitting a function to a set of points. It is different from interpolation in the sense that the least-squares method does not need the fitted function to intersect each point. Instead it seeks only to minimize the sum of the squares of the residuals. The Method of Least Squares can be categorized in two types: Linear and Nonlinear and it also be further classified as follows:

- An ordinary Least Squares
- Weighted Least Squares
- Alternating Least Squares
- Partial Least Squares

For Least Squares Method a very common base problem is curve fitting. Let t be an independent variable and let $y(t)$ represents an unknown function of t that needs to be approximated. Assuming that, there are m observations, i.e. values of y measured at the specified values of t : $y(t) = y(t_i)$, $i = 1, \dots, m$. The idea is to model $y(t)$ by a linear combination of n basis functions:

$$y(t) \approx \beta_1 \phi_1(t) + \dots + \beta_n \phi_n(t)$$

where $\beta_j \phi_j$, $\beta_{j-1} \phi_{j-1}$, $\beta_n \phi_n$ are unknown parameters. In matrix-vector notation, the model is $y \approx X\beta$ (Ljung, 1999), (Gelb et al, 1974), (Goodwin and Sin, 1984), (Mathworks, 2008). The design matrix X is a rectangular matrix of order $m \times n$ with elements $x_{i,j} = \phi_j(t_i)$. The design matrix usually has more rows than columns. The parameter β_j can be calculated from the observations of the design matrix X .

4.3 Data used for parameter estimation

An input/output representation of the dissolved oxygen state space model is considered in Figure 4.1. where $u(k)$, the airflow rate and $s_o(k)$, the dissolved oxygen concentration are measured in real-time.

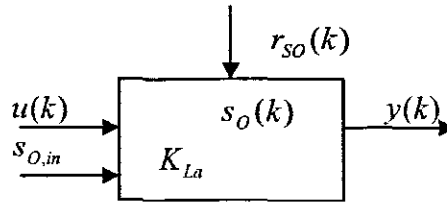


Figure 4.1: Input/output model of DO concentration

It is supposed that these values are available for some period of time $k = [0 \ K]$. The output $y(k)$ is some function of measured variables, which is different for different models of $K_{La}(u, k)$. It is supposed that the inflow concentration of dissolved oxygen $s_{O,in}$ considered as a disturbance is known or measured also. The oxygen uptake rate is unknown and is also considered as a disturbance.

4.4 Application of the least squares method to different models of the oxygen transfer function

A discrete representation of the mass balance equation for dissolved oxygen behaviour is considered

$$s_o(k+1) = s_o(k) + \Delta t \left\{ \frac{Q}{V} [s_{O,in}(k) - s_o(k)] + K_{La}(u, k) [s_{O,sat} - s_o(k)] + r_{SO}(k) \right\} \quad (4.1)$$

where K_{La} can be represented in different ways, according to given in Chapter 3 models. For every case the least squares method is applied and equations for calculation of the parameters are developed. The parameters are considered to be time varying and for every sampling interval they have different values.

4.4.1 Oxygen transfer function represented by a time varying parameter

The case of $K_{La} = k_1(k)$ is considered. The mass balance equation for DO is the same as Equation (4.1), but K_{La} does not depend on the airflow rate. Then the data for it is not used in the estimation process.

In order to apply the method for least squares the Equation (4.1) has to be represented in the input/output form, given in Figure (4.1). To achieve this all measurable variables are moved to the left side of the equation and all parameters are left to the right one, as follows:

$$y(k) = s_o(k+1) - s_o(k) - \Delta t \frac{Q}{V} [s_{o,in}(k) - s_o(k)] = \Delta t k_1(k) [s_{o,sat} - s_o(k)] + \Delta t r_{so}(k) \quad (4.2)$$

In Equation (4.2) it can be seen that

$$y(k) = s_o(k+1) - s_o(k) - \Delta t \frac{Q}{V} [s_{o,in}(k) - s_o(k)] \quad (4.3)$$

The right site of Equation (4.2) can be represented in a vector form using notations for the parameters to be estimated by the letter θ

$$y(k) = \Delta t [\theta_1(k) [s_{o,sat} - s_o(k) + \theta_2]] = \Delta t [(s_{o,sat} - s_o(k)) \quad 1] \begin{bmatrix} \theta_1(k) \\ \theta_2(k) \end{bmatrix} = \varphi(k) \theta(k) \quad (4.4)$$

where $\theta_1 = k_1$, $\theta_2 = r_{so}$. It is obtained that

$$y(k) = \varphi(k) \theta(k), \quad k = \overline{0, K-1} \quad (4.5)$$

is the equation for the output of the mass balance model. The output and the function $\varphi(k) = \Delta t [(s_{o,sat} - s_o(k)) \quad 1] \in R^{1 \times 2}$ are known on the basis of data. In the considered case $\theta(k) \in R^{2 \times 1}$, $\varphi(k) \in R^{1 \times 2}$, $y(k) \in R$.

Equation (4.5) is for every moment of time $k = [0, K-1]$. In order to use the available data and calculate the parameters for every moment of time only, this equation can be represented in a matrix format, as follows;

Equation (4.5) is written for every moment $k = \overline{0, K-1}$

$$y(0) = \varphi(0) \theta(0)$$

$$y(1) = \varphi(1) \theta(1)$$

.

.

$$y(K-1) = \varphi(K-1) \theta(K-1)$$

The obtained set of equations can be written in the following way:

$$\begin{bmatrix} y(0) \\ y(1) \\ \cdot \\ \cdot \\ y(K-1) \end{bmatrix} = \begin{bmatrix} \varphi(0) & 0 & \cdot & \cdot & 0 \\ 0 & \varphi(1) & \cdot & \cdot & 0 \\ \cdot & 0 & \cdot & 0 & \cdot \\ \cdot & \cdot & 0 & \cdot & 0 \\ 0 & 0 & \cdot & \cdot & \varphi(K-1) \end{bmatrix} \begin{bmatrix} \theta(0) \\ \theta(1) \\ \cdot \\ \cdot \\ \theta(K-1) \end{bmatrix}$$

Or equivalently

$$\bar{y} = \bar{\varphi} \cdot \bar{\theta} \quad (4.6)$$

Where: $\bar{\psi} = \text{diag}\{\varphi(0), \varphi(1), \dots, \varphi(K-1)\} \in R^{K \times (2 \cdot K)}$

$$\bar{\theta} = [\theta^T(0), \theta^T(1), \dots, \theta^T(K-1)]^T \in R^{2 \cdot K}$$

$$\bar{y} = [y(0), y(1), \dots, y(K-1)]^T \in R^K$$

The vector $\bar{\theta}$ in Equation (4.6) can be calculated on the basis of least squares approach. Both sides of the equation are multiplied by $\bar{\psi}^T$ to the left side and divided by $\bar{\psi}^T \bar{\psi}$ on the left side.

$$\bar{\psi}^T \bar{y} = \bar{\psi}^T \bar{\psi} \bar{\theta} \quad (4.7)$$

$$\bar{\theta} = [\bar{\psi}^T \bar{\psi}]^{-1} \bar{\psi}^T \bar{y} \quad (4.8)$$

Equation (4.8) is used for calculation of parameters. It can be written also for every moment of time as

$$\theta(k) = [\varphi(k)^T \varphi(k)]^{-1} \varphi(k)^T y(k), \quad k = \overline{0, K-1}$$

If the parameters are considered constant for the given data then Equation (4.5) can be written in a matrix form as follows

$$y(0) = \varphi(0)\theta$$

$$y(1) = \varphi(1)\theta$$

.

.

$$y(K-1) = \varphi(K-1)\theta \text{ or}$$

$$\begin{bmatrix} y(0) \\ y(1) \\ \cdot \\ \cdot \\ y(K-1) \end{bmatrix} = \begin{bmatrix} \varphi(0) \\ \varphi(1) \\ \cdot \\ \cdot \\ \varphi(K-1) \end{bmatrix} \theta$$

From here

$$\bar{y} = \tilde{\psi} \theta \quad (4.9)$$

where $\tilde{\psi} = [\varphi(0), \varphi(1), \dots, \varphi(K-1)]^T \in R^{K \times 2}$, $\theta \in R^2$, $\bar{y} \in R^K$, $\tilde{\psi} \in R^{K \times 2}$ and the vector of the parameters θ is calculated from

$$\theta = [\tilde{\psi}^T \tilde{\psi}]^{-1} \tilde{\psi}^T \bar{y} \quad (4.10)$$

In this case the whole amount of data is used to calculate the constant parameters.

4.4.2 Oxygen transfer function represented by a linear function

$$\text{In this case } K_{La} = k_1(t)u(t) + k_2(t) \quad (4.11)$$

The output $y(t)$ is given by Equation (4.3). In this case $y(k)$ is the same as in the previous case. The left side of Equation (4.4) is

$$\begin{aligned} y(k) &= \Delta t [k_1(k)u(k) + k_2(k)] [s_{O,sat} - s_O(k)] + \Delta tr_{SO} = \\ &= \Delta t [u(k) [s_{O,sat} - s_O(k)] \quad [s_{O,sat} - s_O(k)] \quad 1] \begin{bmatrix} \theta_1 \\ \theta_2 \\ \theta_3 \end{bmatrix} = \varphi(k)\theta(k) \end{aligned}$$

The function $\varphi(k)$ in a vector form is

$$\varphi(k) = \Delta t [u(k) [s_{O,sat} - s_O(k)] \quad [s_{O,sat} - s_O(k)] \quad 1] \in R^{1 \times 3} \quad (4.12)$$

The vector of parameters is

$$\theta = [\theta_1 \quad \theta_2 \quad \theta_3]^T \in R^3 \quad (4.13)$$

where $\theta_1 = k_1$, $\theta_2 = k_2$, $\theta_3 = r_{SO}$

The calculation of the parameters is according to Equation (4.6) for the varying parameters and according to Equation (4.9) for constant parameters. For the considered case $\bar{\psi} \in R^{K \times (3 \times K)}$ has the same structure as in Equation (4.6). $\bar{\theta} \in R^{3 \times K}$ and $y \in R^K$, $\tilde{\psi} \in R^{K \times 3}$, $\theta \in R^3$.

4.4.3 Oxygen transfer function represented by a power function

In this case $K_{La} = k_1(k)u(k)^{k_2(k)}$. This function can be represented as a product of two parameters

$$K_{La} = \zeta_1(k) \cdot \zeta_2(k) \quad (4.14)$$

Where $\zeta_1(k) = k_1(k)$ and $\zeta_2 = u(k)^{k_2(k)}$

The fact that the parameters are multipliers leads to difficulties in forming the input/output form of the mass balance equation. To overcome this difficulty it is proposed to consider not K_{La} but $\ln K_{La}$ during the process of estimation and then to recalculate back K_{La} .

Then

$$\ln K_{La} = \ln \zeta_1(k) + \ln \zeta_2(k) = \theta_1 + \theta_2 \quad (4.15)$$

$$\theta_1 = \ln \zeta_1(k) \text{ and } \theta_2 = \ln \zeta_2(k)$$

The expression of $\ln K_{La}$ can be substituted in the expression of $\varphi(k)$ and the input/output equation is

$$\begin{aligned}
y(k) &= \Delta t[(\theta_1(k) + \theta_2(k))(s_{O,sat} - s_O(k)) + r_{SO}(k)] = \\
&= \Delta t[(s_{O,sat} - s_O(k)) \quad (s_{O,sat} - s_O(k)) \quad 1] \begin{bmatrix} \theta_1 \\ \theta_2 \\ \theta_3 \end{bmatrix} = \varphi(k)\theta(k), \quad k = \overline{0, K-1} \quad (4.16)
\end{aligned}$$

where $\theta_3 = r_{SO}(k)$, $\varphi(k) = \Delta t[(s_{O,sat} - s_O(k)) \quad (s_{O,sat} - s_O(k)) \quad 1] \in R^{1 \times 3}$

The calculation of parameters follows Equation (4.6) for the time varying and Equation (4.9) for constant ones. The difference is in the components of the function $\varphi(k)$ and the number of parameters. When the vector $\theta(k)$ is calculated it is necessary to recalculate the parameters k_1 and \hat{k}_2 . From Equation (4.15)

$$\zeta_1(k) = \ln^{-1} \theta_1(k), \quad \zeta_2(k) = \ln^{-1} \theta_2(k) \quad (4.17)$$

From Equation (4.14) can be written

$$k_1(k) = \zeta_1(k) = \ln^{-1} \theta_1(k), \quad \zeta_2(k) = u(k)^{k_2(k)} \quad (4.18)$$

$$\text{Then } \ln \zeta_2(k) = \theta_2 = k_2(k) \ln u(k) \text{ and } k_2(k) = \frac{\theta_2}{\ln u(k)} \quad (4.19)$$

The dimensions of the vectors and matrices:

$$\bar{\psi} \in R^{K \times (3 \times K)}, \quad \tilde{\psi} \in R^{3 \times K}, \quad \bar{y} \in R^K, \quad \bar{\theta} \in R^{3 \times K}$$

4.4.4 Oxygen transfer function represented by an exponential function

In this case $K_{La} = k_1(k)[1 - e^{-k_2(k)u(k)}]$. This is a complex nonlinear function, which needs some transformations to be done in order to be capable to receive linear representation of the function $y(k)$. The input/output equation is

$$y(k) = \Delta t[k_1(k)(1 - e^{-k_2(k)u(k)}) (s_{O,sat} - s_O(k)) + r_{SO}(k)]$$

It is necessary to select the parameters to be estimated in such a way that $y(k)$ is linear according to these parameters. The following transformations are done:

$$K_{La} = k_1(k)[1 - e^{-k_2(k)u(k)}] = k_1(k) - k_1(k)e^{-k_2(k)u(k)} = \theta_1(k) + \theta_2(k) \quad (4.20)$$

where $\theta_1(k) = k_1(k)$, $\theta_2(k) = -k_1(k)e^{-k_2(k)u(k)}$

Then

$$\begin{aligned}
y(k) &= \Delta t[(\theta_1(k) + \theta_2(k)) (s_{O,sat} - s_O(k)) + r_{SO}(k)] = \\
&= \Delta t[(s_{O,sat} - s_O(k)) \quad (s_{O,sat} - s_O(k)) \quad 1] \begin{bmatrix} \theta_1(k) \\ \theta_2(k) \\ \theta_3(k) \end{bmatrix} \quad (4.21)
\end{aligned}$$

Equation (4.21) has the same structures as Equation (4.16). After calculation of the parameters $\theta(k)$, recalculation of $k_1(k)$ and $k_2(k)$ has to be done following (4.20).

$$k_1(k) = \theta_1(k)$$

$$\theta_2(k) = -\theta_1(k)e^{-k_2(k)u(k)}$$

$$\frac{\theta_2(k)}{\theta_1(k)} = -e^{-k_2(k)u(k)}$$

$$\ln\left(\frac{\theta_2(k)}{\theta_1(k)}\right) = k_2(k)u(k)$$

$$k_2(k) = \frac{1}{u(k)} \ln\left(\frac{\theta_2(k)}{\theta_1(k)}\right)$$

The dimensions of the corresponding vectors and matrices is

$$\bar{y} \in R^K, \bar{\psi} \in R^{K \times (3 \cdot K)}, \bar{\theta} \in R^{3 \cdot K}, \tilde{\psi} \in R^{K \times 3}$$

4.4.5 Oxygen transfer function represented by a square root function

Two cases are considered:

1). In this case $K_{La} = k_1(k)\sqrt{u(k)}$. There is only one parameter to be estimated i.e. k_1 .

The input/output equation is

$$y(k) = \Delta t[k_1(k)\sqrt{u}(s_{O,sat} - s_O(k)) + r_{SO}(k)] = \Delta t[\sqrt{u}(k)(s_{O,sat} - s_O(k)) \quad 1] \begin{bmatrix} \theta_1(k) \\ \theta_2(k) \end{bmatrix} = \varphi(k)\theta(k)$$

where $\varphi(k) = \Delta t[\sqrt{u}(k)(s_{O,sat} - s_O(k)) \quad 1] \in R^{1 \times 2}$, $\theta(k) = [\theta_1(k) \quad \theta_2(k)]^T \in R^2$

The calculation of the parameters is done following Equations (4.6) and (4.9).

where $\bar{\psi} \in R^{K \times (2 \cdot K)}$, $\tilde{\psi} \in R^{K \times 2}$, $\bar{\theta} \in R^{2 \cdot K}$, $\bar{y} \in R^K$

2). In this case $K_{La} = k_1(k)u(k) + k_2(k)\sqrt{u(k) + k_3(k)}$. The following substitutions are done

$$\theta_1(k) = k_1(k)u(k)$$

$$\zeta(k) = k_2(k)\sqrt{u(k) + k_3(k)} = \zeta_1(k) \cdot \zeta_2(k)$$

$$\zeta_1(k) = k_2(k)$$

$$\zeta_2(k) = [u(k) + k_3(k)]^{1/2}$$

Equation (4.21) has the same structures as Equation (4.16). After calculation of the parameters $\theta(k)$, recalculation of $k_1(k)$ and $k_2(k)$ has to be done following (4.20).

$$k_1(k) = \theta_1(k)$$

$$\theta_2(k) = -\theta_1(k)e^{-k_2(k)u(k)}$$

$$\frac{\theta_2(k)}{\theta_1(k)} = -e^{-k_2(k)u(k)}$$

$$\ln\left(\frac{\theta_2(k)}{\theta_1(k)}\right) = k_2(k)u(k)$$

$$k_2(k) = \frac{1}{u(k)} \ln\left(\frac{\theta_2(k)}{\theta_1(k)}\right)$$

The dimensions of the corresponding vectors and matrices is

$$\bar{y} \in R^K, \bar{\psi} \in R^{K \times (3 \times K)}, \bar{\theta} \in R^{3 \times K}, \tilde{\psi} \in R^{K \times 3}$$

4.4.5 Oxygen transfer function represented by a square root function

Two cases are considered:

1). In this case $K_{La} = k_1(k)\sqrt{u(k)}$. There is only one parameter to be estimated i.e. k_1 .

The input/output equation is

$$y(k) = \Delta t [k_1(k)\sqrt{u}(s_{O,sat} - s_O(k)) + r_{SO}(k)] = \Delta t [\sqrt{u}(k)(s_{O,sat} - s_O(k)) \quad 1] \begin{bmatrix} \theta_1(k) \\ \theta_2(k) \end{bmatrix} = \varphi(k)\theta(k)$$

where $\varphi(k) = \Delta t [\sqrt{u}(k)(s_{O,sat} - s_O(k)) \quad 1] \in R^{1 \times 2}$, $\theta(k) = [\theta_1(k) \quad \theta_2(k)]^T \in R^2$

The calculation of the parameters is done following Equations (4.6) and (4.9).

where $\bar{\psi} \in R^{K \times (2 \times K)}$, $\tilde{\psi} \in R^{K \times 2}$, $\bar{\theta} \in R^{2 \times K}$, $\bar{y} \in R^K$

2). In this case $K_{La} = k_1(k)u(k) + k_2(k)\sqrt{u(k) + k_3(k)}$. The following substitutions are done

$$\theta_1(k) = k_1(k)u(k)$$

$$\zeta(k) = k_2(k)\sqrt{u(k) + k_3(k)} = \zeta_1(k) \cdot \zeta_2(k)$$

$$\zeta_1(k) = k_2(k)$$

$$\zeta_2(k) = [u(k) + k_3(k)]^{1/2}$$

Equation (4.21) has the same structures as Equation (4.16). After calculation of the parameters $\theta(k)$, recalculation of $k_1(k)$ and $k_2(k)$ has to be done following (4.20).

$$k_1(k) = \theta_1(k)$$

$$\theta_2(k) = -\theta_1(k)e^{-k_2(k)u(k)}$$

$$\frac{\theta_2(k)}{\theta_1(k)} = -e^{-k_2(k)u(k)}$$

$$\ln\left(\frac{\theta_2(k)}{\theta_1(k)}\right) = k_2(k)u(k)$$

$$k_2(k) = \frac{1}{u(k)} \ln\left(\frac{\theta_2(k)}{\theta_1(k)}\right)$$

The dimensions of the corresponding vectors and matrices is

$$\bar{y} \in R^K, \bar{\psi} \in R^{K \times (3 \times K)}, \bar{\theta} \in R^{3 \times K}, \tilde{\psi} \in R^{K \times 3}$$

4.4.5 Oxygen transfer function represented by a square root function

Two cases are considered:

1). In this case $K_{La} = k_1(k)\sqrt{u(k)}$. There is only one parameter to be estimated i.e. k_1 .

The input/output equation is

$$y(k) = \Delta t [k_1(k)\sqrt{u}(s_{O,sat} - s_O(k)) + r_{SO}(k)] = \Delta t [\sqrt{u}(k)(s_{O,sat} - s_O(k)) \quad 1] \begin{bmatrix} \theta_1(k) \\ \theta_2(k) \end{bmatrix} = \varphi(k)\theta(k)$$

where $\varphi(k) = \Delta t [\sqrt{u}(k)(s_{O,sat} - s_O(k)) \quad 1] \in R^{1 \times 2}$, $\theta(k) = [\theta_1(k) \quad \theta_2(k)]^T \in R^2$

The calculation of the parameters is done following Equations (4.6) and (4.9).

where $\bar{\psi} \in R^{K \times (2 \times K)}$, $\tilde{\psi} \in R^{K \times 2}$, $\bar{\theta} \in R^{2 \times K}$, $\bar{y} \in R^K$

2). In this case $K_{La} = k_1(k)u(k) + k_2(k)\sqrt{u(k) + k_3(k)}$. The following substitutions are done

$$\theta_1(k) = k_1(k)u(k)$$

$$\zeta(k) = k_2(k)\sqrt{u(k) + k_3(k)} = \zeta_1(k) \cdot \zeta_2(k)$$

$$\zeta_1(k) = k_2(k)$$

$$\zeta_2(k) = [u(k) + k_3(k)]^{1/2}$$

Then $\ln \zeta(k) = \ln \zeta_1(k) + \ln \zeta_2(k) = \theta_2(k) + \theta_3(k)$

where $\ln \zeta_1(k) = \ln k_2(k) = \theta_2(k)$, $\ln \zeta_2(k) = \frac{1}{2} \ln[u(k) + k_3(k)] = \theta_3(k)$

Then the oxygen transfer function can be substituted by the following expression

$K_{La} = \theta_1(k) + \theta_2(k) + \theta_3(k)$ and the input/output equation is

$$y(k) = \Delta t[(\theta_1(k) + \theta_2(k) + \theta_3(k))(s_{O,sat} - s_o(k)) + r_{SO}(k)] =$$

$$= \Delta t[(s_{O,sat} - s_o(k)) \quad (s_{O,sat} - s_o(k)) \quad (s_{O,sat} - s_o(k)) \quad 1] \begin{bmatrix} \theta_1 \\ \theta_2 \\ \theta_3 \\ \theta_4 \end{bmatrix}$$

where $\theta_4(k) = r_{SO}(k)$

The dimensions of the corresponding vectors and matrices for the estimation calculation is $\bar{\psi} \in R^{K \times (4 \times K)}$, $\tilde{\psi} \in R^{4 \times K}$, $\bar{y} \in R^K$, $\bar{\theta} \in R^{4 \times K}$

After calculation of the vector θ , the parameters of the transfer function are calculated back as follows:

$$\theta_1(k) = \ln k_1(k)u(k) \rightarrow k_1(k) = \frac{\theta_1(k)}{u(k)}$$

$$\theta_2(k) = \ln k_2(k) \rightarrow k_2(k) = \ln^{-1} \theta_2(k)$$

$$\theta_3(k) = \frac{1}{2} \ln[u(k) + k_3(k)] \rightarrow \ln^{-1} 2\theta_3(k) = u(k) + k_3(k) \rightarrow k_3(k) = \ln^{-1} 2\theta_3(k) - u(k)$$

4.4.6 Oxygen transfer function represented by second order polynomial

In this case $K_{La} = k_1(k)u(k) + k_2(k)u^2(k)$. The vector function $\varphi(k)$ is calculated from the input/output equation

$$y(k) = \Delta t[[k_1(k)u(k) + k_2(k)u^2(k)](s_{O,sat} - s_o(k)) + r_{SO}(k)] =$$

$$= \Delta t[u(k)(s_{O,sat} - s_o(k)) \quad u^2(k)(s_{O,sat} - s_o(k)) \quad 1] \begin{bmatrix} \theta_1(k) \\ \theta_2(k) \\ \theta_3(k) \end{bmatrix} = \varphi(k)\theta(k), \theta \in R^3$$

where $\theta_1(k) = k_1(k)$, $\theta_2(k) = k_2(k)$, $\theta_3(k) = r_{SO}(k)$

and $\varphi(k) = \Delta t[u(k)(s_{O,sat} - s_o(k)) \quad u^2(k)(s_{O,sat} - s_o(k)) \quad 1] \in R^{1 \times 3}$

Other steps in the process are the same as above, where $\bar{\psi} \in R^{K \times (3 \times K)}$, $\tilde{\psi} \in R^{K \times 3}$, $\bar{y} \in R^K$, $\bar{\theta} \in R^{3 \times K}$

4.4.7 Oxygen transfer function represented by a Monod type model

In this case $K_{La} = \frac{k_1(k)u(k)}{u(k) + k_2(k)}$. Some additional transformations have to be done to

equation of the parameters. First the transfer function is represented as a ratio of the two parameters

$$K_{La} = \frac{k_1(k)u(k)}{u(k) + k_2(k)} = \frac{\zeta_1(k)}{\zeta_2(k)}, \text{ where } \zeta_1(k) = k_1(k)u(k), \zeta_2(k) = u(k) + k_2(k)$$

The logarithm of the transfer function is introduced $\ln K_{La} = \ln \zeta_1(k) - \ln \zeta_2(k) = \theta_1 - \theta_2$

where $\theta_1(k) = \ln \zeta_1(k)$, $\theta_2(k) = \ln \zeta_2(k)$. The input/output equation becomes

$$\begin{aligned} y(k) &= \Delta t [(\theta_1(k) - \theta_2(k))(s_{O,sat} - s_O(k)) + r_{SO}] = \\ &= \Delta t [(s_{O,sat} - s_O(k)) \quad -(s_{O,sat} - s_O(k)) \quad 1] \begin{bmatrix} \theta_1(k) \\ \theta_2(k) \\ \theta_3(k) \end{bmatrix} = \varphi(k)\theta(k) \end{aligned}$$

where $\varphi(k) = \Delta t [(s_{O,sat} - s_O(k)) \quad -(s_{O,sat} - s_O(k)) \quad 1] \in R^{1 \times 3}$

The dimensions of the corresponding matrices for estimation are $\bar{\psi} \in R^{K \times (3 \times K)}$, $\tilde{\psi} \in R^{3 \times K}$, $\bar{y} \in R^K$, $\bar{\theta} \in R^{3 \times K}$.

After calculation of the vector θ or $\bar{\theta}$, recalculation back of the transfer function parameters is done. From the steps done for substitution can be written as

$$\zeta_1(k) = k_1(k)u(k) = \ln^{-1} \theta_1(k)$$

$$\zeta_2(k) = k_2(k) + u(k) = \ln^{-1} \theta_2(k)$$

From here, $k_1(k) = \frac{\ln^{-1} \theta_1(k)}{u(k)}$, $k_2(k) = \ln^{-1} \theta_2(k) - u(k)$, $k = \overline{0, K-1}$

4.5 Calculation of the parameters in the software environment of Matlab

4.5.1 Algorithm for parameter estimation

Matlab software is developed for calculation of the parameters of the dissolved oxygen concentration mass balance equation. The algorithm for calculation is following:

- Input of the data from measurement of $s_O(k)$ and $u(k)$ for a given period of time $k = [0, K]$
- Input of constants necessary for calculation

Estimation steps:

- Calculation of $y(k)$ according to Equation (4.3), $k = \overline{0, K-1}$
- Calculation of $\varphi(k)$ for the considered case of K_{La} , $k = \overline{0, K-1}$
- Building of the vector \bar{y} and the matrix $\bar{\psi}$ according to Equation (4.6)
- Calculation of the parameters $\bar{\theta}$ according to Equation (4.8)

Verification steps:

- Simulation of the dissolved oxygen mass balance equation using the estimated parameters with the same values of $u(k)$, $k = \overline{0, K-1}$ as these used to produce data.
- Comparison of the obtained dissolved oxygen trajectory with the data used for the estimation
- Calculation of errors between the data $s_o(k)$, $k = [0, K]$ and the trajectory of $s_o(k)$ obtained from the simulation

The software uses data for the ASM1 model, where the concentration of the dissolved oxygen is taken from its simulation done with $K_{La} = 240/day$ and $s_{O,sat} = 8mg/l$. The inflow concentration is considered to be very low $s_{O,in} = 0.2mg/l$. The results obtained from the estimation are done for every case of K_{La} separately.

4.6 Conclusion

This chapter discussed different models of the oxygen transfer function, for the development of a method and algorithm for estimating the values of K_{La} . The value of K_{La} varies according to the wastewater quality and diffusers clogging. Matlab software is developed for calculation of the parameters of the dissolved oxygen concentration mass balance equation and is given in Appendix B. The least squares method is developed for estimation of the OUR and the oxygen transfer function parameters.

Estimation steps:

- Calculation of $y(k)$ according to Equation (4.3), $k = \overline{0, K-1}$
- Calculation of $\varphi(k)$ for the considered case of K_{La} , $k = \overline{0, K-1}$
- Building of the vector \bar{y} and the matrix $\bar{\psi}$ according to Equation (4.6)
- Calculation of the parameters $\bar{\theta}$ according to Equation (4.8)

Verification steps:

- Simulation of the dissolved oxygen mass balance equation using the estimated parameters with the same values of $u(k)$, $k = \overline{0, K-1}$ as these used to produce data.
- Comparison of the obtained dissolved oxygen trajectory with the data used for the estimation
- Calculation of errors between the data $s_o(k)$, $k = [0, K]$ and the trajectory of $s_o(k)$ obtained from the simulation

The software uses data for the ASM1 model, where the concentration of the dissolved oxygen is taken from its simulation done with $K_{La} = 240/day$ and $s_{O,sat} = 8mg/l$. The inflow concentration is considered to be very low $s_{O,in} = 0.2mg/l$. The results obtained from the estimation are done for every case of K_{La} separately.

4.6 Conclusion

This chapter discussed different models of the oxygen transfer function, for the development of a method and algorithm for estimating the values of K_{La} . The value of K_{La} varies according to the wastewater quality and diffusers clogging. Matlab software is developed for calculation of the parameters of the dissolved oxygen concentration mass balance equation and is given in Appendix B. The least squares method is developed for estimation of the OUR and the oxygen transfer function parameters.

CHAPTER FIVE

OVERVIEW OF THE METHODS FOR ANALYSIS AND CONTROL DESIGN OF NONLINEAR SYSTEMS

5.1 Introduction

The theory of automatic control has been well developed for the decades ever since the establishment of the Nyquist criterion in the 1930s due to World War II (Dorf and Bishop, 2001) and other methods of linear system analysis. (http://www.worldscibooks.com/etextbook/6862/6862_preface.pdf). The fact is that almost all physical systems are nonlinear in nature. Sometimes it is possible to describe the operation of a physical system by a linear model, using ordinary linear differential equations to solve a problem where a mode of operation of the physical system does not deviate too much from the nominal set of operating conditions; sometimes this condition is called exact linearization. But at times the linearized model can be deemed inadequate and thus giving an introduction of nonlinear systems theory (<http://www.control.aau.dk/~raf/NonLinear/Nonlinea.htm>).

Nonlinear control theory is used for analysis and design of nonlinear control systems. This chapter gives an introduction in section 5.1. Section 5.2 considers nonlinear systems definition. The nonlinear methods for analysis and control design of nonlinear systems are compared in subsections 5.2.1 to 5.2.4. Section 5.3 deals with mathematical models of the nonlinear systems. Section 5.4 gives different types of nonlinear controller design methods and discussed lastly is methods for analysis of the nonlinear systems

5.2 Nonlinear system determination

Linear models are frequently sufficient enough to describe the dynamics of processes in steady-state operations if disturbances to the process are fairly small. Given the latter statement, it is one of the reasons for the attractiveness of making use of linear dynamical models in system estimation and control. Furthermore, linear systems theory and the resulting control design have been well recognized for past decades. The examples like, the least-square (LS) method and linear programming problems are based on somewhat complete theory and take place in a variety of applications (<http://www.math.ucla.edu/~tom/LP.pdf>), (Ikonen and Najim, 2002). Common accepted mathematical representation of a linear system in state space is given by the following set of equations (http://www.me.berkeley.edu/ME237/2_general_properties.pdf)

$$\dot{x} = Ax(t) + Bu(t), \quad x(0) = x_0 \quad (5.1)$$

$$y = Cx(t) + Du(t) \quad (5.2)$$

where $x \in R^n$, $u \in R^m$, $y \in R^l$ are respectively state, control and output vectors and $A \in R^{n \times n}$, $B \in R^{n \times m}$, $C \in R^{l \times n}$, $D \in R^{l \times m}$ are state, control output state and output control matrices, x_0 is the initial state space vector.

Linear systems theory is based on the following main points

(http://www.me.berkeley.edu/ME237/2_general_properties.pdf):

1. Superposition principle: meaning a linear combination of any two solutions for a linear system is also a solution.
2. Unique Equilibrium: Equilibrium is a solution $x(t)$, by way of making the control input $u(t) = 0$, for which the state x is steady. A generic linear system has a distinctive equilibrium at the origin $x(t) = 0$ which guarantees easily achievable stability.
3. Controllability: There are acknowledged necessary and sufficient conditions under which a control can manoeuvre the state of a linear system from any original value to any desired absolute value in fixed time.
4. Observability: There are known necessary and sufficient conditions under which the system's state history can be determined from its input and output history.
5. Control design tools: Assortments of controller and observer design techniques are readily available for linear systems, e.g. Classical techniques, pole placement method, H^∞ etc.

But on the other hand, it cannot be said that nonlinear systems have a convenient consistent theory. The stage, on which the existing powerful analysis tools for linear systems are sitting on, is *superposition principle*. But, it is of interest to note that the superposition principle is not applicable to nonlinear systems. Therefore, analysis tools for nonlinear systems engage more complex mathematics, and the tools for analysis and design are restricted to specialised categories (Slotine and Li, 1991). Linear control is an established subject with a variety of powerful methods and long history of successful industrial applications. But, now many researchers and designers, from such broad areas like aircraft and spacecraft control, robotics, process control, and biomedical engineering, have recently shown a growing interest in the development and applications of nonlinear control methodologies. It can be seen that many reasons exist why? Even if linear system theory has contributed to valuable methodologies for dynamical modelling,

system identification, and control design, it has its boundaries. There are many conditions where linear methodologies are rendered insufficient, for instance, when steady-states are changing unexpectedly or frequently. In such situations it might be indispensable to utilize the nonlinear models in order to express the system more accurately (Slotine and Li, 1991).

A system can be described as a nonlinear system when its behaviour or performance cannot be described by the equations of first order. It is currently not possible to model and identify general nonlinear systems because of their great variety and because of their structural complexity. There are numerous nonlinear systems which must be controlled in the present industrial world. Thus, it is important to develop methods to model nonlinear systems and to estimate the model parameters. Once the models are available, it is also important to investigate how they can be used to establish an understanding and an effective control of the relevant system. The general schematic representation of a nonlinear system is shown on Figure 5.1.

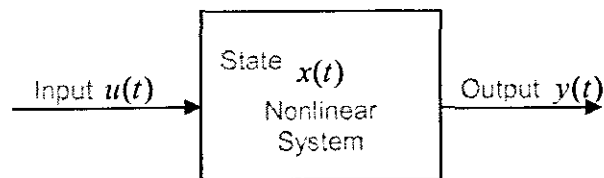


Figure 5.1: General nonlinear system model.

The general mathematical representation of a nonlinear system in state space domain is given by the Equations (5.3) and (5.4) (Slotine and Li, 1991),

State equation

$$\dot{x}(t) = f(x, u, t), \quad x(0) = x_0 \quad (5.3)$$

Output equation

$$y(t) = h(x, u, t) \quad (5.4)$$

where $f \in \mathbf{R}^n$ is the vector nonlinear function of the state, control and time and $h \in \mathbf{R}^l$ is the vector nonlinear output function of the state, control and time.

5.2.1 Improvement of existing control systems

It is a known fact that linear control methods mostly rely on key assumptions of small range operations for the linear model to be valid. Once the required operation range becomes large, then a linear controller is likely to perform poorly or be unstable, simply because of the nonlinearities in the system that cannot be properly compensated for. Nonlinear controller, on the other hand, may handle the nonlinearities in large operations directly. The example is that of a robot motion problem, that when a linear controller is used, it does not take into consideration the nonlinear forces associated with the motion of robot links (Slotine and Li, 1991).

5.2.2 Analysis of hard nonlinearities

One of the assumptions of the linear control is that the model is indeed linearizable. However, in control systems there are much nonlinearities whose discontinuous nature does not allow linear approximation. Examples of hard nonlinearities include, but are not limited to coulomb friction, saturation, dead-zones, backlash, and hysteresis which are often found in control engineering. Their effects cannot be derived from linear methods, and as a result nonlinear analysis techniques must be developed to predict a system's performance in the presence of these inherent nonlinearities (Slotine and Li, 1991). These nonlinearities are frequently causing undesirable behaviour of the control systems, such as instabilities or spurious limit cycles and because of this their effects must be predicted and properly compensated for.

5.2.3 Dealing with model uncertainties

When designing linear controllers, it is usually necessary to assume that the parameters of the system model are reasonably well known. However, many control problems involve uncertainties in the model parameters. This may be due to a slow time variation of parameters, or to a sudden change in parameters. A linear controller based on inaccurate or outmoded values of the model parameters may exhibit significant performance degradation or even instability (Slotine and Li, 1991). Nonlinearities can intentionally be introduced into the controller system so that model uncertainties can be tolerated. Two modes of nonlinear controllers for this purpose are robust controllers and adaptive controllers.

5.2.4 Design simplicity

Good nonlinear controller designs may be simpler and more intuitive than their linear counterparts. This a priori paradoxical result comes from the fact that nonlinear controller designs are often deeply rooted in the physics of the plant (Slotine and Li, 1991).

5.3 Mathematical models of the nonlinear systems

Physical systems are naturally nonlinear, meaning, that all control systems are nonlinear to a certain extent. Nonlinear control systems can be described by nonlinear differential equations. However, if the operating range of a control system is small, and if the involved nonlinearities are smooth, then the control system may be reasonably approximated by a linearized system, whose dynamics is described by a set of linear differential equations. Nonlinear systems are mathematically represented systems whose behaviour cannot be described by the equation of first order or whose behaviour is not expressible as a linear function of their descriptors, meaning, such, systems are not linear and are not subject to the principle of superposition, as linear systems are. Nonlinear system is one whose behaviour is not simply the sum of its parts or multiples.

Nonlinear systems frequently have more than one equilibrium point. The general objective of the nonlinear control strategy is to make the closed-loop system to behave more linearly by keeping the loop gain constant. However, if the operating range of a control system is very small, and the involved nonlinearities of system are believed to be smooth, then the control system may be reasonably approximated by a linearized system whose dynamics are described by a set of linear differential equations (Slotine and Li, 1991).

Nonlinearities of the system can be classified as inherent and artificial. Natural or inherent nonlinearities normally come with the system's hardware and motion. The artificial ones are intentional if introduced by the control design engineer. The nonlinearities can also be classified in terms of their mathematical properties, as continuous and discontinuous. The discontinuous nonlinearities cannot locally be approximated by linear functions, thus they are so called hard nonlinearities (Slotine and Li, 1991).

Nonlinear equations are more complex, and much harder to understand because of their lack of simple superposed solutions. For nonlinear equations the solutions to the equations do not in general form a vector space and cannot be superposed to produce

new solutions. This makes solving the equations much harder than in linear systems. Some nonlinear equations are well understood, for example $x^2 - 1 = 0$, and other polynomial equations. Systems of nonlinear polynomial equations, however, are more complex. Similarly, first order nonlinear ordinary differential equation such as $d_x u = u^2$ are easily solved. Higher order differential equations like $d_x^2 u + g(u) = 0$, where g is any nonlinear function, can be much more challenging. For partial differential equations the picture is even poorer, although a number of results involving existence of solutions, stability of a solution and dynamics of solutions have been proven. The type of control that is convenient for nonlinear systems is nonlinear control. Nonlinear affine standard form equation is presented below:

$$\dot{x}(t) = f(x, t) + g(x, t)u(t), \quad x(0) = 0 \quad (3.6)$$

$$y(t) = h(x, t)$$

where x is a state vector, u is the control vector, w is the disturbance vector and $f(x)$ and $g(x)$ are nonlinear functions, y is the output vector and h is the output matrix. This equation represents big class of nonlinear processes and this equation is used for the development of nonlinear linearizing controller based on Lyapunov second method for stability or input/output feedback linearization.

5.4 Nonlinear control design

The type of control that is convenient for nonlinear systems is nonlinear control.

Types of nonlinear controller design methods can be listed in the following way:

1. Feedback linearization
2. Input/Output Linearization
3. Sliding mode control
4. Lyapunov theory of stability
5. Adaptive control

5.4.1 Feedback linearization

Jacobian Linearization method is a renowned approach and is based on local linearization of nonlinear model, but it is constrained to a certain operating range, which is most of the time too small for practical purpose and as a result cannot guarantee the wider controllability of the system. A different approach founded on techniques from differential geometry has been established and for that matter has gained much attention, the reason being; it gives rather effective tools for investigating and designing

nonlinear systems control. The approach in question is called exact feedback linearization and is less restrictive than the Jacobian method, because it has a much broader control range (Ervadi-Radhakrishnan and Voit, 2005). More is discussed in chapter 6.

5.4.2 Input/Output linearization

Most of the feedback linearization approaches are based on input/output linearization or state space linearization. The main objective of input/output (I/O) linearization approach is to linearize the map between the transformed inputs (v) and the actual outputs (y). Detailed discussion is given in chapter 6; this method is used to design the linearizing controller for dissolved oxygen concentration in the thesis.

5.4.3 Sliding mode control

Sliding mode controller design provides a systematic approach to the problem of maintaining stability and consistent performance in the face of modelling imprecision (Slotine and Li, 1991:277). Sliding mode control is suitable to control first order systems. It is standard approach to tackle the parametric and modelling uncertainties of nonlinear systems. The sliding mode approach is a method which transforms a higher order system into first order system. In this way, a simple control algorithm can be applied, which is very straightforward and robust (http://scholar.lib.vt.edu/theses/available/etd-5440202339731121/unrestricted/CHAP4_DOC.pdf). It has been successfully applied to robot manipulators, underwater vehicles, automotive transmissions and engines, high-performance electric motors, and power systems.

5.4.4 Lyapunov theory of stability

Presented with a control system, the first thing that comes to mind in regard to its different properties is whether it is stable. because unstable control system is basically ineffective and prospectively dangerous. Given the degree of distinction, a system is described as stable if starting the system somewhere near its desired operating point implies that it will stay around that point forever (Slotine and Li, 1991), (Bandyopadhyay, 2003: 255).

The linearization method is said to be drawing conclusions about a nonlinear system's local stability around an equilibrium point from the stability properties of its linear approximation, while the direct method is not restricted to local motion, but instead it

expands to determining the stability properties of a nonlinear system by constructing a scalar energy-like function for the system and examining the function's time variation. The uniqueness of this particular method is that, only the form of the model differential or difference equations is needed to be known but not their solutions.

Linearization method constitutes the theoretical justification of linear control, while the direct method has become the most important tool for nonlinear systems analysis and design and the latter is used in the thesis in chapter 7 for nonlinear linearizing controller design. Both methods give rise to Lyapunov stability theory because they determine important directions for investigation of the control systems.

5.4.5 Adaptive control

The fundamental idea in adaptive control of nonlinear systems is to control the system with uncertainty parameters (Slotine and LI, 1991), (Yang and Wang, 2006). There are many control predicaments that require the feedback, but confronted by different design goals, there are different approaches relating to the control problem. The undertaking of stability, tracking, disturbance rejection and attenuation results in a number of control problems and as a result, in each problem there is a feedback version for all state variables to be measured, whose dimension is less than the dimension of the state.

The desire for optimization of control design leads to many problems of optimal control. When considering model uncertainty, then the issues of sensitivity and robustness come into play, simply because the design of feedback control handles a wide range of model uncertainty and leads to either robust or adaptive control problems. Robust control characterises model uncertainty as per perturbation of a nominal model. Nominal model may be thought as a point in space and perturbed models as points encompassing the nominal model. Robust control design is mainly due to meeting the control objectives for model uncertainty in the sphere. The adaptive control on the other hand deals with parameter uncertainties in terms of certain unknown parameters and strives to use feedback to learn parameters on-line, meaning during the operation of the system.

The main focus of nonlinear control deals with the analysis and design of nonlinear control system meaning control systems contain at least one nonlinear component. In the analysis it is assumed that, nonlinear closed-loop systems have been designed and the characteristic behaviour of the system is being determined. In the design, a nonlinear plant to be controlled and some specifications of the closed-loop system behaviour are

given and the task at hand will be to construct a controller in such a way that the closed-loop system meets the desired characteristics. In practical terms, the issue of design and analysis are interlinked, simply because the design of a nonlinear control system usually entails repetitive process of analysis and design (Slotine and Li, 1991).

5.5 Methods for analysis of the nonlinear systems

The analysis of nonlinear systems is very difficult and many methods have been proposed in the literature, but the first two are being discussed briefly:

1. Phase plane analysis
2. Describing functions
3. Lyapunov method

5.5.1 Phase plane analysis

Phase plane analysis is regarded as a graphical method for studying second order systems. The fundamental idea for the method is to solve second order differential equations graphically by generating in state space of the second order dynamic system, motion trajectories corresponding to various initial conditions, and then to examine the qualitative features of the trajectories (Slotine and Li, 1991), (Bandyopadhyay, 2003).

Phase plane analysis has a number of useful properties. First, as a graphical method, it allows one to picture what goes on in a nonlinear system starting from an assortment of initial conditions, without having to solve nonlinear equations analytically. Secondly, it is not restricted to small or smooth nonlinearities, nevertheless, it applies equally well to strong nonlinearities and to “hard” nonlinearities. Ultimately, it is of great importance to note that some practical control systems can indeed be adequately approximated as second order systems, and by so doing, the fundamental disadvantage concerning this is, this restricting them to second order systems (Slotine and Li, 1991). The graphical study of high order systems is computationally and geometrically complex.

An example of a phase plane analysis method can be presented using a phase portraits described by the second order autonomous system as

$$\dot{x}_1 = f_1(x_1, x_2), \quad x_1(0) = x_{10} \quad (5.5)$$

$$\dot{x}_2 = f_2(x_1, x_2), \quad x_2(0) = x_{20} \quad (5.6)$$

where x_1 and x_2 are the states of the system, and f_1 and f_2 are the nonlinear functions of the states. Geometrically, the state space of the above system is a plane having x_1 and x_2 as coordinates (Hassan Saeed, 2002).

Singular point is an imperative notion in phase plane analysis, meaning, a singular point is an equilibrium point in the phase plane. The reason being, an equilibrium point is defined as a point where the system states can stay forever, implying that $\dot{x} = 0$ and by using the above system, therefore,

$$f_1(x_1, x_2) = 0 \qquad f_2(x_1, x_2) = 0 \qquad (5.7)$$

Linear system usually has one singular point, but a nonlinear system often has more than one isolated singular point. It can be argued as to why an equilibrium point of a second order system is called a singular point. The answer to this is, the slope of the phase orbits passing through a point (x_1, x_2) is determined based on Equations (5.5) and (5.6) with functions f_1 and f_2 believed to be single valued, generally there is a specific value for this slope at any given point in phase plane. This means that the phase trajectories will not intersect. However, at singular points, the value of the slope is at (0,0) meaning that the slope is undefined.

Singular points are of great significance characteristics in phase plane analysis. Examination of the singular points can reveal important information about the properties of a system. When dealing with nonlinear systems, in addition to singular points, there might be further complex features, such as limit cycles. Although phase plane method is primarily developed for second order systems, it is also applicable to the analysis of first order systems.

It should however be noted that phase plane analysis of nonlinear systems is related to that of their linear counterparts, meaning the local behaviour of nonlinear system can be approximated by that of a linear system. Nevertheless, nonlinear systems can display much more complicated patterns in the phase plane, such as multiple equilibrium points and limit cycles. Limit cycle can be defined as an isolated closed curve. The trajectory has closed both, signifying the periodic nature of the motion, and isolated, representing the limiting nature of the cycle (Glad and Ljung, 2000).

5.5.2 Describing functions

Describing function method is a method used as an approximation procedure for studying nonlinear systems. Its primary objective is to approximate the nonlinear components in the nonlinear control system by making their linear equivalents and then using frequency domain techniques to evaluate the resulting systems (Slotine and Li, 1991), (Hassan Saeed, 2002). It differs from neither phase plane method in the sense that, it is restrictive to second order systems, nor Lyapunov method, which will be defined later, whose application to particular systems centres around the success of a trial-and-error searching for a Lyapunov function. It can be applied easily to nonlinear systems in order to satisfy some easy to check conditions (Slotine and Li, 1991). The most important application for this method is to predict limit cycles in nonlinear systems. Describing functions can be utilized to determine the system stability, both in the case in the closed loop frequency response and transient response. The describing function describes the nonlinearity and then the stability can be easily assessed by Nyquist diagram (Hassan Saeed, 2002), (Bandyopadhyay, 2003), (Glad and Ljung, 2000).

5.5.3 Lyapunov method

The two methods of Lyapunov can be used for system analysis or controller design. The first method is based on solution of the system of differential equations representing the system model and evaluation behaviour of the solution. The second method is based on construction of a Lyapunov function and evaluating the sign of its derivative for the differential equations describing the system model.

5.6 Conclusion

The control theory has been in existence for centuries. But the mostly used theory had been linear control. Since linear control has limitations it is the reason why nonlinear control theory has been so important in today's world. In this chapter, nonlinear control theory has been studied. Some of the existing methods for design of controllers of the nonlinear systems are discussed. *Three methods for analysis of the nonlinear system* have been discussed, namely phase plane analysis, describing functions and Lyapunov method. Chapter 6 is discussing the input-output feedback linearization out of which the linearizing controller is designed based on.

CHAPTER SIX

DESIGN OF A NONLINEAR LINEARIZING CONTROL OF DISSOLVED OXYGEN CONCENTRATION

6.1 Introduction

Feedback linearization is a principle which has drawn much attention in the field of nonlinear control systems (Slotine and Li, 1991). The advantage of feedback linearization is that its design can be used generically, in the sense that the same principle can be used on all systems of the right type. Feedback linearization is an approach to nonlinear control design in the form of algebraic transformation of nonlinear system dynamics into a fully or partial linear one, the reason being that, the linear control techniques can be applied. It differs from conservative linearization in the sense that feedback linearization is achieved by exact state transformation and feedback, as opposed to linear approximations of the dynamics. Its techniques can be viewed as ways to transform original system model into equivalent model of a simpler form (Henson and Seborg, 1997).

In this chapter, the feedback linearization is given in section 6.2. Section 6.3 linearization approaches, where two types of linearization input/state and input/output are discussed and compared. Importance of the Dissolved oxygen concentration control is given in section 6.4. Section 6.5 introduces nonlinear linearizing controller design on the basis of the geometrical approach. The design of the nonlinear linearizing controller is described in section 6.6. Section 6.7 shows Simulink block diagram which is used for simulation of the controller. Section 6.8 describes a Matlab program for the controller. Simulation results are given in section 6.9 and those results are being discussed in section 6.10.

6.2 Feedback Linearization

Generally the control systems can either be classified as linear or nonlinear and their control equations can be formulated as follows: (Slotine and Li, 1991).

- For linear control system

$$\dot{x}(t) = Ax(t) + Bu(t) \quad (6.1)$$

- For nonlinear control system

$$\dot{x}(t) = Ax(t) + Bu(t) + f(x, u, t) \quad (6.2)$$

Where $x \in R^n$ is the vector of the state variables, $u \in R^m$ is a control vector, A and B are $n \times n$ and $n \times m$ continuous matrices, respectively, $f: R^n \times R^m \rightarrow R^n$ is a matrix

continuous function. Conventionally, controllability has been defined for linear state space systems. For nonlinear systems, the concept controllability refers to the case where control acts on the system state, even supposing it may be insufficient to transfer the system to the final state. The most common approach to investigate controllability of the nonlinear control system is to linearize it around an operating point x_0 , followed by use of linear control methods. Expressing the dependent variables and control functions as deviations from some nominal operating state x_0 and control u_0 ,

$$x(t) = x_0 + \Delta x(t) \quad (6.3)$$

$$u(t) = u_0 + \Delta u(t) \quad (6.4)$$

and using Taylor expansion about x_0, u_0 , the given nonlinear control system can be written as

$$\frac{d\Delta x(t)}{dt} = [A + J_x(x_0, u_0)]\Delta x(t) + [B + J_u(x_0, u_0)]\Delta u(t) \quad (6.5)$$

where $J_x(x_0, u_0)$ and $J_u(x_0, u_0)$ are the Jacobian matrices evaluated at the reference operating point. The method is simple but rather limited, as the linear approximation is often only sufficiently accurate in small range of around (x_0, u_0) . As a consequence, the control is approximate and often fails for target states that are moderately far from the initial state (Henson and Seborg, 1997).

Feedback linearization has been used successfully to address some practical problems. The fundamental idea of the feedback linearization is to cancel the nonlinearities and impose a desired linear dynamics which can simply be applied to a class of nonlinear systems described by the following forms: companion form or controllability canonical form. A system is termed to be in companion form if its dynamics are represented by (Slotine and Li, 1991)

$$x^{(n)}(t) = f(x, t) + b(x, t)u(t) \quad (6.6)$$

where u is the scalar control input, x is the scalar output of interest, $x(t) = [x(t) \ \dot{x}(t), \dots, x(t)^{(n-1)}]^T$ is the state vector, and $f(x)$ and $b(x)$ are nonlinear functions of the states. The uniqueness of this form is that it only shows the derivatives of x , does not show the derivative of the input u .

If the system is expressed in a controllability canonical form, utilizing the control input, whereby b is assumed to be non-zero of the kind, the nonlinear control can be calculated as

$$u(t) = \frac{1}{b}[v(t) - f(t)] \quad (6.7)$$

then the nonlinearities can be cancelled and the simple input-output relation obtained.

$$x^{(n)}(t) = v(t) \quad (6.8)$$

As a result, the linear control law can be determined of the following form

$$v(t) = -k_0x(t) - k_1\dot{x}(t) - \dots - k_{n-1}x(t)^{(n-1)} \quad (6.9)$$

with k_i chosen so that the polynomial $p^n + k_{n-1}p^{n-1} + \dots + k_0$ has its roots strictly in the left-half complex plane. This leads to the exponential stable dynamics of the closed loop system

$$x^{(n)}(t) + k_{n-1}x(t)^{(n-1)} + \dots + k_0x(t) = 0 \quad (6.10)$$

Implying that $x(t) \rightarrow 0$. For the tasks involving tracking of a desired output $x_d(t)$, the control law becomes

$$v(t) = x_d^{(n)}(t) - k_0e - k_1\dot{e}(t) - \dots - k_{n-1}e^{(n-1)}(t) \quad (6.11)$$

where $e(t) = x(t) - x_d(t)$ is the tracking error, which leads to exponentially convergent tracking.

On the basis of the above for nonlinear dynamics to be properly controlled they have to be in a controllability canonical form, or else algebraically transformations are to be first applied to put the dynamics into the controllability form before using feedback linearization, or relying on partial linearization of the original dynamics instead of full linearization.

There are two approaches to convert the nonlinear system into controllable canonical form: Input-state linearization and input-output linearization. These approaches are considered below. These two approaches use special kind of nonlinear control law. In some applications, the control aims can be achieved with a nonlinear static state feedback control law of the form,

$$u(t) = \alpha(x(t)) + \beta(x(t))v(t) \quad (6.12)$$

where α is an m -dimension vector for nonlinear functions and β is an $m \times m$ matrix of nonlinear functions. But it is not applicable to all processes as it is not always possible to satisfy the control objective with a static controller. In this case a dynamic state feedback control law ought to be used as follows:

$$\dot{\zeta} = \gamma(x, \zeta) + \delta(x, \zeta)v(t) \quad (6.13)$$

$$u(t) = \alpha(x, \zeta) + \beta(x, \zeta)v(t) \quad (6.14)$$

where ζ is a q – dimensional vector of controller state variables; γ is a q – dimensional vector of nonlinear functions; and δ is a $q \times m$ matrix of nonlinear functions (Henson and Seborg, 1997).

6.3 Linearization approaches

6.3.1 Input-State linearization

A class of nonlinear control strategies that can produce a linear model that is an exact representation of the original nonlinear model over a large set of operating conditions is presented. Characteristically the model is called feedback linearization; the universal approach and the model are based on two operations:

- Nonlinear change of coordinates
- Nonlinear state feedback

The emphasis is put on local feedback linearization, meaning, the coordinate transformation and control law may only be locally defined, as to keep away from difficulties associated with the global problem.

Nonlinear system represented by

$$\dot{x}(t) = f(x, t) + g(x, t)u(t), \quad (6.15)$$

$$y(t) = h(x, t) \quad (6.16)$$

$x(0) = x_0$ is considered

The emphasis is put on whether the state feedback control exists of the form of equation (6.12) and a change of variables

$$z = T(x) \quad (6.17)$$

also exists for all states variables, in order to transform the nonlinear system into a controllable canonical form that transforms the original nonlinear to a linear state space system of the form

$$\dot{z}(t) = Az(t) + Bv(t), \quad z(0) = z_0 \quad (6.18)$$

$$y(t) = h(T^{-1}(z)) \quad (6.19)$$

The above is referred to as input-state linearization. Despite the fact that linear control design can stabilize the system in small region just around the equilibrium point, it is not guaranteed whether the controller can do the same for the larger region. The input-state linearization is achievable through the combination of state transformation and input transformation, with state feedback used in both. As a result, it is a linearization by feedback, or feedback linearization. This is necessarily different from a Jacobian

linearization for small range operation, over which linear control is founded. A definition for the conditions of nonlinear system has to fulfil in order to be input-state linearizable is given in (Slotine and Li, 1991), (Henson and Seborg, 1997).

Definition 6.1: A nonlinear system $\dot{x} = f(x,t) + g(x,t)u(t)$, where $f : D \rightarrow R^n$ and $g : D \rightarrow R^{n \times p}$ are sufficiently smooth on a domain $D \subset R^n$, is said to be feedback linearizable, if there exists a diffeomorphism $T : D \rightarrow R^n$ such that $D_z = T(D)$ contains the origin and the change of variables $z(t) = T(x)$ transforms the nonlinear system into the form $\dot{z}(t) = Az(t) + B\gamma(x)[u(t) - \alpha(x)]$ with (A,B) controllable and $\gamma(x)$ non-singular for all $x \in D$.

The feedback linearization and Jacobian Linearization approaches can be compared. When considering the Jacobian linearization for a nonlinear system for the following equilibrium point (u_0, x_0, y_0) using deviation variables, the Jacobian model can be written as a linear state space system of the form

$$\dot{x}(t) = Ax(t) + Bu(t) \quad (6.20)$$

$$y(t) = Cx(t) \quad (6.21)$$

in the company of apparent definitions for the matrices A , B and C . It is of significance to note that the Jacobian model is an exact representation of the nonlinear model only at the point (x_0, u_0) . Accordingly, a control strategy based on a linearized model may lead to unsatisfactory performance and robustness at other operating points.

When feedback linearization is done, the input/output model is then linear,

$$\dot{z}(t) = Az(t) + Bv(t) \quad (6.22)$$

$$\omega(t) = Cz(t) \quad (6.23)$$

where z is an r -dimensional vector of transformed state variables; v is an m -dimensional vector of transformed input variables; ω is an m -dimensional vector of transformed output variables, and the matrices A , B and C have a special canonical formation. If $r < n$, then an additional $n-r$ state variables must be introduced to complete the coordinate transformation of the model. The integer r is called the relative degree and is an essential feature of the nonlinear system.

Linear controller is designed for the linearized input/output model, but there is a subsystem that is normally not linearized,

$$\dot{\eta}(t) = q(\eta, z) \quad (6.24)$$

where η is an $(n-r)$ -dimensional vector of transformed state variables and q is a $(n-r)$ -dimensional vector of nonlinear functions. Input/state linearization methods are limited to processes in which these alleged zero dynamics are stable.

6.3.2 Input/Output Linearization

The linearizing of the state equations does not automatically linearize the I/O map. Consider the single-input single-output (SISO) system.

$$\dot{x}(t) = f(x, t) + g(x, t)u(t) \quad (6.25)$$

$$y(t) = h(x, t) \quad (6.26)$$

The derivate of the output is

$$\dot{y}(t) = \frac{\partial h}{\partial x} [f(x(t)) + g(x(t))u(t)] = L_f h(x(t)) + L_g h(x)u(t) \quad (6.27)$$

where $L_f h(x, t) = \frac{\partial h}{\partial x} f(x, t)$ and $L_g h(x, t) = \frac{\partial h}{\partial x} g(x, t)$ are called Lie derivative of h

along f and g functions.

Further definitions for the Lie derivatives are:

$$L_g L_f h(x, t) = \frac{\partial (L_f h(x))}{\partial x} g(x, t) \quad (6.28)$$

$$L_f^2 h(x, t) = \frac{\partial (L_f h(x, t))}{\partial x} f(x, t) \quad (6.29)$$

$$L_f^k h(x, t) = L_f L_f^{k-1} h(x, t) = \frac{\partial (L_f^{k-1} h(x, t))}{\partial x} f(x, t) \quad (6.30)$$

$$L_f^0 h(x) = h(x, t) \quad (6.31)$$

Reflecting back to the term \dot{y} , it can be written

$$\dot{y}(t) = L_f h(x, t) + L_g h(x, t)u(t) \quad (6.32)$$

It is evident that if $L_g h(x) = 0$, then

$$\dot{y}(t) = L_f h(x, t) \quad (6.33)$$

is independent of u .

If the higher order derivative is considered for y then,

$$\ddot{y}(t) = \frac{d^2 y}{dt^2} = y^{(2)}(t) = \frac{\partial(L_f h(x,t))}{\partial x} [f(x,t) + g(x,t)u(t)] = L_f^2 h(x,t) + L_g L_f h(x,t)u(t) \quad (6.34)$$

This once more proves that if $L_g L_f h(x,t) = 0$ then $\ddot{y} = L_f^2 h(x,t)$ which again is independent of u .

The process can be repeated as to deduce if $h(x)$ satisfies

$$0 = L_g L_f^{i-1} h(x,t) \quad (i=1,2,\dots,p-1) \quad (6.35)$$

$$0 \neq L_g L_f^{p-1} h(x,t) \quad (6.36)$$

Then control u does not appear in the equations of $y, \dot{y}, \dots, y^{p-1}$ and it can therefore be easy to rewrite the p^{th} order differential equation for y is such that

$$y^{(p)} = L_f^p h(x,t) + L_g L_f^{p-1} h(x,t)u(t) \quad (6.37)$$

This clearly illustrates that the system is input/output linearizable if the control variable expressed analytically as:

$$u(t) = \frac{1}{L_g L_f^{p-1} h(x,t)} [-L_f^p h(x,t) + v(t)] \quad (6.38)$$

This nonlinear control reduces the I/O map to

$$y^{(p)}(t) = v(t) \quad (6.39)$$

which is a chain of p integrators. p is sometimes referred to as the relative degree of the nonlinear system.

6.3.3 Comparison between the two approaches

When dealing with state space linearization approach, the objective is to linearize the map between the transformed inputs and the entire vector of transformed state variables. This goal is realized by deriving artificial outputs (ω) that yield a feedback linearized representation with state dimension $r = n$. A linear controller is then created for the linear state-input model. Nevertheless, this approach may fail simply if the controller design is assigned as the map between the transformed inputs and the original outputs (y) which normally is nonlinear one. Accordingly, input/output linearization is favoured over state space linearization for the most process control applications. It is also possible to simultaneously linearize both the input-state and input/output maps for a number of processes for the reason that the original outputs give a linear model with dimension $r = n$. The input/output linearization approach is applied for the design of linearizing control of the dissolved oxygen concentration (Henson and Seborg, 1997).

6.4 Importance of the Dissolved oxygen concentration control

The dissolved oxygen concentration (DO) in the aerobic part of an activated sludge process should be sufficiently high to supply adequate oxygen to the micro-organisms in the sludge, as it plays an integral part for control of wastewater treatment plants. On the other hand, an excessively high DO (which requires a high airflow rate) leads to high energy consumption and may also deteriorate the sludge quality. A high DO concentration in the internally re-circulated water also means the denitrification is less efficient. Hence, both for economical and process reasons, it is of great importance to control the DO.

Dissolving oxygen in the wastewater is a nonlinear process which makes it difficult to be controlled. A lot of different control techniques have been tried in the past, but none came close to solving the exact problem. High control performance for all operating conditions is not easily achievable with any type of linear controllers. In order to attain a high performance controller for all operating conditions, the main focus is to take into consideration the nonlinear characteristics of the oxygen transfer function K_{La} when designing the controller.

Dissolved oxygen concentration is characterised by two important parameters, oxygen transfer function K_{La} and oxygen uptake rate r_{so} (Respiration). The oxygen transfer depends on several variables in the form of oxygen transfer rate and mass transfer coefficient as the literatures describes (Lindberg, 1997).

Automatic control techniques were used for DO control in wastewater treatment processes for many years, the reason being:

- The sensors for measurement of DO were available.
- The DO control reduces the amount of energy for blowing of air in the aeration basin.
- The effluent characteristics and process performance depend on the proper DO concentration in the aeration tank.

The normally used controllers over the years are proportional integral (PI) or proportional integral differential (PID). The work performed by the said controllers above led to not very good system performance, simply because

- The set-points are selected according to some nominal system requirements and not according to the operating conditions of the process at the moment of control.
- The parameters of the controllers are not determined according to the operating conditions of the process.
- The controllers are designed for linear process, whereas the process of dissolving of oxygen into the wastewater is a nonlinear process.

These drawbacks are being dealt with in the thesis by addressing the following points:

1. The optimal set-point for the DO controller is determined through the solution of optimal control problem on the basis of measurement of the process variables and prediction of the process disturbances as a part of the process control strategy 1. The problem for optimal control is solved in the scheme of repetitive optimization every two hours depending on the dynamics of the system disturbances. This problem is not considered in the thesis. The obtained desired DO trajectory is used in the thesis in order to calculate the optimal set point and controller parameters.
2. The DO model parameters are estimated every two hours on the basis of the real values of the measured DO concentration and airflow rate.
3. The controller parameters are determined on the basis of the estimated model parameters and the optimal set-point for the dissolved oxygen concentration.

The design of the controller parameters is done by the method developed in the thesis and this method is based on the consideration that DO process is a nonlinear one. The idea is to keep the industry standard PI controller, but some additional control to be introduced in order to cope with the nonlinear character of the process (Lindberg and Carlsson, 1996) developed a strategy for DO controller based on the nonlinear DO transfer function, the reason being to illustrate that nonlinear DO controller can outperform a standard PI controller.

Development of a cascaded PI control of ammonia concentration in the aeration tank has been done (S.Gerkšič *et al*, 2006) and (Lindberg *et al*, 1996). This type of control is a nonlinear linearizing control. With its help the nonlinear process is linearized for the purposes of PI controller implementation. The proposed structure is given in Figure 6.1.

The developed method in the thesis consists of two steps:

- Design of a nonlinear linearizing controller using the input/output method of *geometrical control theory* on the basis of a given linear reference model.
- Design of a linear (PI) controller for the linearized by the nonlinear controller system.

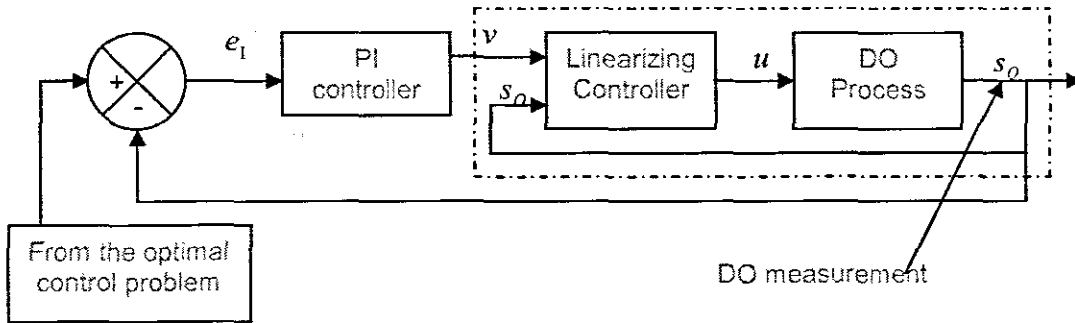


Figure 6.1: Control strategy for the DO concentration process.

6.5 Nonlinear Linearizing Controller Design on the basis of input/output linearization

Equation (3.6) is a nonlinear equation. It describes the state space and the output behaviour of the DO process. The process has to be linearized in order to use PI controller for regulation according to the set-point. The theory for design of linearizing controllers is used. The controller equation is assumed in the following way:

$$u(t) = \gamma(s_o, r_{s_o}, v, s_{o,m}) \quad (6.40)$$

Where γ is a nonlinear function and $v(t)$ is the external nonlinear controller reference signal which can be used to increase and improve the closed loop system performance. This signal will be generated by the PI controller.

The process for design of the nonlinear linearizing controller is done for the equation (3.8) where the control $u(t)$ is represented by the affine control $u_1(t)$ and is based on the following steps:

- Calculation of the output relative degree
- Selection of a linear reference model as a desired model for the closed loop linearized system.
- Comparison of the desired and the DO models and derivation of the expression for the DO controller.

Calculation of the Lie derivatives of the DO process to determine the system relative degree.

The equation:

$$\dot{s}_o(t) = f(s_o, t) + g(s_o, t)u_1(t) + g_1(s_o, t)s_{o,im}(t) + g_2(s_o, t)r_{so}(t), \quad s_o(0) = s_o$$

$$y = s_o = h(s_o)$$

is considered

In order to find the relative degree, the derivative of the output according to the state space variable is calculated

$$\frac{dy}{dt} = \frac{dh(s_o)}{dt} = \dot{s}_o = f(s_o) + g(s_o)u_1 + g_1(s_o)s_{o,im} + g_2(s_o)r_{so}$$

It is obtained that the control u_1 appears in the derivative ($g(s_o) \neq 0$) and the relative degree $r = 1$. In this case the state space equation directly can be used for calculation of the linearizing controller.

The process for DO is of the first order. That is why the desired model can be selected in such a way that the closed loop linearized system is stable.

$$\dot{s}_{o,des}(t) = as_{o,des}(t) + bv(t) \quad (6.41)$$

Where s_o is the desired value of the DO and a is a coefficient giving dynamics of the closed loop system. In order to derive the expression for the DO linearizing controller the right hand parts of equations (3.8) from the chapter 3 for modelling and (6.40) are compared for calculation of u_1 . In this case $s_{o,des} = s_o$ is assumed.

$$as_o(t) + bv(t) = f(s_o(t)) + g(s_o(t))u_1(t) + g_1(s_o) s_{o,im}(t) + g_2(s_o) r_{so}(t) \quad (6.42)$$

$$g(s_o(t))u_1(t) = as_o(t) + bv(t) - f(s_o(t)) - g_1(s_o) s_{o,im}(t) - g_2(s_o) r_{so}(t) \quad (6.43)$$

$$u_1(t) = \frac{as_o(t) + bv(t) - f(s_o(t)) - g_1(s_o) s_{o,im}(t) - g_2(s_o) r_{so}(t)}{s_{o,sat} - s_o(t)} = \quad (6.44)$$

$$= \alpha(s_o) + \beta(s_o)v(t) - \beta_1(s_o) s_{o,im}(t) - \beta_2(s_o) r_{so}(t)$$

where $f(s_o) = -\frac{Q}{V}s_o(t) + k_1(s_{o,sat} - s_o(t))$; $g(s_o) = (s_{o,sat}(t) - s_o(t))$,

$$g_1(s_o) = \frac{Q}{V} = \text{Constant}, \text{ and } g_2(s_o) = 1 = \text{Constant}$$

$$\alpha(s_o) = \frac{as_o - f(s_o(t))}{s_{o,sat} - s_o(t)}$$

$$\beta(s_o) = \frac{b}{s_{O,sat} - s_o(t)}$$

$$\beta_1(s_o) = \frac{g_1(s_o)}{s_{O,sat} - s_o(t)}$$

$$\beta_2(s_o) = \frac{g_2(s_o)}{s_{O,sat} - s_o(t)}$$

After some transformations, the equation (6.44) can be represented as

$$u_1(t) = \frac{\left(a + \frac{Q}{V} + k_1\right)s_o(t) + bv(t) - k_1s_{O,sat} - \frac{Q}{V}s_{O,in}(t) - r_{SO}(t)}{(s_{O,sat} - s_o(t))} \quad (6.45)$$

In order to calculate the original nonlinear control $u(t)$, the proposed substitution in chapter 3 is used,

$$u_1(t) = -k_1 e^{-k_2 u(t)}$$

where Equation (6.45) is substituted. The original control can be obtained from the above equation following the transformations

$$e^{-k_2 u(t)} = \frac{u_1}{-k_1}$$

$$\ln\left(\frac{u_1}{-k_1}\right) = \ln(e^{-k_2 u(t)}) = -k_2 u(t)$$

$$\begin{aligned} u(t) &= -\frac{1}{k_2} \ln\left[\frac{u_1(t)}{-k_1}\right] = -\frac{1}{k_2} \ln\left[\frac{\left(a + \frac{Q}{V} + k_1\right)s_o(t) + bv(t) - k_1s_{O,sat} - \frac{Q}{V}s_{O,in}(t) - r_{SO}(t)}{-k_1(s_{O,sat} - s_o(t))}\right] = \\ &= -\frac{1}{k_2} \ln\frac{1}{-k_1} (\alpha(s_o(t)) + \beta(s_o)v(t) + g_1(s_o)s_{O,in}(t) + g_2(s_o)r_{SO}) = \\ &= \gamma(s_o, v, s_{O,in}, r_{SO}) \end{aligned} \quad (6.46)$$

This equation represents the nonlinear, linearizing controller. The linear control $v(t)$ in it is unknown and it can be determined by design of a PI controller in such a way that some requirements for the characteristics of the transition behaviour of the closed loop system are fulfilled.

6.5.1 PI controller design

The nonlinear process with nonlinear linearizing controller (6.46) results in a linear closed loop system given by the equation of the desired linear system, Equation (6.41). For this system it is very easy to apply PI control. The equation of the PI controller is given as follows;

$$v(t) = K_p \left[e(t) + \frac{1}{T_i} \int e(t) dt \right] \quad (6.47)$$

where $e(t) = s_o^{sp} - s_o(t)$ is the control error, K_p and T_i are the controller parameters.

The problem for designing of a PI controller is to find the coefficients of the controller K_p and T_i , such that the dissolved oxygen concentration is kept at the given set-point and the poles of the closed loop system are situated at desired positions. The theory of pole placement for design of the controller is used and the application of the method is done in Laplace domain using transfer functions approach (Ogata, 2002). The following steps are done:

6.5.2 Transfer function of the linearized process

$\dot{s}_o(t) = as_o(t) + bv(t)$, where s_o is a state and output of the process and $v(t)$ is a control input.

In Laplace domain:

$$ss_o(s) = as_o(s) + bv(s) \quad (6.48)$$

$$(s - a)s_o(s) = bv(s) \quad (6.49)$$

$$G_p(s) = \frac{s_o(s)}{d(s)} = \frac{b}{s - a} \quad (6.50)$$

Where $G_p(s)$ is the transfer function of the linearized closed loop system.

6.5.3 Transfer function of the PI controller

In Laplace domain with $v(t)$ being the output and $e(t)$ as the input of the controller, the transfer function of the PI controller is derived as follows:

$$V(s) = K_p \left[E(s) + \frac{1}{T_i s} E(s) \right] \quad (6.51)$$

$$G_c(s) = \frac{V(s)}{E(s)} = K_p \left[1 + \frac{1}{T_i s} \right] \quad (6.52)$$

6.5.4 Transfer function of the closed loop system

The transfer function of the closed loop system is derived according to the closed loop system structure, Figure 6.3.

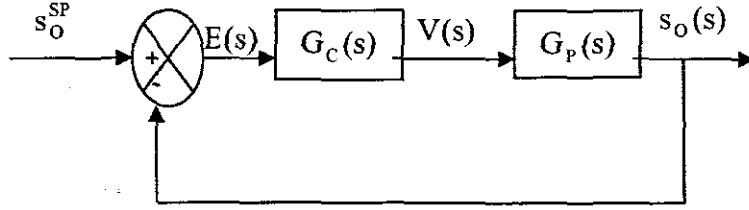


Figure 6.2: Block diagram of the closed loop system with PI controller

The transfer function of the closed loop system is

$$\begin{aligned}
 G_{CL}(s) &= \frac{G_C(s)G_P(s)}{1+G_C(s)G_P(s)} = \frac{K_P \left[\frac{T_i s + 1}{T_i s} \right] \frac{b}{s-a}}{1+K_P \left[\frac{T_i s + 1}{T_i s} \right] \frac{b}{s-a}} = \\
 &= \frac{K_P [T_i s + 1] b}{T_i s (s-a) + K_P [T_i s + 1] b} = \frac{K_P [T_i s + 1] b}{s^2 T_i + [K_P T_i b - T_i a] s + K_P} = \\
 &= \frac{K_P [T_i s + 1] b}{T_i s^2 + s T_i (K_P - a) + K_P b} \tag{6.53}
 \end{aligned}$$

The characteristic equation of this transfer function is used for the controller design.

6.5.5 Characteristic equation of the closed loop system

The characteristic equation of the closed loop system is given by the denominator of the closed loop transfer function $T_i s^2 + s T_i (K_P b - a) + K_P b = 0$. It is of order two. This equation can be written with coefficient 1 in front of s^2 .

$$s^2 + s \frac{T_i (K_P b - a)}{T_i} + \frac{K_P b}{T_i} = 0 \tag{6.54}$$

$$s^2 + s (K_P b - a) + \frac{K_P b}{T_i} = 0 \tag{6.55}$$

The coefficients of the controller appear in equation (6.55). They can be found if equation (6.55) is compared with characteristic equation of the closed loop system with the desired performance.

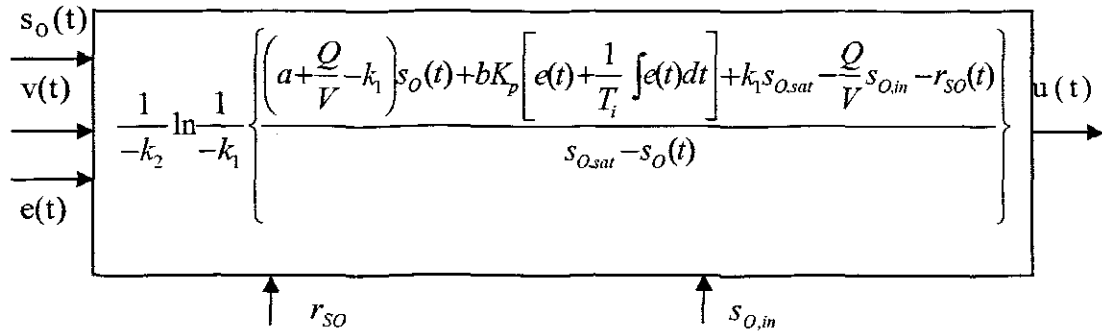


Figure 6.3: Structure of the nonlinear linearizing controller.

6.7 Simulink block diagram of the nonlinear linearizing controller

The system is simulated in Simulink. The Simulink diagram of the linear and nonlinear linearizing control of the closed loop DO control system, called "Paki.mdl" is shown in Figure 6.4. It has one subsystem:

- Nonlinear Linearizing controller subsystem (Figure 6.5)

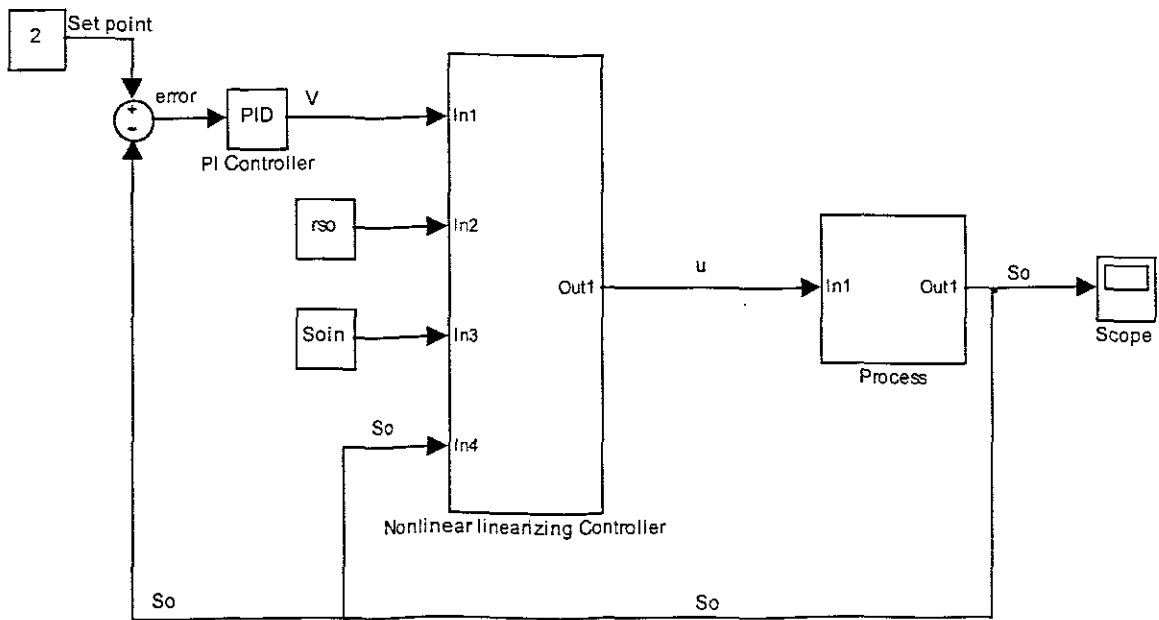


Figure 6.4: Closed loop, based on linear and nonlinear linearizing control of the DO control system Simulink diagram

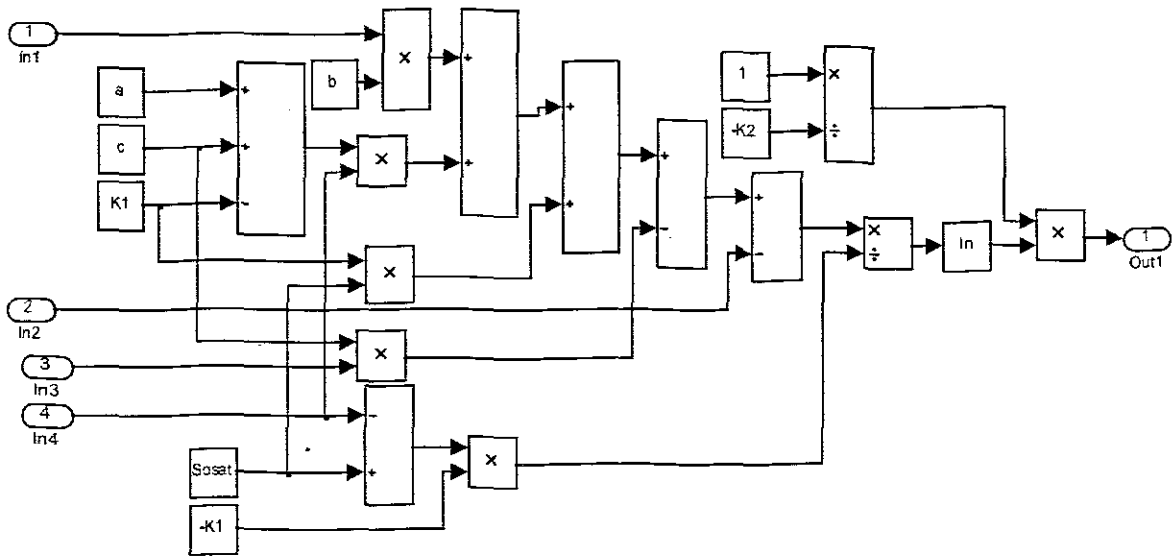


Figure 6.5: The nonlinear linearizing controller Simulink diagram

6.8 Matlab program for calculation of PI parameters, process model coefficients and the closed loop system *Paki.mdl*

```

%=====
%PI Controller Parameters
%=====

Ti= b*(4+a)/6
Kp= 4+a
P=Kp
I=P/Ti

%=====
%Coefficients
%=====

a=-0.8
b=15000
K1=240
K2=1.96 e-04

```

The program "*Linearizing_controller.m*" is run Matlab work space. The calculated parameters are sent to Simulink program "*Paki.mdl*" Figure 6.4 for simulation of the closed loop behaviour.

6.9 Simulation results of the closed loop system with the combined linear and nonlinear linearizing control

Parameters for simulation of the Dissolved Oxygen Concentration are introduced in Matlab workspace by the program "*Linearizing_controller .m*". The program is given in the Appendix C. The corresponding Simulink model "*Paki .mdl*" is given in Figure 6.4. The input variables are the disturbances $s_{O,in}$, and r_{SO} . v and u are calculated by the PI and nonlinear linearizing controllers, r_{SO} is calculated according to Equation (3.2) and the parameters are $\mu_H, Y_H, \mu_A, Y_A, K_{NH}, K_{OA}, K_{OH}, K_S$. The variables s_S, s_{NH} , and s_O are taken as steady state values from the Benchmark. The output variable is dissolved oxygen concentration s_O . The values of the parameters are taken from the ASM1 biological model and are given in Table 3.5. The values of k_1 and k_2 are calculated from the value $K_{La} = 240 \text{ day}^{-1}$ by a curve fitting for a given value of the airflow rate u_1 .

Table 6.1: Values of the r_{SO} model parameters and variables

Par	μ_H	Y_H	μ_A	Y_A	s_S	s_{NH}	K_{NH}	K_{OA}	K_{OH}	K_S	s_O
Val	4	0.67	0.5	0.24	0.889	1.733	1.0	0.4	0.2	10.	0.491

Table 6.2: Values of the model parameter for controller calculation

Par	k_1	k_2	r_{SO}	$s_{O,in}$	a	b
Val	240	$1.961e^{-04}$	-764.6982	0.2	-0.8	15000

The DO process has two main disturbances $s_{O,in}$, and r_{SO} . They can influence the process considerably. To investigate what are the limits of the values of the disturbances for which the proposed control can still be applicable, simulations of the closed loop system with different values of the set-point, disturbances, and the value of the parameter a are provided. Table 6.3 shows the variations of the above parameters.

Table 6.3: Parameters table for nonlinear control design

Set point	r_{SO} Calculations				Resultant	$s_{O,in}$	a
	X_{ba}		X_{bn}		r_{SO}		
1.8	X_{ba}	149.797	X_{bn}	2559.444	-764.6982	0.2	-0.8
1.8	$X_{ba}-10\%$	134.8173	$X_{bn}+10\%$	2315.3864	-746.7435	0.2	-0.8
1.8	$X_{ba}+10\%$	164.7767	$X_{bn}-10\%$	2303.4096	-762.6757	0.2	-0.8

1.8	Xba-25%	112.3478	Xbh+25%	3199.305	-719.7945	0.2	-0.8
1.8	Xba+25%	187.2463	Xbh-25%	1919.583	-809.6251	0.2	-0.8
1.8	Xba-40%	89.8782	Xbh+40%	3583.2216	-692.8452	0.2	-0.8
1.8	Xba+40%	209.7158	Xbh-40%	1535.6664	-836.5741	0.2	-0.8
2	Xba	149.797	Xbh	2559.444	-764.7096	0.2	-0.8
2	Xba-10%	134.8173	Xbh+10%	2815.3864	-746.7435	0.2	-0.8
2	Xba+10%	164.7767	Xbh-10%	2303.4996	-782.6757	0.2	-0.8
2	Xba-25%	112.3478	Xbh+25%	3199.305	-719.7945	0.2	-0.8
2	Xba+25%	187.2463	Xbh-25%	1919.583	-809.6251	0.2	-0.8
2	Xba-40%	89.8782	Xbh+40%	3583.2216	-692.8452	0.2	-0.8
2	Xba+40%	209.7158	Xbh-40%	1535.6664	-836.5741	0.2	-0.8
3	Xba	149.797	Xbh	2559.444	-764.7096	0.2	-0.8
3	Xba-10%	134.8173	Xbh+10%	2815.3864	-746.7435	0.2	-0.8
3	Xba+10%	164.7767	Xbh-10%	2303.4996	-782.6757	0.2	-0.8
3	Xba-25%	112.3478	Xbh+25%	3199.305	-719.7945	0.2	-0.8
3	Xba+25%	187.2463	Xbh-25%	1919.583	-809.6251	0.2	-0.8
3	Xba-40%	89.8782	Xbh+40%	3583.2216	-692.8452	0.2	-0.8
3	Xba+40%	209.7158	Xbh-40%	1535.6664	-836.5741	0.2	-0.8

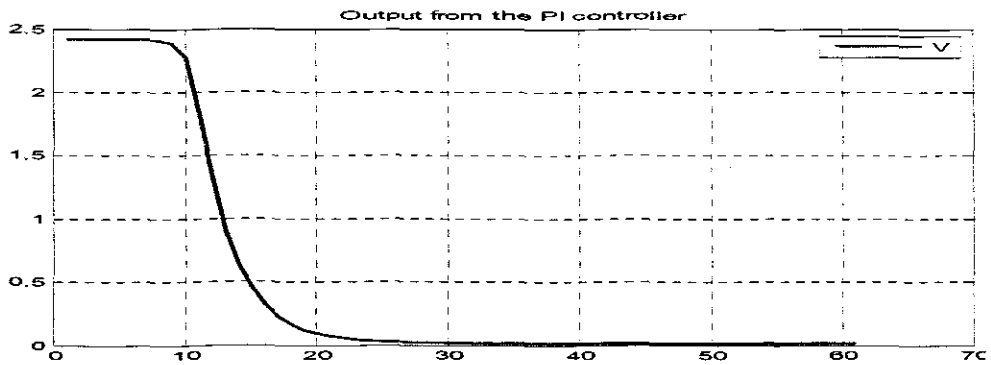


Figure 6.6: Output response of PI controller.

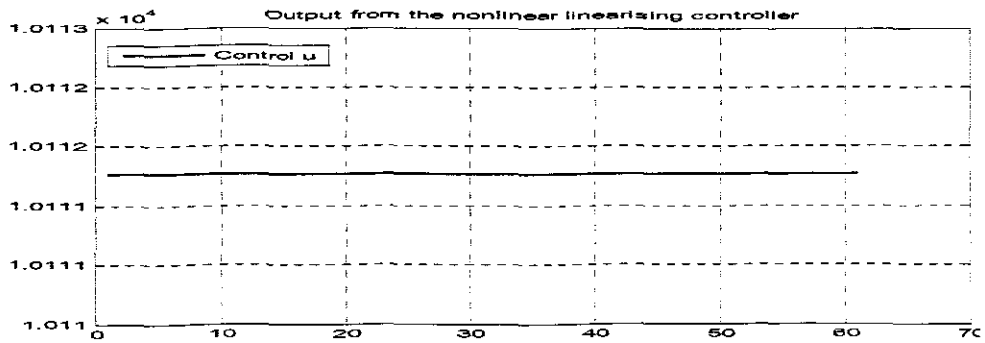


Figure 6.7: Output response of the nonlinear linearizing controller

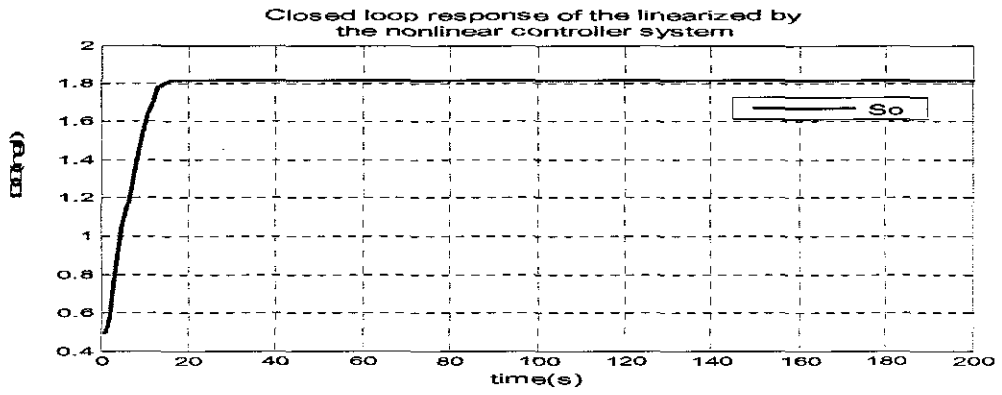


Figure 6.8: Closed loop response of the linearized by the nonlinear controller system when $S_{oin}=0.2$, $a=-0.8$, $r_{so}=-764.6982$ and the set point is 1.8

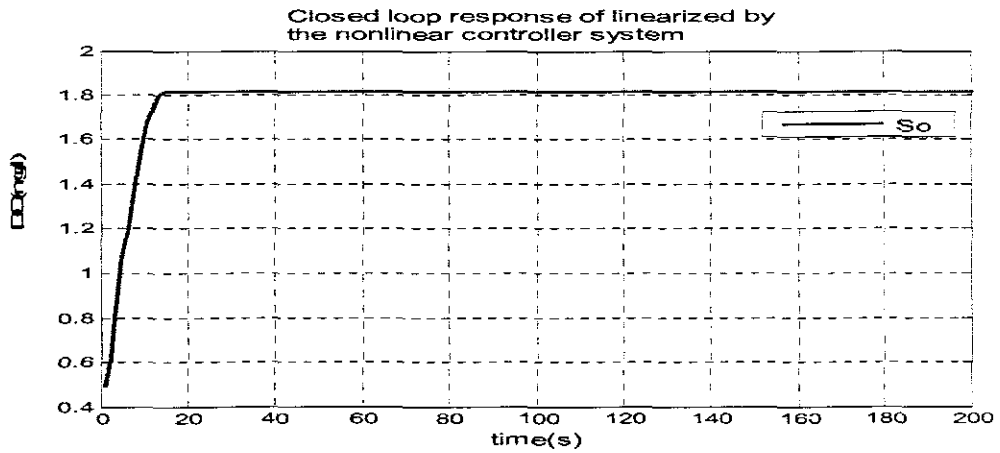


Figure 6.9: Closed loop response of the linearized by the nonlinear controller system when $S_{oin}=0.2$, $a=-0.8$, $r_{so}=-746.7435$ and the set point is 1.8

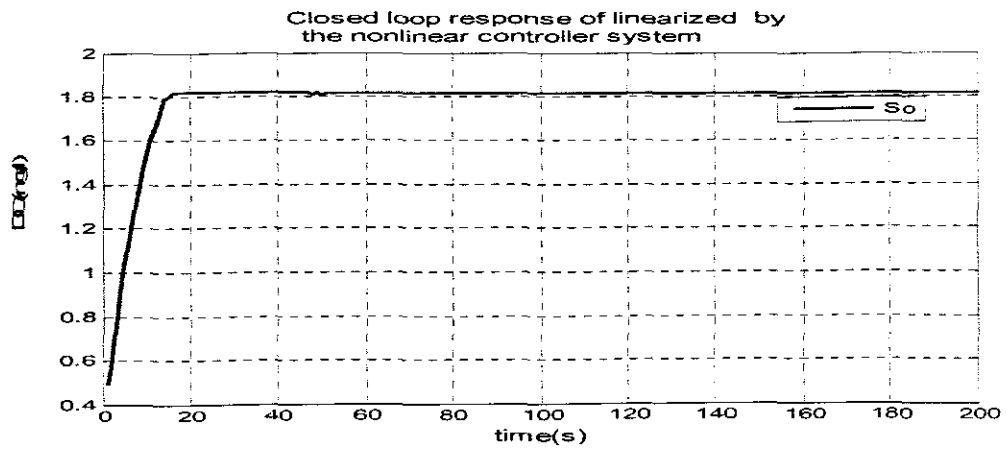


Figure 6.10: Closed loop response of the linearized by the nonlinear controller system when $S_{oin}=0.2$, $a=-0.3$, $r_{so}=-782.6757$ and the set point is 1.8

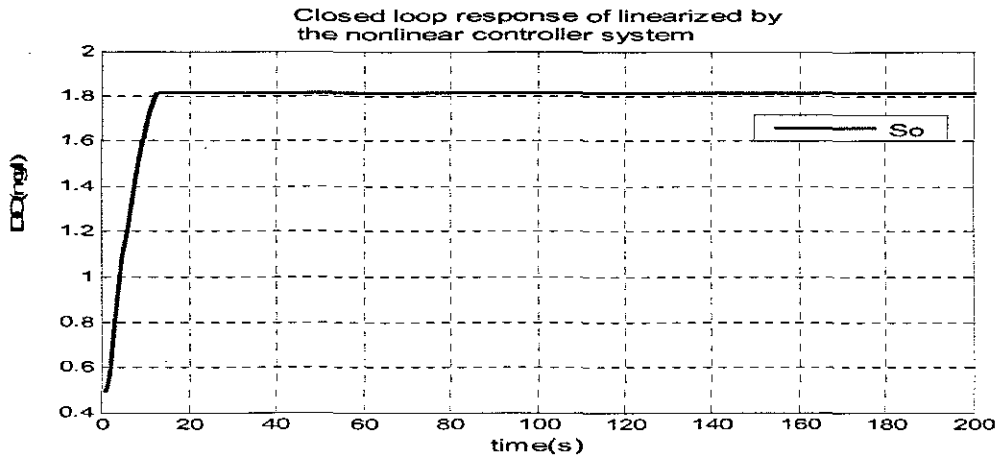


Figure 6.11: Closed loop response of the linearized by the nonlinear controller system when $S_{oin}=0.2$, $a=-0.8$, $r_{so}=-719.7945$ and the set point is 1.8

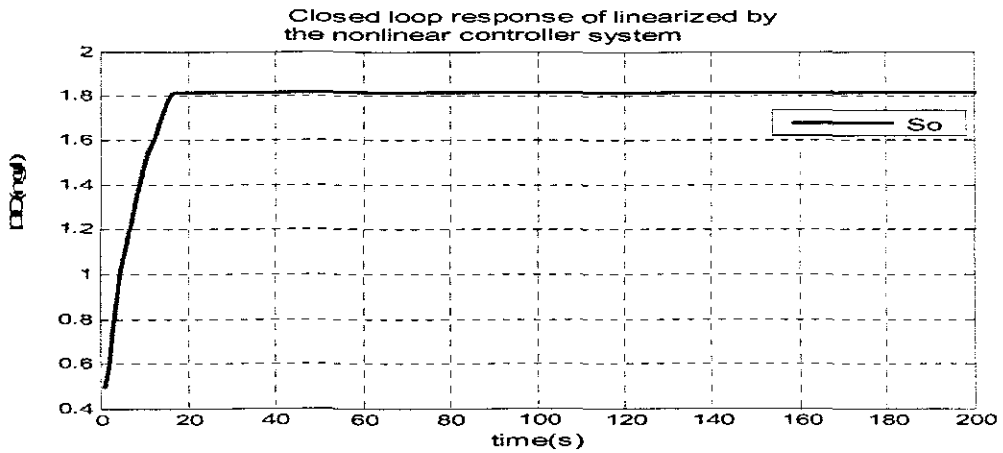


Figure 6.12: Closed loop response of the linearized by the nonlinear controller system when $S_{oin}=0.2$, $a=-0.8$, $r_{so}=-809.6251$ and the set point is 1.8

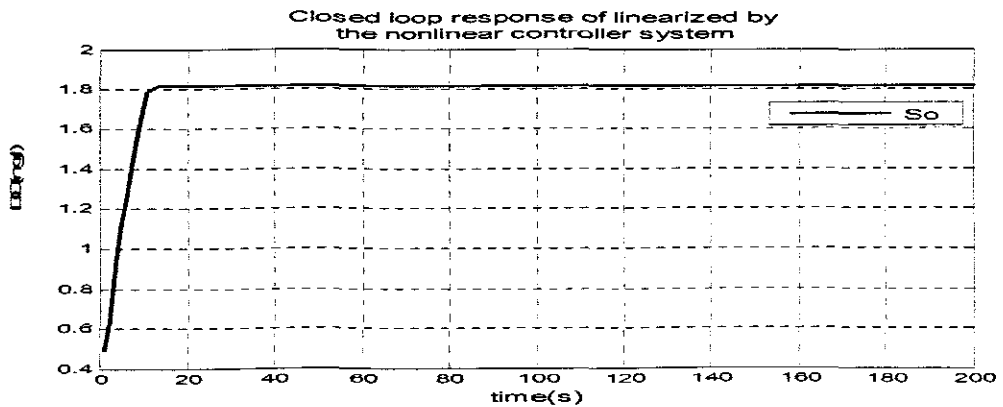


Figure 6.13: Closed loop response of the linearized by the nonlinear controller system when $S_{oin}=0.2$, $a=-0.8$, $r_{so}=-692.8452$ and the set point is 1.8

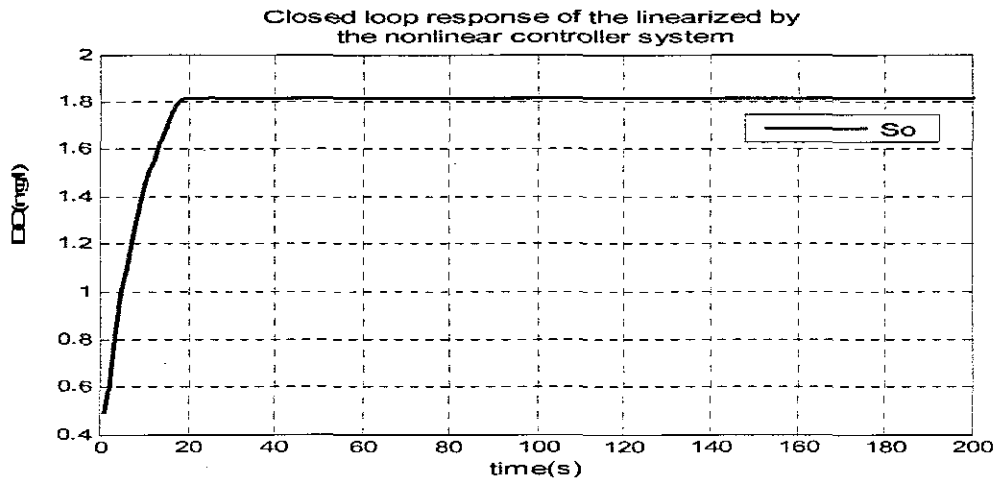


Figure 6.14: Closed loop response of the linearized by the nonlinear controller system when $S_{oin}=0.2$, $a=-0.8$, $r_{so}=-836.5741$ and the set point is 1.8

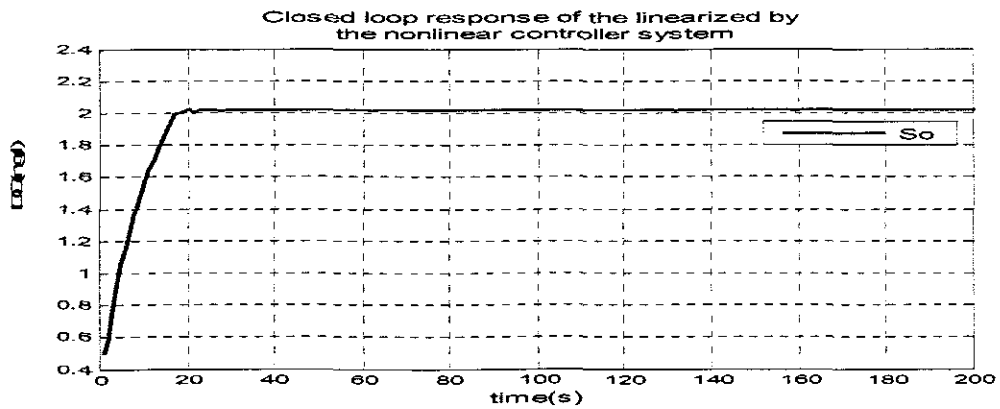


Figure 6.15: Closed loop response of the linearized by the nonlinear controller system when $S_{oin}=0.2$, $a=-0.8$, $r_{so}=-764.6982$ and the set point is 2

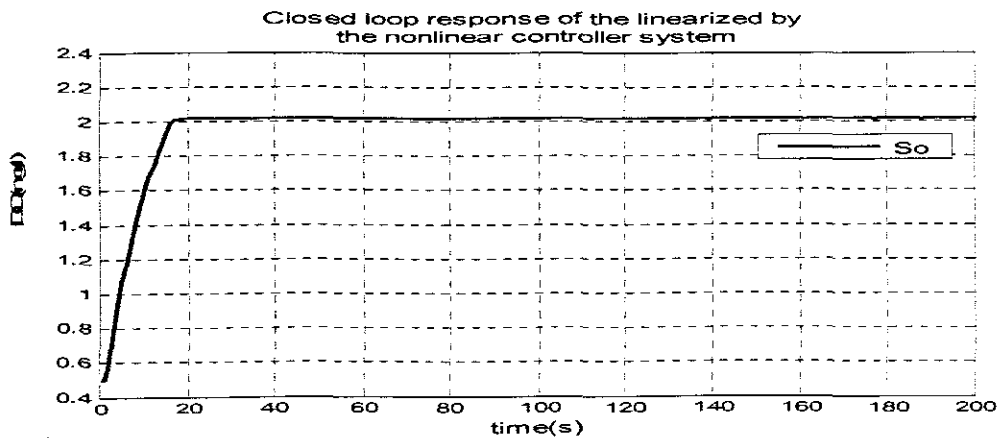


Figure 6.16: Closed loop response of the linearized by the nonlinear controller system when $S_{oin}=0.2$, $a=-0.8$, $r_{so}=-746.7435$ and the set point is 2

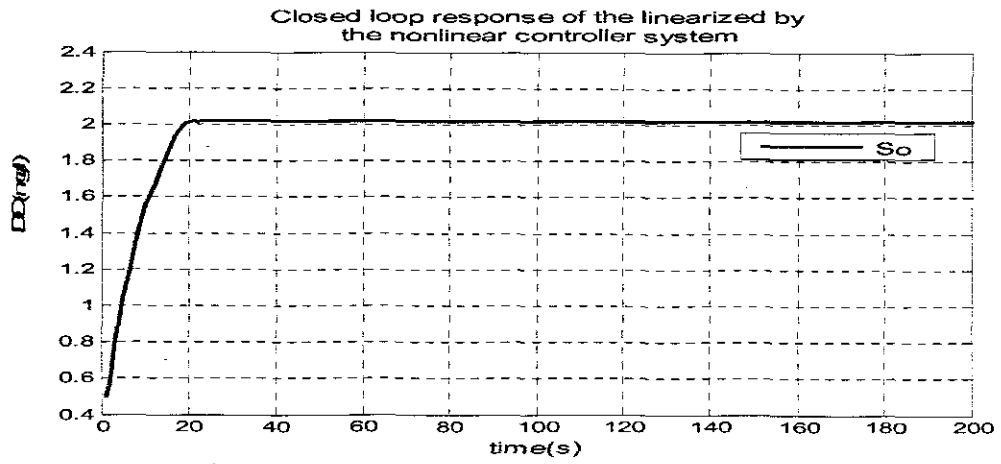


Figure 6.17: Closed loop response of the linearized by the nonlinear controller system when $S_{oin}=0.2$, $a=-0.8$, $r_{so}=-782.6757$ and the set point is 2

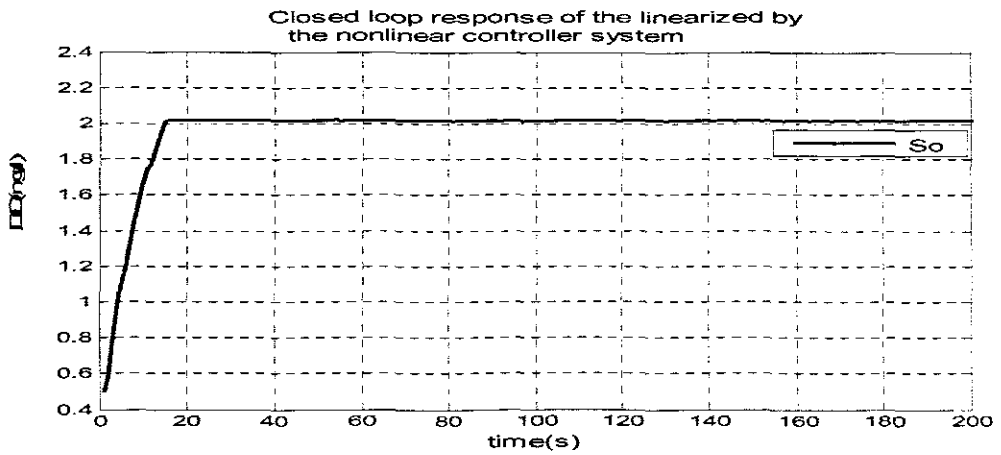


Figure 6.18: Closed loop response of the linearized by the nonlinear controller system when $S_{oin}=0.2$, $a=-0.8$, $r_{so}=719.7945$ and the set point is 2

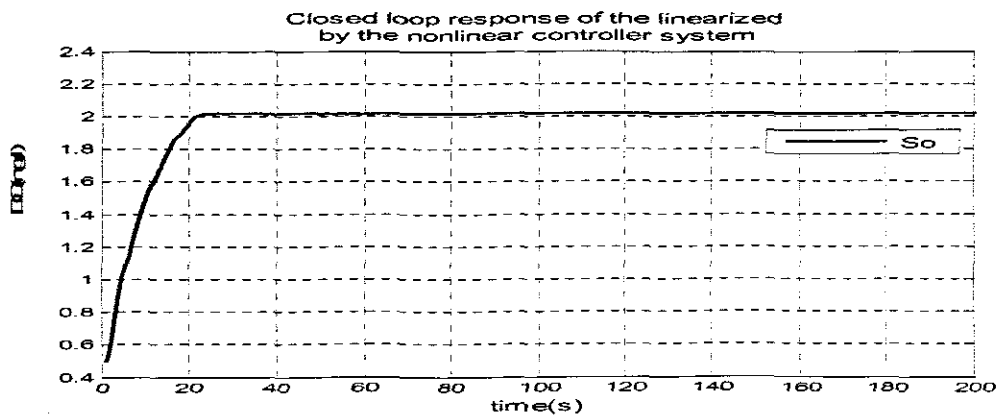


Figure 6.19: Closed loop response of the linearized by the nonlinear controller system when $S_{oin}=0.2$, $a=-0.8$, $r_{so}=-809.6251$ and the set point is 2

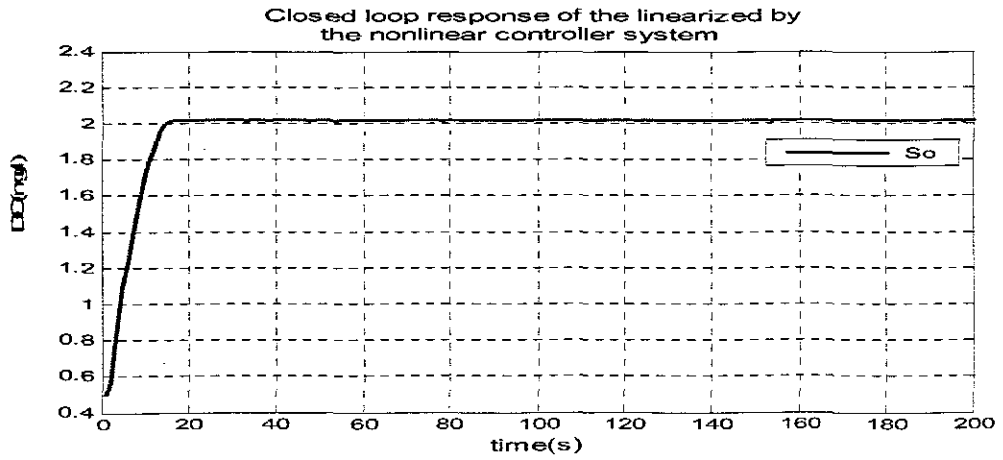


Figure 6.20: Closed loop response of the linearized by the nonlinear controller system when $S_{oin}=0.2$, $a=-0.8$, $r_{so}=-692.8452$ and the set point is 2

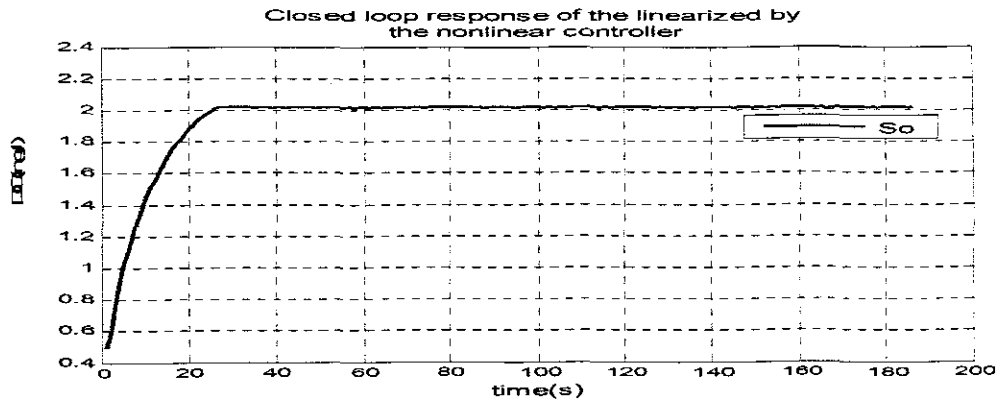


Figure 6.21: Closed loop response of the linearized by the nonlinear controller system when $S_{oin}=0.2$, $a=-0.8$, $r_{so}=-836.5741$ and the set point is 2

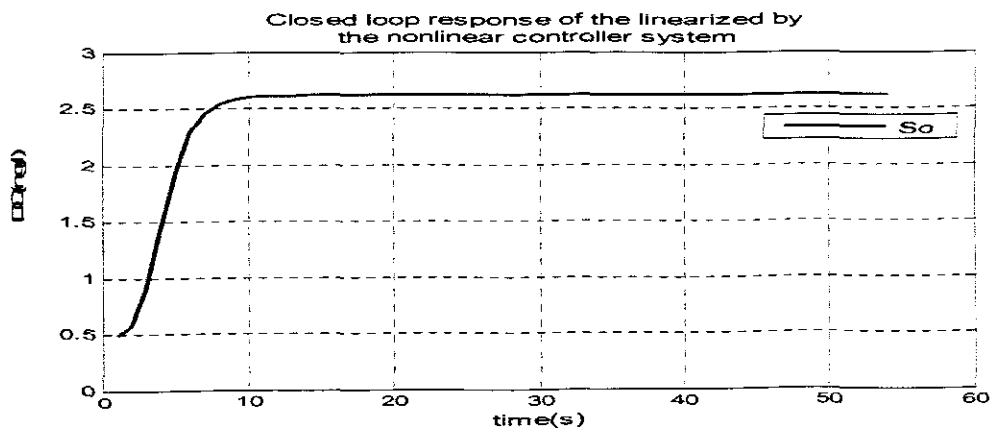


Figure 6.22: Closed loop response of the linearized by the nonlinear controller system when $S_{oin}=0.2$, $a=-0.8$, $r_{so}=-764.6982$ and the set point is 3

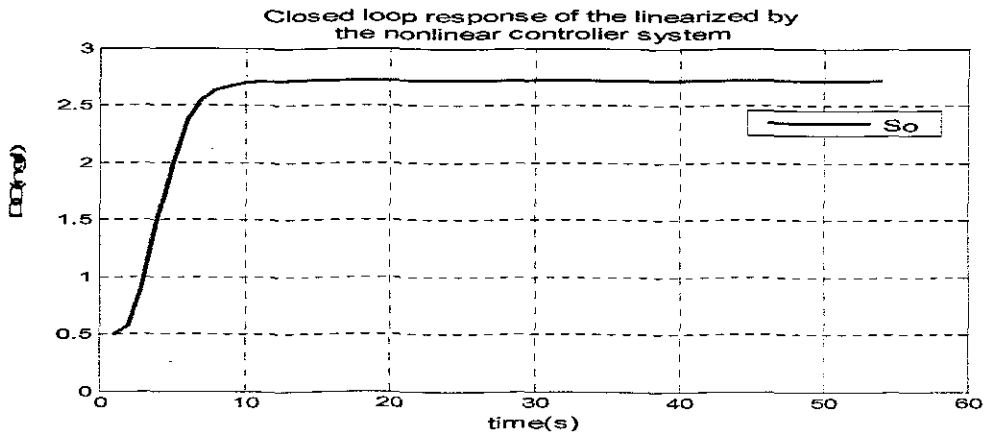


Figure 6.23: Closed loop response of the linearized by the nonlinear controller system when $S_{oin}=0.2$, $a=-0.8$, $r_{so}=-746.7435$ and the set point is 3

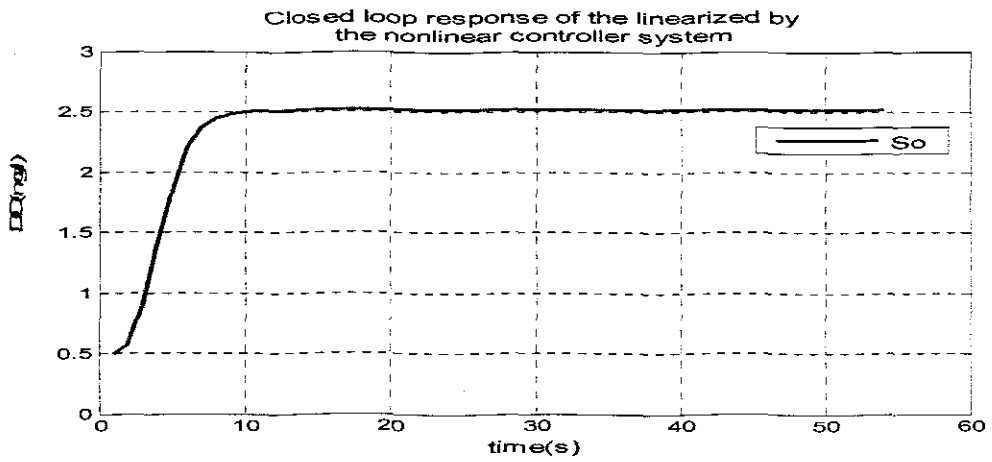


Figure 6.24: Closed loop response of the linearized by the nonlinear controller system when $S_{oin}=0.2$, $a=-0.8$, $r_{so}=-782.6757$, and the set point is 3

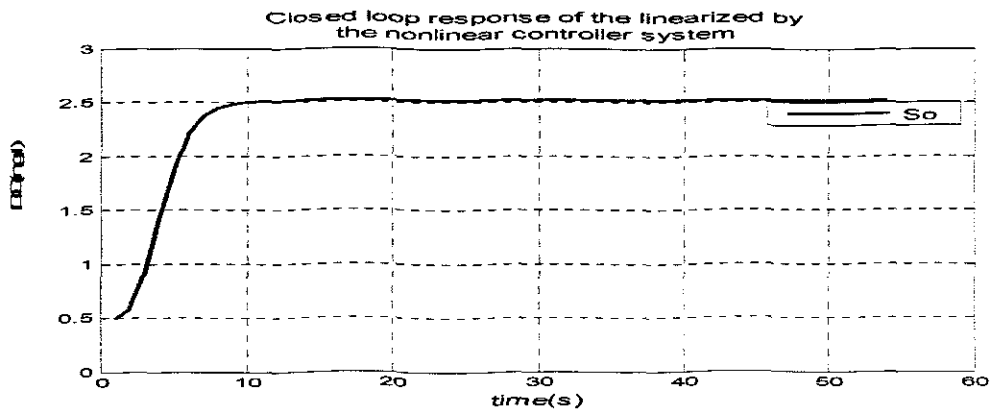


Figure 6.25: Closed loop response of the linearized by the nonlinear controller system when $S_{oin}=0.2$, $a=-0.8$, $r_{so}=719.7945$ and the set point is 3

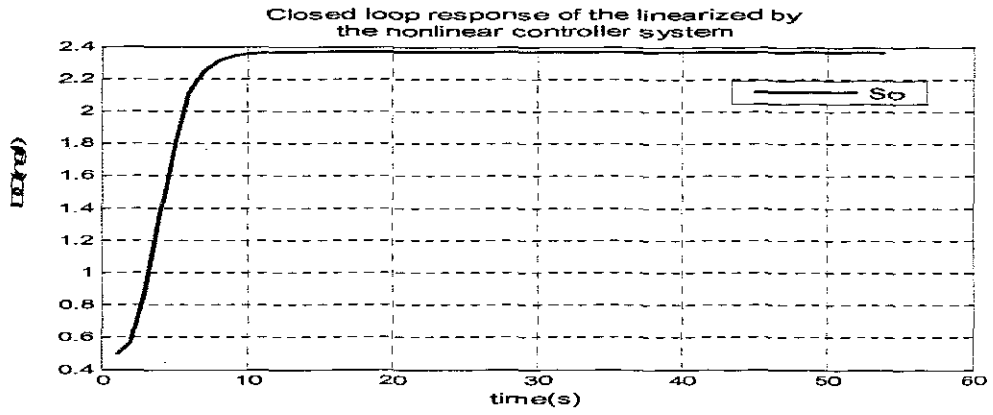


Figure 6.26: Closed loop response of the linearized by the nonlinear controller system when $S_{oin}=0.2$, $a=-0.8$, $r_{so}=-809.6251$ and the set point is 3

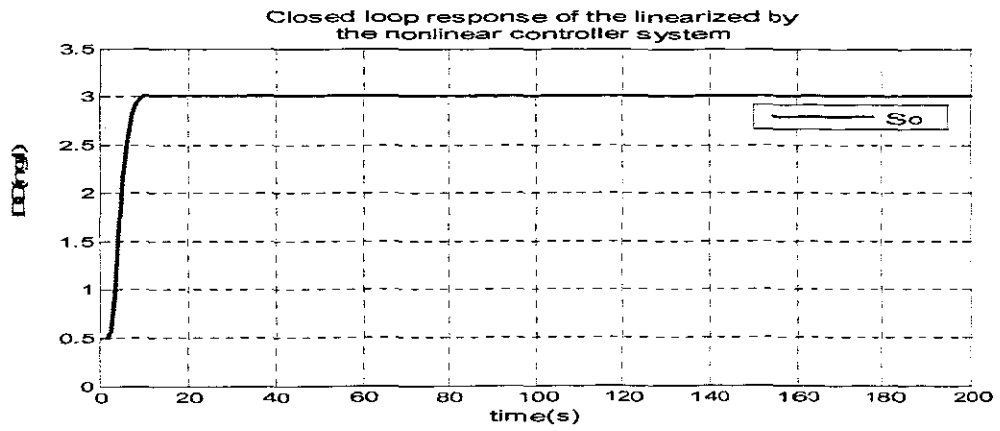


Figure 6.27: Closed loop response of the linearized by the nonlinear controller system when $S_{oin}=0.2$, $a=-0.8$, $r_{so}=-692.8452$ and the set point is 3

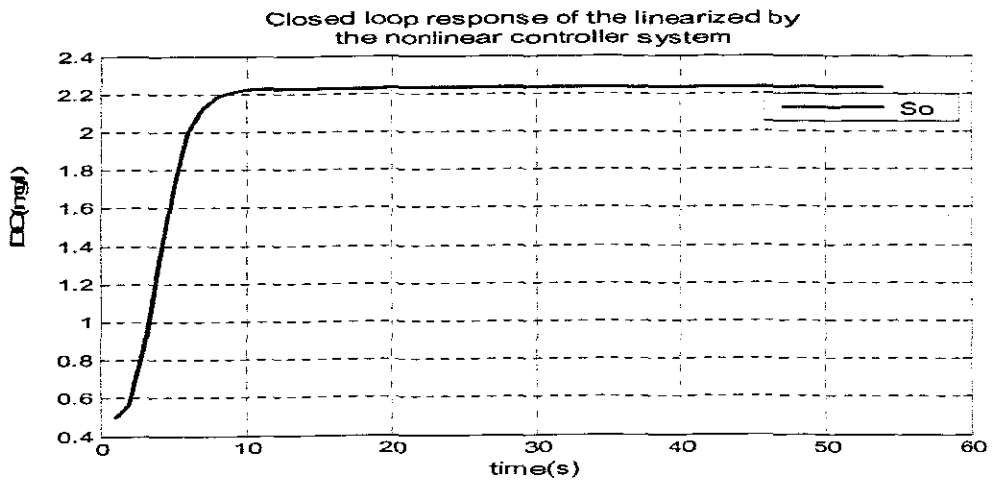


Figure 6.28: Closed loop response of the linearized by the nonlinear controller system when $S_{oin}=0.2$, $a=-0.8$, $r_{so}=-836.5741$ and the set point is 3

6.10 Discussion of the results

For the behaviour of the closed loop linearized system; the investigation of the influence disturbances $s_{0.in}$, r_{SO} and the value of the coefficient α showed close to critical behaviour of the whole system (linear and nonlinear controllers). The obtained graphs are compared according to the values of time delay, steady state error, settling time, and rising time.

The following conclusions can be done:

- The time delay is the same for all values of set-points and r_{SO}
- The settling time depends on the value of the set-point, when the set point is smaller, the settling time is smaller, on the other hand for the same set-point the settling time is bigger for the bigger values of r_{SO}
- The steady state error is not very sensitive towards the values of r_{SO} , but varies for different values of the set-points.
- The rising time also varies with the changes in the values of the set-point. For bigger set-points values, the value of the rising time is bigger.

The specifications of the dynamic output behaviour of the closed loop system are given below in Table 6.4.

Table 6.4 Simulation results comparison

Set point	Parameters			Characteristics			
	α	r_{SO}	$s_{0.in}$	Time delay (td)	Steady state error (ss)	Settling time (ts)	Rising time (tr)
1.8	-0.8	-784.6982	0.2	0	0.05	15	2
1.8	-0.8	-746.7435	0.2	0	0.05	12	2
1.8	-0.8	-782.6757	0.2	0	0.05	12	2
1.8	-0.8	-719.7945	0.2	0	0.05	12	2
1.8	-0.8	-809.6251	0.2	0	0.05	12	2
1.8	-0.8	-692.8452	0.2	0	0.05	12	2
1.8	-0.8	-836.5741	0.2	0	0.05	15	2
2	-0.8	-764.7096	0.2	0	0.05	15	2
2	-0.8	-746.7435	0.2	0	0.05	20	2
2	-0.8	-782.6757	0.2	0	0.05	12	2
2	-0.8	-719.7945	0.2	0	0.05	24	2
2	-0.8	-809.6251	0.2	0	0.05	15	2
2	-0.8	-692.8452	0.2	0	0.05	30	2
2	-0.8	-836.5741	0.2	0	0.05	10	2

3	-0.8	-764.7096	0.2	0.5	0.2	10	2
3	-0.8	-746.7435	0.2	0.5	0.01	0.19	2
3	-0.8	-782.6757	0.2	0.5	0.5	9	2
3	-0.8	-719.7945	0.2	0.5	0.1	12	2
3	-0.8	-809.6251	0.2	0.5	0.01	15	2
3	-0.8	-692.8452	0.2	0.5	0.05	12	2
3	-0.8	-836.5741	0.2	0.5	0.05	12	2

6.11 Conclusion

The developed method for design of linear and nonlinear linearizing controllers based on pole placement and geometric approach is described in this chapter. The simulation results show that the designed linear and nonlinear linearizing controllers can control the DO process according to the proposed requirements. The method allows

- The linearized by the nonlinear controller closed loop system to be equivalent to a linear stable desired system
- The closed loop system with linear and nonlinear controller to have determined by the design desired behaviour.

Nonlinear controller based on Lyapunov direct method is discussed in chapter 7.

CHAPTER SEVEN

DESIGN OF NONLINEAR LINEARIZING REFERENCE MODEL CONTROL OF THE DISSOLVED OXYGEN PROCESS ON THE BASIS OF LYAPUNOV THEORY

7.1 Introduction

The integral and general approach for the stability of nonlinear control systems is contained in the theory of stability of motion for the solution of ordinary differential equations introduced by the Russian mathematician Alexandr Michailovich Lyapunov in 1892 in "The general problem of motion stability" which includes two methods of stability namely linearization (quantitative) and direct (qualitative) methods (Slotine and LI, 1991) and (Crayson, 1965). The stability of dynamical systems can be investigated in a very accurate way with Lyapunov's methods if the corresponding mathematical models are written as systems of ordinary differential equations (Hachicho, 2006).

From the above statement, this chapter introduces Lyapunov stability theory in sections 7.2 and 7.3, with nonlinear controller design procedure as follows: section 7.4 gives the common nonlinear controller design based on the Lyapunov's direct method and reference control method. Section 7.5 uses the common controller developed in section 7.4 applied to the model of dissolved oxygen concentration. Simulink block diagrams are provided for the sole purpose of simulations and their simulation results are shown in section 7.8

7.2 Nonlinear Systems and Equilibrium Points

A nonlinear homogeneous dynamic system can often be represented by a set of nonlinear differential equations in the form

$$\dot{x}(t) = f(x,t) , x(0) = x_0 \quad (7.1)$$

where f is $n \times 1$ nonlinear vector function, and x is the $n \times 1$ state vector. A particular value of the state vector is called a point due to the fact it corresponds to a point in the state-space. The number of states n is called the *order* of the system. Hence, it is possible for a system trajectory to correspond only to a single point; such a point is called an equilibrium point.

7.2.1 Autonomous and non-autonomous systems

Definition 7.1: The nonlinear is said to be autonomous if f does not depend explicitly on time, meaning, if the system's state equation can be written as

$$\dot{x}(t) = f(x) , x(0) = x_0 \quad (7.2)$$

or else, the system is called non-autonomous (Slotine and Li, 1991), .

Apparently, time-invariant systems are autonomous and linear time-varying are non-autonomous. Truly speaking, all physical systems are non-autonomous, the reason being that none of their dynamic characteristics are strictly time-invariant.

It is significant to notice that for control systems, the above definition is made on closed loop dynamics

$$\dot{x}(t) = f(x, u) , x(0) = x_0 \quad (7.3)$$

which way leads to a non-autonomous closed loop system, if a controller depends on time t :

$$u(t) = g(x, t) \quad (7.4)$$

meaning that, the adaptive controllers for the linear time-invariant plants usually make the closed loop systems nonlinear and non-autonomous.

The elemental distinction involving autonomous and non-autonomous systems lies in the fact that trajectory of an autonomous system does not depend on the initial time, while the same is opposite for the non-autonomous systems. Autonomous systems have rather simpler properties and their investigation is much easier.

7.2.2 Equilibrium Points

Definition 7.2: A state x^* is an equilibrium state of the system if once $x(t)$ is equal to x^* , it remains equal to x^* for all future times.

Linear system equations are often transformed in such way that equilibrium point of the system is the origin of the state space.

7.2.3 Concepts of stability

The notion of stability is believed to be well-behaviour of a system around a desired operating point. However, in terms of nonlinear systems the case of stability is not the same as their linear counterparts as they may have much more complex and exotic behaviour, meaning that by taking a mere notion of stability is not enough to describe the

essential features of their motion. A number of more refined stability concepts, such as asymptotic stability, exponential stability and global asymptotic stability, are needed.

7.2.4 Stability and Instability

Definition 7.3: *The equilibrium state $x=0$ is said to be stable if for any $L > 0$, there exists $\delta > 0$, such that if $\|x(0)\| < \delta$, then $\|x(t)\| < L$ for all $t \geq 0$. Otherwise, it is believed that the equilibrium point is unstable.*

Lyapunov stability means that the system trajectory can be kept arbitrarily close to the origin by starting sufficiently close to it. More appropriate it can be defined as states that their origin is stable, only if the state trajectory $x(t)$ will not get out of a ball of arbitrarily specified radius, whereas the idea is that the starting state from within the ball at time 0 guarantees that the state will stay within ball thereafter.

The following standard mathematical abbreviation symbols will be used throughout the discussion of Lyapunov's stability theory:

\forall to mean "for any"

\exists for "there exists"

\in for "in the set"

\Rightarrow for "implies that"

Instability of an equilibrium point is characteristically undesirable, for the reason that it often leads the system into limit cycles or results in damage to the involved mechanical or electrical components. In linear system, volatility is equivalent to the blowing up, because unbalanced poles lead to exponential growth of the system states.

7.2.5 Asymptotic Stability and Exponential Stability

When considering a wide variety of engineering applications and the fact that for them to be stable Lyapunov stability is applied, it deems at times that this stability concept is not enough. The typical example can be that of a satellite. When its attitude is disturbed a bit from its nominal position, it is needed for the satellite to maintain its attitude in a range specifically assigned to it by the magnitude of the disturbance meaning, Lyapunov stability is applied. But on the other hand the attitude is gradually required to go back to its original value and this requires the concept of asymptotic stability to be determined.

Definition 7.4: It is of importance to note that an equilibrium point $\mathbf{0}$ is asymptotically stable if it is stable, and if in addition there is existence of some $I > 0$ such that $\|x(0)\| < I$ implies that $x(t) \rightarrow 0$ as $t \rightarrow \infty$.

The asymptotic stability means that the equilibrium is stable, and that in addition, means that when considering the states starting close to $\mathbf{0}$, they actually converge to $\mathbf{0}$ as the time t goes to infinity. An equilibrium point which is Lyapunov stable but not asymptotically stable is called marginally stable. It is easy to construct counter examples that illustrate that state convergence does not necessarily imply stability.

Definition 7.5: An equilibrium point $\mathbf{0}$ is exponentially stable if there exists two strictly positive numbers α and λ such that

$$\forall t > 0, \|x(t)\| \leq \alpha \|x(0)\| e^{-\lambda t}$$

Meaning that, the state vector of an exponentially stable system converges to the origin faster than an exponential function. The positive number λ is often called the rate of the exponential convergence. Notice must be taken that exponential stability implies asymptotic stability. But asymptotic stability does not guarantee exponential stability, as can be seen from the system

$$\dot{x} = -x^2 \quad x(0) = 1 \tag{7.5}$$

Whose solution is $x = 1/(1+t)$, a function slower than any exponential function $e^{-\lambda t}$ with $\lambda > 0$.

The definition given to exponential convergence endows with a clear bound on the state at any time. By inscription the positive constant α as $\alpha = e^{\lambda \tau_0}$, it is easy to see that, after a time of $\tau_0 + (1/\lambda)$, the magnitude of the state vector decreases to less 35% ($\approx e^{-1}$) of its original value, in the same way to the notion of time-constant in a linear system. After $\tau_0 + (3/\lambda)$, the magnitude $\|x(t)\|$ will be less than 5% ($\approx e^{-3}$) of $\|x(t)\|$.

7.2.6 Local and Global stability

Definition 7.6: If asymptotic (or exponential) stability holds for any initial states, the equilibrium point is said to be asymptotically (or exponentially) stable in the large. It is also called globally asymptotically (or exponentially) stable.

Linear time-invariant systems are either asymptotically stable, or marginally stable, or unstable, as can be seen from modal decomposition of linear system solutions; linear asymptotic stability is always global and exponential, and linear instability always implies exponential blown-up.

7.2.7 Linearization and Local stability

Lyapunov's linearization method is of particular concern to local stability of nonlinear systems. It is a prescription of the perception that nonlinear systems should be of similar behaviour approximated to their linear counterparts for small range motions. This is attributable to the fact that all physical systems are inherently nonlinear, so a result Lyapunov's linearization method provides the fundamental validation of using linear control techniques in practise as to show that stable design pertaining to linear control guarantees the stability of the original physical system locally. On the basis of the linearized model of the systems the necessary conditions for stability of the nonlinear system are based on the position of the poles of the linearized system as follows:

1. If the linearized system is strictly stable, that is if all eigenvalues of Jacobian matrix A are strictly in the left-half complex plane, then the equilibrium point is asymptotically stable (for the actual nonlinear system).
2. If the linearized system is unstable, that is if at least one eigenvalues of Jacobian matrix A is strictly in the right-half of the complex plane, then the equilibrium point is unstable (for the nonlinear system).
3. If the linearized system is marginally stable, meaning when all eigenvalues of Jacobian matrix A are on the left-half of the complex plane, at least one of them is on the $j\omega$ axis, then one cannot conclude for the nonlinear system stability.

7.3 Lyapunov's Direct method

The fundamental values of Lyapunov's direct method are mathematical extension of an essential physical observation. If the total energy of a dynamic system is continuously dissolute, then the system whether being linear or nonlinear, finally ought to settle down to an equilibrium point. Hence the stability of the dynamic system can be examined by the variation of a single scalar function (Slotine et al, 1991). Lyapunov's direct method is said to be a standard tool for stability analysis of ordinary differential equations. It has long been recognised as one of the most fundamental tools for analysis and synthesis of nonlinear systems. The significance of the criterion shoots from the fact that it allows

stability of a system to be substantiated without solving the differential equation explicitly (Rantzer, 2000).

7.3.1 Positive definite functions and Lyapunov functions

In analysis, the task in applying the method is to construct a function V such that it and its first time derivative \dot{V} demonstrate certain properties. As soon as these properties of V and \dot{V} are made known, the stability behaviour is acknowledged. The difficulty, nevertheless, happens when the necessary conditions cannot be achieved, for then no conclusions can be drawn about stability. It can be seen that each problem presents a new challenge, simply because the functions must be shaped anew for each specified system, or a class of systems. It is however noted that, a proper choice of V thus depends to an extent upon experience, creativity and most of time, good fortune of the analyst.

When dealing with the problem of synthesis, functions V and \dot{V} are being selected and the system parameters adjusted to satisfy the functions. It is always considered an easier procedure on the basis that great latitude in choice of functions and in the selection of the parameters exists. The following procedure underwrites that the system will be stable:

1. Select a Lyapunov function V to be positive definite
2. Find a time derivative of the Lyapunov function for the trajectory of the system under study $-\dot{V}$
3. Determine the sign of the Lyapunov function derivative along the system trajectory: if $\dot{V} < 0$, the system is stable, if $\dot{V} = 0$ the system is marginally stable, if $\dot{V} > 0$ the system is unstable.

Lyapunov functions play a very important role similar to potential functions and energy functions. Moreover, when asymptotic stability of equilibrium has been proven using Lyapunov function as a storage function. But is rather difficult to find a specific Lyapunov function for a specific practical nonlinear control problem, it proves a very fundamental drawback of the direct method. Hence, presented with specific systems, the controller designer has to use experience, basic instinct, and physical insights to search for an appropriate Lyapunov function. But of all the above, the use of physical insights is most preferred, because when applicable, it represents by far the most powerful and elegant way of approaching the problem, because of its close proximity in spirit to the original

intuition underlying the direct method. Consider a function $V(x):R^n \rightarrow R$ such that $V(x) \geq 0$ with equality if and only if $x=0$ (positive definite functions which are convex) and $\dot{V}(x) < 0$ (negative definite). Then $V(x)$ is called a Lyapunov function candidate and the system is asymptotically stable in the sense of Lyapunov. (Note that $V(0) = 0$ is required, otherwise $V(x) = 1/(1+|x|)$ would prove that $\dot{x}(t) = -x(t)$, is locally stable. An additional condition called "properness" or radial unbounded is required in order to conclude global asymptotic stability).

It is a well known fact that Lyapunov functions are closely related to cost functions in optimal control theory. In fact, one way to interpret a Lyapunov function V for global stable dynamic system $\dot{x} = f(x)$ is to view $V(x_0)$ as the cost to go from the initial state x_0 to the equilibrium. The Lyapunov function for a dynamic system is assumed to be done by a quadratic form

$$V(x) = x^T(t)Px(t) \tag{7.6}$$

where $P \in R^{n \times n}$ is a positive definite real symmetrical matrix. The most important application area of Lyapunov function is the synthesis of stabilising feedback controllers. Dynamic systems may use a set of convex Lyapunov functions, based on the computation of quadratic Lyapunov functions using linear matrix inequalities (LMI).

7.3.2 Barbalat's lemma

Assume that f is a function of time only.

Having $\dot{f}(t) \rightarrow 0$ does not imply that $f(t)$ has a limit at $t \rightarrow \infty$.

Having $f(t)$ approaching a limit as $t \rightarrow \infty$ does not imply that $\dot{f}(t) \rightarrow 0$.

Having $f(t)$...lower bounded and decreasing ($\dot{f} \leq 0$) implies it converges to a limit. But it does not say whether or not $\dot{f} \rightarrow 0$ as $t \rightarrow \infty$.

Barbalat's Lemma says:

If $f(t)$ has a finite limit as $t \rightarrow \infty$ and if \dot{f} is uniformly continuous (or \ddot{f} is bounded), then $\dot{f}(t) \rightarrow 0$ as $t \rightarrow \infty$.

It is always difficult to investigate the asymptotic stability of time-varying systems on the bases of finding a Lyapunov functions with negative definite derivative. For autonomous systems if \dot{V} is negative semi-definite, then, it is possible to know the asymptotic behaviour of the system by calling up the invariant-set theorems. However, this flexibility is not the case in terms of time-varying system, hence Barbalat's lemma come into fore. Then it can be said that $V(x,t)$ satisfies the following conditions:

$V(x,t)$ is lower bounded

$\dot{V}(x,t)$ is negative semi-definite

$\dot{V}(x,t)$ is uniformly continuous in time, then $\dot{V}(x,t) \rightarrow 0$ as $t \rightarrow \infty$

The system

$$\dot{e}(t) = -e(t) + gw(t) \quad (7.7)$$

$$\dot{g}(t) = -e(t)w(t) \quad (7.8)$$

is non-autonomous because the input w is a function of time. Assume that the input $w(t)$ is bounded.

Taking $V(t) = e^2(t) + g^2(t)$ gives $\dot{V}(t) = -2e^2(t) \leq 0$. This says that $V(t) \leq V(0)$ by first two conditions and hence e and g are bounded. But it does not say anything about the convergence of e to zero. Moreover, the invariant set theorem cannot be applied, because the dynamics is non-autonomous.

Using Barbalat's lemma the function of Lyapunov can be constructed as

$V(t) = -4e(t)(-e(t) + g(t)w(t))$ this function is bounded because e , g and w are bounded. This implies

$V \rightarrow 0$ as $t \rightarrow \infty$ and hence $e \rightarrow 0$. This proves that the error converges.

7.4 Controller design

7.4.1 Nonlinear continuous control of the dissolved oxygen

Method for design of a nonlinear linearizing controller based on a reference model and Lyapunov stability direct method theory in combination with an additional linear controller to improve the performance of the closed loop system is developed. A strategy for designing a nonlinear DO controller was developed. The design is for the case of the nonlinear oxygen transfer function as a function of control action in the controller design process of the type given by Equation (3.9).

7.4.2 Model reference control systems, Design of a nonlinear controller in common case.

One useful method for specifying system performance is by means of a model that will produce the desired output for a given input. The model needs not to be actual hardware. It can only be a mathematical model simulated on a computer. In a model reference control, the output of the model and that of the plant are compared and the difference is used to generate the control signals.

The method for the design of a nonlinear controller consists of the following steps:

7.4.3 The plant is described by the nonlinear state equation

$$\dot{x}(t) = f(u, x, t), \quad x(0) = x_0 \quad (7.9)$$

$$y(t) = Cx(t) \quad (7.10)$$

where $x \in R^n$ is the state vector, $u \in R^m$ is the control vector, and $f \in R^n$ is a vector valued function, $y \in R^l$ is the plant output, $C \in R^{l \times n}$ is the output matrix.

7.4.4 Determination of the specifications for the behaviour of the closed loop system

It is desired that the output of the closed loop system follows closely some reference model system output. The problem for design of a controller is to find a controller that always generates a signal that forces the plant state towards the reference model state. The closed loop system configuration is given on Figure 7.1.

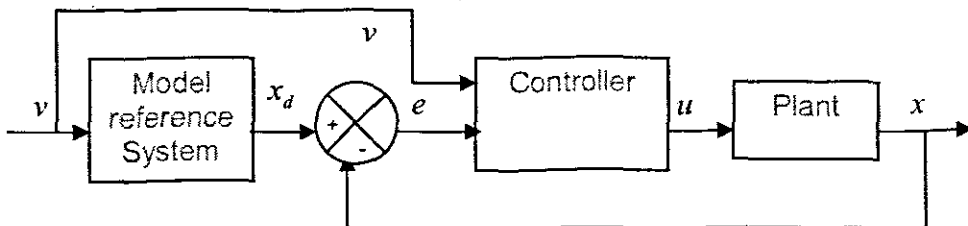


Figure 7.1: The closed loop system configuration diagram

where $v \in R^m$ is the reference control input, $e \in R^n$ is the error between the reference and plant states.

The model reference system can be different. It is assumed in the project that it is linear, given by the equations

$$\dot{x}_d(t) = Ax_d(t) + Bv(t) \quad (7.11)$$

$$y(t) = Cx(t) \quad (7.12)$$

where $x_d \in R^n$ is the state vector of the reference model, $v \in R^m$ is the control vector for the reference model, $A \in R^{n \times n}$ is a constant state matrix and $B \in R^{n \times m}$ is a constant control matrix.

It is assumed that the eigenvalues of the A have negative real parts so that the model reference system has an asymptotically stable equilibrium state. The control input v can be selected in such way that x_d follows some desired trajectory, which then will be followed by the plant.

7.4.5 Determination of the error between the reference model and plant state.

The error is

$$e(t) = \dot{x}_d(t) - x(t), e \in R^n \quad (7.13)$$

The requirements towards the closed loop systems are that the error $e(t)$ has to be reduced to zero by a suitable control vector $u(t)$. In order to include the model equation and the plant equation in the error equation (7.13) it is necessary to differentiate the error equation (7.13) according to the time

$$\begin{aligned} \dot{e}(t) &= \dot{x}_d(t) - \dot{x}(t) = Ax_d(t) + Bv(t) - f(x, u, t) = \\ &= Ax_d(t) + Ax(t) - Ax(t) + Bv(t) - f(x, u, t) = \\ &= A(x_d - x(t)) + Ax(t) + Bv(t) - f(x, u, t) = \\ &= Ae(t) + Ax(t) - f(x, u, t) + Bv(t) \end{aligned} \quad (7.14)$$

Equation (7.14) is a differential equation for the error vector. The problem now is to design a controller such that at the equilibrium state $x = x_d, \dot{x} = \dot{x}_d$ or $e = \dot{e} = 0$. Thus the equilibrium $e = 0$ will be the origin of the coordinate system

7.4.6 Design of a controller

7.4.6.1 Construction of a Lyapunov functions for the system.

The Lyapunov function is assumed to be done by a quadratic form

$$V(e) = e^T(t)Pe(t) \quad (7.15)$$

Where $P \in R^{n \times n}$ is a positive definite real symmetrical matrix.

7.4.6.2 Calculation of the first derivative of the function of Lyapunov according to the trajectory of the error equation

$$\begin{aligned}
 \dot{V}(e) &= \dot{e}^T(t)Pe + e^T(t)P\dot{e}(t) = [Ae(t) + Ax(t) - f(x,u,t) + Bv(t)]^T Pe(t) + \\
 &+ e^T(t)P[Ae(t) + Ax(t) - f(x,u,t) + Bv(t)] = \\
 &= [e^T(t)A^T + x^T(t)A^T - f^T(x,u,t) + v^T(t)B^T]Pe(t) + e^T(t)[Ae(t) + Ax(t) - f(x,u,t) + Bv(t)] = \\
 &= e^T A^T Pe(t) + x^T A^T Pe(t) - f^T(x,u,t)Pe(t) + v^T(t)B^T Pe(t) + \\
 &+ e^T PAe(t) + e^T(t)PAx(t) - e^T(t)Pf(x,u,t) + e^T(t)PBv(t) = \\
 &= e^T(t)[A^T P + PA]e(t) + 2M
 \end{aligned} \tag{7.16}$$

where

$$\begin{aligned}
 2M &= x^T(t)A^T Pe(t) + e^T(t)PAx(t) - \\
 &- f^T(x,u,t)Pe(t) - e^T(t)Pf(x,u,t) + v^T(t)B^T Pe(t) + e^T(t)PBv(t) = \\
 &= e^T(t)PAx(t) + e^T(t)PAx(t) - e^T Pf(x,u,t) - e^T(t)Pf(x,u,t) + \\
 &+ e^T PBv(t) + e^T(t)PBv(t) = 2e^T(t)P[Ax(t) - f(x,u,t) + Bv(t)]
 \end{aligned} \tag{7.17}$$

This derivation is based on the fact that P is a symmetrical matrix and $P^T = P$ or

$$M = e^T(t)P[Ax - f(x,u,t) + Bv(t)] \tag{7.18}$$

M is a scalar quantity.

7.4.6.3 Calculation of the control vector u

The assumed function $V(e)$ is a Lyapunov function. If its derivative is negative definite, then the system (7.16) will be stable. It can be seen that the derivative is sum of two expressions

$$\dot{V}(e) = e^T(t)[A^T P + PA]e(t) + 2M \tag{7.19}$$

In order $\dot{V}(e)$ to be negative definite, the two terms have to be negative definite.

1. $e^T(t)[A^T P + PA]e(t) < 0 \rightarrow A^T P + PA = -Q$

Where Q is a positive definite matrix.

2. $M < 0$

On the basis of (7.18) and (7.19) above it can be concluded that M can be made negative or equal to zero through convenient choice of the plant control vector $u(t)$, which is included in the derivative $\dot{V}(e)$. Then noting that $V(e) \rightarrow \infty$ as $\|e\| \rightarrow \infty$, can be seen that the equilibrium state $e = 0$ is asymptotically stable in the large. Condition (1) can always be fulfilled by a proper choice of P since the eigenvalues of the matrix A are selected to be with negative real parts. The problem now is to choose an appropriate

vector $u(t)$ so that M is either zero, or negative scalar quantity. The calculations of $u(t)$ can be done with selected values of the matrix P or the matrix Q . The obtained control u makes the process to be stable and to follow the desired trajectory determined by the reference model. The method is applied to the nonlinear model of dissolved oxygen concentration.

7.5 Design of the nonlinear Lyapunov controller for the model of the Dissolved Oxygen Concentration

7.5.1 Dissolved oxygen model

The procedure described above is applied as follows. The nonlinear model of the dissolved oxygen as developed in chapter 3 is:

$$\dot{s}_o(t) = f(s_o(t)) + g(s_o(t))u(t) + g_1(s_o(t))s_{o,m}(t) + g_2(s_o(t))r_{so}(t) \quad (7.20)$$

$$y(t) = Cs_o(t) \quad (7.21)$$

7.5.2 The model of the desired system (reference model)

The model of the DO is of first order. That is why the desired model is selected to be of the first order too.

$$\dot{s}_{o,d}(t) = as_{o,d}(t) + bv(t) \quad (7.22)$$

$$y_d(t) = Cs_{o,d}(t) \quad (7.23)$$

Where $s_{o,d} \in R$ is the desired state space vector, $v \in R$ is the control vector for the reference model, $a \in R$ and $b \in R$ are the state space and control coefficients of the reference model, $C = 1$ is the output coefficient for the dissolved oxygen concentration.

The coefficient a is negative in order for the reference model to be stable. The transfer function corresponding to the reference model can be determined after Laplace transform of the reference model equation.

$$L\{\dot{s}_o(t)\} = L\{as_{o,d} + bv(t)\}$$

$$ss_o(s) = as_o(s) + bv(s)$$

$$(s - a)s_o(s) = bv(s) \quad (7.24)$$

$$s_o(s) = \frac{bv(s)}{(s - a)}$$

$$W_d(s) = \frac{s_o(s)}{v(s)} = \frac{b}{s - a}$$

The Laplace transform of the output is

7.6 Design of the control

7.6.1 Construction of a Lyapunov function for the error differential equation

The Lyapunov function is selected of the form:

$$V(e) = e^T(t)Pe(t) = Pe^2(t) \quad (7.28)$$

where P is positive definite coefficient, $P \in R$

7.6.2 Calculation of the first derivative of the function of Lyapunov

$$\begin{aligned} \dot{V}(e(t)) &= 2Pe(t)e(t) = \\ &= 2P \begin{bmatrix} ae(t) + as_o(t) + bv(t) - f(s_o(t)) - g(s_o(t))u_1(t) - \\ -g_1(s_o(t))s_{o,in}(t) - g_2(s_o(t))r_{s_o}(t) \end{bmatrix} e(t) = \\ &= 2Pae^2(t) + 2Pe(t) \begin{bmatrix} as_o(t) + bv(t) - f(s_o(t)) - g(s_o(t))u_1 - \\ -g_1(s_o(t))s_{o,in}(t) - g_2(s_o(t))r_{s_o}(t) \end{bmatrix} = \\ &= 2Pae^2(t) + 2M < 0 \end{aligned} \quad (7.29)$$

$$M = e(t)P[as_o(t) + bv_d(t) - f(s_o(t)) - g(s_o(t))u_1(t) - g_1(s_o(t))s_{o,in}(t) - g_2(s_o(t))r_{s_o}(t)] \quad (7.30)$$

The obtained equation (7.30) is the equation of the first derivative of the function of Lyapunov. In order for the error in the closed loop system to go to zero as time $t \rightarrow \infty$ it is necessary for the first derivative of the function of Lyapunov to be negative. The first part is negative as a is selected to be negative (in a unit circle) for discrete system. Then the second part M can be made negative $M < 0$ by a proper selection of the control $u_1(t)$.

7.6.3 Calculation of the control $u_1(t)$

$$\begin{aligned} M &= e(t)P[as_o(t) + bv_d(t) - f(s_o(t)) - g(s_o(t))u_1(t) - g_1(s_o(t))s_{o,in}(t) - g_2(s_o(t))r_{s_o}(t)] < 0 \\ M &= e(t)P[as_o(t) + bv_d(t) - f(s_o(t))] - e(t)P[g(s_o(t))u_1(t) + g_1(s_o(t))s_{o,in}(t) + g_2(s_o(t))r_{s_o}(t)] < 0 \\ &+ e(t)P[as_o(t) + bv_d(t) - f(s_o(t))] < e(t)P[g(s_o(t))u_1(t) + g_1(s_o(t))s_{o,in}(t) + g_2(s_o(t))r_{s_o}(t)] \end{aligned} \quad (7.31)$$

$$\begin{aligned} Pe(t)[as_o(t) + bv(t) - f(s_o(t))] &< Pe(t)g(s_o(t))u_1(t) + Pe(t)g_1(s_o(t))s_{o,in}(t) + \\ &+ Pe(t)g_2(s_o(t))r_{s_o}(t) \end{aligned} \quad (7.32)$$

All expressions without $u_1(t)$ are put to one side and the one containing $u_1(t)$ is put on the other side.

$$\begin{aligned} Pe(t)[as_o(t) + bv_d(t) - f(s_o(t)) - g_1(s_o(t))s_{o,in}(t) - g_2(s_o(t))r_{s_o}(t)] &< \\ < Pe(t)g(s_o(t))u_1(t) \end{aligned} \quad (7.33)$$

From here:

$$\frac{Pe(t)[as_o(t) + bv(t) - f(s_o(t)) - g_1(s_o(t))s_{o,in}(t) - g_2(s_o(t))r_{so}(t)]}{Pe(t)g(s_o(t))} < u_1(t) \quad (7.34)$$

The coefficient P in the numerator and denominator can be cancelled and the nonlinear control that will make the closed loop system stable and having the same behaviour as the reference model is

$$u_1(t) > \frac{[as_o(t) + bv(t) - f(s_o(t)) - g_1(s_o(t))s_{o,in}(t) - g_2(s_o(t))r_{so}(t)]e(t)}{e(t)g(s_o(t))} \quad (7.35)$$

After substitution of the expressions for the nonlinear functions f and g , it is obtained that,

$$u_1(t) > \frac{\left[as_o(t) + bv(t) + \frac{Q}{V}s_o(t) + k_1s_{o,sat} - k_1s_o(t) - \frac{Q}{V}s_{o,in}(t) - r_{so}(t) \right] e(t)}{[s_{o,sat}(t) - s_o(t)]e(t)}$$

$$u_1(t) > \frac{\left[\left(a + \frac{Q}{V} - k_1 \right) s_o(t) + bv(t) + k_1s_{o,sat} - \frac{Q}{V}s_{o,in}(t) - r_{so}(t) \right] e(t)}{[s_{o,sat}(t) - s_o(t)]e(t)} \quad (7.36)$$

Finally the air airflow rate $u(t)$ is calculated following derivation in chapter 3 and 6 as

$$u(t) = \frac{-1}{k_2} \ln \left[\frac{u_1}{-k_1} \right] > \frac{-1}{k_2} \ln \left\{ \frac{\left[\left(a + \frac{Q}{V} - k_1 \right) s_o(t) + bv(t) + k_1s_{o,sat} - \frac{Q}{V}s_{o,in}(t) - r_{so}(t) \right] e(t)}{-k_1[s_{o,sat}(t) - s_o(t)]e(t)} \right\} \quad (7.37)$$

The control $u_1(t)$ can be selected to be a couple of times bigger than the expression in the right side of equation (7.37). This selection can be done after some simulations. It can be seen that the control $u(t)$ depends on the coefficients and the control of the reference model, oxygen transfer function coefficients k_1 and k_2 , process state $s_o(t)$, the inflow concentration of the dissolved oxygen and oxygen uptake rate.

7.7 Design of a controller for the reference model

Design is done for PI controller using pole placement method. The structure of the closed loop system is given in Figure 7.2. The control of the reference model can be selected in such way that additional characteristics of the closed loop behaviour could be obtained. The aim here is the current process of dissolved oxygen concentration has to be equal to the desired set-point, determined from the process optimization. This means that the

control $v(t)$ has to move the desired output $s_o(t)$ to be equal to the s_o^{SP} , the dissolved oxygen set-point without steady state error, or $e_1(t) = s_o^{SP} - s_{o,d}(t) \rightarrow 0$, when $t \rightarrow \infty$

The desired behaviour can be achieved with PI control. As the control $v(t)$ determines the behaviour of the reference model, and the reference model determines the behaviour of the plant, it can be concluded that also $e_1(t) = s_o^{SP} - s_o(t)$ can be achieved if $v(t)$ is PI controller.

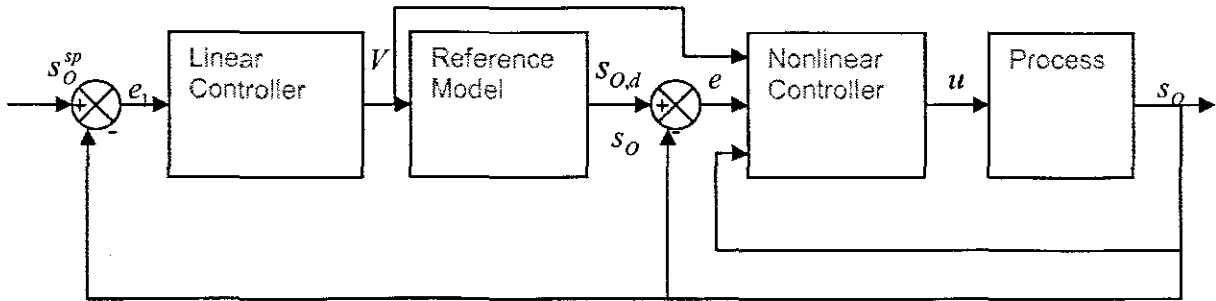


Figure 7.2: Closed loop system of the nonlinear controller.

7.7.1 Design of the PI controller

PI controller implemented here is similar to the one designed in chapter 6

$$v(t) = K_p \left[e_1(t) + \frac{1}{T_i} \int e(t) dt \right] \quad (7.38)$$

7.7.2 Final expression for the control $u(t)$

The equation is presented in such way that the following components are described, control input $u(t)$, k_1 and k_2 of which their values of are calculated from the value $K_{La} = 240 \text{ day}^{-1}$, the values of a and b are selected such that the closed loop system can be determined with the following desired characteristics

- System stability.
- With small overshoot and quick response.

Two disturbance inputs $s_{o,m}$ and r_{SO} and one state/output s_o

V [m^3] is the volume of the tank and Q is the total flow rates. The description of the PI controller is the same as the one in chapter 6. The representation of the combined

control equation of the linear and the Lyapunov second method based reference model nonlinear linearizing controller is given below

$$u(t) = \frac{-1}{k_2} \ln \left[\frac{\left[\left(a + \frac{Q}{V} - k_1 \right) s_o(t) + bK_p \left[e_1(t) + \frac{1}{T_1} \int e(t) dt \right] + k_1 s_{o,sat} - \frac{Q}{V} s_{o,in}(t) - r_{so}(t) \right] e(t)}{-k_1 [s_{o,sat}(t) - s_o(t)] e(t)} \right] \quad (7.39)$$

It can be seen from Equations (7.39) and (6.63) that the expressions for the combined control are very similar but are obtained using different theories and control structures.

7.8 Simulation study of the behaviour of the designed closed loop system

Simulation of the closed loop system is done in the Matlab/Simulink environment. The related m-file *Parameters_Nketoane.m* and the Simulink block diagram *Closed_Loop1.mdl* are first introduced, and then followed by simulation results of the dissolved oxygen concentration closed loop system. The DO model parameters are the same as the used in chapter 6. In order to investigate the capability of the combined control to overcome the influence of the disturbances $s_{o,in}$ and r_{so} different values of these disturbances are used in closed loop simulation. These values are shown in Table 7.1

Table 7.1: Parameters table for nonlinear control design

Set point	r_{so} Calculations				Resultant	$s_{o,in}$	α
					r_{so}		
1.8	Xba	149.797	Xbh	2559.444	-764.6982	0.2	-0.8
1.8	Xba-10%	134.8173	Xbh+10%	2816.3884	-746.7435	0.2	-0.8
1.8	Xba+10%	164.7767	Xbh-10%	2303.4996	-782.6757	0.2	-0.8
1.8	Xba-25%	112.3478	Xbh+25%	3199.305	-719.7945	0.2	-0.8
1.8	Xba+25%	187.2463	Xbh-25%	1919.583	-809.6251	0.2	-0.8
1.8	Xba-40%	89.8782	Xbh+40%	3583.2216	-692.8452	0.2	-0.8
1.8	Xba+40%	209.7158	Xbh-40%	1536.6664	-836.5741	0.2	-0.8
2	Xba	149.797	Xbh	2559.444	-764.7096	0.2	-0.8
2	Xba-10%	134.8173	Xbh+10%	2816.3884	-746.7435	0.2	-0.8
2	Xba+10%	164.7767	Xbh-10%	2303.4996	-782.6757	0.2	-0.8
2	Xba-25%	112.3478	Xbh+25%	3199.305	-719.7945	0.2	-0.8
2	Xba+25%	187.2463	Xbh-25%	1919.583	-809.6251	0.2	-0.8
2	Xba-40%	89.8782	Xbh+40%	3583.2216	-692.8452	0.2	-0.8
2	Xba+40%	209.7158	Xbh-40%	1536.6664	-836.5741	0.2	-0.8
3	Xba	149.797	Xbh	2559.444	-764.7096	0.2	-0.8
3	Xba-10%	134.8173	Xbh+10%	2816.3884	-746.7435	0.2	-0.8

3	Xba+10%	164.7767	Xbh-10%	2303.4996	-782.6757	0.2	-0.8
3	Xba-25%	112.3478	Xbh+25%	3199.305	-719.7945	0.2	-0.8
3	Xba+25%	187.2463	Xbh-25%	1919.583	-809.6251	0.2	-0.8
3	Xba-40%	89.8782	Xbh+40%	3583.2216	-692.8452	0.2	-0.8
3	Xba+40%	209.7158	Xbh-40%	1535.6664	-836.5741	0.2	-0.8

7.8.1 Simulink block diagram

The system is simulated in Simulink. The closed loop based on Lyapunov direct based method Simulink block diagram of the dissolved oxygen process "Closed_Loop1.mdl" is shown in Figure 7.3. It consists of three important subsystems:

- Reference model subsystem (Figure 7.4)
- Nonlinear Linearizing controller subsystem (Figure 7.5)
- Respiration model subsystem (Figure 7.6)

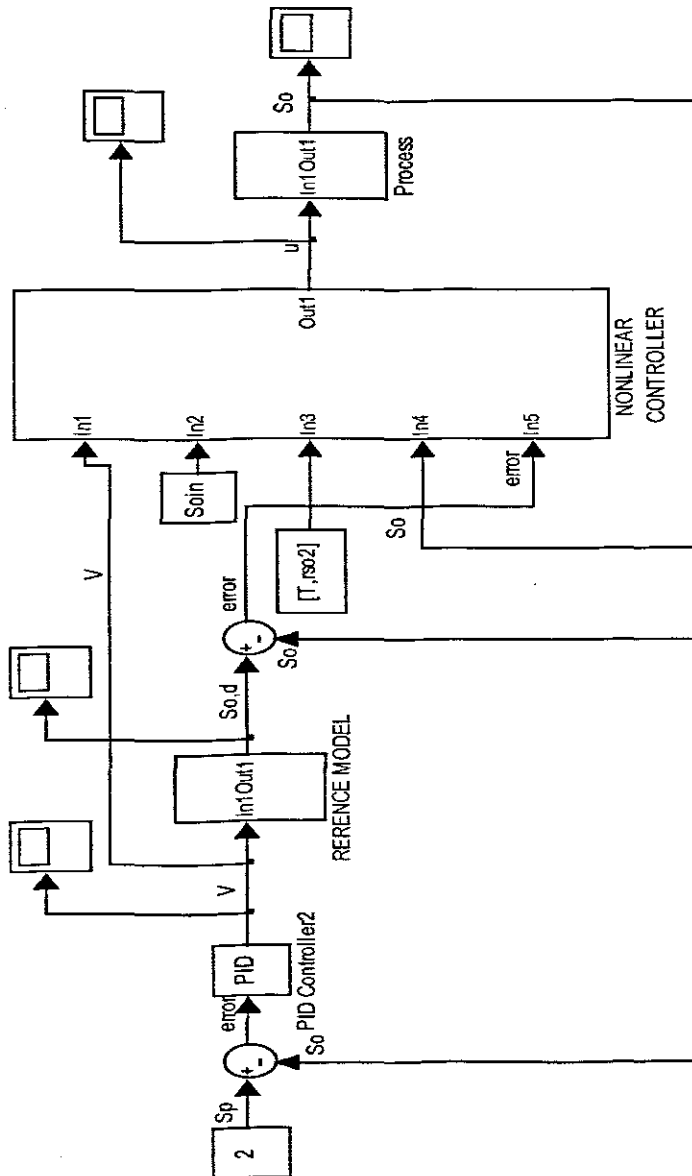


Figure 7.3: Closed loop Lyapunov direct method based on reference model Simulink block diagram

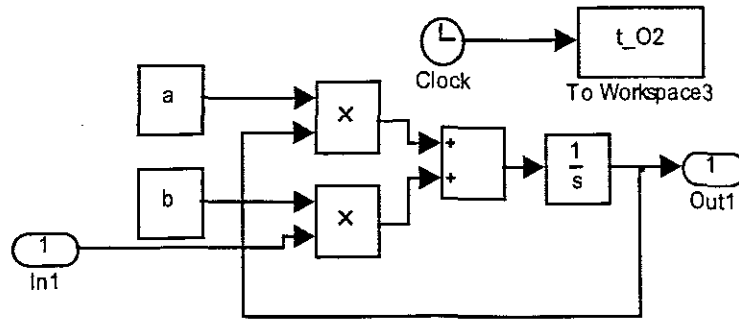


Figure 7.4: Reference model Simulink block diagram

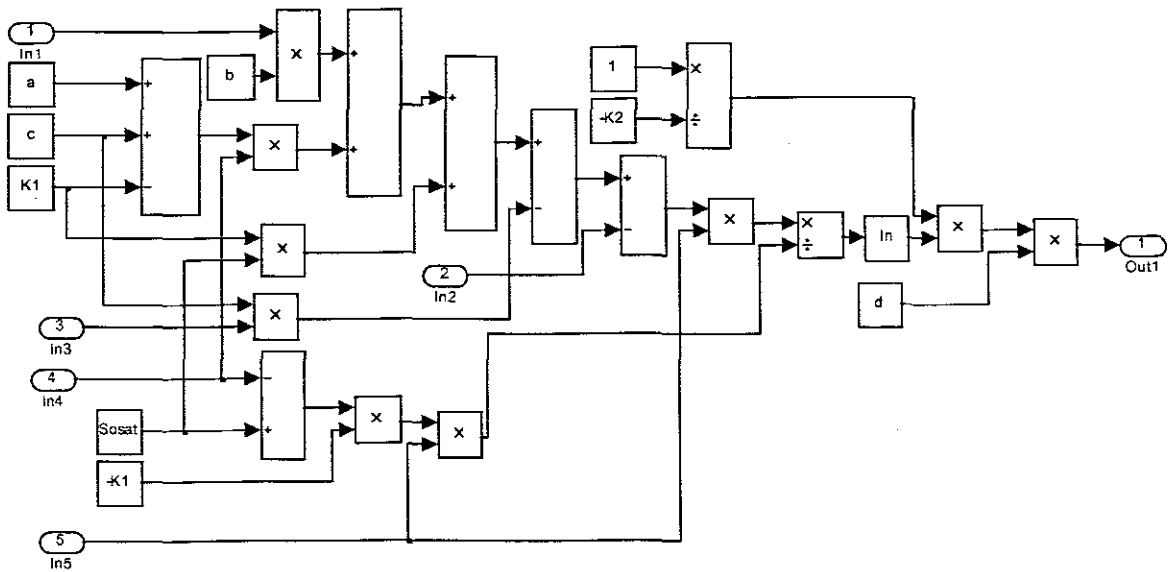


Figure 7.5: Nonlinear Linearizing controller Simulink block diagram

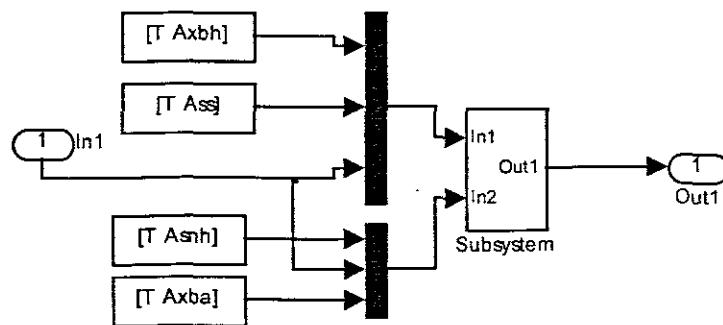


Figure 7.6: Respiration Simulink block diagram

7.8.2 Matlab program for the Lyapunov based nonlinear controller with reference model

```

%=====
%PI Controller Parameters
%=====
Ti= b*(4+a)/6
Kp= 4+a
P=Kp
I=P/Ti
%=====
%Coefficients
%=====
a=-0.8
b=15000
K1=240
K2=1.96 e-04
d=1

```

The above Matlab program is used for the simulation of both the PI controller and Lyapunov based nonlinear linearizing controller for the dissolved oxygen concentration model.

Parameters for simulation of the Dissolved Oxygen Concentration are introduced in Matlab workspace by the program "*Parameters_Nketoane .m*". The program is given in the Appendix D. The corresponding Simulink model "*Closed_Loop1 .mdl*" is given in Figure 7.3. The input variables are the disturbances $s_{O,in}$, and r_{SO} the control signal u is calculated by the nonlinear controller, v is calculated by the PI controller and the parameters for calculation of r_{SO} are μ_H , Y_H , μ_A , Y_A , K_{NH} , K_{OA} , K_{OH} , K_S . The variables s_S , s_{NH} and s_O are the steady state Benchmark process values (Copp, 2002). The output variable is dissolved oxygen concentration s_O . The values of the parameters are taken from the ASM1 biological model and are given in Table 3.5. The values of k_1 and k_2 are calculated from the value $K_{La} = 240 \text{ day}^{-1}$ by a curve fitting for a given value of the airflow rate u_1 .

Table 7.2: Values of the r_{SO} model parameters and variables

Par	μ_H	Y_H	μ_A	Y_A	s_S	s_{NH}	K_{NH}	K_{OA}	K_{OH}	K_S	s_O
Val	4	0.67	0.5	0.24	0.889	1.733	1.0	0.4	0.2	10.	0.491

Table 7.3: Values of the model parameter for controller calculation

Par	k_1	k_2	r_{SO}	$s_{O,in}$	a	b	d
Val	240	$1.961e^{-20}$	-764.6982	0.2	-0.8	15000	1

The simulations are provided according to the Table 7.1. The results are given in Figures 7.9 till 7.29

7.8.3 Simulation results

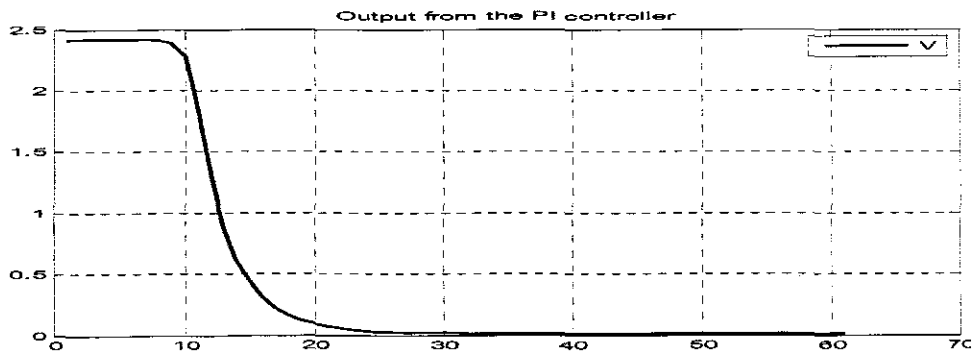


Figure 7.7: PI controller signal

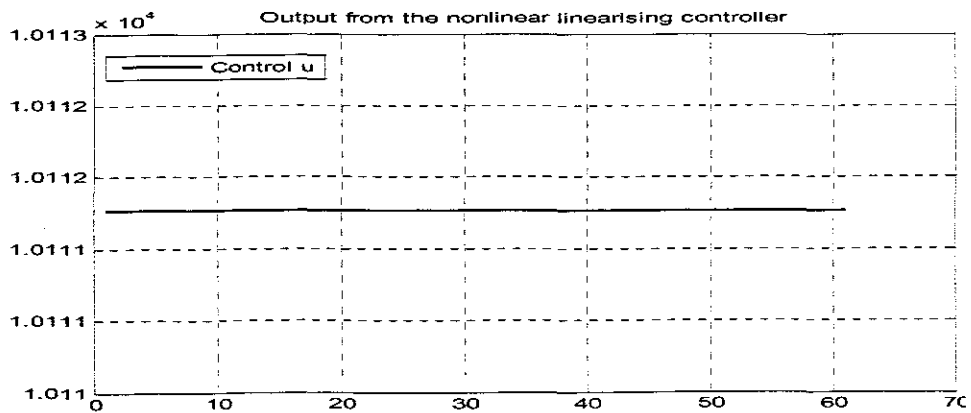


Figure 7.8: Nonlinear controller output

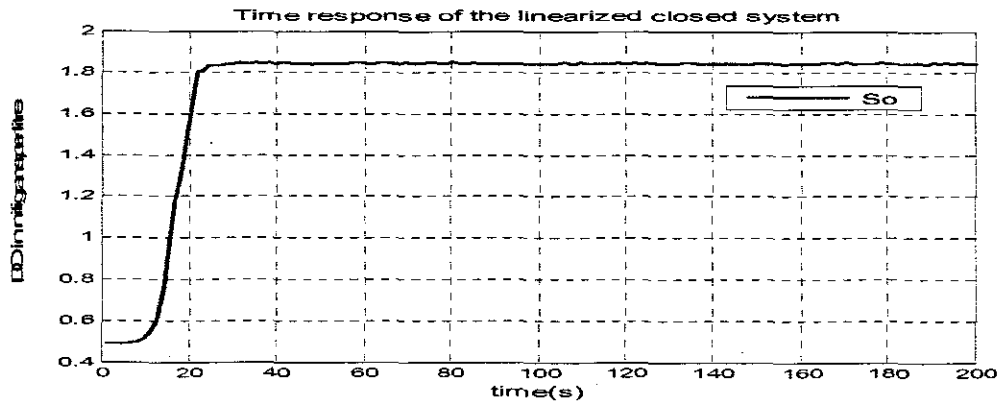


Figure 7.9: Closed loop response for the linearized by Lyapunov reference based nonlinear controller when $S_{oin}=0.2$, $a=-0.8$, $r_{so}=-764.6982$ and the set point is 1.8

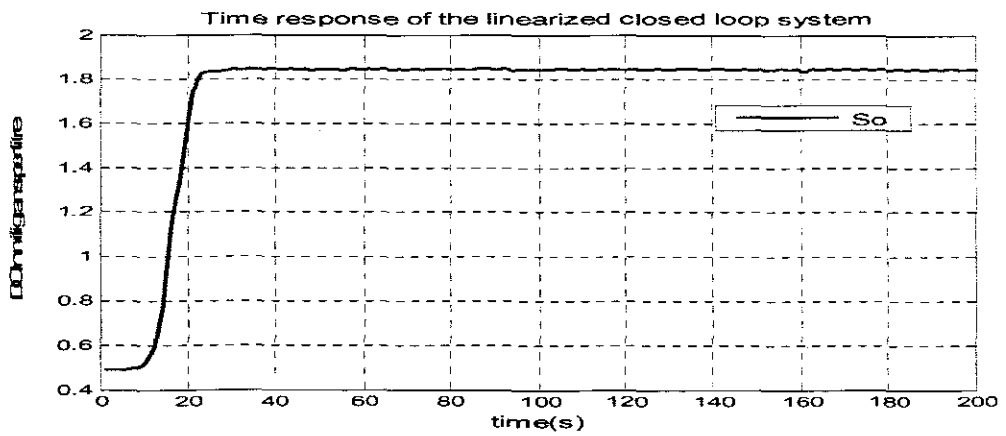


Figure 7.10: Closed loop response for the linearized by Lyapunov reference based nonlinear controller when $S_{oin}=0.2$, $a=-0.8$, $r_{so}=-746.7435$ and the set point is 1.8

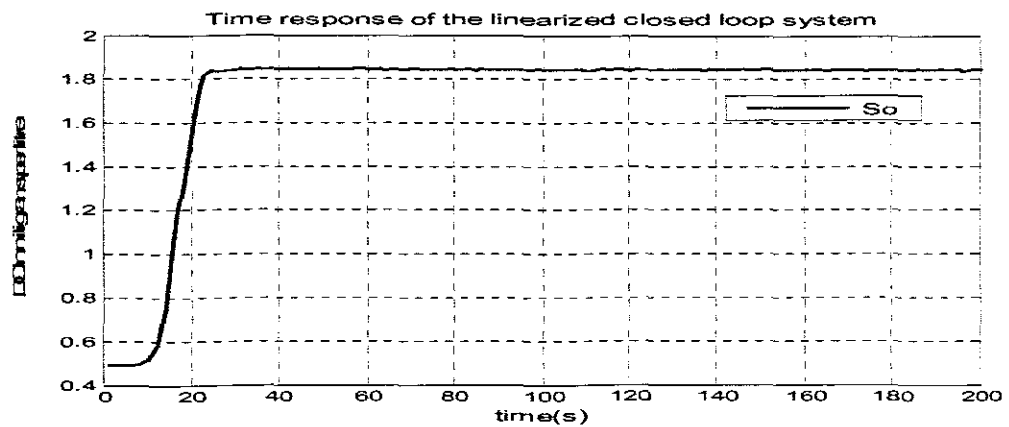


Figure 7.11: Closed loop response for the linearized by Lyapunov reference based nonlinear controller when $S_{oin}=0.2$, $a=-0.8$, $r_{so}=-782.6757$ and the set point is 1.8

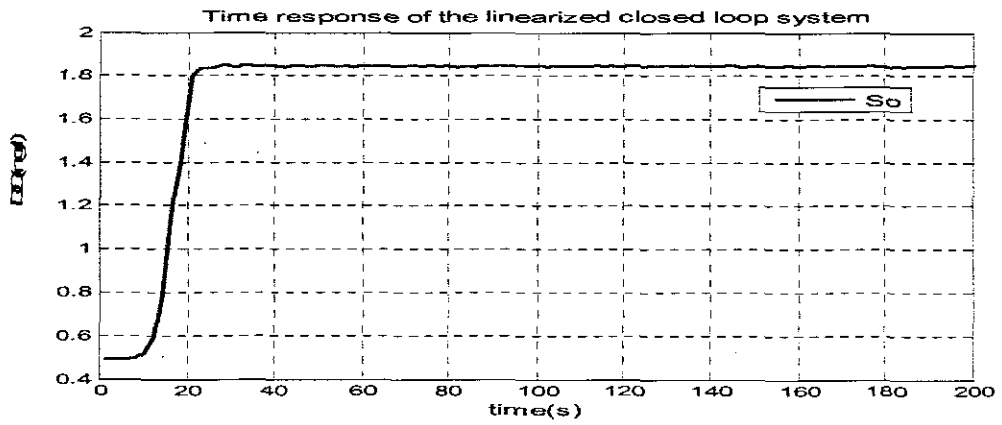


Figure 7.12: Closed loop response for the linearized by Lyapunov reference based nonlinear controller when $S_{oin}=0.2$, $a=-0.8$, $r_{so}=-719.7945$, and the set point is 1.8

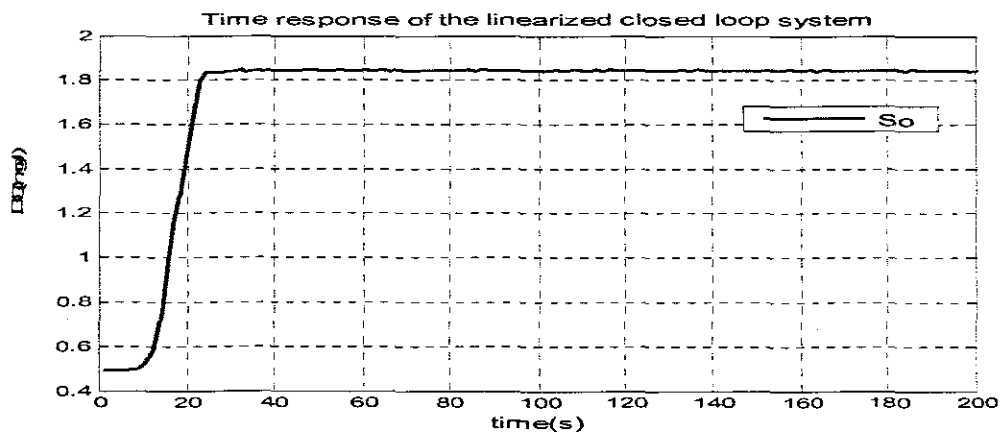


Figure 7.13: Closed loop response for the linearized by Lyapunov reference based nonlinear controller when $S_{oin}=0.2$, $a=-0.8$, $r_{so}=-809.6251$, and the set point is 1.8

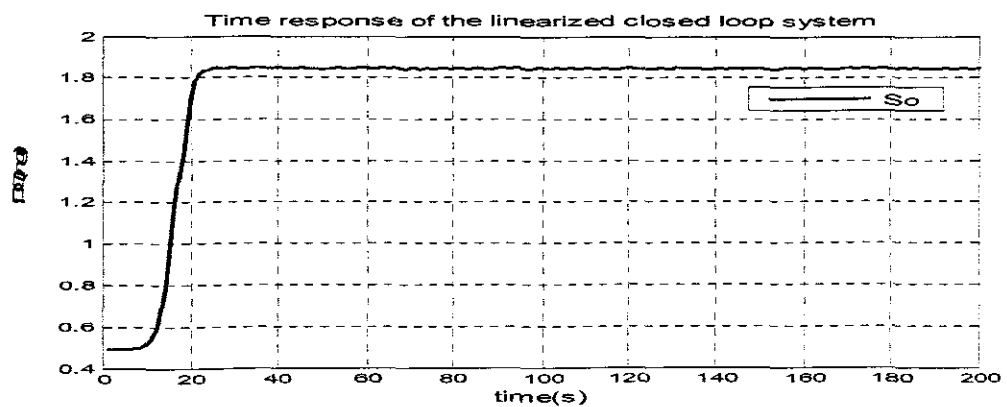


Figure 7.14: Closed loop response for the linearized by Lyapunov reference based nonlinear controller when $S_{oin}=0.2$, $a=-0.8$, $r_{so}=-692.8452$, and the set point is 1.8

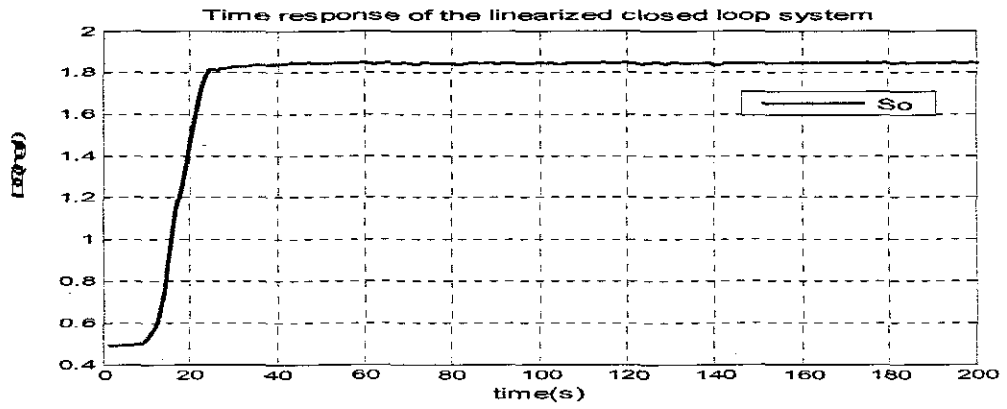


Figure 7.15: Closed loop response for the linearized by Lyapunov reference based nonlinear controller when $S_{oin}=0.2$, $a=-0.8$, $r_{so}=-836.5741$, and the set point is 1.8

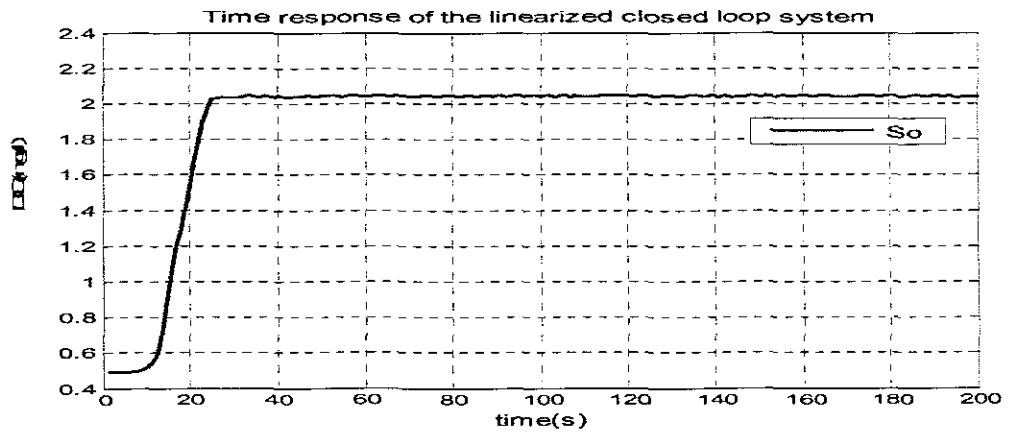


Figure 7.16: Closed loop response for the linearized by Lyapunov reference based nonlinear controller when $S_{oin}=0.2$, $a=-0.8$, $r_{so}=-764.6982$, and the set point is 2

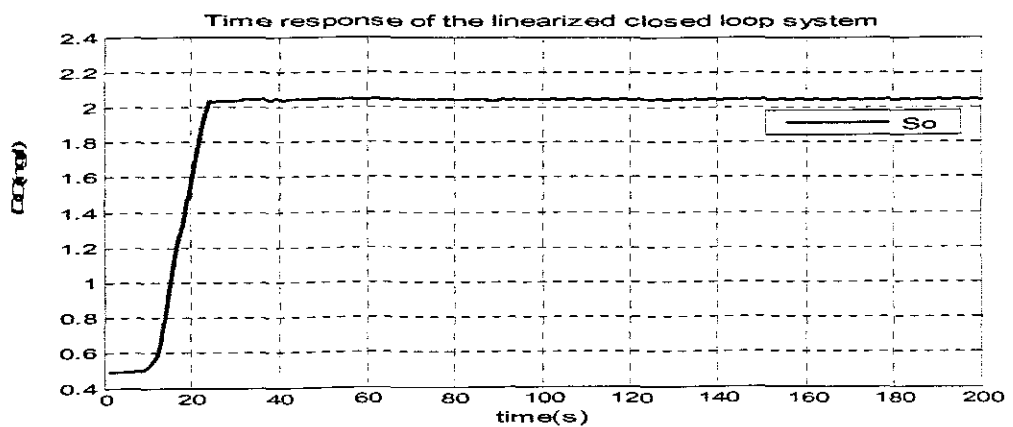


Figure 7.17: Closed loop response for the linearized by Lyapunov reference based nonlinear controller when $S_{oin}=0.2$, $a=-0.8$, $r_{so}=-746.7435$ and the set point is 2

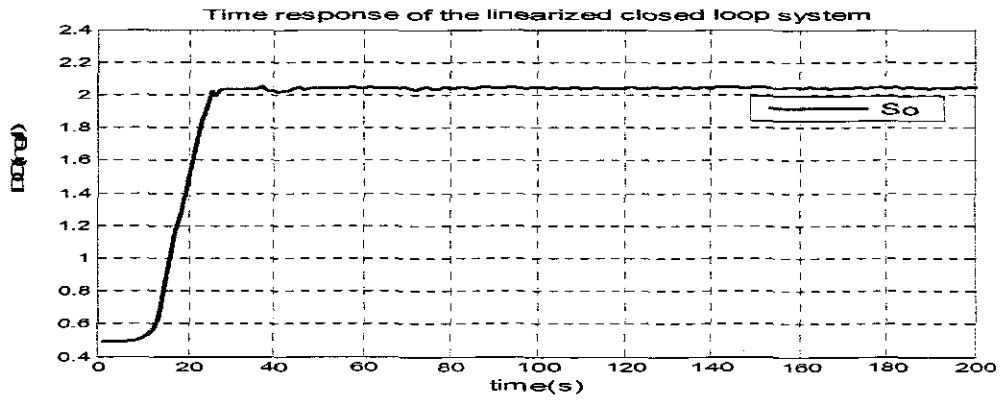


Figure 7.18: Closed loop response for the linearized by Lyapunov reference based nonlinear controller when $S_{oin}=0.2$, $a=-0.8$, $r_{so}=-782.6757$, and the set point is 2

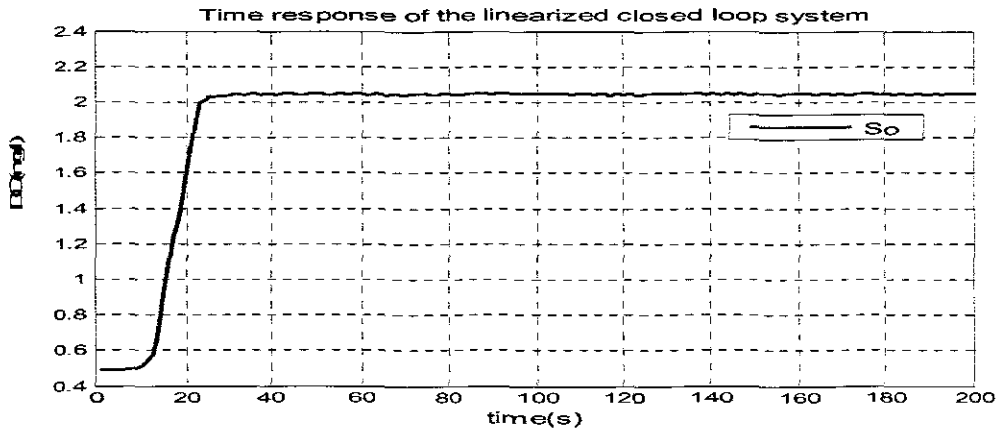


Figure 7.19: Closed loop response for the linearized by Lyapunov reference based nonlinear controller when $S_{oin}=0.2$, $a=-0.8$, $r_{so}=-719.7945$, and the set point is 2

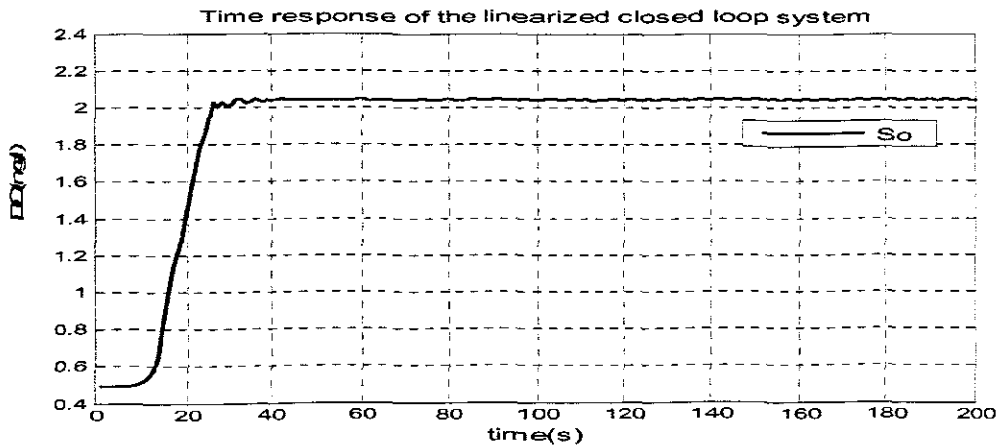


Figure 7.20: Closed loop response for the linearized by Lyapunov reference based nonlinear controller when $S_{oin}=0.2$, $a=-0.8$, $r_{so}=-809.6251$, and the set point is 2

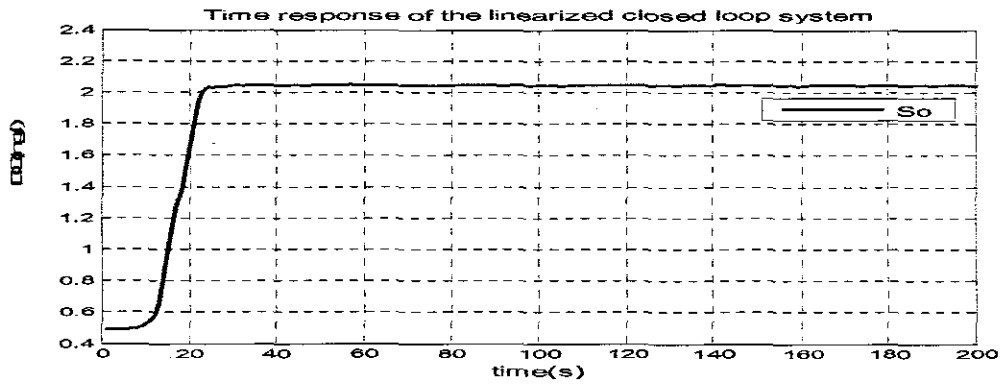


Figure 7.21: Closed loop response for the linearized by Lyapunov reference based nonlinear controller when $S_{oin}=0.2$, $a=-0.8$, $r_{so}=-692.8452$, and the set point is 2

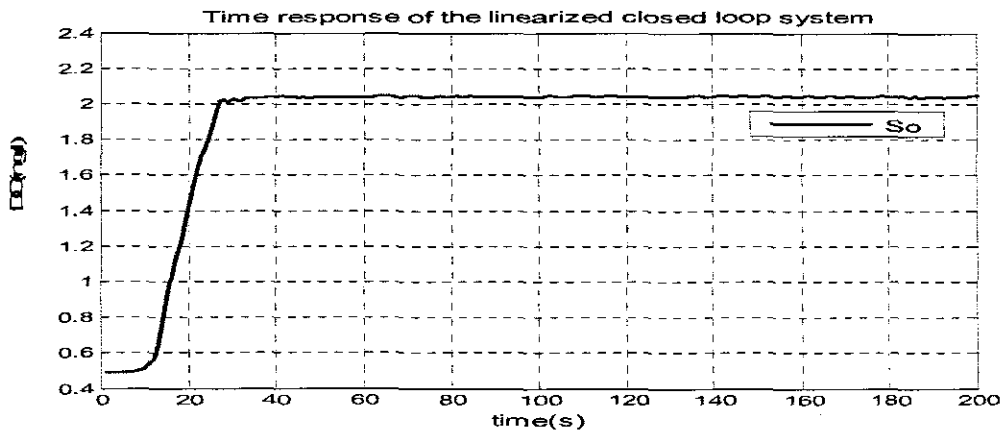


Figure 7.22: Closed loop response for the linearized by Lyapunov reference based nonlinear controller when $S_{oin}=0.2$, $a=-0.8$, $r_{so}=-836.5741$, and the set point is 2

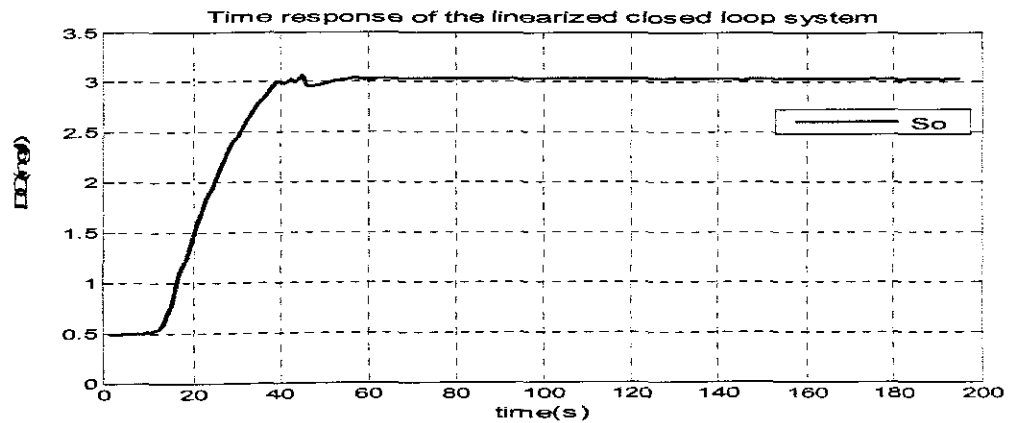


Figure 7.23: Closed loop response for the linearized by Lyapunov reference based nonlinear controller when $S_{oin}=0.2$, $a=-0.8$, $r_{so}=-764.6982$, and the set point is 3

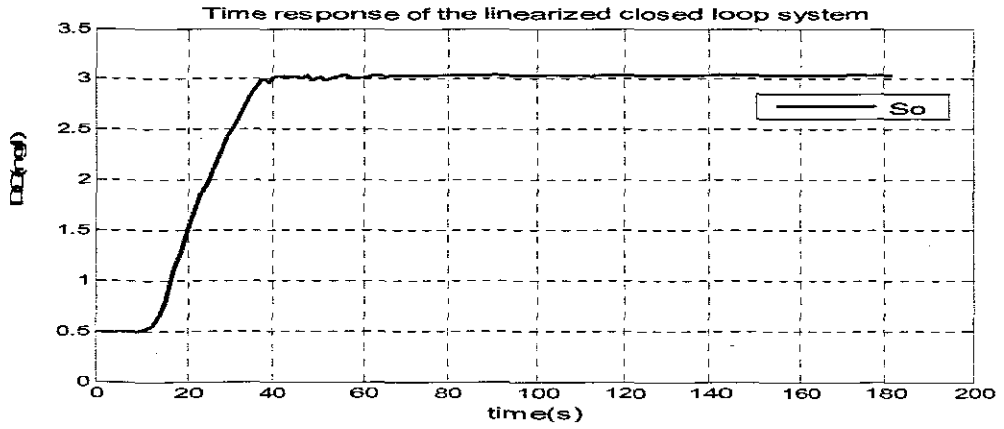


Figure 7.24: Closed loop response for the linearized by Lyapunov reference based nonlinear controller when $S_{oin}=0.2$, $a=-0.8$, $r_{so}=-746.7435$ and the set point is 3

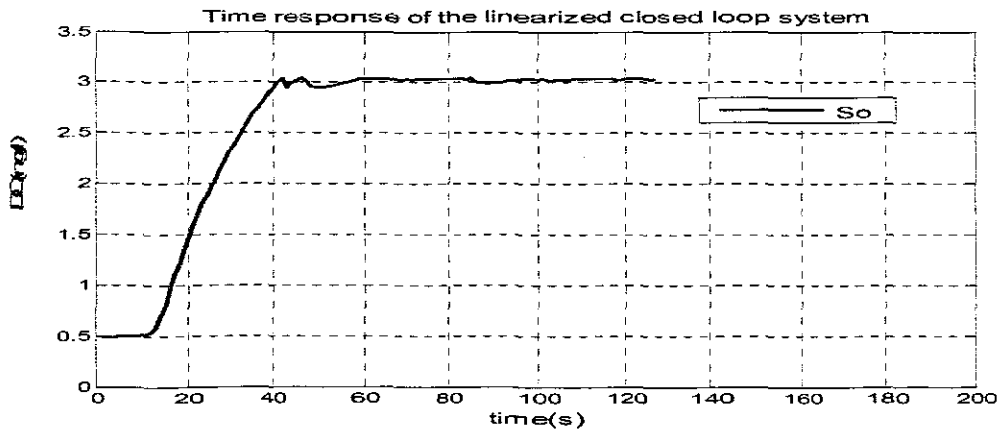


Figure 7.25: Closed loop response for the linearized by Lyapunov reference based nonlinear controller when $S_{oin}=0.2$, $a=-0.8$, $r_{so}=-782.6757$, and the set point is 3

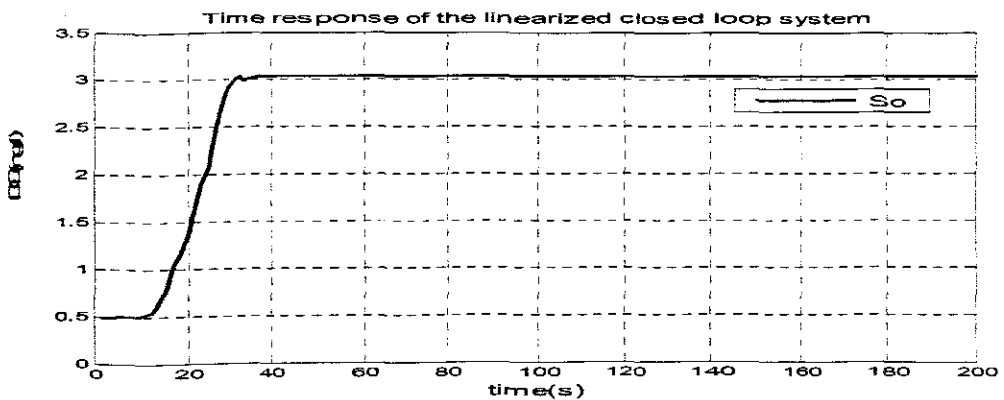


Figure 7.26: Closed loop response for the linearized by Lyapunov reference based nonlinear controller when $S_{oin}=0.2$, $a=-0.8$, $r_{so}=-719.7945$, and the set point is 3

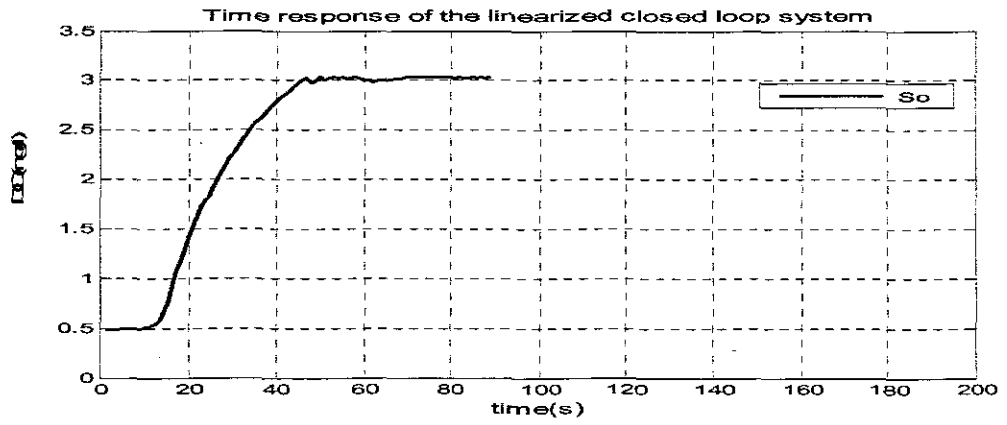


Figure 7.27: Closed loop response for the linearized by Lyapunov reference based nonlinear controller when $S_{oin}=0.2$, $a=-0.8$, $r_{so}=-809.6251$, and the set point is 3

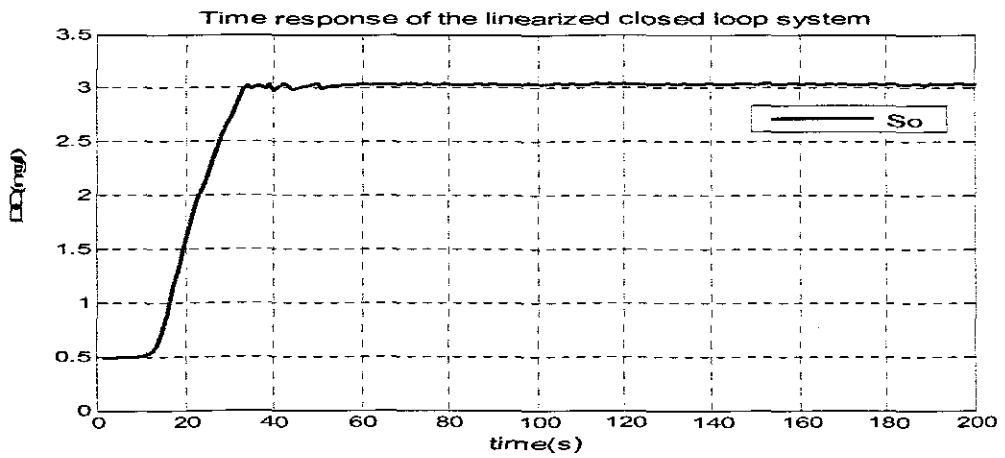


Figure 7.28: Closed loop response for the linearized by Lyapunov reference based nonlinear controller when $S_{oin}=0.2$, $a=-0.8$, $r_{so}=-692.8452$, and the set point is 3

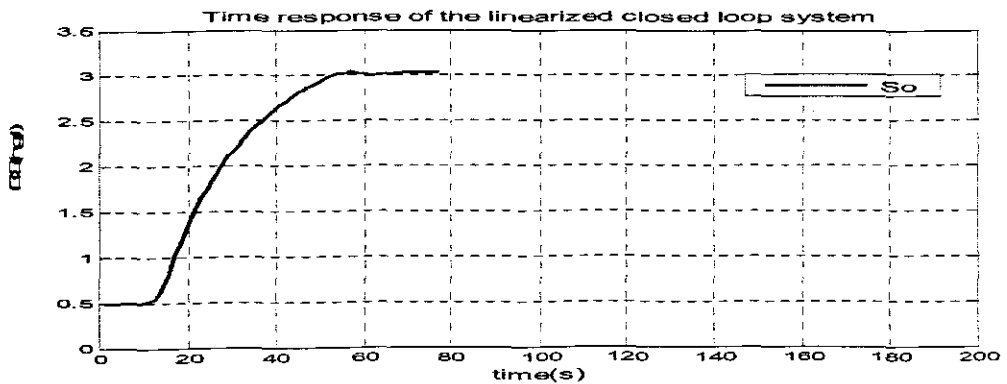


Figure 7.29: Closed loop response for the linearized by Lyapunov reference based nonlinear controller when $S_{oin}=0.2$, $a=-0.8$, $r_{so}=-836.5741$, and the set point is 3

7.9 Discussion of the results

For the simulation of the closed loop behaviour of the dissolved oxygen concentration the following parameters were varied: the two disturbance; external $s_{O,in}$, and internal r_{SO} , the reference model parameter α and the set-point. The following closed loop transition behaviour parameters were observed to investigate the performance of the controller: time delay, steady state error, settling time, rising time. The following characteristics have been seen:

- The closed loop system is stable
- The output follows the reference model and the set point trajectories
- The derivative of the of the Lyapunov function is smaller than 0 when $t \rightarrow \infty$ and $\dot{V} \rightarrow 0$ (this can be calculated)

The following conclusions can be done:

- The time delay is the same for all values of set-points and r_{SO}
- The settling time depends on the value of the set-point, when the set point is smaller, the settling time is smaller, on the other hand for the same set-point the settling time is bigger for the bigger values of r_{SO}
- The steady state error is not very sensitive towards the values of r_{SO} , but varies for different values of the set-points.
- The rising time also varies with the changes in the values of the set-point. For bigger set-points values, the value of the rising time is bigger. The Lyapunov reference model based nonlinear controller causes slight oscillations of the steady state value of the DO concentration

The specifications of the dynamic output behaviour of the closed loop system are given below in Table 7.4.

Table 7.4 Simulation results comparison

Set point	Parameters			Characteristics			
	α	r_{SO}	$s_{O,in}$	Time delay (td)	Steady state error (ss)	Settling time (ts)	Rising time (tr)
1.8	-0.8	-764.6982	0.2	0.01	0.018	22	0.10
1.8	-0.8	-746.7435	0.2	0.01	0.018	22	0.10
1.8	-0.8	-782.6757	0.2	0.01	0.018	22	0.10

1.8	-0.8	-719.7945	0.2	0.01	0.018	22	0.10
1.8	-0.8	-809.6251	0.2	0.01	0.018	22	0.10
1.8	-0.8	-692.8452	0.2	0.01	0.018	22	0.10
1.8	-0.8	-836.5741	0.2	0.01	0.018	22	0.10
2	-0.8	-764.7096	0.2	0.01	0.03	22	0.10
2	-0.8	-746.7435	0.2	0.01	0.03	30	0.10
2	-0.8	-782.6757	0.2	0.01	0.03	26	0.10
2	-0.8	-719.7945	0.2	0.01	0.03	30	0.10
2	-0.8	-809.6251	0.2	0.01	0.03	26	0.10
2	-0.8	-692.8452	0.2	0.01	0.03	28	0.10
2	-0.8	-836.5741	0.2	0.01	0.03	30	0.10
3	-0.8	-764.7096	0.2	0.01	0.05	50	0.16
3	-0.8	-746.7435	0.2	0.01	0.05	38	0.16
3	-0.8	-782.6757	0.2	0.01	0.058	56	0.16
3	-0.8	-719.7945	0.2	0.01	0.058	38	0.16
3	-0.8	-809.6251	0.2	0.01	0.058	50	0.16
3	-0.8	-692.8452	0.2	0.01	0.05	36	0.16
3	-0.8	-836.5741	0.2	0.01	0.05	60	0.16

7.10 Conclusion

The developed nonlinear controller based on Lyapunov direct method and linear reference model is described in this chapter. The proper selection of the reference model plays an important part in the system design as the plant output follows the desired model output. The simulation results show that the designed nonlinear controller according to the Lyapunov direct method was designed successfully. The designed controller will be implemented in chapter 8 for control of the dissolved oxygen concentration using PLC and SCADA system.

CHAPTER EIGHT

IMPLEMENTATION OF THE NONLINEAR CONTROLLER IN A PROGRAMMABLE LOGIC CONTROLLER (PLC) AS A PART OF THE THREE LAYER CONTROL STRATEGY

8.1 Introduction

Automation of many different processes, such as controlling machines, chemical processes or factory assembly lines, is done through the use of small specialized computers called programmable logic controllers (PLCs). They are designed as computers for the purpose of industrial use. Programmable logic controllers were first introduced in the market to serve the automobile industry. The first programmable logic controller was developed as project for General Motors in 1968 to replace hard-wired relay systems with much more sophisticated electronic controller. From that time till today the PLCs have evolved in terms of hardware and software (Clements-Jewery and Jeffcoat, 1996). PLCs are similar to computers, but the difference is, computers are optimized for calculation and display tasks, as for PLCs they are optimized for control tasks and industrial surroundings (Bolton, 1996).

This chapter introduces programmable logic controllers (PLCs) in section 8.2. Section 8.3 discusses the PLCs hardware. Program scan is given in section 8.4. Section 8.5 introduces how PLCs are being programmed. Modicon M340 PLCs using Unity Pro S V4.0 software is discussed and this PLC is the one that is used for programming purposes in the thesis.

8.2 Programmable Logic Controller (PLC)

PLC is actually a control device that consists of a programmable microprocessor which is able to store instructions and implement functions such as logic, sequencing, timing, counting and arithmetic in order to control processes or machines, and is programmed using a specialized computer language. In the beginning, programmable logic controller would have been programmed in ladder logic, which is similar to schematic of relay logic. A modern programmable logic controller is usually programmed in any one of several languages, ranging from ladder to Visual Basic or C. Typically, the program is written in a development environment on a personal computer (PC), and later downloaded onto the programmable logic controller platform directly through a cable connection. The written program is then stored in the programmable logic controller through a non-volatile memory. PLCs have the following characteristics:

- PLCs are rugged and designed to withstand vibrations, temperature, humidity, and noise.
- They have interfaces for inputs and outputs already inside the controller.
- They are easily programmed and have an easily understood programming language which is primarily concerned with logic and switching operations.

PLC Advantages are:

1. Enhanced Reliability
2. More Flexibility
3. Cost effective for controlling complex systems
4. Answer more rapidly than computers
5. Easier to troubleshoot
6. Remote control capability
7. Communication capability

PLC Disadvantages are:

1. Distinctively to microcontroller systems that have what is called an open architecture, most PLCs manufactures offer only closed architecture for their products.
2. PLC devices are proprietary, which means that parts and software from one manufacturer can't easily be used in partnership with parts of another manufacturer, which limits the design and cost options.

Programmable logic controllers contain a number of variable Input/Output (I/O) ports, and are typically Reduced Instruction Set Computer (RISC) based. They are designed for real-time use, and always must withstand hostile environments on the shop floor. The programmable logic controller circuitry monitors the status of multiple sensor inputs, and controls output actuators, like motors starters, solenoids, lights, displays and valves.

The programmable logic controller has made a very significant contribution to factory automation. In the early days, automation systems were utilising thousands of individual relays and timers. Recently timers and relays within a factory are replaceable by a single programmable logic controller. Presently, programmable logic controllers provide a wide range of functionality, in the company of basic relay, motion control, process control and much more complex networking, as well as being used in Distributed systems as a measure of control. Digital signal gives an on and off signal, which the programmable

logic controller sees as Boolean values. Analog signals may also be employed, from devices such as volume controls, and these signals are seen by the programmable logic controllers as floating point values.

There are many different types of interfaces that are available for operators when they have to interact with the programmable logic controller to configure or to work with it. This may take the form of simple lights, switches, text displays, or for more complex systems, a computer Web interface and a Supervisory Control and Data Acquisition (SCADA) system.

8.3 PLC Hardware

A PLC has the following five basic components:

1. Programming Devices (Personal Computer)
2. Central Processing Unit (CPU)
3. Power Supply
4. Input/Output modules (both Discrete and Analog)

The relationship amongst these components is displayed on Figure 8.1.

8.3.1 Programming Device

This is used to enter the necessary programs into the memory of the processor.

8.3.2 Central Processing Unit (CPU)

The CPU is the element enclosing the microprocessor. It reads the input signals and brings out the control actions, according to the program stored in its memory, and communicates the results as action signal to the outputs.

8.3.3 Power Supply

It is the unit that is required to convert the mains A.C. voltage to low D.C voltage of about 5V needed for the processor and the circuits in the input and output interface modules.

8.3.4 Input/Output Modules

Input and output (I/O) modules work as an interface between the processor and the devices attached to the PLC and they enable the PLC to both sense and control the process (NIIT, 2005). Input interface modules accept signals from the machine or process devices and convert them into signals that can be used by the controller, meaning that the input interface allows status information regarding the processes to be communicated to the CPU. Output interface modules convert controller signals that can be used to control the machine or the process, which allows the CPU to communicate operating signals to the process devices under its control.

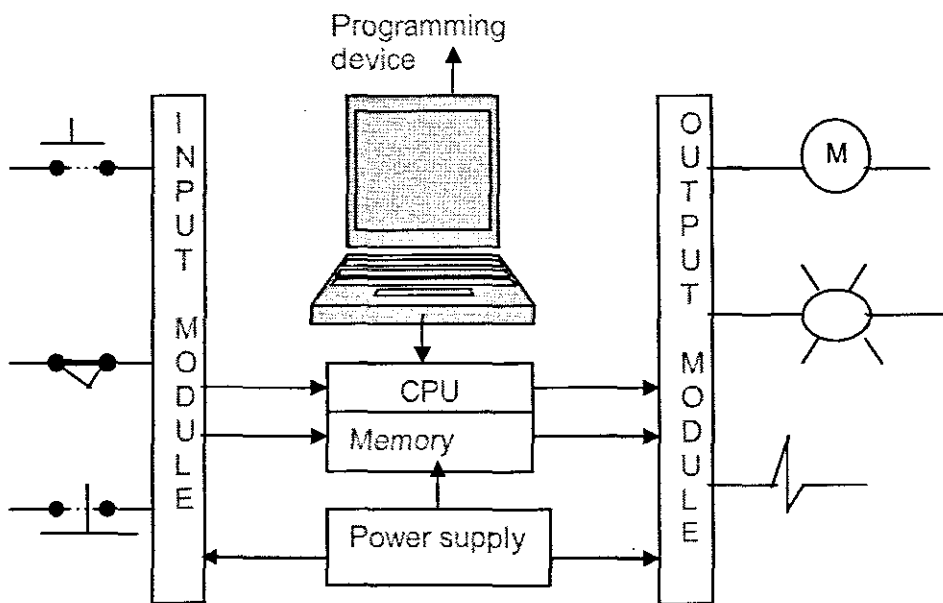


Figure 8.1: Block diagram of the standard components of PLC (NIIT,2005)

8.3.4.1 Discrete Input Module

Discrete input modules accept and recognize only two states of the device, which are digital or ON/OFF type signals. The input module transforms each input into a logic voltage level. An open contact is transformed into a logic 0 voltage and closed contact into logic 1 voltage.

8.3.4.2 Discrete Output Module

Discrete output modules operate on digital or ON/OFF signals and control the current flow of real-world devices or processes, such as lamps, motor starter coils, control relay and solenoids.

8.3.4.3 Analog Input Module

Analog input modules use analog signals to influence data and translate it into digital signals with a digital converter.

8.3.4.4 Analog Output Module

Analog output modules collect data in digital form and convert it into voltage or current to control the analog apparatus. The binary number is converted into analog voltage or current by the digital-to-analog (D/A) converter.

8.4 Program Scan

As soon as the PLC is powered ON, the processor does an internal audit check to ensure that each part is functional. Following this, the processor starts the program scan. A watchdog timer is used by the processor to check correct completion of a program in the allotted time and perform internal testing. It is reset on each program scan. If an error in the program causes the scan ceases before completion, the watchdog timer times out. Presented below is the program scan process.

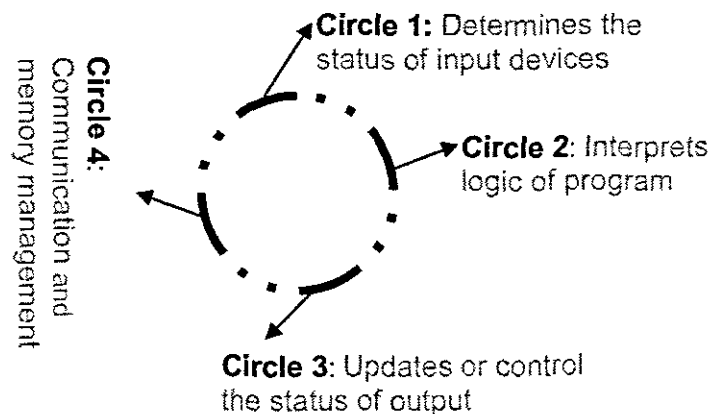


Figure 8.2: Program's scan process Diagram.

The process scan above is illustrated in four-steps

8.3.4.2 Discrete Output Module

Discrete output modules operate on digital or ON/OFF signals and control the current flow of real-world devices or processes, such as lamps, motor starter coils, control relay and solenoids.

8.3.4.3 Analog Input Module

Analog input modules use analog signals to influence data and translate it into digital signals with a digital converter.

8.3.4.4 Analog Output Module

Analog output modules collect data in digital form and convert it into voltage or current to control the analog apparatus. The binary number is converted into analog voltage or current by the digital-to-analog (D/A) converter.

8.4 Program Scan

As soon as the PLC is powered ON, the processor does an internal audit check to ensure that each part is functional. Following this, the processor starts the program scan. A watchdog timer is used by the processor to check correct completion of a program in the allotted time and perform internal testing. It is reset on each program scan. If an error in the program causes the scan ceases before completion, the watchdog timer times out. Presented below is the program scan process.

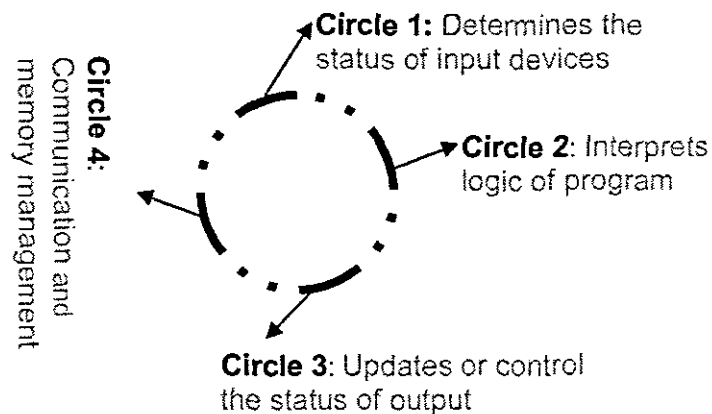


Figure 8.2: Program's scan process Diagram.

The process scan above is illustrated in four-steps

8.3.4.2 Discrete Output Module

Discrete output modules operate on digital or ON/OFF signals and control the current flow of real-world devices or processes, such as lamps, motor starter coils, control relay and solenoids.

8.3.4.3 Analog Input Module

Analog input modules use analog signals to influence data and translate it into digital signals with a digital converter.

8.3.4.4 Analog Output Module

Analog output modules collect data in digital form and convert it into voltage or current to control the analog apparatus. The binary number is converted into analog voltage or current by the digital-to-analog (D/A) converter.

8.4 Program Scan

As soon as the PLC is powered ON, the processor does an internal audit check to ensure that each part is functional. Following this, the processor starts the program scan. A watchdog timer is used by the processor to check correct completion of a program in the allotted time and perform internal testing. It is reset on each program scan. If an error in the program causes the scan ceases before completion, the watchdog timer times out. Presented below is the program scan process.

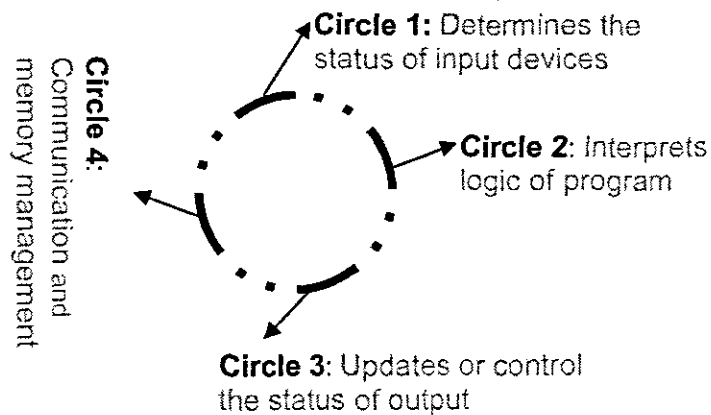


Figure 8.2: Program's scan process Diagram.

The process scan above is illustrated in four-steps

1. Provides status monitoring of the input devices
2. Interprets the logic of the ladder program, which is stored in the memory
3. Monitors the output status of devices
4. Communicates with the other attached devices and participate in memory management.

8.5 Programming of PLCs

In the beginning PLCs were being programmed using a method that was based on relay logic wiring schematics. The reason for this was to eliminate the need to teach Electricians, Technicians and Engineers how to program a computer, but to great surprise it is still the method that is commonly used for programming PLCs till today.

There are two types of programming languages in the computer world, machine language and programming language. Machine language programs are thoroughly understood and well executed by the computer and programs written in the programming languages characterize the operation of the software. Machine language is made up of 0s and 1s, also called bits and bytes. Programs written in programming languages such as Visual Basic, C, C++ or Java, are written in plain English Language, which is the language that a programmer can understand and be able to write programs with greater ease than using 0s and 1s of the machine language.

Parallel to computer languages, PLCs programming as well uses two types of languages:

1. Machine language is written using 0s and 1s, which normally symbolizes OFF and ON status of circuits inside a PLC.
2. Ladder Logic language which encompasses input and output symbols. It is an advanced graphic-based language and it uses logic gates such as AND, OR, or XOR to specify and control the input and output state of affairs.

8.5.1 Ladder Logic

Ladder logic is the main programming method used for PLCs. Ladder logic has been developed to mimic the relay logic. The decision to use the relay logic diagrams has been a strategic one, as the retraining of engineers, technicians and electricians was greatly reduced by selecting ladder logic as main programming method.

8.5.2 Symbols used in Ladder Logic diagrams

Ladder logic diagrams are used in PLCs to write programming instructions. A ladder logic diagram consists of three basic elements:

1. Input devices
2. Output devices
3. Rung

8.5.3 Input Devices (Contacts)

Contacts are input devices that are similar to normal electrical switches. They have two states, ON and OFF. PLCs offer two types of contacts:

8.5.4 Normally Open Contact

Normally open (NO) contact, which is a contact that does not allow current to follow through it when switched OFF. When the contact is switched ON, the circuit is completed and the current streams through the circuit. Below is the illustration of the normally open contact.

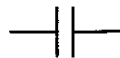


Figure 8.3: Normally Open Contact.

8.5.5 Normally Closed Contact

Normally closed (NC) contact allows the current to pass through it as soon as it is switched OFF. But the situation is different the moment the contact is switched ON; the circuit is broken and current stops following through the circuit. They are normally used for safety measures. Normally closed contact is shown below.



Figure 8.4: Normally Closed Contact.

8.5.6 Output Devices (Coils)

Coils are output devices that are controlled by the PLCs. If the input conditions of the ladder logic yield an ON value, then the coil is set to the ON position and the machine or process performs its designated function. An illustration of an output device is given below.

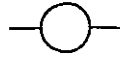


Figure 8.5: Structure of a coil.

8.5.7 Rung

The rung is a horizontal line. It contains both inputs and outputs elements of the ladder logic. Two vertical lines at the two ends of the rungs represent the voltage potential of the ladder logic diagram. The one on the left hand-side is called Live or mains, in terms of D.C voltage it is positive and one on the right is called neutral or negative in terms of D.C voltage. Figure illustrates the rungs of the ladder logic diagram.

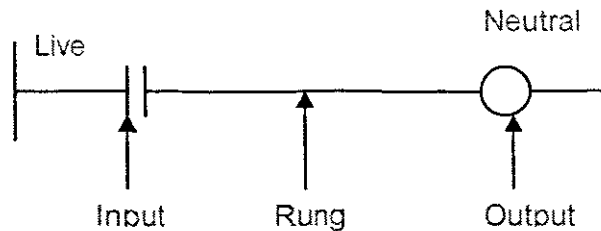


Figure 8.6: Simple ladder logic diagram

Even today modern control systems still consist of relays, but only for logic. A relay is a simple device that employs magnetic field to control a switch. When a voltage is affected to the input coil, then the consequential current generates a magnetic field. The magnetic field hauls a metal switch towards it and the contacts touch, as a result closing the switch. A normally open contact closes when the coil is energized. The normally closed contacts touch when the input coil is not energized.

8.6 Modicon M340 PLC using Unity Pro S V4.0 Software

Modicon M340 PLC is used for this project in conjunction with software called Unity Pro S V4.0 which is a High performance configuration tool for an economical realization of the multitude of tasks involved in drive engineering and automatic control science and technology. Unity Pro S software provides the user with unified configuration environment for effective systems configuration in compliance with all regulations of the international IEC 61131-2 Ed.2 (2003) standard. Modicon M340 automated platform processors manage the entire PLC station, which is made up of discrete I/O (input/output) modules, analogue I/O modules. These are distributed across one or more racks connected on the local bus. Each rack must include a power supply module; the main rack supports the CPU. The following diagram in Figure 8.7 shows a configuration example for the Modicon M340 PLC with one rack:

The Modicon M340 PLC with analog-mixed module AMM-0600 is used with default settings. This PLC is used with four analog inputs and two analog outputs.

The input channels are injected with 1...5V or 4...20mA.

The output channels are injected with 0...mA to 20mA

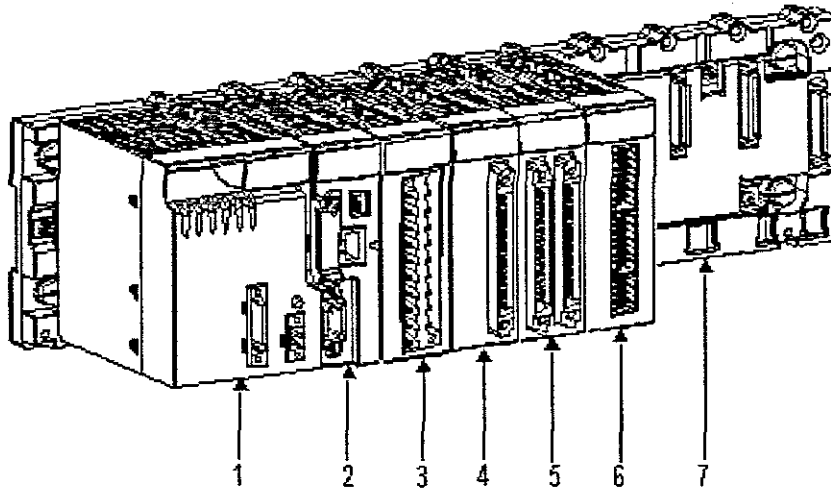


Figure 8.7: A diagram for a configuration example for the Modicon M340 PLC with one rack

Table 8.1 describes the numbered components of the PLC station above.

Table 8.1: Number Table

Number	Description
1	Power supply module
2	Processor
3	20-pin terminal block I/O module

4	40-pin single connector I/O module
5	40-pin 2-connector I/O module
6	Counting module
7	8-slot rack

Note that the four analog input addresses are assigned to the conductivity, pH, DO, and the Turbidity sensors, while the two analog out addresses are allocated to actuators, i.e. Channel 0 is reserved for Proportional valve and Channel 1 is Spare. The output channel 0 and channel 1 fallback are selected to zero

The CPU of this PLC supports Function Block diagram.

Functional equipments are divided into major functional blocks. (Filters, valves, pump, etc.) One block may represent a filtration plant, and another a raw water pump station. Each one of the functional equipment is monitored and controlled by measuring equipment and final actuators.

The signals generated and required by this equipment are wired to a PLC (Modicon M340 PLC with the software called Unity Pro S V4.0), generally one plant PLC for each functional block of the plant. The PLC is wired together to the central SCADA computer by means of a medium-speed data highway. (This can be either copper wire or fibre optic.) The SCADA software which runs in the computer comprises a number of software modules. Basically to the whole system is a database (MySQL). This device stores information; *does not do anything by itself. The data just sit there and wait for other software modules to read what is already in the data base or to overwrite existing data with new values*

The most important is the communication driver module. This module scans the PLC continuously for values of all the input variables and writes them in the appropriate records in the database. The communication driver also scans those records in the databases which are associated with the final actuators

Next, a real control system is connected to the computer via a PLC to test the algorithm on a real physical model. The PLC serves only for I/O as all computations are still being done in the simulation environment--MATLAB/Simulink. MATLAB/Simulink receives a

data from the physical model output and sends the action value to the physical model input.

In the third phase the control algorithm is completely ported into the PLC. Monitoring of the process and parameters configuration may still be done using the connected PC (Adroit) with MATLAB/Simulink.

For development of control algorithms, especially advanced control algorithms such as Nonlinear, predictive, optimal and neural algorithms and etc; it is necessary to start in a simulation environment such as MATLAB.

MATLAB (Matrix Laboratory) is a general, high-performance language for technical computing. It integrates computation, visualization and programming in a common environment. MATLAB is an interactive system and includes a large library of predefined mathematical functions. It also provides the user with the possibility to extend this library with new functions. MATLAB is available for most hardware platforms and is considered to be one of the most fundamental software tools at many technical universities as well as industries all over the world.

In the last step, the control algorithm is transmitted and the real model directly controlled by the PLC. The connection between MATLAB/Simulink and PLC can be used only for real-time monitoring of process inputs, process outputs or other control parameter

8.7 The closed loop system of Waste Water Treatment plant.

The block diagram below Figure 8.8 indicates the industrial standard PLC with PID controller closed loop setup for the wastewater treatment plant.

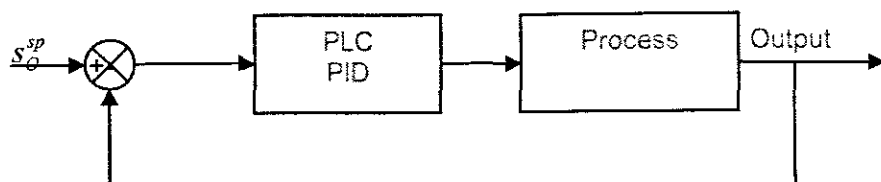


Figure 8.8: The closed loop system of wastewater treatment plant.

In order to overcome this drawback, the developed nonlinear controllers had to be used in order to control the plant. As indicated from the block diagram below; Figure 8.9, the PLC has to communicate with database and Matlab.

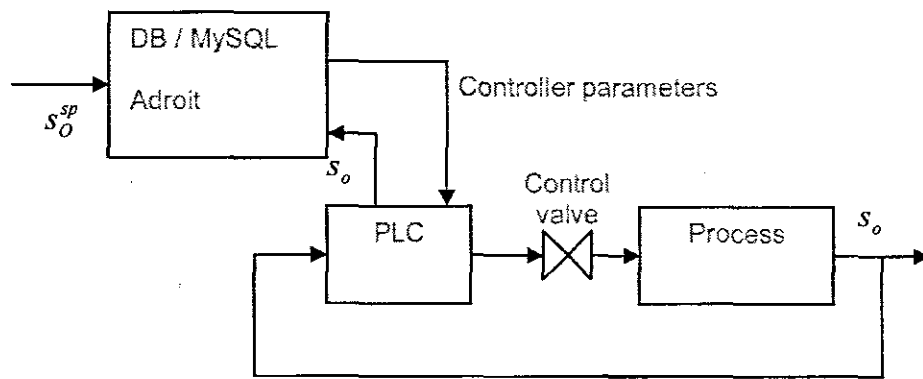


Figure 8.9: The PLC has to communicate with database and Adroit.

This closed loop drawing represents the operational structure of the wastewater treatment plant. There are three main steps in the three layer scheme of repetitive optimization with given calculations

- Receiving the values of the inflow and r_{sO} disturbances from MySQL database in Matlab/Simulink
- Calculation of the updated values of the controller parameters and sending them to MySQL, Adroit and PLC registers for implementation.
- Real-time control performed by PLC

The controller in PLC is to achieve stabilization of the system by comparing the DO raw value with the DO set-point of 2 mg/l. Thus the following steps of interfacing between real time and simulation can be described as:

Set-point is generated by the optimal control problem and is send to MySQL and from MySQL is send to Matlab for controller design and to PLC for controller implementation.

Capture DO raw value from sensor:

- Send this value to Adroit
- Send value to MySQL

The control action:

- Export the controller parameters to MySQL
- Send parameters values to Adroit
- Send these values to PLC registers

Note: that the diagram below for a visual display of the interfacing structure of the controller and plant, Figure 8.10. It shows the interfacing of the real time with Matlab and Simulink design environment. This diagram displays the interface structure of the Waste water Treatment plant control.

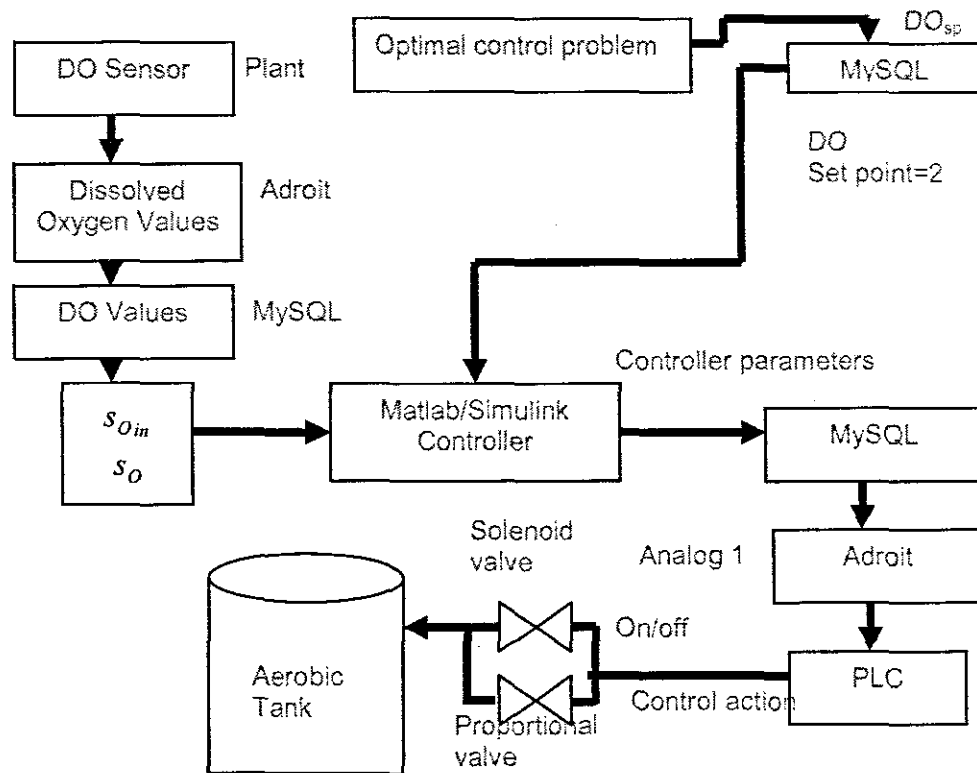


Figure 8.10: The interfacing structure of the controller and plant.

8.8 Process Variables to be measured

Process variables that are measured for this project in order to meet the project requirements are pH, Temperature, DO_2 , Conductivity and Turbidity. Each of them is discussed as follows:

8.8.1 pH

The pH of a sample of water is a measure of the concentration of Hydrogen ions. The term pH was derived from the manner in which the hydrogen ion concentration is calculated; it is the negative logarithm of hydrogen ion (H^+) concentration.

The pH of water determines the solubility (amount that can be dissolved in water) and biological availability (amount that can be utilized by aquatic life) of chemical constituents such as nutrients (phosphorous, nitrogen and carbon) and heavy metals (lead, copper, cadmium). For example in addition to affecting how much and what form of phosphorous is most abundant in the water, pH may also determine whether aquatic life can survive in it.

Photosynthesis uses up dissolved carbon dioxide, which acts like carbonic acid (H_2CO_3) in water. CO_2 removal in fact reduces the acidity of the water and so pH increases. When pollution results in higher algal and plant growth (e.g. from increased temperature or excess of nutrients), pH levels may increase, as allowed by the buffering capacity of the lake. A change in pH may increase the solubility of phosphorous, making it more available for plant growth and resulting in greater long-term demand for dissolved oxygen.

Generally during the summer months in the upper portion of a productive or eutrophic lake, pH will change between 7.5 and 8.5. In the bottom of the lake or in less productive lakes pH will be lower between 6.5 and 7.5. This is the very general statement to provide an example of the differences the user might measure.

8.8.2 Turbidity

Turbidity is a measure of the degree to which light is scattered by suspended particulate material and soluble colour compounds in the water. It provides an estimate of the muddiness or cloudiness of the water due to clay, silt, finely divided organic and inorganic matter, soluble colour organic compounds and microscopic organisms.

8.8.3 Conductivity

Conductivity of liquids is based on the electrolytic dissociation acids, bases or salts in water into electrically charged particles. The magnitude of the electrical conductivity is the reciprocal value of the electric resistance of the solution.

8.8.4 DO

Dissolved oxygen is the amount of oxygen in the effluent. If there is no oxygen or insufficient one, the aquatic animals will die or their growth or production will be affected. The dissolved oxygen should be as high as possible.

8.8.5 Communication

The equipment used for this project must be able to communicate with each other. Ethernet cable is used to interface PLC and PC with Adroit.

8.9 Implementation of the designed controllers in PLC

PLC program that is used to acquire data from sensors, the data acquired from sensors is sent or saved in the holding registers in the PLC to be available in Adroit. The program is written in Function Block diagram logic using blocks for reading of raw data from the sensors. These sensors measure the current status of the waste water to be displayed at Adroit. The Function Block logic, allows the operator to switch the solenoid or proportional valve from Adroit window and run the program which is developed in the PLC. The operator can also make changes of the threshold any time as possible. Figure 8.11 below is a PLC bus for which the PLC modules in the form of processor, digital input, digital output and analog mixed enabling the user to make the settings according to the different needs of the project.

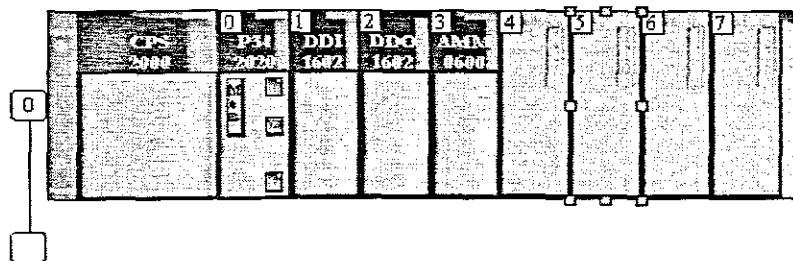


Figure 8.11: PLC bus

8.9.1 PLC program for input and output data

PLC program for input and output of data is written in such a manner that it enables communication between software and hardware environments. The module that is used for implementation is analog mixed card, where Analog Input Channel 0 receives turbidity raw value from the turbidity sensor; analog input channel 1 receives DO raw value from

DO sensor, input channel 2 receives conductivity raw value from the conductivity sensor, analog input channel 3 receives pH raw value, analog output channel 0 receives control action from the PLC to the proportional Valve, analog output channel 1 – Spare. The program is the same for both linearizing and nonlinear Lyapunov reference based model controllers.

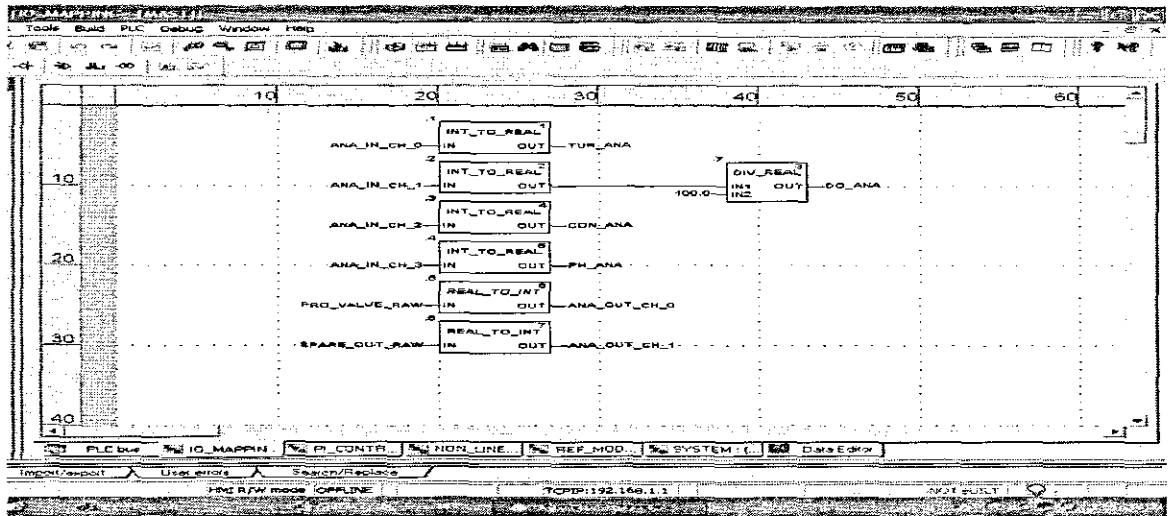


Figure 8.12: I/O Mapping diagram for the input sensors and output actuators

8.9.1.1 PLC program for implementation of PI controller

PI controller is designed for controlling the linearized closed loop system. It is developed for both linearizing and nonlinear Lyapunov reference based model controllers.

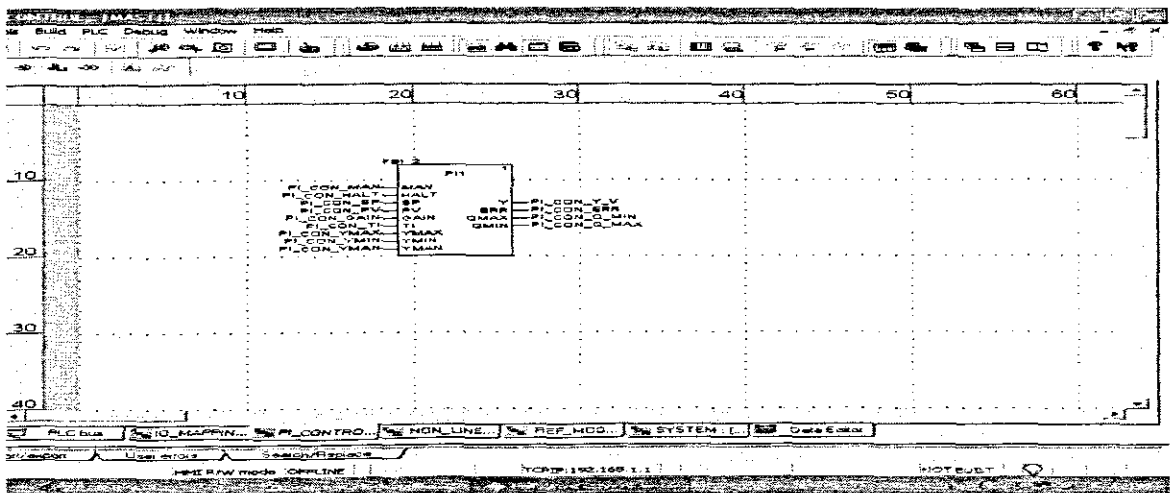


Figure 8.13: PI Controller diagram

8.9.1.2 PLC program implementation of the linearizing controller

The linearizing controller program in PLC is implemented according to diagram Figure 8.14. The diagram is similar to the controller designed in chapter 6.

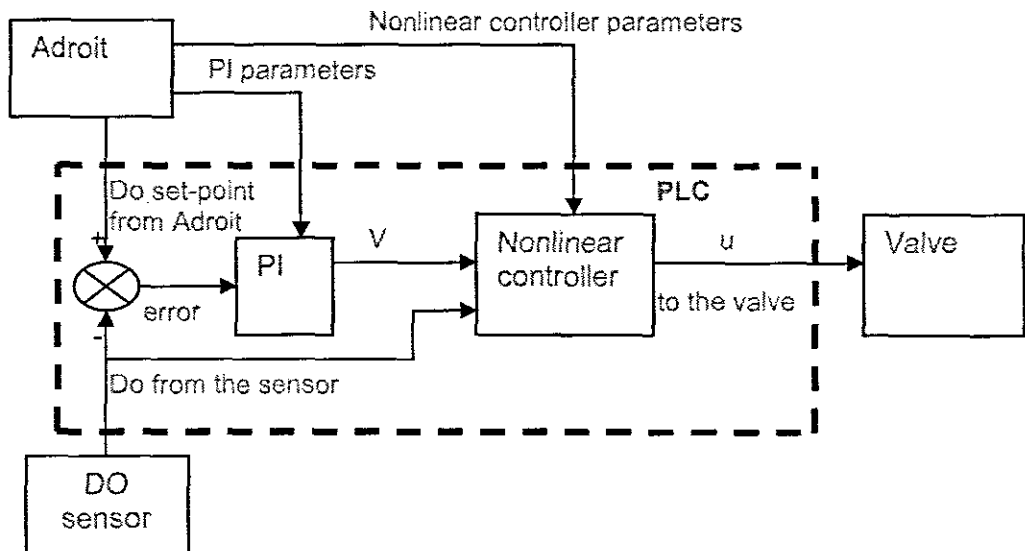


Figure 8.14: Linearizing controller structure for PLC implementation

In order to achieve full control of the process the following different programs in PLC are developed:

- Receiving set-point from MySQL and Adroit
- Receive DO measurements from the DO sensor
- Forming of error in PLC
- Implementation of PI controller
- Implementation of the reference model (Only applicable for Lyapunov based controller)
- Forming the error between reference model output and the measured DO (only applicable for Lyapunov based controller)
- Implementation of the nonlinear controller

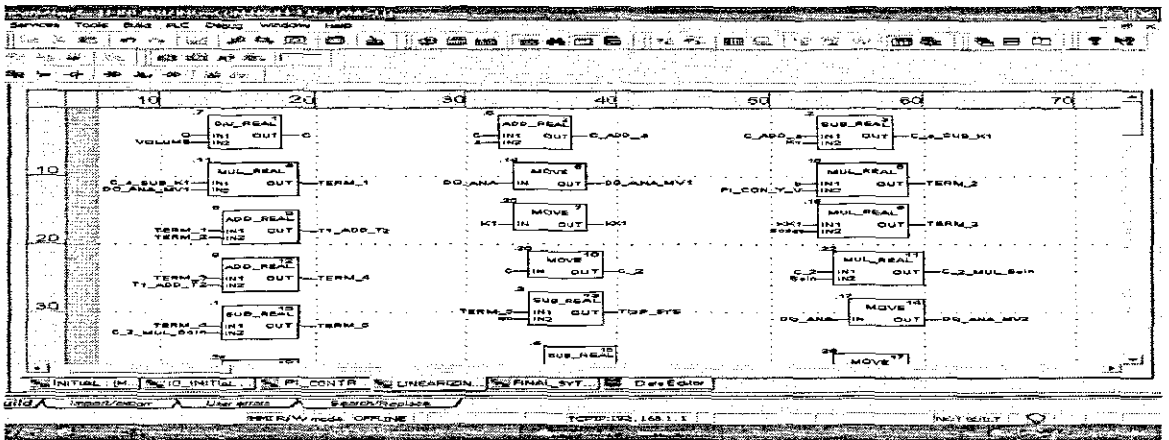


Figure 8.15A: Linearizing controller diagram

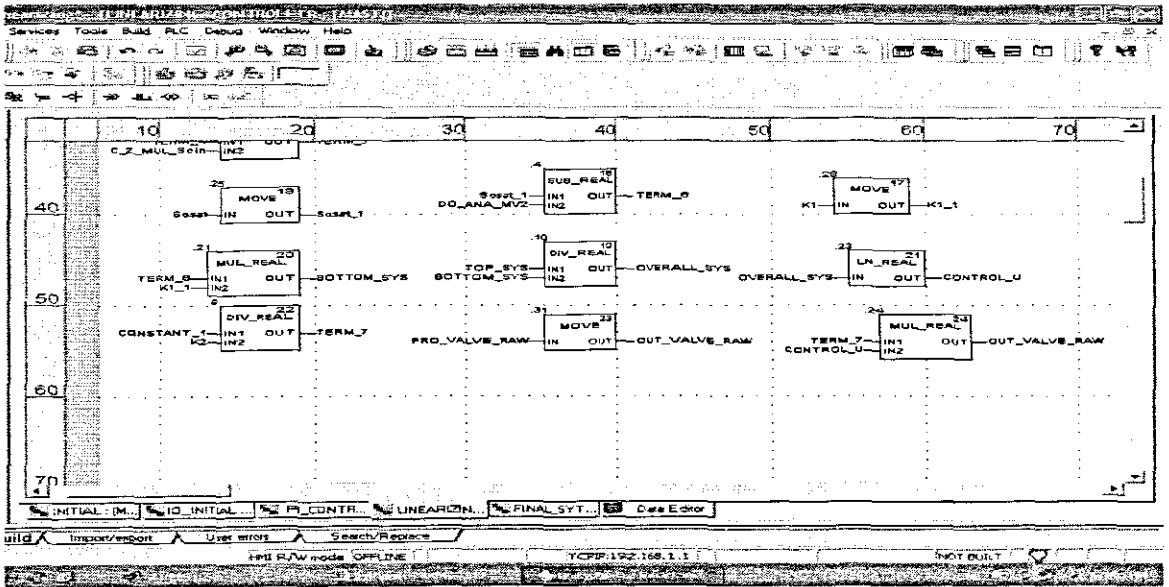


Figure 8.15B: Linearizing controller diagram-continuation

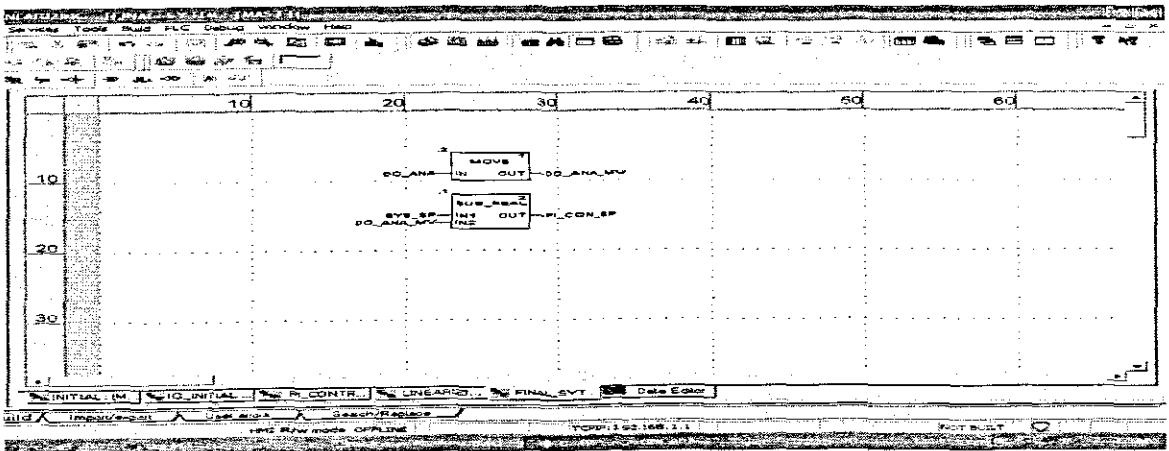


Figure 8.16: Error calculation structure

8.9.2 PLC program for implementation of the nonlinear Lyapunov reference based model controller

The nonlinear Lyapunov reference based model controller program in PLC is implemented according to diagram Figure 8.17. The diagram is similar to the controller designed in chapter 7.

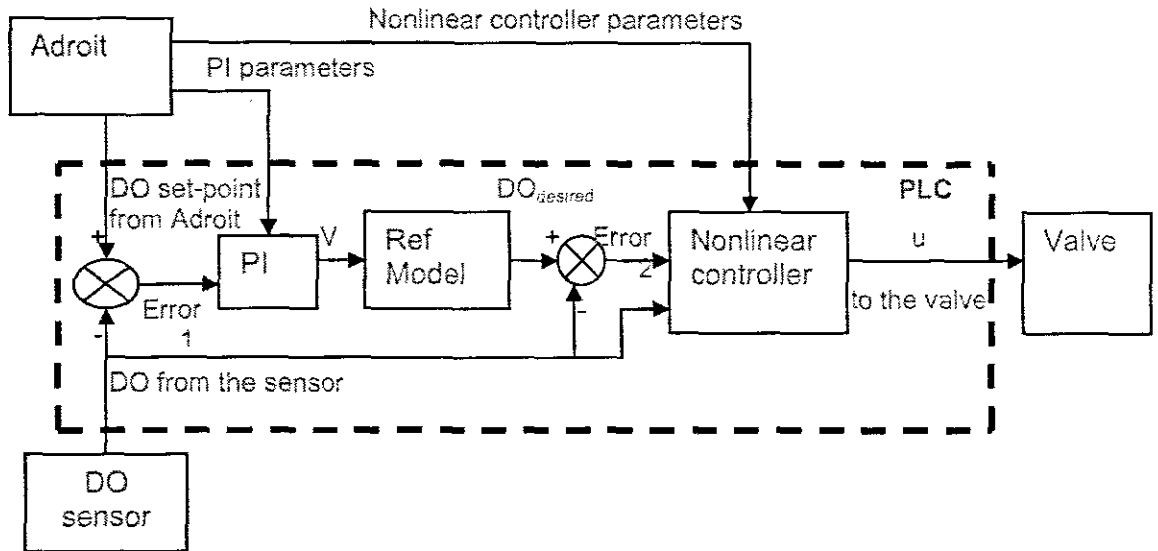


Figure 8.17: Nonlinear Lyapunov reference based controller structure for PLC implementation

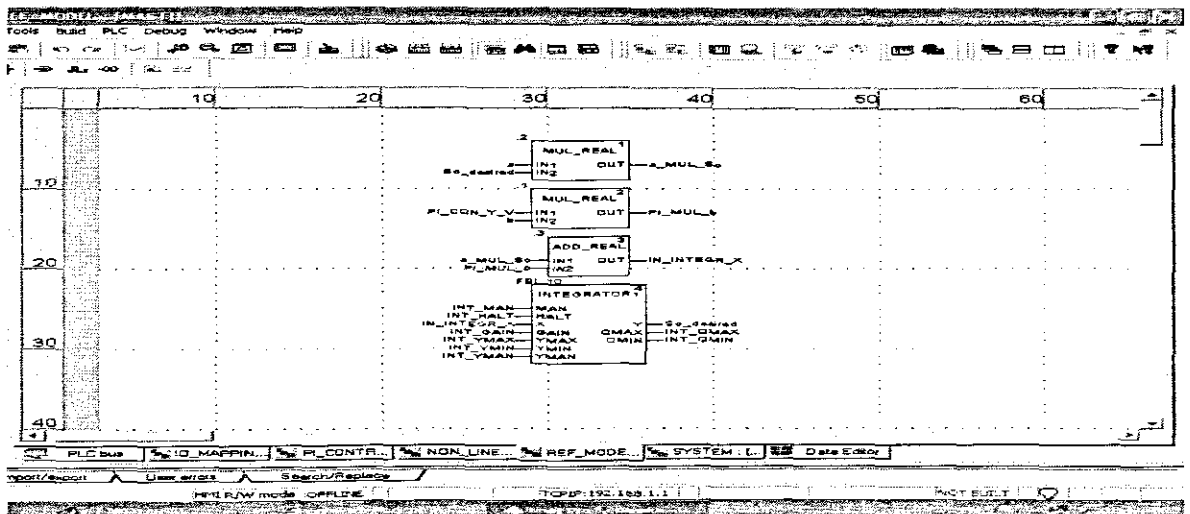


Figure 8.18: Reference model diagram

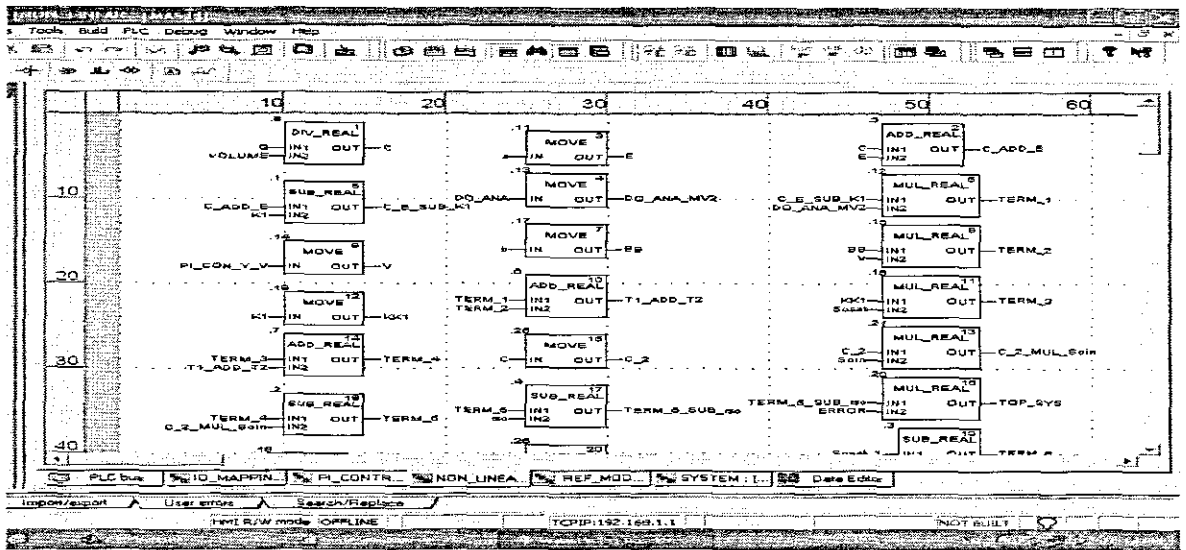


Figure 8.19A: Nonlinear controller

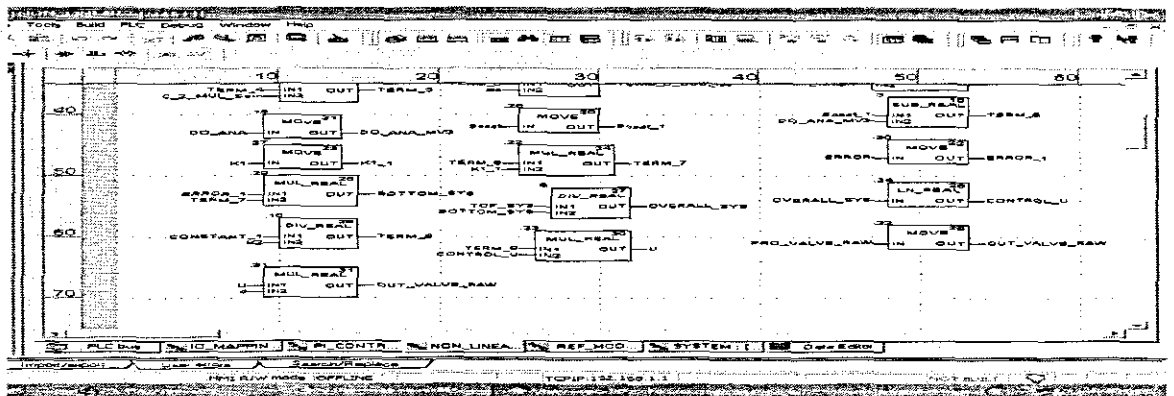


Figure 8.19B: Nonlinear controller-continuation

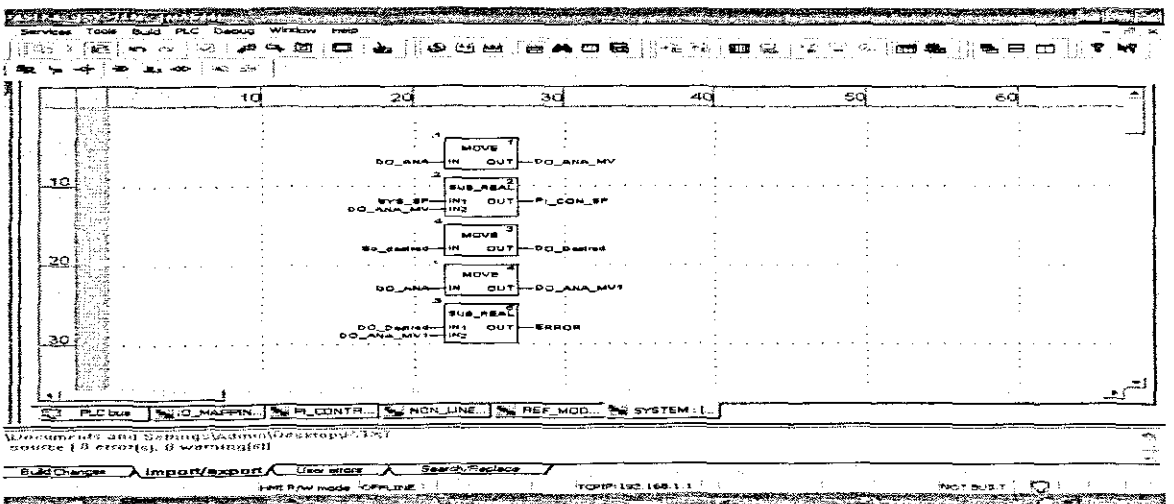


Figure 8.20: Calculations of errors in the nonlinear controller structure

8.9.3 Definition of variables in the PLC programs

Table 8.2: Elementary variables for the design of both Nonlinear Linearizing and Nonlinear reference model, Lyapunov based controllers

Variable Name	Address	Data Type	Comment
a	%MW22	REAL	
a_MUL_So	%MW26	REAL	
ANA_IN_CH_0	%IW0.3.0	INT	Analog Input Channel 0 - Turbidity
ANA_IN_CH_1	%IW0.3.1	INT	Analog Input Channel 1 - DO
ANA_IN_CH_2	%IW0.3.2	INT	Analog Input Channel 2 - Conductivity
ANA_IN_CH_3	%IW0.3.3	INT	Analog Input Channel 3 - PH
ANA_OUT_CH_0	%QW0.3.4	INT	Analog Output Channel 0 - Proportional Valve
ANA_OUT_CH_1	%QW0.3.5	INT	Analog Output Channel 1 - Spare
b	%MW28	REAL	
BB	%MW60	REAL	
BOTTOM_SYS	%MW100	REAL	
C	%MW44	REAL	
C_2	%MW74	REAL	
C_2_MUL_Soin	%MW78	REAL	
C_ADD_E	%MW48	REAL	
C_E_SUB_K1	%MW52	REAL	
CON_ANA	%MW4	REAL	
CONSTANT_1	%MW106	REAL	
CONTROL_U	%MW104	REAL	
d	%MW114	REAL	
DIG_IN_0	%I0.1.0	EBOOL	Spare
DIG_IN_1	%I0.1.1	EBOOL	Spare
DIG_IN_2	%I0.1.2	EBOOL	Spare
DIG_IN_3	%I0.1.3	EBOOL	Spare
DIG_IN_4	%I0.1.4	EBOOL	Spare
DIG_IN_5	%I0.1.5	EBOOL	Spare
DIG_IN_6	%I0.1.6	EBOOL	Spare
DIG_IN_7	%I0.1.7	EBOOL	Spare
DIG_IN_8	%I0.1.8	EBOOL	Spare
DIG_IN_9	%I0.1.9	EBOOL	Spare
DIG_IN_10	%I0.1.10	EBOOL	Spare
DIG_IN_11	%I0.1.11	EBOOL	Spare
DIG_IN_12	%I0.1.12	EBOOL	Spare
DIG_IN_13	%I0.1.13	EBOOL	Spare
DIG_IN_14	%I0.1.14	EBOOL	Spare
DIG_IN_15	%I0.1.15	EBOOL	Spare
DIG_OUT_1	%Q0.2.1	EBOOL	Spare
DIG_OUT_2	%Q0.2.2	EBOOL	Spare
DIG_OUT_3	%Q0.2.3	EBOOL	Spare
DIG_OUT_4	%Q0.2.4	EBOOL	Spare
DIG_OUT_5	%Q0.2.5	EBOOL	Spare
DIG_OUT_6	%Q0.2.6	EBOOL	Spare
DIG_OUT_7	%Q0.2.7	EBOOL	Spare
DIG_OUT_8	%Q0.2.8	EBOOL	Spare
DIG_OUT_9	%Q0.2.9	EBOOL	Spare
DIG_OUT_10	%Q0.2.10	EBOOL	Spare
DIG_OUT_11	%Q0.2.11	EBOOL	Spare
DIG_OUT_12	%Q0.2.12	EBOOL	Spare
DIG_OUT_13	%Q0.2.13	EBOOL	Spare
DIG_OUT_14	%Q0.2.14	EBOOL	Spare
DIG_OUT_15	%Q0.2.15	EBOOL	Spare
DO_ANA	%MW2	REAL	

DO ANA MV	%MW12	REAL	
DO ANA MV1	%MW36	REAL	
DO ANA MV2	%MW54	REAL	
DO ANA MV3	%MW88	REAL	
DO Desired	%MW34	REAL	
E	%MW46	REAL	
ERROR	%MW38	REAL	
ERROR 1	%MW98	REAL	
IN_INTEGR_X	%MW32	REAL	
INT_GAIN		REAL	
INT HALT		BOOL	
INT MAN		BOOL	
INT_QMAX		BOOL	
INT_QMIN		BOOL	
INT_YMAN		REAL	
INT_YMAX		REAL	
INT_YMIN		REAL	
K1	%MW50	REAL	
K1_1	%MW94	REAL	
K2	%MW108	REAL	
KK1	%MW68	REAL	
OUT_VALVE_RAW	%MW116	REAL	
OVERALL_SYS	%MW102	REAL	
PH ANA	%MW6	REAL	PH Meter Raw Value
PI_CON_ERR		REAL	
PI_CON_GAIN		REAL	
PI_CON_HALT		BOOL	
PI_CON_MAN		EBOOL	PI Controller Man/Auto Select
PI_CON_PV		REAL	
PI_CON_Q_MAX		BOOL	
PI_CON_Q_MIN		BOOL	
PI_CON_SP	%MW16	REAL	PI Controller Set point
PI_CON_TI	%MW20	TIME	
PI_CON_YMAN		REAL	
PI_CON_YMAX		REAL	
PI_CON_YMIN		REAL	
PI_MUL_b	%MW30	REAL	
PRO_VALVE_RAW	%MW8	REAL	Proportional Valve Analog Output Raw
Q	%MW40	REAL	
rso	%MW82	REAL	
So desired	%MW24	REAL	
Soin	%MW76	REAL	
Sosat	%MW68	REAL	
Sosat_1	%MW90	REAL	
SPARE_OUT_RAW	%MW10	REAL	Spare Analog Output Raw
SYS_SP	%MW14	REAL	
T1_ADD_T2	%MW64	REAL	
TERM_1	%MW56	REAL	
TERM_2	%MW62	REAL	
TERM_3	%MW70	REAL	
TERM_4	%MW72	REAL	
TERM_5	%MW80	REAL	
TERM_5 SUB_rso	%MW84	REAL	
TERM_6	%MW92	REAL	
TERM_7	%MW96	REAL	
TERM_8	%MW110	REAL	

TOP_SYS	%MW86	REAL	
TUR_ANA	%MW0	REAL	
U	%MW112	REAL	
V	%MW58	REAL	
VOLUME	%MW42	REAL	
PI_CON_YMAX		REAL	

8.10 Conclusion

In this chapter, the general introduction of PLCs is given, Modicon M340 PLC together with Unity Pro S software were used for the development of linearizing and nonlinear Lyapunov reference based model controllers. The process variables for measure are also introduced. The developed nonlinear controllers were successfully implemented in PLC for the control of dissolved oxygen concentration using Adroit SCADA systems and MySQL database. In the next chapter, the project is reviewed and concluded.

CHAPTER NINE

CONCLUSION AND FUTURE DIRECTION OF RESEARCH

9.1 Introduction

The theory of automatic control has been well developed for the decades ever since the establishment of the Nyquist criterion in the 1930s due to World War II. All physical systems are nonlinear in nature, it is possible to describe the operation of a physical system by a linear model, using ordinary linear differential equations to solve a problem where a mode of operation of the physical system does not deviate too much from the nominal set of operating conditions; sometimes this condition is called exact linearization. But at times the linearized model can be deemed inadequate and thus giving an introduction of nonlinear systems theory, hence the need for nonlinear theory. Nonlinear control theory is used for analysis and design of nonlinear control systems.

In this thesis, the problem of modelling, parameter estimation and identification and control of dissolved oxygen (DO) concentration in the aeration tank of the activated sludge process (ASP) of WWTP using nonlinear control theory has been considered.

9.1.1 Aims and objectives

Derived from the problem of the statement, the project aim and objectives were developed and investigated using the methods for design of linear and nonlinear controllers of the concentration of the DO in the aeration tank of the ASP and the implementation of the designed controllers in the frameworks of Modicon PLC, Adroit SCADA, MYSQL database and MATLAB/SIMULINK software. The objectives are as follows:

1. Review of the literature for modelling and control of DO concentration
2. Development of models of the DO concentration with different representations of the oxygen transfer function.
3. Development of method for design of parameter estimation of the DO model coefficients and oxygen uptake rate for different mathematical representations of the oxygen transfer function
4. Development of method for design of a linear controller of the DO concentration based on pole placement theory.
5. Development of method for design of a nonlinear controller of the DO concentration based on Lyapunov stability theory and reference model control theory.

6. Development of method for design of a nonlinear linearizing controller of the DO concentration based on the nonlinear geometrical control theory.
7. Implementation of the controllers in the frameworks of the PLC as a part of the Adroit SCADA system.
8. Development of software for communication between SCADA, MySQL, Matlab and PLC in real time

9.2 Deliverables

In achieving the aim and objectives of the project, the following deliverables were done:

9.2.1 Literature review, analysis and comparison of the models and approaches for control of DO concentration

Literature review of the methods for modelling, estimation and control of the process for dissolving of oxygen in wastewater using automatic control and parameter estimation of dissolved oxygen concentration in wastewater treatment plants is done. Particularly, the activated sludge process modelling and control is considered. A design method, which gives a high performance controller for all operating conditions, is discussed. The design method consists of two parts: estimation part where the oxygen transfer function and oxygen uptake rate (respiration) are determined and a controller design part.

In ensuring the effective control of the process (ASP) by controlling dissolved oxygen concentration, two factors that affect the dynamics of the DO, oxygen uptake rate (respiration) and nonlinear oxygen transfer function were taken into consideration. Review of the methods for application of respiration and of the DO model parameter estimation has been performed.

9.2.2 Review of the theory for design of the nonlinear controller

The type of control that is convenient for nonlinear systems is nonlinear control; two methods were used in designing nonlinear controller according to the theory:

1. Input/Output Linearization
2. Lyapunov theory of stability

Review of the theory of the above two methods was done.

9.2.3 Development of a method for parameter estimation of the nonlinear model of DO with different representations of the oxygen transfer function

The oxygen uptake rate has a very complex nonlinear representation according to the Patterson matrix of ASM1 model. This representation includes different variables of the ASP. Their on-line measurement is not possible because of lack of respective sensors. This means that real-time use of the model of dissolved oxygen (DO) for control purposes is not possible if the oxygen uptake rate is calculated according to Patterson matrix. It is necessary to find some estimated value of the oxygen uptake rate (OUR) on the basis of the available measurements, which are the DO concentration values.

Considered in the thesis are different models of the oxygen transfer function. In order to develop a method and algorithm for this estimation it is necessary to know the values of K_{La} . This value of K_{La} varies according to the wastewater quality and diffusers clogging. It shows the efficiency of the aerator system. K_{La} has a typically nonlinear character: as the airflow rate increases, then K_{La} tends to a saturation value characterized by different parameters, which are not known. Their estimation is also necessary to be performed. A least squares method is developed for estimation of the OUR and the oxygen transfer function parameters is developed in the thesis. The considered models are used for design and simulation of the nonlinear closed loop control. Different models of OUR are considered:

1. Oxygen transfer function represented by a time varying parameter
2. Oxygen transfer function represented by a linear function
3. Oxygen transfer function represented by a power function
4. Oxygen transfer function represented by an exponential function
5. Oxygen transfer function represented by a square root function
6. Oxygen transfer function represented by second order polynomial
7. Oxygen transfer function represented by a Monod type model

9.2.4 Development of a method for nonlinear linearizing reference model control of the dissolved oxygen process on the basis of Lyapunov theory

A method for design of nonlinear linearizing reference model control of the DO process on the basis of the second method of Lyapunov is developed. Linear pole placement design of a linear controller for linearized closed loop system is performed. The resulted closed loop system is stable; it has the desired transition behaviour determined by the

selected poles. The linearized by the nonlinear controller closed loop system follows the behaviour of the reference model.

9.2.5 Development of a method for design of a nonlinear linearizing control of dissolved oxygen concentration

A method for design of a nonlinear controller linearizing the closed loop systems based on geometric control theory is developed using reference linear model for the desired behaviour of the closed loop system. A linear PI controller is designed for the purposes of control of the linearized closed loop system. The obtained closed loop system is stable and with desired transition behaviour. The reference model is embedded in the method and does not appear explicitly in the control structure as in the previous method.

9.2.6 Software development

The methods for design described above are examined through simulation implementation using Matlab and Simulink. Separate software programs are developed for every of the deliverables from 9.2.3 till 9.2.5, Appendix A-D. The developed software for different simulations is grouped in Tables 9.1 and 9.2 respectively.

Table 9.1: Programs used for parameter estimation of different models of the oxygen transfer function

Transfer Function	Software	Parameter
Time varying parameter	New_parameter_estimation.m	K1, rso
Linear function	Linear.m	K1, K2 and rso
Power function	Power.m	K1, K2 and rso
Exponential function	Exponential.m	K1, K2 and rso
Square root function	Square root.m	K1, K2 and rso
Second order polynomial	Second order polynomial.m	K1, K2 and rso
Monod type mode	Monod.m	K1, K2 and rso

Table 9.2: Programs used for nonlinear linearizing controllers design and nonlinear controller design and simulation of the closed loop system

Method	Design	Simulation
Lyapunov	Paseka_Nketoane.m	Closed_loop1.mdl
Linearizing	Linearizing_controller.m	Paki.mdl

Table 9.3: Programs for nonlinear controller implementation in the embedded environment of PLC

Method	Design	Subsystems
Lyapunov	Paseka	IO_MAPPING: [MAST]
		PI_CONTROL: [MAST]
		REF_MOD: [MAST]
		NON_LINER: [MAST]
		SYSTEM: [MAST]
Linearizing	Linearizing	IO_MAPPING: [MAST]
		PI_CONTROL: [MAST]
		LINEARIZING_COTROLLER: [MAST]
		FINAL_SYSTEM: [MAST]

9.3 Application of the results

The developed models, controllers and software in the thesis serve the following:

- Better engineering understanding of many of the control process characteristics for the operational personal
- Research base for further investigations of the problem for modelling and control of the dissolved oxygen concentration in WWTP
- Education: operators will have insightful about on-line sensors and other equipment for process monitoring and control. The results also can be used for educational purposes as a learning tool for control engineering students used on a lab-scale plant for demonstration and practical purposes.
- The developed software can provide on-line data to control the process and thus making it easy for prediction purposes.
- The methods and software can be applied to wastewater treatment plants for the municipalities as well for industrial operations to achieve better performance of the controllers as most of the plants are nonlinear in nature.

9.4 Future research

The future research is seen to be useful in the following directions:

- The problem for identifiability of the DO models for different mathematical representations of the oxygen transfer function
- Further research is needed in the field of real-time parameter estimation for the parameters of the oxygen transfer function and of the oxygen uptake rate

- Design of nonlinear controller with not only linearizing capabilities, but bringing optimality to the closed loop system
- Implementation of the embedded in PLC nonlinear controllers in real-time on the place of existing on/off or PID controllers in the Municipality's treatment plants

9.5 Publications

1. Nketoane P., R. Tzoneva (2009). Method for design of Lyapunov nonlinear linearizing reference model based controller for the dissolved oxygen concentration process in the wastewater treatment, submitted to SAIEE Research Journal.
2. Nketoane P., R. Tzoneva (2009). Methods for design of nonlinear input/output linearizing controller for the dissolved oxygen concentration process in the wastewater treatment, submitted to SAIEE Research journal

APPENDIX B

APPENDIX D:MATLAB: Script file-DO_Open_Loop_Parameters

```

%=====
%Parameters for simulation of the Dissolved Oxygen Concentration
%=====
%System Variables
%=====
clear
Sosat=8;           % Dissolved oxygen saturation
K1=240;           % Constant calculated from KLa=240 metres cubed per day
K2=1.0961e-004;  % Constant calculated from KLa=240 metres cubed per day
Soo=0.491;       % Oxygen
V=1333;          % Volume of Tanks 3,4&5
Soin=0.6;        % Internal disturbance
t=0:1:8;
u=50000.0*ones (1,9) %Air flow rate
Qq=55338;        %Internal recycle flow rate
Qr=18446;        % Influent flow rate
Qo=18446;        % Recycle flow rate
Q=Qq+Qr+Qo;
c=Q/V; %=====
%State variables and kinetic values for ASM1
%=====
muA=0.5;         %the maximum autotrophic growth rate
muH=4;           %the maximum heterotrophic growth rate
Koh=0.20         %Half-saturation heterotrphic oxygen growth rate
Yh=0.67;        %Heterotrophic yeild
Ya=0.24;        %is the autotrophic yield
Ks=10;          %Half-saturation heterotrphic growth rate
Knh=1.0;        %Half-saturation autotrophic growth rate
Koa =0.4;        %Half-saturation autotrophic oxygen growth rate
Xbhs=3839.166;  %Active heterotrophic biomass
Xbas=74.8985;   %Active autotrophic biomass
Snh=1.733;      %Ammonia and ammonium nitrogen
Sss=0.889;      %Readily biodegradable substrate
Snh=Snh*ones (1,9);
Ss=Sss*ones (1,9);
Xba=Xbas*ones (1,9);
Xbh=Xbhs*ones (1,9);
T=t';
U=u'
Ass=Ss';
Asnh=Snh';
Axba=Xba';
Axbh=Xbh';

```

APPENDIX B

APPENDIX B

THE DEVELOPED MATLAB M-FILES FOR PARAMETER ESTIMATION

The m-files used for design of parameter estimation are presented in Appendix B. The files are for calculation of different expressions of oxygen transfer functions and they are used to estimate parameters K1, K2 and oxygen uptake rate.

B.1: MATLAB script file-New_parameter_estimation.m

```
clc
Sosat=8;
V=1333;
Qq=55338;
Qr=18446;
Qo=18446;
Q=Qq+Qr+Qo;
c=Q/V;
Sosat=8;
dt=0.0104;
K=10;
Soin1=[0.7379 0.2691 0.4228 0.5479 0.9427 0.4177 0.9831 0.3015 0.7011 0.6663]
Soin=0.2*ones(1,K)+Soin1;
SO=2.0*ones(1,K+1)+rand(1,K+1);
%=====
%Calculation of ybar
%=====
for k=1:K
    y(k)=SO(k+1)-SO(k)-dt*c*(Soin(k)-SO(k));
end
ybar=y';
%=====
%Calculation of psibar
%=====
for k=1:K
    j=2*k;
    psibar(k,(j-1):j)=dt*[(Sosat-SO(k)) 1]
end
%=====
%Calculation of THETHA
%=====
thetha=(psibar'*psibar)^(-1)*psibar'*ybar
%=====
%Copying the coefficients trajectories of K1
%=====
for i=1:K;
    j=2*i-1
    K1(i)=thetha(j);
end
%=====
%Copying the coefficients trajectories of rso
%=====
for i=1:K;
    j=2*i
    rso(i)=thetha(j);
```

```

end
k=1:K;
plot(k,K1,'g',k,rso,'r')
title('Coefficients trajectories of rso')
xlabel('time (k)')
ylabel('SO')
hold off
%=====
%Calculate K1, rso estimates
%=====
SOest(1)=SO(1)
for k=1:K-1
SOest=SO(k)-dt*c*(Soin(k)-SO(k))+K1*(Sosat-SO(k))+rso(k);
end
%=====
%calculate error
%=====
for k=1:K
error(K+1)=SO(k)-SOest(k);
end
plot (error)
title('Error Signal')
xlabel('time (k)')
ylabel('SOest')

```

B.2: MATLAB script file-Linear.m

```

Sosat=8;
V=1333;
Qq=55338;
Qr=18446;
Qo=18446;
Q=Qq+Qr+Qo;
c=Q/V;
dt=0.0104;
K=10;
Soin1=[0.7379 0.2691 0.4228 0.5479 0.9427 0.4177 0.9831 0.3015 0.7011 0.6663]
u=5000.0+1000*Soin1
Soin=0.2*ones(1,K)+0.5*Soin1;
SO=2.0*ones(1,K+1)+rand(1,K+1);
%=====
%Calculation of ybar
%=====
for k=1:K
    y(k)=SO(k+1)-SO(k)-dt*c*(Soin(k)-SO(k));
end
ybar=y';
%=====
%Calculation of psibar
%=====
for k=1:K
    j=3*k;
    a1(k)=u(k)*(Sosat-SO(k))
    a2(k)=Sosat-SO(k)
    a3(k)=1
    psibar(k,(j-2):j)=dt*[a1(k) a2(k) a3(k)]
end
%=====
%Calculation of THETHA
%=====
theta=(psibar*psibar)^(-1)*psibar*ybar
%=====
%Copying the coefficients trajectories of K1
%=====
for i=1:K;
    j=3*i-2
    K1(i)=theta(j);
end
%=====
the coefficients trajectories of K2
%=====
for i=1:K;
    j=3*i-1
    K2(i)=theta(j);
end
%=====
the coefficients trajectories of rso
%=====
for i=1:K;
    j=3*i
    rso(i)=theta(j);
end
k=1:K;
plot(k,K1,'blue',k,K2,'red',k,rso,'green')

```

```

title('Coefficients trajectories of rso')
xlabel('time (k)')
ylabel('SO')
hold off
%=====
e K1,K2, rso estimates
%=====SOest(1)=
SO(1)
for k=1:K-1
SOest=SO(k)-dt*c*(Soin(k)-SO(k))+K1*u(k)*(Sosat-SO(k))+K2*(Sosat-SO(k))+rso(k);
end
%=====
e error
%=====
for k=1:K
error(K+1)=SO(k)-SOest(k);
end
plot (error)
title('Error Signal')
xlabel('time (k)')
ylabel('SOest')

```

```

title('Coefficients trajectories of rso')
xlabel('time (k)')
ylabel('SO')
hold off
%===== %Calculat
e K1,K2, rso estimates
%=====SOest(1)=
SO(1)
for k=1:K-1
SOest=SO(k)-dt*c*(Soin(k)-SO(k))+K1*u(k)*(Sosat-SO(k))+K2*(Sosat-SO(k))+rso(k);
end
%===== %Calculat
e error
%=====
for k=1:K
error(K+1)=SO(k)-SOest(k);
end
plot (error)
title('Error Signal')
xlabel('time (k)')
ylabel('SOest')

```

B.3: MATLAB script file-Power.m

```
Sosat=8;
V=1333;
Qq=55338;
Qr=18446;
Qo=18446;
Q=Qq+Qr+Qo;
c=Q/V;
dt=0.0104;
K=10;
Soin1=[0.7379    0.2691    0.4228    0.5479    0.9427    0.4177    0.9831
0.3015    0.7011    0.6663]
u=5000.0+1000*Soin1
Soin=0.2*ones(1,K)+0.5*Soin1;
SO=2.0*ones(1,K+1)+rand(1,K+1);
%=====
%Calculation of ybar
%=====
for k=1:K
    y(k)=SO(k+1)-SO(k)-dt*c*(Soin(k)-SO(k));
end
ybar=y';
%=====
%Calculation of psibar
%=====
for k=1:K
    j=3*k;
a1(k)=Sosat-SO(k)
a2(k)=Sosat-SO(k)
a3(k)=1
    %psibar(k,(j-2):j)=dt*[(Sosat-SO(k)) (Sosat-SO(k)) 1]
psibar(k,(j-2):j)=dt*[a1(k) a2(k) a3(k)]
end
%=====
%Calculation of THETHA
%=====
thetha=(psibar'*psibar)^(-1)*psibar'*ybar
%=====
%Copying the coefficients trajectories of K1
%=====
KK=(3*K)-2
for i=1:K;
j=3*i-2
    thetha1(i)=thetha(j);
end
K1=exp(thetha1)
%=====
%Copying the coefficients trajectories of K2
%=====
KK2=(3*K)-1
for i=1:K;
j=3*i-1
    thetha2(i)=thetha(j);
end
K2=thetha2/log(u)
%=====
%Copying the coefficients trajectories of rso
%=====
KK3=3*K
```

```

for i=1:K;
j=3*i
    rso(i)=thetha(j)
end
k=1:K;
plot(k,K1,k,K2,k,rso)
title('Coefficients trajectories of rso')
xlabel('time (k)')
ylabel('SO')
hold on
%=====
%Calculate K1, rso estimates
%=====
SOest(1)=SO(1)
for k=1:K
SOest=SO(k)-dt*c*(Soin(k)-SO(k))+K1*(Sosat-SO(k))+dt*rso(k);
end
% =====
% Calculate error
% =====
for k=1:K
error(K+1)=SO(k)-SOest(k);
end
hold off
plot (error)
title('Error Signal')
xlabel('time (k)')
ylabel('SOest')

```

B.4: MATLAB script file-Exponential.m

```
Sosat=8;
V=1333;
Qq=55338;
Qr=18446;
Qo=18446;
Q=Qq+Qr+Qo;
c=Q/V;
dt=0.0104;
K=10;
Soin1=[0.7379    0.2691    0.4228    0.5479    0.9427    0.4177    0.9831
0.3015    0.7011    0.6663]
u=5000.0+1000*ones(1,K+1)+rand(1,K+1);
Soin=0.2*ones(1,K)+0.5*Soin1;
SO=2.0*ones(1,K+1)+rand(1,K+1);
%=====
%Calculation of ybar
%=====
for k=1:K
    y(k)=SO(k+1)-SO(k)-dt*c*(Soin(k)-SO(k));
end
ybar=y';
%=====
%Calculation of psibar
%=====
for k=1:K
    j=3*k;
    a1(k)=Sosat-SO(k)
    a2(k)=Sosat-SO(k)
    a3(k)=1
    %psibar(k,(j-2):j)=dt*[(Sosat-SO(k)) (Sosat-SO(k)) 1]
    psibar(k,(j-2):j)=dt*[a1(k) a2(k) a3(k)]
end
%=====
%Calculation of THETHA
%=====
thetha=(psibar'*psibar)^(-1)*psibar'*ybar
%=====
%Copying the coefficients trajectories of K1
%=====
for i=1:K;
    j=3*i-2
    K1(i)=thetha(j);
end
%=====
%Copying the coefficients trajectories of K2
%=====
for i=1:K;
    j=3*i-1
    thetha2(i)=thetha(j);
    K2(i)=(1/u)*log(thetha2/K1)
end
%=====
%Copying the coefficients trajectories of rso
%=====
for i=1:K;
    j=3*i
    rso(i)=thetha(j)
end
```

B.4: MATLAB script file-Exponential.m

```
Sosat=8;
V=1333;
Qq=55338;
Qr=18446;
Qo=18446;
Q=Qq+Qr+Qo;
c=Q/V;
dt=0.0104;
K=10;
Soin1=[0.7379    0.2691    0.4228    0.5479    0.9427    0.4177    0.9831
0.3015    0.7011    0.6663]
u=5000.0+1000*ones(1,K+1)+rand(1,K+1);
Soin=0.2*ones(1,K)+0.5*Soin1;
SO=2.0*ones(1,K+1)+rand(1,K+1);
%=====
%Calculation of ybar
%=====
for k=1:K
    y(k)=SO(k+1)-SO(k)-dt*c*(Soin(k)-SO(k));
end
ybar=y';
%=====
%Calculation of psibar
%=====
for k=1:K
    j=3*k;
    a1(k)=Sosat-SO(k)
    a2(k)=Sosat-SO(k)
    a3(k)=1
    %psibar(k,(j-2):j)=dt*[(Sosat-SO(k)) (Sosat-SO(k)) 1]
    psibar(k,(j-2):j)=dt*[a1(k) a2(k) a3(k)]
end
%=====
%Calculation of THETHA
%=====
thetha=(psibar'*psibar)^(-1)*psibar'*ybar
%=====
%Copying the coefficients trajectories of K1
%=====
for i=1:K;
    j=3*i-2
    K1(i)=thetha(j);
end
%=====
%Copying the coefficients trajectories of K2
%=====
for i=1:K;
    j=3*i-1
    thetha2(i)=thetha(j);
    K2(i)=(1/u)*log(thetha2/K1)
end
%=====
%Copying the coefficients trajectories of rso
%=====
for i=1:K;
    j=3*i
    rso(i)=thetha(j)
end
```

```

k=1:K;
plot(k,K1,k,K2,k,rso)
title('Coefficients trajectories of rso')
xlabel('time (k)')
ylabel('SO')
hold on
%=====
%Calculate K1, rso estimates
%=====
SOest(1)=SO(1)
for k=1:K
SOest=SO(k)-dt*c*(Soin(k)-SO(k))+K1*(Sosat-SO(k))+dt*rso(k);
end
% =====
% Calculate error
% =====
for k=1:K
error(K+1)=SO(k)-SOest(k);
end
hold off
plot (error)
title('Error Signal')
xlabel('time (k)')
ylabel('SOest')

```

B.5: MATLAB script file-Square root.m

```
Sosat=8;
V=1333;
Qq=55338;
Qr=18446;
Qo=18446;
Q=Qq+Qr+Qo;
c=Q/V;
dt=0.0104;
K=10;
Soin1=[0.7379    0.2691    0.4228    0.5479    0.9427    0.4177    0.9831
0.3015    0.7011    0.6663]
u=5000.0+1000*Soin1
Soin=0.2*ones(1,K)+0.5*Soin1;
SO=2.0*ones(1,K+1)+rand(1,K+1);
%=====
%Calculation of ybar
%=====
for k=1:K
    y(k)=SO(k+1)-SO(k)-dt*c*(Soin(k)-SO(k));
end
ybar=y';
%=====
%Calculation of psibar
%=====
for k=1:K
    j=2*k;
    a1(k)=sqr(u(k))*(Sosat-SO(k))
    a2(k)=1
    %psibar(k,(j-1):j)=dt*[u(k)*(Sosat-SO(k)) (Sosat-SO(k)) 1]
    psibar(k,(j-1):j)=dt*[a1(k) a2(k)]
end
%=====
%Calculation of THETHA
%=====
theta=(psibar'*psibar)^(-1)*psibar'*ybar
%=====
%Copying the coefficients trajectories of K1
%=====
for i=1:K;
    j=2*i-2
    K1(i)=theta(j);
end
%=====
%Copying the coefficients trajectories of K2
%=====
for i=1:K;
    j=3*i-1
    K2(i)=theta(j);
end
%=====
%Copying the coefficients trajectories of rso
%=====
for i=1:K;
    j=3*i
    rso(i)=theta(j);
end
k=1:K;
plot(k,K1,k,K2,k,rso)
```

```
title('Coefficients trajectories of rso')
xlabel('time (k)')
ylabel('SO')
hold on
% =====
% Calculate error
% =====
for k=1:K
error(K+1)=SO(k)-SOest(k);
end
hold off
plot (error)
title('Error Signal')
xlabel('time (k)')
ylabel('SOest')
```

```

k=1:K;
plot(k,K1,k,K2,k,rso)
title('Coefficients trajectories of rso')
xlabel('time (k)')
ylabel('SO')
hold on
% =====
% Calculate error
% =====
for k=1:K
error(K+1)=SO(k)-SOest(k);
end
hold off
plot (error)
title('Error Signal')
xlabel('time (k)')
ylabel('SOest')

```

B.7: MATLAB script file-Monod.m

```

Sosat=8;
V=1333;
Qq=55338;
Qr=18446;
Qo=18446;
Q=Qq+Qr+Qo;
c=Q/V;
dt=0.0104;
K=10;
Soin1=[0.7379    0.2691    0.4228    0.5479    0.9427    0.4177    0.9831
0.3015    0.7011    0.6663]
u=5000.0+1000*Soin1
Soin=0.2*ones(1,K)+0.5*Soin1;
SO=2.0*ones(1,K+1)+rand(1,K+1);
%=====
%Calculation of ybar
%=====
for k=1:K
    y(k)=SO(k+1)-SO(k)-dt*c*(Soin(k)-SO(k));
end
ybar=y';
%=====
%Calculation of psibar
%=====
for k=1:K
    j=3*k;
a1(k)=Sosat-SO(k)
a2(k)=- (Sosat-SO(k))
a3(k)=1
    %psibar(k, (j-2):j)=dt*[(Sosat-SO(k)) -(Sosat-SO(k)) 1]
psibar(k, (j-2):j)=dt*[a1(k) a2(k) a3(k)]
end
%=====
%Calculation of THETHA
%=====
theta=(psibar'*psibar)^(-1)*psibar'*ybar
%=====
%Copying the coefficients trajectories of K1
%=====
for i=1:K;
j=3*i-2
    K1(i)=theta(j);
end
%=====
%Copying the coefficients trajectories of K2
%=====
for i=1:K;
j=3*i-1
    theta2(i)=theta(j);
K2(i)=(1/u(i))*log(theta2(i)/K1(i));
end
%=====
%Copying the coefficients trajectories of rso
%=====
for i=1:K;
j=3*i
    rso(i)=theta(j);
end

```

```

k=1:K;
plot(k,K1,k,K2,k,rso)
title('Coefficients trajectories of rso')
xlabel('time (k)')
ylabel('SO')
hold on
% =====
% Calculate error
% =====
for k=1:K
error(K+1)=SO(k)-SOest(k);
end
hold off
plot (error)
title('Error Signal')
xlabel('time (k)')
ylabel('SOest')

```

APPENDIX C

APPENDIX C: MATLAB: Script file-Linearizing_Controller.m

```

%=====
%Parameters for Closed control of the linearizing controller
%Dissolved Oxygen Concentration
%=====
%System Variables
%=====
clear
Sosat=8           %Dissolved oxygen saturation
K1=240;          %Constant calculated from KLa=240 metres cubed per day
K2=1.0961e-004; %Constant calculated from KLa=240 metres cubed per day
Soo=0.491;       %Oxygen
V=1333;          %Volume of Tanks 3,4&5
Soin=0.6;        %Internal disturbance
t=0:1:8;
Qq=55338;        %Internal recycle flow rate
Qr=18446;        %Influent flow rate
Qo=18446;        %Recycle flow rate
Q=Qq+Qr+Qo;
c=Q/V;
a=-0.8;
b=15000;
%=====
%State variables and kinetic values for ASM1
%=====muA=0.5;
           %the maximum autotrophic growth rate
muH=4;      %the maximum heterotrophic growth rate
Koh=0.20;   %Half-saturation heterotrphic oxygen growth rate
Yh=0.67;    %Heterotrophic yeild
Ya=0.24;    %is the autotrophic yield
Ks=10;      %Half-saturation heterotrphic growth rate
Knh=1.0;    %Half-saturation autotrophic growth rate
Koa =0.4;   %Half-saturation autotrophic oxygen growth rate
Xbhs=2559.444; %Active heterotrophic biomass
Xbas=149.797; %Active autotrophic biomass
Snhs=1.733; %Ammonia and ammonium nitrogen
Sss=0.889; %Readily biodegradable substrate
Snh=Snh*ones(1,9);
Ss=Sss*ones(1,9);
Xba=Xbas*ones(1,9);
Xbh=Xbhs*ones(1,9);
T=t;
Ass=Ss';
Asnh=Snh';
Axba=Xba';
Axbh=Xbh';

%=====
%Calculation of the oxygen uptake rate
%=====
rso=-muH*((1-Yh)/Yh)*(Ss/(Ks+Ss))*(Soo/(Koh+Soo))*Xbhs-muA*((4.57-
Ya)/Ya)*(Snhs/(Knh+Snhs))*(Soo/(Koa+Soo))*Xbas
rso1=rso*ones(1,9);
rso2=rso1';
%=====

```

%PI Controller Parameters

%=====

$$Ti=b*(4+a)/6$$

$$Kp=4+a$$

$$P=Kp;$$

$$I=P/Ti$$

APPENDIX D

APPENDIX D:MATLAB: Script file-Parameters_Nketoane.m

```
%=====
%Parameters for Closed control of the Nonlinear linearizing controller
%Dissolved Oxygen Concentration
%=====
%System Variables
%=====
clear
Sosat=8;           %Dissolved oxygen saturation
K1=240;           %Constant calculated from KLa=240 metres cubed per day
K2=1.0961e-004;  %Constant calculated from KLa=240 metres cubed per day
Soo=0.491;       %Oxygen
V=1333;          %Volume of Tanks 3,4&5
Soin=0.6;        %Internal disturbance
t=0:1:8;
Qq=55338;        %Internal recycle flow rate
Qr=18446;        %Influent flow rate
Qo=18446;        %Recycle flow rate
Q=Qq+Qr+Qo;
c=Q/V;
a=-0.8;
b=15000;
d=1;
%=====
%State variables and kinetic values for ASM1
%=====
muA=0.5          %the maximum autotrophic growth rate
muH=4;          %the maximum heterotrophic growth rate
Koh=0.20;       %Half-saturation heterotrphic oxygen growth rate
Yh=0.67;        %Heterotrophic yeild
Ya=0.24;        %is the autotrophic yield
Ks=10;          %Half-saturation heterotrphic growth rate
Knh=1.0;        %Half-saturation autotrophic growth rate
Koa =0.4;       %Half-saturation autotrophic oxygen growth rate
Xbhs=2559.444;  %Active heterotrophic biomass
Xbas=149.797;   %Active autotrophic biomass
Snhs=1.733;     %Ammonia and ammonium nitrogen
Sss=0.889;     %Readily biodegradable substrate
Snh=Snhs*ones(1,9);
```

```

Ss=Sss*ones(1,9);
Xba=Xbas*ones(1,9);
Xbh=Xbhs*ones(1,9);
T=t';
Ass=Ss';
Asnh=Snh';
Axba=Xba';
Axbh=Xbh';
%=====
%Calculation of the oxygen uptake rate
%=====
rso=-muH*((1-Yh)/Yh)*(Ss/(Ks+Ss))*(Soo/(Koh+Soo))*Xbhs-muA*((4.57-
Ya)/Ya)*(Snhs/(Knh+Snhs))*(Soo/(Koa+Soo))*Xbas
rso1=rso*ones(1,9);
rso2=rso1';
%=====
%PI Controller Parameters
%=====
Ti=b*(4+a)/6
Kp=4+a
P=Kp;
I=P/Ti

```

APPENDIX E

E.1: Modicon M340 PLC description

E1 BMX XBP 0600 rack (6 slots)

There are four sizes of racks, chosen according to the number of modules needed to be used:

- BMX XBP 0400 rack (4 slots)
- BMX XBP 0600 rack (6 slots)
- BMX XBP 0800 rack (8 slots)
- BMX XBP 1200 rack (12 slots)

The list above gives the number of usable slots.

Each rack includes one extra slot that is reserved for the power supply module, and one slot on the right is reserved for the BMX XBE 1000 rack extender module

The following diagram shows the BMX XBP 0600 rack

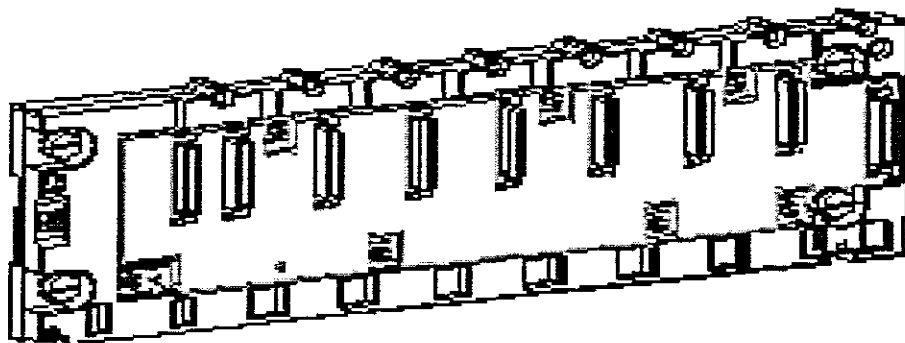


Figure E1.1: BMX XBP 0600 rack diagram

Grounding a Modicon M340 PLC configuration involves the racks and the power supply modules. Protective grounding of the racks must be performed by connecting a ground cable between the protective earth of the installation and the screw located on the left-hand side of the rack, close to the power supply module. This screw is used to connect two cables (1.5 to 2.5 mm² or in AWG size, 16 to 13). Every rack in the PLC station must be grounded.

E1.1 BMX CPS 2000 Power Supply

Each rack requires one power supply module defined according to the distributed network (alternating or direct current) and the power necessary at rack level. Power supply modules are used to supply each rack and its modules. The choice of power

supply module depends on the distributed network (alternating or direct current) and the power required. There are two types of power supply module:

- power supply modules for alternating current networks
- power supply modules for direct current networks

The power supply module is installed in the first two slots of each BMX XBP 0600 rack.

E1.2 Auxiliary Functions of the Power Supply Modules

Each power supply module has the following auxiliary functions:

- display panel
- alarm relay.
- pencil tip push button which causes a reset of the rack when pressed
- 24 VDC sensor supply (only on modules powered by an alternating current network).

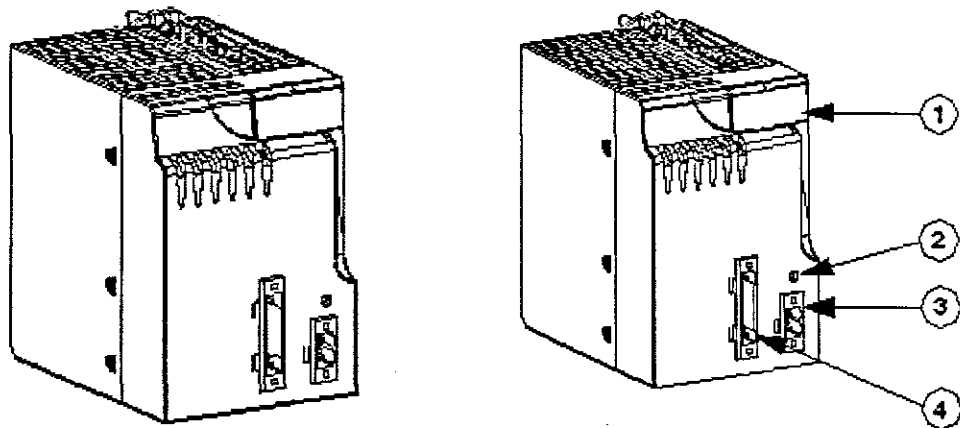


Figure E1.2: The BMX CPS 2000 power supply module and components numbers

E1.3 Sensor Power Supply

The BMX CPS 2000 alternating current power supply modules have a built-in power supply providing a voltage of 24 VDC which is used to supply power to the sensors. The following illustration identifies the various components of a BMX CPS 2000 power supply module

Table E1.1: The following table describes the components of a power supply module.

Number	Function
1	Display panel consisting of: <ul style="list-style-type: none"> • 1 OK LED (green) on if rack power supply module is present and operating correctly • One 24 V LED (green) on when sensor power supply is present. This LED is only to be found on BMX CPS 2000/3500 alternating current power supply modules
2	RESET button

3	Alarm relay connector
4	Connector for the input network (and the 24 VDC sensor power supply for BMX CPS 2000/3500 alternating current power supply modules)

E1.4 Grounding of the Power Supplies

The power supplies are equipped with ground connection contacts. Just like the rack, the Protective Earth (PE) terminal located on the power supply module must be connected to the protective earth of the installation in one of the following two ways: Using a separate cable, independent of the rack ground cable, and directly connected to the protective earth of the installation. Using a cable connecting the ground screw of the rack to the Protective Earth (PE) terminal of the module from the power supply (where the rack is already grounded)

E2 BMX P34 2020 Processor

BMXP34 2020/2030 processors support communication via an Ethernet link. These processors have a built-in communication channel dedicated to Ethernet communication. The BMX P34 2020/2030 processor has only one IP address. 2 rotary switches enable easy selection of the IP address processor.

E2.1 Introduction to the Ethernet Port

The following illustration shows the processor of the RJ45 Ethernet port from the BMX P34 2020

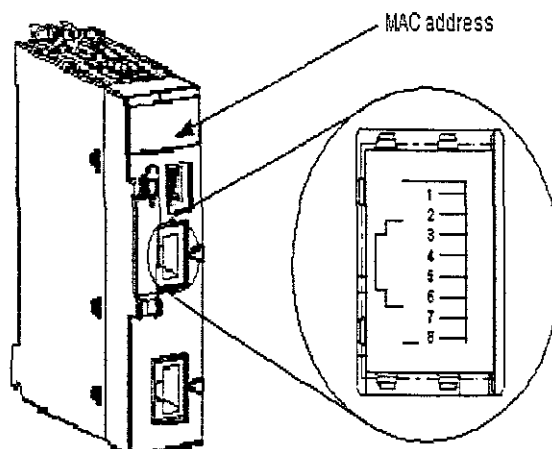


Figure E1.3: BMX P34 2020 diagram showing an RJ45 Ethernet port.

Table E1.2: The following illustration shows the pin assignment of the Ethernet port for the BMX P34 2020/2030 processor:

1	TD+
2	TD-
3	RD+
4	Not connected
5	Not connected
6	RD-
7	Not connected
8	Not connected

The MAC address is located on the front panel of the processor below the processor display panel. The BMX P34 2020/2030 operates as a single node on an Ethernet and possibly other networks. The module must have a unique IP address. The 2 rotary switches on the back of the module provide a simple way to select an IP address

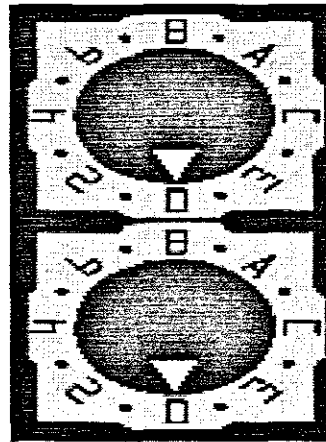


Figure E1.5: MAC diagram for selection an IP address

Ethernet port on a BMX P34 2020 processor is identifiable by a green ring, Figure E.6

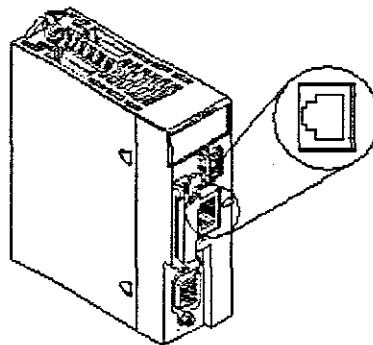


Figure E1.6: Ethernet port on a BMX P34 2020 processor

Ethernet communication essentially targets applications of:

- coordination between PLCs
- local or centralized monitoring
- communication with the production management information system
- communication with remote inputs/outputs

Acting as an agent, Ethernet communication also supports management of the network monitoring standard SNMP. The following illustration shows an Ethernet network

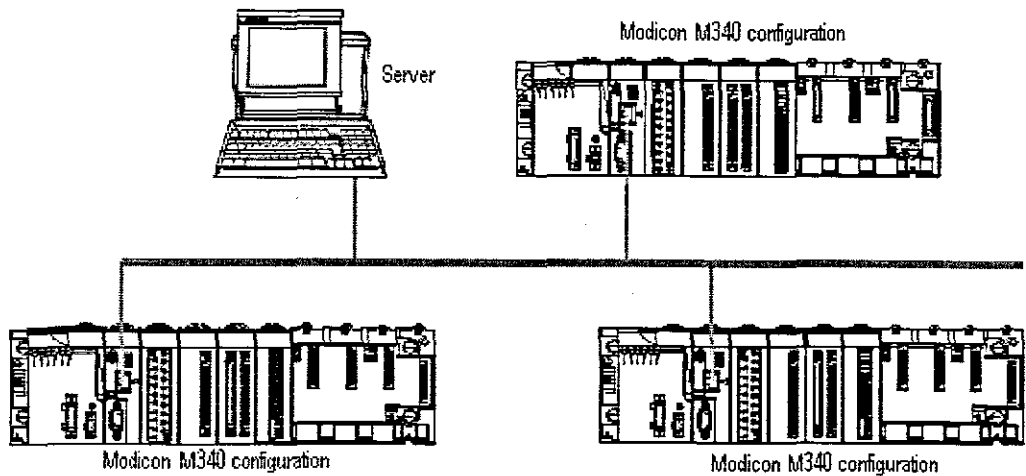


Figure E1.7: Ethernet network diagram

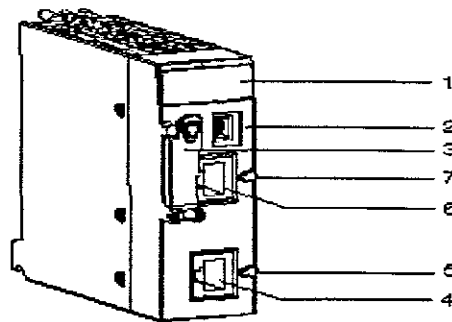


Figure E1.8: The components of a BMX P34 2020 processor diagram

Table E1.3: The following table shows the components of a BMX P34 2020 processor

Number	Function
1	Display panel

2	USB port
3	Memory card protection port
4	Serial port
5	Serial port identification ring (black)
6	Ethernet port
7	Ethernet port identification ring (green)

E2.2 Connecting a Console to a Processor

Two connection cables are available to connect a human-machine interface to the processor USB port

- BMX XCA USB 018, 1.8 m in length
- BMX XCA USB 045, 4.5 m in length

Both of these cables are fitted with a connector at each end:

- Type A USB: connects to the console
- Type mini B USB: connects to the processor

On the type A USB connector side, these cables are fitted with a metallic ground connection to be screwed to a grounded object

On the type mini B USB connector side, these cables are fitted with a:

- Metallic ground connection to be screwed to a grounded object
- Bare section to be fastened to the protection bar with a clamp ring

Note: When using the M340, it is strongly recommended to use a USB 2.0 shielded cable following the USB international standard. The cables BMX XCA USB 018 and BMX XCA USB 045 are designed for this type of use and avoid unexpected behaviour of the PLC. Those cables are shielded and tested against electrical noises.

Display

There are several LEDs available on the front panel of each processor, enabling rapid diagnosis of the PLC status. These LEDs provide information on:

- PLC functioning
- the memory card
- communication with the modules
- serial communication
- communication on the CANopen network

- communication on the Ethernet network

The following diagram shows the diagnostic LEDs on the BMX P34 2020 processor. Note that two displays exist, depending on whether you are using V1 or V2 (or greater) of the processor.

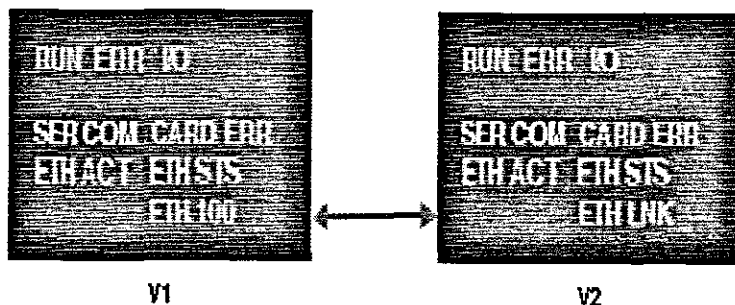


Figure E1.9: The diagnostic diagram of LEDs on the BMX P34 2020 processor

The characteristics of the BMX P34 2020 processor are presented below

Table E1.4: The characteristics of the BMX P34 2020 processor

Characteristics			Available
Functions	Maximum number of channels	Discrete	1024
		Analog rack inputs/outputs	256
		Expert channels	36
		Ethernet channels	3
	Number of embedded connections	USB	1
		Serial modbus link	1
		CANopen master	-
Ethernet		1 (embedded)	
Savable real-time clock		Yes	
Savable Application Data Memory Capacity			256 Kb
Application Structure	MAST task		1
	FAST task		1
	Event processing		64
Application Code Execution Speed	Internal RAM	100% Boolean	8.1 Kins/ms(1)
		65% Boolean + 35% digital	6.4 Kins/ms(1)
Execution Time	One basic Boolean instruction		0.12
	One basic digital instruction		0.17
	One floating point instruction		1.1

E3 Discrete inputs/outputs

The discrete input/output modules are powered by the rack bus. The modules may be installed and uninstalled without turning off power supply to the rack, without causing any hazards and without there being any risk of damage or disturbance to the PLC. The discrete input/output modules of the Modicon M340 range are standard format modules (occupying one single position), fitted with either:

- one 20-pin terminal block or
- one or two 40-pin connectors

For modules fitted with 40-pin connector outputs, a series of products known as TELEFAST 2 is available that enables discrete input/output modules to be quickly connected to operational parts.

Inputs

Inputs receive signals from the sensors and carry out the following functions:

- acquisition
- adaptation
- galvanic insulation
- filtering
- protection against interference

Outputs

Outputs store the orders given by the processor, in order to control pre-actuators via decoupling and amplification circuits

A wide range of discrete input/output modules enables the user to select the module best suited to his/her needs. The characteristics of these modules differ as follows:

Table E1.5: Different characteristics of discrete input/output module

Characteristics	Description
Modularity	<ul style="list-style-type: none">• 8 channels• 16 channels• 32 channels• 64 channels
Type of Inputs	<ul style="list-style-type: none">• Modules with direct current inputs (24 VCC and 48 VCC)• Modules with alternating current inputs (24 VCA, 48 VCA and 120 VCA)
Type of Outputs	<ul style="list-style-type: none">• Modules with relay outputs• Modules with direct current static outputs (24 VCC / 0.1 A - 0.5 A - 3 A)• Modules with alternating current static outputs (24 VCC / 240 VAC / 3 A)

Type of Connector	<ul style="list-style-type: none"> • 20-pin terminal blocks • 40-pin connectors allowing connection to sensors and pre-actuators by means of the TELEFAST 2 pre-wiring system
--------------------------	---

The following illustration shows a discrete input/output module with 40-pin connectors:

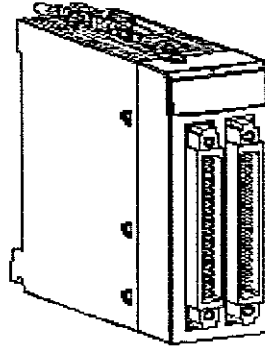


Figure E1.10: A discrete input/output module with 40-pin connectors:

E3.1 BMX DDI 1602 Input Module

It is a 24 VDC discrete module connected via a 20-pin terminal block. It is a positive logic (or sink) module, its 16 input channels receive current from the sensors.

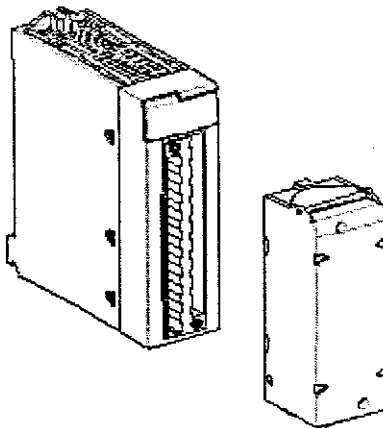


Figure E1.11: 24 VDC discrete module connected via a 20-pin terminal block

The following diagram shows the connection of the module to the sensors

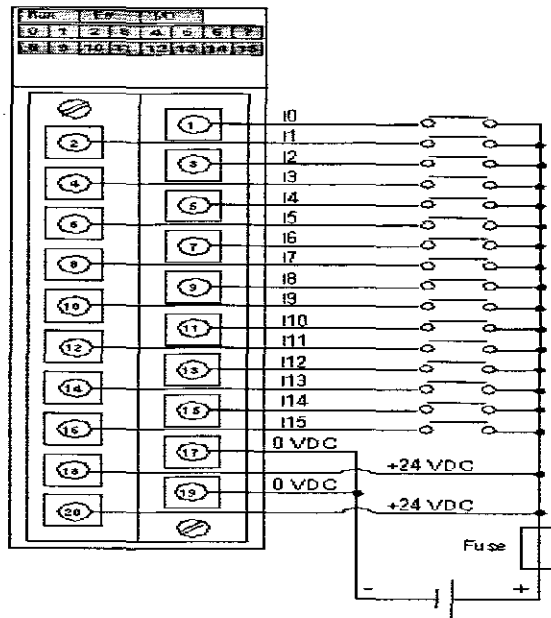


Figure E1.12: Wiring diagram for a 20 pin out for a digital output module

Table E1.6: General Characteristics for the BMX DDI 1602 module

BMX DDI 1602 Module		24V DC positive logic inputs	
Nominal input values		Voltage	24 VDC
		Current	3.5 mA
Threshold input values	at 1	Voltage	≥ 11 V
		Current	> 2 mA (for $U \geq 11$ V)
	at 0	Voltage	5 V
		Current	< 1.5 mA
Sensor supply (including ripple)		19-30V (possible up 34 V, limited 1 hour/day)	
Input impedance	at nominal U	6.8 k Ω	
Response time	typical	4 ms	
	maximum	7 ms	
Reliability	MTBF in hours at ambient $T=30^{\circ}\text{C}$	798 237	
Reverse polarity		Protected	
IEC 1131-2 compliance		Type 3	
2-wire/3-wire proximity sensor compatibility		IEC 947-5-2	
Dielectric strength		1500 V actual, 50/60 Hz for 1 min	
Resistance of insulation		>10 M Ω (below 500 VDC)	
Type of input		Current sink	
Paralleling of inputs (1)		Yes	
Sensor voltage: monitoring threshold	Ok	>18 VDC	
	Error	<14 VDC	
Sensor voltage: monitoring	On appearance	1 ms $< T < 3$ ms	

response time at 24 V (-15%...+20%)	On disappearance	8 ms<T<30 ms
Power consumption 3.3 V	typical	76 mA
	maximum	107 mA
Sensor supply consumption	typical	46 mA
	maximum	73 mA
Power dissipation		2.5 W max
Temperature derating		None

(1) This characteristic is used to connect several inputs to the same module in parallel, or to different modules for input redundancy.

E3.2 BMX DDO 1602 Output Module

The BMX DDO 1602 module is 24 VDC discrete modules connected via 20-pin terminal block. It is a positive logic (or source) module, its 16 output channels provide to the pre-actuators.

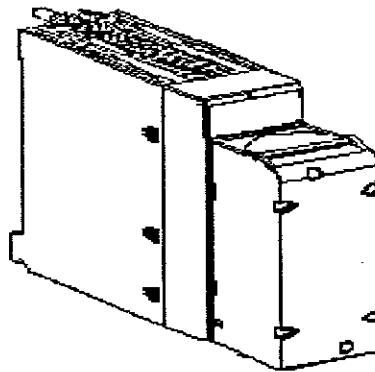


Figure E1.13: 20 pin out digital module diagram

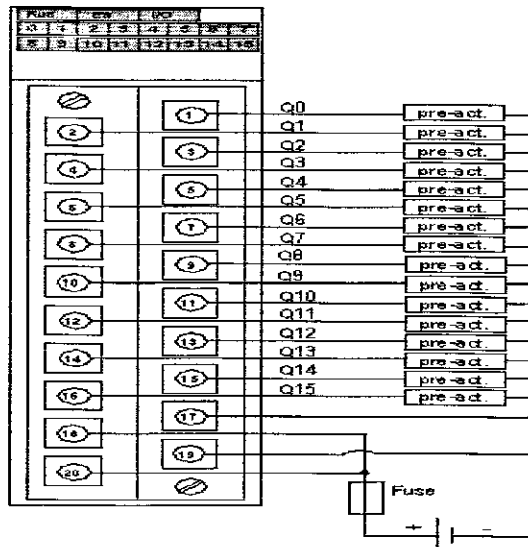


Figure E1.14: Wiring diagram for a 20 pin out for a digital output module

Table E1.7: General characteristics of the BMX DDO 1602 module

BMX DDO 1602 Module		24 VDC positive logic static outputs
Nominal values	Voltage	24 VDC
	Current	0.5 A
Threshold values	Voltage (including ripple)	19...30 V (34 V possible for 1 hour/day)
	Current/channel	0.625 A
	Current/module	10 A
Power of tungsten filament lamp	maximum	6 W
Leakage current	at 0	< 0.5 mA
Voltage drop	at 1	<1.2 V
Load Impedance	minimum	48Ω
Response time (1)		1.2 ms
Reliability	MTBF in hours at $T_{amb,op} = 30^{\circ}\text{C}$	409 413
Frequency of switching to inductive load		0.5/LI ² Hz
Paralleling of outputs		Yes (maximum of 2)
Compatibility with IEC 1131-2 DC direct inputs		Yes (type 3 and not IEC)
Built-in protection	against overvoltage	Yes, by Transil diode
	against inversions	Yes, by inverted diode (2)
	against short-circuits and overloads	Yes, by current limiter and electric circuit-breaker 1.5 In<Id<2 In
Pre-actuator voltage: monitoring threshold	Ok	> 18 V
	Error	< 14 V
Pre-actuator	on appearance	8 ms<T<30 ms

voltage: monitoring response time	on disappearance	1 ms<T<3 ms
Power consumption 3.3 V	typical	79 mA
	maximum	111 mA
24 V pre-actuator consumption	Typical	23 mA
	maximum	32 mA
Power dissipation		4 W max
Dielectric strength	Output/ground or output/internal logic	1500 V actual, 50/60 Hz for 1 min
Resistance insulation		> 10MΩ (below 500 VDC)
Temperature derating		None

E4 Analog inputs/outputs

The analog input/output modules are powered by the rack bus. The modules may be installed and uninstalled without turning off power supply to the rack, without causing any hazards and without there being any risk of damage or disturbance to the PLC. The analog modules may be installed in any of the positions in the rack except for the first two (marked PS and 00) which are reserved for the rack's power supply module and the processor module respectively. Power is supplied by the bus at the bottom of the rack (3.3 V and 24 V).

Table E1.8: The general input characteristics of BMX AMM 0600 module

Type	
Nature of inputs	Voltage/Current (250Ω internally protected sensors)
Number of channels	4 Inputs
Acquisition cycle time:	
<ul style="list-style-type: none"> Fast (periodic acquisition for the declared channels used) 	1ms + 1ms x number of channels used
<ul style="list-style-type: none"> Default (periodic acquisition for all channels) 	5ms
Resolution	14 bit in +/-10V 12 bit in 0.....5V
Digital filtering	1 st order
Isolation:	
<ul style="list-style-type: none"> Between inputs channels group and output channels group 	750 VDC
<ul style="list-style-type: none"> Between channels and bus 	1400 VDC
<ul style="list-style-type: none"> Between channels and ground 	1400 VDC
Maximum overload authorized for inputs	Voltage inputs: +/-30 VDC Current inputs: +/-90mA

Power consumption (3.3V)	Typical	0.35 W
	Maximum	0.48 W
Power consumption (24V)	Typical	1.3 W
	Maximum	2.8 W

A wide range of analog input/output modules enables you to select the module best suited to your needs. The characteristics of these modules differ as follows

Table E1.9: Different characteristics of analog input/output module

Characteristics	Description
Modularity	<ul style="list-style-type: none"> • 2 channels • 4 channels
Performance and range of signals offered	<ul style="list-style-type: none"> • Voltage/current • Thermocouple • Thermowell
Type of Connector	<ul style="list-style-type: none"> • 20-pin terminal blocks • 40-pin connectors allowing connection to sensors and pre-actuators by means of the TELEFAST 2 pre-wiring system

The following illustration shows an analog input/output module with one 40-pin connector

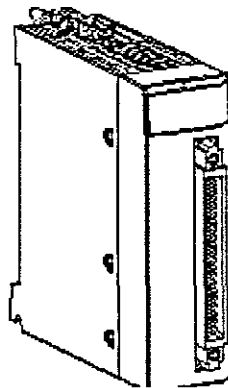


Figure E1.15: 40 pin Analog module diagram

The following illustration shows an analog input/output module with 20-pin terminal block:

Power consumption (3.3V)	Typical	0.35 W
	Maximum	0.48 W
Power consumption (24V)	Typical	1.3 W
	Maximum	2.8 W

A wide range of analog input/output modules enables you to select the module best suited to your needs. The characteristics of these modules differ as follows

Table E1.9: Different characteristics of analog input/output module

Characteristics	Description
Modularity	<ul style="list-style-type: none"> • 2 channels • 4 channels
Performance and range of signals offered	<ul style="list-style-type: none"> • Voltage/current • Thermocouple • Thermowell
Type of Connector	<ul style="list-style-type: none"> • 20-pin terminal blocks • 40-pin connectors allowing connection to sensors and pre-actuators by means of the TELEFAST 2 pre-wiring system

The following illustration shows an analog input/output module with one 40-pin connector

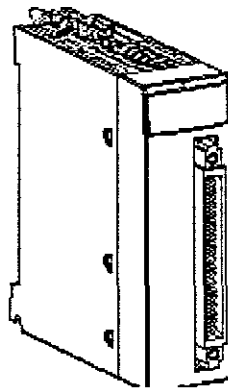


Figure E1.15: 40 pin Analog module diagram

The following illustration shows an analog input/output module with 20-pin terminal block:

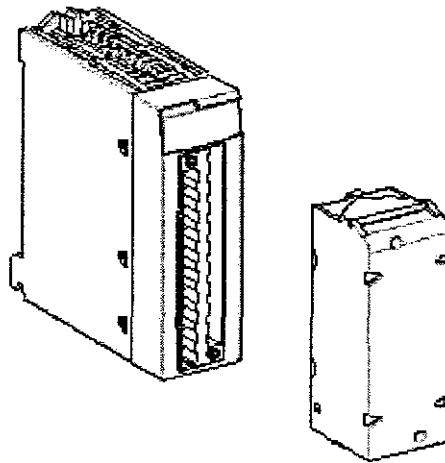


Figure E1.16: 20 pin Analog module diagram

E4.1 BMX AMM 0600 Analog Modules

The BMX AMM 0600 Input/Output module combines 4 non-isolated analog inputs with 2 non-isolated analog outputs. The BMX AMM 0600 module offers the following range, according to the selection made during configuration.

- Voltage input range +/-10 V/0..10 V/0..5 V/1..5 V
- Current input range 0...20 mA/4...20 mA
- Voltage output range +/-10 V
- Current output range 0...20 mA/4...20 mA

The actuators are connected using the 20-point terminal block.

The terminal block connection, the sensors, and the actuators wiring are as follows:

U_x is the positive pole input for channel x

COM_x is the negative pole input for channel x

U/IO_x is the positive output for channel x

COM_x is the negative output for channel x

Note: The current loop is self-powered by the output and does not request any external power supply.

Table E1.10: Connection points for Analog module

Channel	Positive	Negative	Comment
0	1&2	5	Turbidity
1	6&7	8	DO
2	9&10	11	Conductivity
3	12&13	14	PH

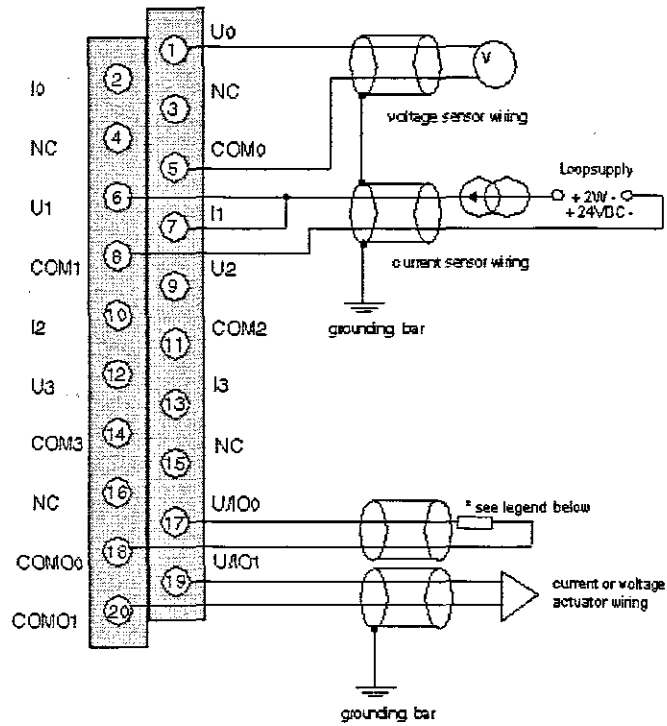
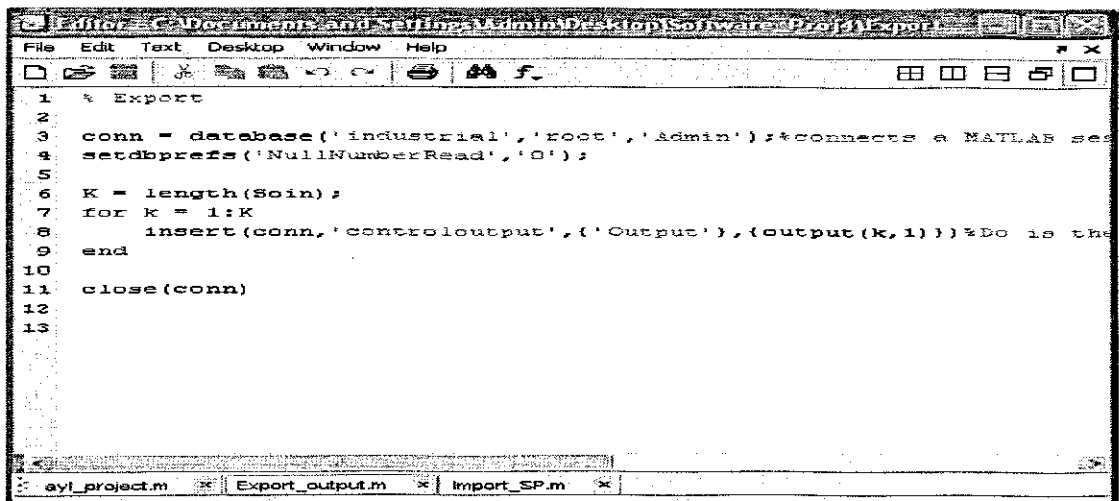


Figure E1.17: wiring diagram of the Analog module for a 20 pin out connection

E.2: MySQL database

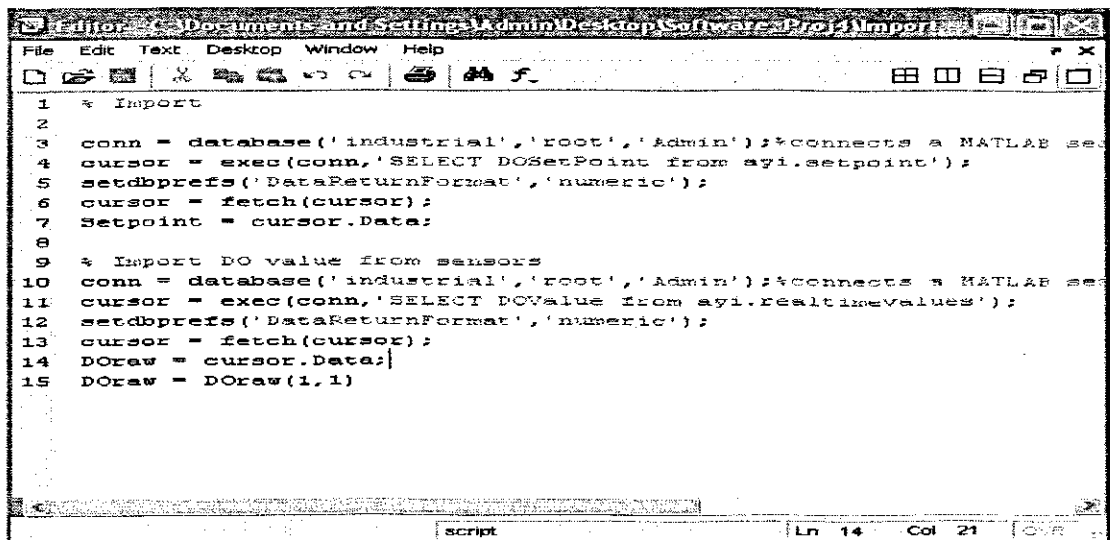
This figure below indicates how the data can be imported and exported from Matlab to MySQL. An mfile is created in Matlab and executed when required as indicated below.

The aim of retrieving and sending data from MySQL and Adroit is fulfilled in the Adroit application. Initially communication between the two applications is established; then through Adroit programming data can be retrieved and exported



```
1 % Export
2
3 conn = database('industrial','root','Admin');%connects a MATLAB sea
4 setdbprefs('NullNumberRead','0');
5
6 K = length(Soin);
7 for k = 1:K
8     insert(conn,'controlooutput',{'Output'},{output(k,1)})%Do is the
9 end
10
11 close(conn)
12
13
```

Figure E2.1: M-File for Export of data



```
1 % Import
2
3 conn = database('industrial','root','Admin');%connects a MATLAB sea
4 cursor = exec(conn,'SELECT DOSetPoint from ayi.setpoint');
5 setdbprefs('DataReturnFormat','numeric');
6 cursor = fetch(cursor);
7 Setpoint = cursor.Data;
8
9 % Import DO value from sensors
10 conn = database('industrial','root','Admin');%connects a MATLAB sea
11 cursor = exec(conn,'SELECT DOValue from ayi.realtimevalues');
12 setdbprefs('DataReturnFormat','numeric');
13 cursor = fetch(cursor);
14 DOraw = cursor.Data;|
15 DOraw = DOraw(1,1)
```

Figure E2.2: M-File for Import of data

The following dialog boxes indicate the configuration of tags in the Adroit environment. Here the analog agent has been selected and tags can be scanned to PLC.

Tables can then also be created in MySQL DB Manager in order to store all imported and exported data from Matlab and Adroit. This dialog box is therefore important, for interfacing simulated values with real time.

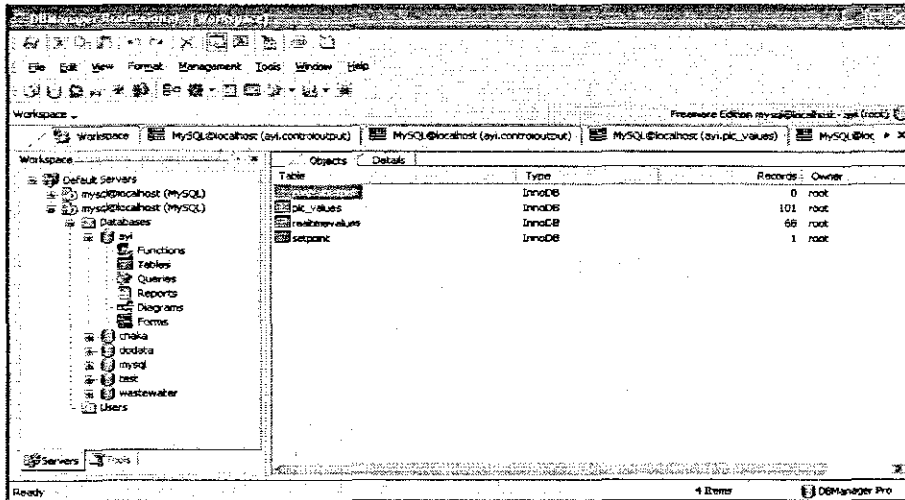


Figure E2.3: MySQL DB Manager

Raw values from the sensors can now be imported to Matlab via the database. The following dialog box displays the raw values that are received from the sensors.

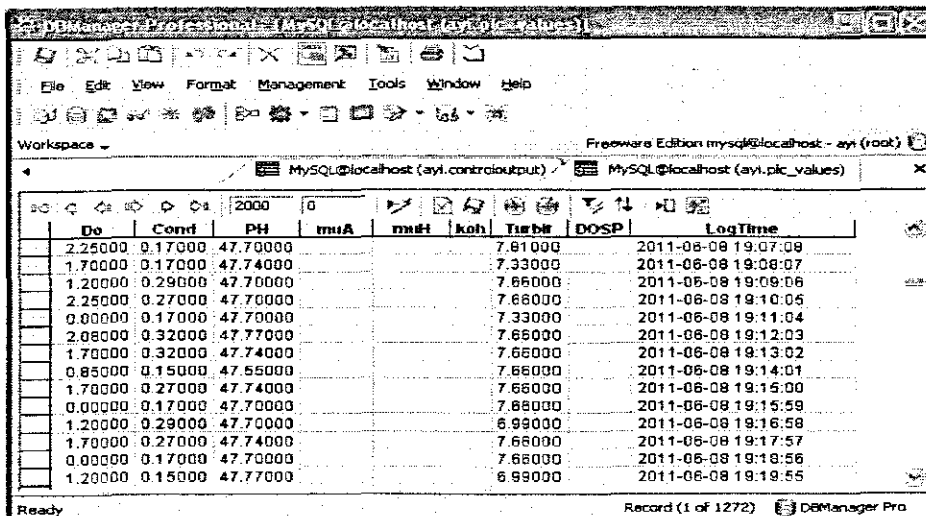


Figure E2.4: MySQL DB Manager Import data from Matlab and Adroit.

Since the main focus is on the monitoring of the DO values, these values are extracted separately and are being compared with the set-point value of 2 in the PLC

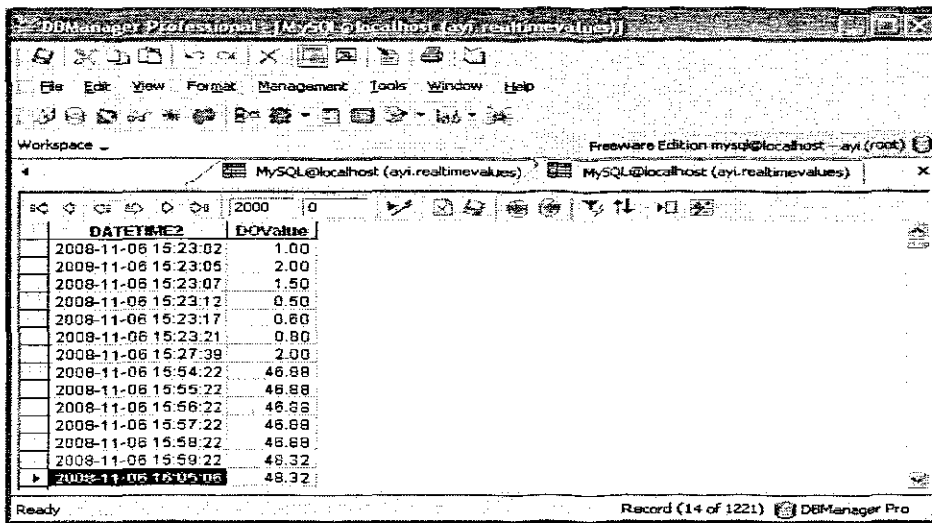


Figure E2.5: MySQL DB Manager import DO Value from PLC and Adroit.

The set-point is being created in MySQL and is being send to PLC where the DO values will be compared with the set-point values or to Matlab where design of the controller parameters can be provided

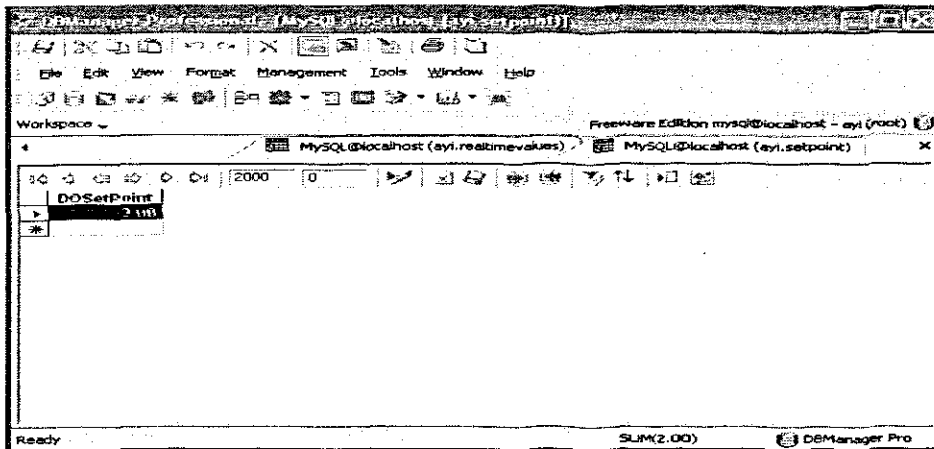


Figure E2.6: Dialog box diagram

This dialog box Figure E2.6 displays the set-point that has been imported to Matlab. This dialog box Figure E2.7 displays the analog tags. Note that all the tags are being scanned to the PLC, before any operation can be executed.

E.3. Adroit program

The SCADA and automation program Adroit (A Distributed Real-time Object oriented Intelligent Toolkit) is used to achieve the following:

1. Acquire sensor data from the PLC,
2. Store this data in a Database,
3. Acquire coefficient and set point values from a Database,
4. Update these values to PLC in real-time and
5. Allow the user to change parameters and observe process response and trends.

Figure E3.1 shows the mimic window of the main menu. This is the default screen of the user interface and all other parts of the GUI can be accessed from this main user screen. This mimic has five buttons that enable the user to access other parts of the project.

The 'DO Trend Graph' button allows the user to call up a historical graph (trend) window that displays the measured value of DO in the aerobic zone of the plant. The 'Aerobic Tank' button brings up another mimic that displays the real-time plant, with the DO measurement and state of the air inlet valve. The 'Browse Database' button executes a command that runs the MySQL Query Browser. The user is prompted for a password and can then browse through the data of the plant.

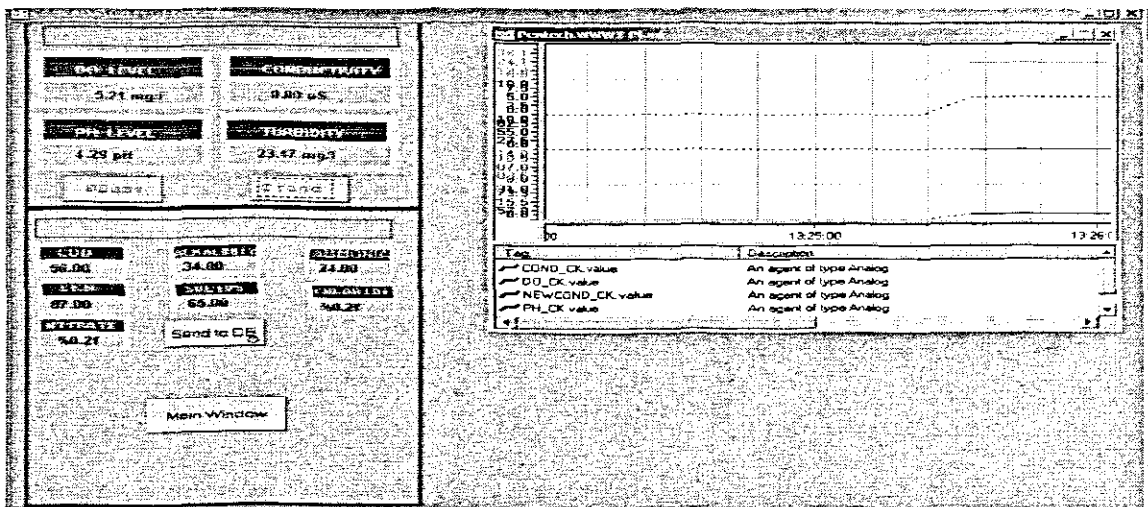


Figure E3.1: Adroit Program

The developed Adroit program shown in Figure E3.1 is used to acquire data of variables from the PLC and from Lab measurements. The data acquired from PLC is for DO

(dissolved oxygen), Conductivity, pH and Turbidity. The button marked DBase is associated with the program for sending online data to the Database in MySQL when this button is pressed it opens the database table in Microsoft Access. Button Trend is associated with the program for viewing graph for online variables, when this button is pressed it opens the trend plotting the current status of variables. The button Send to DB is for sending lab-measured data to database, when this button is pressed variables go to the database in MySQL and that can be viewed by pressing the DBase button, which will open database. From the database it can be seen that lab-measured data has been entered to the database.

E.4. Sensors used in the lab-scale plant

Dissolved Oxygen Sensor
Turbidity Sensor
Ph Sensor
Conductivity Sensor

Each of these sensors has transmitters where the currently measured variable can be displayed and the signal can be send to the PLC.

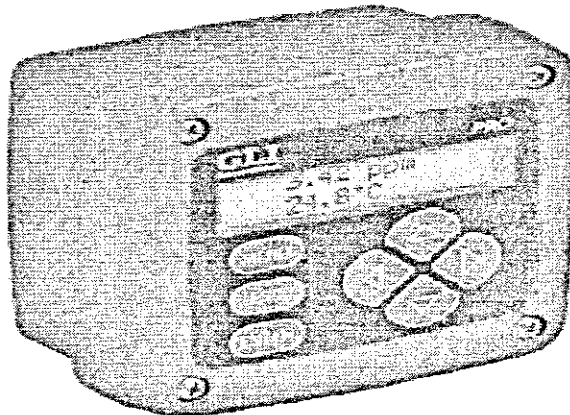


Figure E4.1: DO Transmitter

DO, pH and Conductivity transmitters have the same type of boxes and displays as show for DO in Figure E4.1. All these transmitters are mounted in a Box together with PLC, Turbidity meter and power supplies for all transmitters and for PLC

E.4.1 Solenoid Valve

3/2- WAY SOLENOID VALVE, G1/4, monostable Mod.434-015. The Series 4, G1/4, 3/2-way solenoid valves, which have electro pneumatic actuation and spring return, are available in the N.C.(closed) or N.O.(open) version. This model operates at a flow rate of 1250 Nl/min and a operating pressure of min 2 to max 10 Bar. Their main characteristics are in their electro pneumatic actuated and spring design.

The main advantage of these solenoid valves is their small overall dimensions and low energy consumption and can also be assembled on a pneumatic or electric manifold.

This model can be operated at a temperature of 0 to 60 Degrees Celsius using dry air at 20 Degrees Celsius. See Figure E4.2



Figure E4.2: Solenoid Valve.

E.4.2. Proportional Pressure Regulators

This is a MPPE type and is being used in parallel with the solenoid valve. The valves' technical data can be displayed as follows: See Figure E4.3

Table E4.1: MPPE valve data

Flow rate	Pressure regulation ranges	Voltage	Variants
350 ... 5,500 l/min	0 ... 1 bar 0 ... 2.5 bar 0 ... 6 bar 0 ... 10 bar	18 ... 30 V DC	• Setpoint value input as analogue voltage signal 0 ... 10 V
Type of pilot control	Pilot actuated using 2/2-way valves		Setpoint value input as analogue current signal 4 ... 20 mA
Constructional design	Pilot actuated piston regulator	Actuation type	Electrical

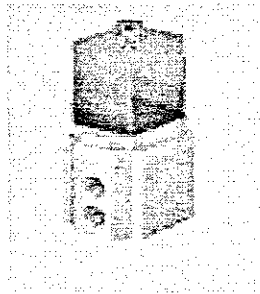


Figure E4.3: Proportional Pressure Regulators

E.5. Sensor wiring

E.5.1. Connecting DO sensor

- After properly mounting the transmitter, install the GLI membrane dissolved oxygen sensor.
- Route the six conductors inter-connect cable to the transmitter.
- At the transmitter end of the inter-connect cable, twist the two shield wires together. Then insulate them with plastic tubing or tape to prevent inadvertent shorting, and connect the combined shield to transmitter Terminal 3 on TB2.
- Connect the other sensor interconnect cable wires to the transmitter terminals on TB2, matching colours as indicated in the diagram Figure E5.1.

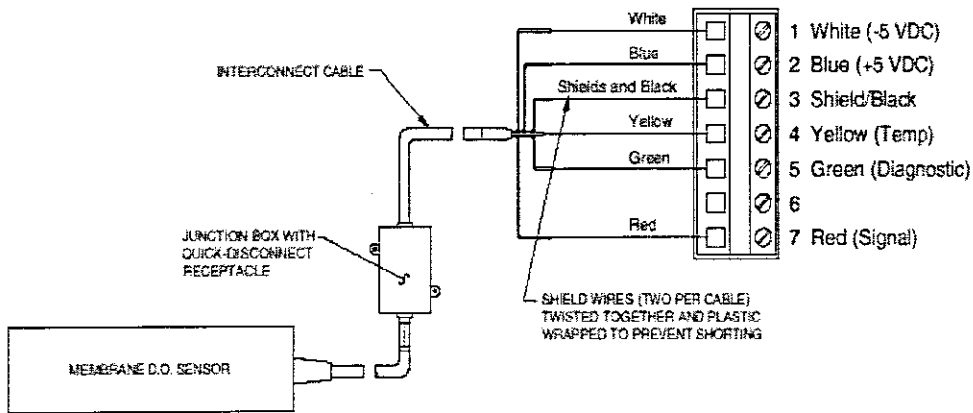


Figure E5.1: DO Sensor Wiring

The DO sensor has been wired according to this diagram.

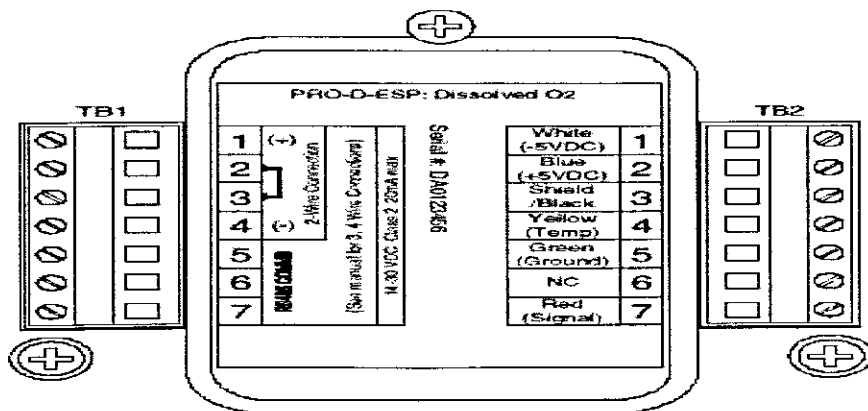


Figure E5.2: DO Transmitter inside view

The diagram in Figure E5.2 shows how the DO, Conductivity and pH Transmitters look like inside. From TB1 is the connection for power supplies and is the same for all three Transmitters and from TB2 is connection for the sensor and it differs for all three sensors according to their colour-coding.

E.5.2. Connecting conducting sensor

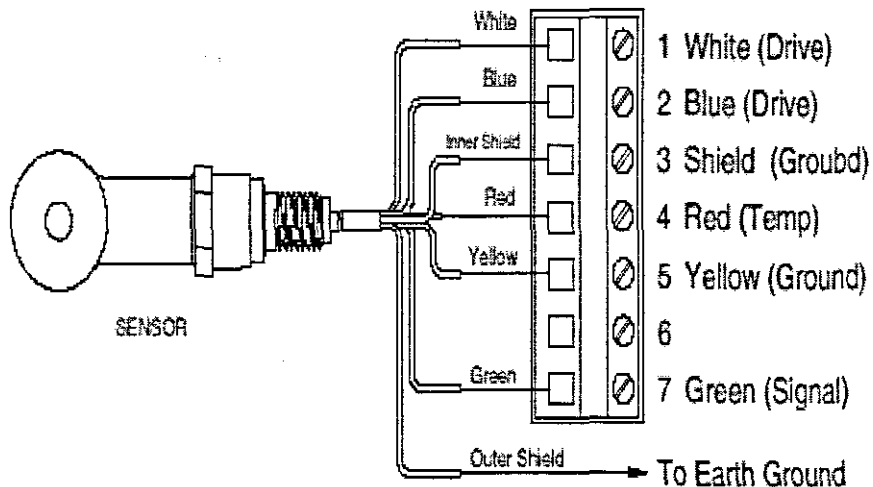


Figure E5.3: Conductivity Sensor Wiring

This sensor has been wired according to the diagram in Figure E5.3.

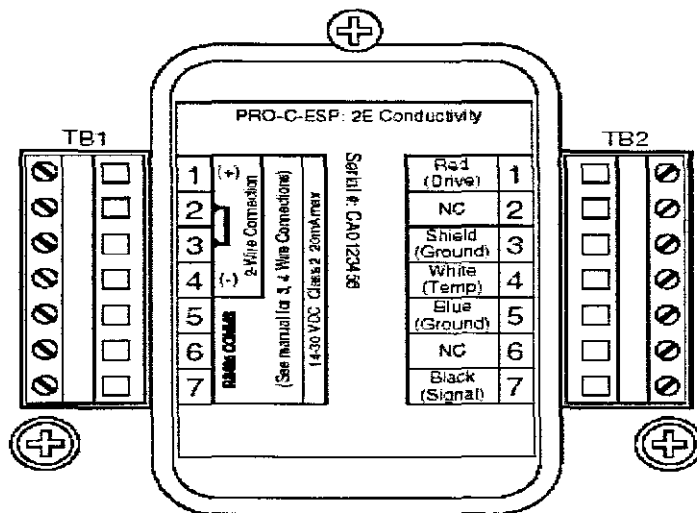


Figure E5.4: Conductivity Transmitter Inside view

BIBLIOGRAPHY/REFERENCES

ABUSAM, A. KEESMAN, K.J., SPANJERS, H., VAN STRATEN, G., & MEINEMA, K. 2002. A procedure for benchmarking specific full scale activated sludge plants used for carbon and nitrogen removal. 2002 IFAC 15th Triennial World Congress, Barcelona, Spain. <http://www.citeseer.nj.nec.com>

ALEKSEI, K.O., & TENO, T. 2001. Estimation of biodegradation parameters of phenolic compounds on activated sludge by respirometry. *Chemosphere*. 44:1273-1280

ALEXANDER, W.V., EKAMA G.A., & MARAIS G.V.R. 1979. The contact stabilization of activated sludge process, University of Cape Town, South Africa. 228-238, 2002. Activated sludge models ASM1, ASM2, ASM2d, and ASM3. By IAW task group on mathematical modelling for design and operation of biological wastewater treatment. 43-120. 1995. Activated sludge model no.2. By IAWQ task group on mathematical modelling for design and operation of biological wastewater treatment. 2-3. 1986. Anaerobic digestion model no.1. By IAW task group on mathematical modelling of anaerobic digestion process. 2-18

ANDREWS, J.F. 1974. Review Paper: Dynamic models and control strategies for wastewater treatment processes. *Water Research*, 8:261-289.

APPLICATION DATA SHEET. 2006. Dissolved Oxygen Measurement in Wastewater Treatment-Two different technologies. Water and Wastewater Industry, ADS 4950-01/rev.E

ARCEIVALA J.S., & ASOLEKAR, R.S. 2007. Wastewater Treatment for Pollution Control and Reuse. *Tata McGraw-Hill Publishing Company Limited, 7 west Patel Nagar, New Delhi. ISBN 0-07-062099-7*

BANDYOPADHYAY, M.N. 2003. Control Engineering: Theory and practice. *Printice-Hall of India Private Limited, New Delhi. ISBN-81-203-1954-0*

BILLING, A.E. 1987: Modelling Techniques for Biological Systems. PhD thesis. University of Cape Town. Department of Chemical Engineering. South Africa

BOLTON, W. 1996. Programmable Logic Controllers, An Introduction. *Newnes. An imprint of Butterworth-Heinemann, Linacre House, Jordan Hill, Oxford OX2 8DP, 225 Wildwood Avenue, Woburn, MA 01801-2041. ISBN-0 7506 3119 8.*

- CADET, C., & BETEAU, J.F. 2002. New control strategy design to improve effluent quality in wastewater treatment plants. *2002 IFAC 15th Triennial World Congress, Barcelona, Spain.*
<http://www.citeseer.nj.nec.com>
- CHECCHI, N., & MARSILI-LIBELLI, S. 2005. Reliability parameters estimation in respirometric models. *Water Research*. 39:3686-3696.
- CHEN, C.Y., ROTH, J.A., & ECKENFELDER JR, W.W. 1980. Response of dissolved oxygen to changes in influent organic loading to activated sludge systems. *Water Research*, 14:1449-1457.
- CLEMENTS-JEWERY, K., & JEFFCOAT, W. 1996. The PLC workbook. Programmable Logic Controllers made easy. *Prentice Hall international UK) limited Campus 400, Maylands Avenue.* ISBN-0-13-489840-0
- COSTANZO, M.P.B. 1997. Programmable Logic Controllers. *Halesowen College, UK.* ISBN 0 340 69258 8.
- COUILLARD, D, & ZHU, S. 1992. Control strategies for the activated sludge process under shock loading. *Water Research*, 26(5):649-655
- CRAYSON, L.P. 1965. The status of synthesis using Lyapunov method. *Automatica*, 3:91-121
- DOMNIK, C.S. 1997. Activated sludge treatment of chemi-thermo mechanical pulp effluent, A theoretical and experiment investigation of response to effluent variation. Masters thesis.
- DORF, R.C., & BISHOP, R.H. 2001. Morden Control Systems. *Printice-Hall Inc. Upper Saddle River, New Jersey 07458.* ISBN 0-13-03031411-0.
- EKMAN, M. 2005. Modelling and control of bilinear systems, application to the activated sludge. PHD thesis. Apsala University Sweden. ISBN 91-554-6342-8
- ELLIS G.T., BARBEAU S.D., SMETS F.B., & GRADY C.P. LESLIE J.R. 1996. Respirometric technique for determination of extant kinetic parameters describing biodegradation. *Water Environment Research*, 68(.5):917-926

FUJIMOTO, E., SEKINE, T., IWAHORI, K., & FURUYA, N. 1983. Studies on dissolved oxygen concentration and sludge retention time affecting the full-scale Activated sludge process. *Water Research*, 17(12):1829-1845

GEORGE, L. & BATTEN, J.R. 1988. Programmable Controllers: Hardware, Software, and Applications. *TAB Professional and Reference Books, Division of TAB BOOKS Inc. Blue Ridge Summit, PA. ISBN 0-8306-3147-X*

GERKŠIČ, S., VREČKO, D., & HVALA, H. 2006. Improving oxygen concentration in activated sludge process with estimation of respiration and scheduling control. *Water science and Technology*, 53(4):283-291

GERNEAEY, A.K., PETERSEN, B., OTTOY, J.P & VANROLLEGHEM, P. 2001. Activated sludge monitoring with combined respirometric-titrimetric measurements. *Water Research*, 35(5): 1280-1294.

GERNAEY, K, BOGAERTH, H., VANROLLENGHEM, P., VAN VOOREN, L., GUTIERREZ, G. & VEGA, P. 1998. Process synthesis applied to activated sludge processes. A framework with MINLP optimisation models. *Dept. Ingenieria de Sistemas Automatica. Facultad de Ciencias. Universidad de Valladolid. <http://www.citesser.nj.nec.com>*

GUTIERREZ, G., & VEGA, P. 2002. Integrated design of biological processes and their control system including closed loop properties for disturbances rejection. *2002 IFAC 15th Triennial World Congress, Barcelona, Spain. <http://www.citeseer.nj.nec.com>*

HACHICHO, O. 2006. A novel LMI-based optimization algorithm for the guaranteed estimation of the domain of attraction using Lyapunov functions. *Faculty of Civil Engineering, Mechanical Engineering, Safety Engineering, University of Wuppertal Germany. . www.Elsevier.com/locate/jfranklin.*

HENSON, M.A., & SEBORG, D.E. 1997. Nonlinear Process Control. *Prentice Hall PTR, Upper Saddle River, New Jersey 07458. ISBN 0-13-625179-X.*

HENZE M., HARREMOËS P., JANSEN, J.La C., & ARVIN E. 1995. Wastewater Treatment, Biological and Chemical Processes. Springer, Berlin, Heidelberg, Germany

HENZE, M., LESLIE GRADY JR, C.P., GUJAR, W., MARAIS, G.V.R., & MATSUO T.1987. Activated Sludge Process Model No.1. Scientific and Technical Report 1, IAWQ, 1987. London UK.

HOLENDA, B., DOMOKOS, E., RÉDEY, Á., & J. FAZAKAS. 2008. Dissolved oxygen control of the activated sludge wastewater treatment using model predictive control. *Computers and Chemical Engineering*, 32:1270-1278

HOLENDA, B. 2007. Development of modelling, control and optimization tools for the activated sludge process. PHD thesis. University of Pannonia.

HOLMBERG, U., & OLSSON, G. 1985. Simultaneous On-line estimation of oxygen transfer rate and respiration rate. *Modelling and Control of Biotechnological Process. IFAK, Noordwijkerhout. 205-209*

<http://press.princeton.edu/math/blondel/part3.pdf>

http://scholar.lib.vt.edu/theses/available/etd-5440202339731121/unrestricted/CHAP4_DOC.pdf

<http://www.control.aau.dk/~raf/NonLinear/Nonlinea.htm>

<http://www.cs.ele.tue.nl/MLazar/TechnicalReport.pdf>

<http://www.math.ucla.edu/~tom/LP.pdf>

http://www.me.berkeley.edu/ME237/2_general_properties.pdf

<http://www.wfw.wtb.tue.nl/benelux2002/nmpc.pdf>

HULL, V., PARRELLA, L., & FALCUCCI, M. 2008. Modelling dissolved oxygen dynamics in coastal lagoons. *Ecological Modelling*, 211:468-480.

IKONEN, E., & NAJIM, K. 2002. Advanced process Identification and control. *Marcel Dekker, Inc. 270 Madison Avenue, New York, NY 10016. ISBN 0-8247-0648-X*

infoscience.epfl.ch/record/28423/files/fulltext.pdf

NGILDSEN, P. 2002. Realising full-scale control in wastewater treatment systems using In Situ

sensors. *PHD thesis. Lund university, Sweden. ISBN-91-88934-22-5*

JEPPSON, U.I.F. 1996. Modelling Aspects of Wastewater Treatment Processes. CODEN: LUTEDX/TEIE-1010/1-444/1998, Lund, Sweden: 42.

JEPPSSON, U.I.F. 1993: On the verifiability of the Activated Sludge System Dynamics. *PhD thesis. Lund Institute of Technology. Department of Industrial Electrical Engineering and Automation. S-221 00 LUND.*

KATEBI, R., JOHNSON, M., & WILKIE, J. 1999. Control and Instrumentation for Wastewater Treatment Plants. *Springer-Verlag London Limited. Great Britain. ISBN 1-85233-054-6.*

KO, K.U., McINNIS, B.C., & GOODWIN, G.C. 1982. Adaptive control and Identification of the Dissolved Oxygen Process. *Automatica*, 18(6):727-730.

LJUNG, L & TORSTEN, S. 1983. Theory and Practice of Recursive Identification. *MIT Press. Cambridge. Massachusetts London, England. ISBN 9780262120.*

LI, K.Y., & ZHANG, Y.B. 1996. Oxygen transfer limitation in respirometer. *Water Environment Research*, 68(1):36-41

LILLEY, I.D., PYBUS P.J., & POWER S.P.B. 1997: Operating Manual for Biological Nutrient Removal Wastewater Treatment Works. Steward Scott Inc. *Water Research Commission Report No. TT 83/97. South Africa. ISBN 1 86845 2727.*

LINDBERG, C.F., & CARLSSON, B. 1996. Estimation of the respiration rate and oxygen transfer function utilizing a slow DO sensor. *Water science and Technology*, 33(1):325-333.

LINDBERG, C.F., & CARLSSON, B. 1996. Nonlinear and Set-Point control of the dissolved oxygen concentration in activated sludge process. *Water science and Technology*, 34 (3-4):135-142.

LINDBERG, C.F. 1997: Control and Estimation strategies applied to the Activated Sludge Process. PhD thesis. Uppsala University. Department of Materials Science Systems and Control Group. SE-751 03 Uppsala. Sweden

LING, B.K. 2006. A diffusive stage-structured model in a polluted environment. *Nonlinear*

LIRA, V.V., PÉRICLES, B.R., DA ROCHA NETO, J.S., VAN HAANDEL, A.C. 2004. Estimation of Dissolved oxygen Dynamics for Sequencing Batch Aerobic Reactors. *IEEE Transactions on Instrumentation and Measurement Conference. Como. Italy, 18-20 May: 14-19*

LUKASSE, L.J.S., KEESMAN, K.J., & VAN STRATEN, G. 1997. Estimation of BOD_{st}, Respiration rate and Kinetics of Activated Sludge. *Water Research. 31(9):2278-2286*

LUKASSE, L, KEESMAN, K., SPANJERS, H., & BLOEMEN, M. 2000. Diagnosis and Identification of Respirometer Dynamics and Sludge Kinetics in Continuous-Flow Respirometers. *Water Environment Research, 72(3):340-347.*

MANFRED, R., BUTTER, D., & BECK, B.M. 2002. Modelling, Simulation and control urban wastewater systems, Springer, London: 230-270.

MARSILI-LIBELLI, S., & TABANI, F. 2002. Accuracy analysis of a respirometer for activated sludge dynamic modelling. *Water Research, 36:1181-1192.*

MARSILI-LIBELLI, S., & VAGGI, A. 1997. Estimation of respirometric activities in bioprocesses. *Journal of Biotechnology, 52:182-192.*

MATHIEU, S., & ETIENNE, P. 2000. Estimation of wastewater biodegradable COD fractions by combining respirometric experiments in various SO/XO ratios. *Water Research. 34(4):1233-1246.*

METCALF& EDDY, INC. 1979. Wastewater Engineering: Treatment Disposal.Reuse. *McGraw-Hill Book Company. ISBN 0-07-041677-X*

NATIONAL LIME ASSOCIATION. 1987. Principles of sewage treatment, *Washington D.C. 15-76.*

OGATA, K 2002. Morden Control Engineering, *Fourth Edition. Prentice-Hall, Inc, Upper Saddle River, New Jersey 07458. ISBN: 0-13-043245-8*

OLSSON, G., & NEWELL, B. 1999. Wastewater Treatment Systems, Modelling, Diagnosis and

control. IWA publishing

OLSSON, G., & ANDREWS, J.F. 1978. The Dissolved Oxygen Profile-A Valuable Tool for control of the activated sludge process. *Water Research*, 12:985-1004

PÉREZ-CORREA, R.J., LÓPEZ, F., & SOLAR, I. 1991. Dissolved oxygen control through an adaptive nonlinear model approach: a simulation study. *Journal of Process Control*, 1:152-160.

PERISINI, T. & ZOPPOLO, R. 1985. A receding horizon regulator for nonlinear systems and neural approximation. *Automatica*, 31(10):1443-1451.

PETERSEN, B., GERNAEY, K., & VANROLLEGHEM, P.A. 2001. Practical Identifiability of model parameters by combined respirometric-titrimetric measurements. *Water Science and Technology*, 43(7):347-355

PIOTROWSKI, R., BRDYS, M.A., ONARCZAK, K., DUZINKIEWICZ, K., & CHOTKOWSKI, W. 2008. Hierarchical dissolved oxygen control for activated sludge processes. *Control Engineering Practice*, 16:114-131.

RANTZER, A. 2000. A dual to Lyapunov's stability theorem. *Department of Automatic Control, Lund Institute of Technology Lund Sweden*. <http://dx.doi.org/10.1109/CDC.2000.914264>

RICHARD, M. 1989. The Bench Sheet monograph on Activated Sludge Microbiology. *The Water Pollution Control Federation*. ISBN # 0-943-244-27-7

RICHALET, J., RAULT, A., TESTUD, J., & PAPON, J. 1976. Algorithm control of industrial processes. *Proceedings of the 4th IFAC Symposium on Identification and system parameter estimation*. 1119-1167

RIOS-GUTIERREZ, F. 2007. Overview of Programmable Controllers (PLCs). <http://www.d.umn.edu/~snorr/ece4951s7/Lect4.pdf> 15-02-09)

ROŠ, M, DULAR, M, & FARKAS, P.A. 1988. An improved method using respirography for the design of activated sludge aeration systems. *Water Research*. 22(12):1483-1489

ROSEN, C. 2001. A chemometric approach to process monitoring and control, with application

to wastewater treatment operation. *PHD thesis. Lund university, Sweden. ISBN-91-88934-20-9*

RYDER, R.A. 1972. Dissolved oxygen control of Activated sludge aeration. *Water Research Pergamon Press, 6:441-445.*

SAEED, S.H. 2002. Automatic Control Systems: With Matlab Programs. S.K. KATATARIA & SONS, 4424/6, Guru Nanak Market, Nai Sarak, Delhi-110006. ISBN 81-88458-03-1

SAMUELSSON, P. 2005. Control of nitrogen removal in activated sludge processes. PHD thesis. *Uppsala Universitet Sweden. ISBN 91-554-6311-8*

SINGMAN, J. 1998. Efficient control of wastewater treatment plants-a benchmark study *Uppsala University school of Engineering. <http://www.citeseer.nj.nec.com>. 2-14.*

SLOTINE, J-J, & LI, W. 1991. Applied nonlinear control. Massachusetts institute of Technology. Printice Hall, Englewood Cliffs, New Jersey 07632. ISBN 0-13-040890-5

SPANJERS, H., VANROLLEGHEM, P., OLSSON, G., & DOLD, P. 1996. Respirometry in control of the activated sludge process. *Water science and Technology, 34(3-4):117-126.*

SPANJERS, H., & VANROLLEGHEM, P. 1995. Respirometry as a tool for rapid characterization of wastewater and Activated sludge. *Water Science and Technology. 31(2):105-114*

SOLLFRANK, U., & GUJER, W., 1990. Simultaneous determination of oxygen uptake rate and oxygen transfer coefficient in activated sludge systems by an on-line method. *Water science and Technology, 24(6)725-732*

SOTOMAYOR, O.A.Z., PARK, S.W., & GARCIA, C. 2001. Software sensor for on-line estimation of the microbial activity in activated sludge systems. *ISA Transactions, 41:127-143*

STENSTROM, K.M., & PODUSKA, R.A. 1980. The effects of dissolved oxygen concentration on nitrification. *Water Research, 14:643-649.*

SURMACZ-GORSKA, J., GERNAEY, K., DEMUYNCK, C., VANROLLEGHEM, P., & VERSTRAETE, W. 1996. Nitrification monitoring in activated sludge by oxygen uptake rate

OUR) measurements. *Water Research*, 30(5):1228-1236.

TRIVERS, S.M., & LOVETT, D.A. 1984. Activated sludge treatment of abattoir wastewater-II, influence of dissolved oxygen concentration. *Water Research*, 18(4).435-439

VANROLLEGHEM, P.A, & LEE D.S. 2003. On-line monitoring equipment for wastewater treatment process: state of the art. *Water science and Technology*, 47(2):1-34.

VANROLLEGHEM P.A., & SPANJERS, H. 1998. A Hybrid respirometric method for more reliable assessment of activated sludge model parameter. *Water science and Technology*, 37(12):237-246

VANROLLEGHEM, A.P., SPANJERS, H., PETERSEN, B., GINESTET, P, & TAKACS, I. 1999. Estimation Combinations of) Activated Sludge Model No.1 Parameters and Components by Respirometry. *Water Science and Technology*, 39(1):195-214.

VANROLLEGHEM, P.A., VAN DAELE, M., & DOCHAIN, D. 1995. Practical Identifiability of a biokinetic model of Activated Sludge Respiration. *Water Research*, 29(11):2561-2570

WILÉN, B., & BALMÉR, P. 1999. The effect of dissolved oxygen concentration on the structure, size and size distribution of activated sludge flocs. *Water Research*, 33(2):391-400

YOO, C., LEE, J., & LEE, I. 2004. Nonlinear model-based dissolved control in the biological wastewater treatment process. *Korean Journal of Chemical Engineering*, 21(1):14-19.

YOO, C., LEE, H., & LEE, I. 2002. Comparisons of process identification methods and supervisory DO control in full scale wastewater treatment plant. 2002 IFAC 15th Triennial World Congress, Barcelona, Spain. <http://www.citeseer.nj.nec.com>

ZHAO, H., ISAACS, S.H., SØEBERG, H., & KÜMMEL, M. 1995. An analysis of nitrogen removal and control strategies in an alternating Activating sludge process. *Water Research*, 29(2):. 535-544.

ZHINGUO R.B, & KELLER, J. 2008. Partial nitrification to nitrite using low dissolved oxygen concentration as the main selection factor. *Biodegradation*. 19:303-312